3D printing
of thermo-sensitive drug substances
via Fused Deposition Modeling (FDM™)

Inaugural-Dissertation

zur Erlangung des Doktorgrades
der Mathematisch-Naturwissenschaftlichen Fakultät
der Heinrich-Heine-Universität Düsseldorf

vorgelegt von

Lena Hoffmann
aus Datteln

Düsseldorf, Oktober 2023

aus dem Institut für Pharmazeutische Technologie und Biopharmazie
der Heinrich-Heine-Universität Düsseldorf

Gedruckt mit der Genehmigung der
Mathematisch-Naturwissenschaftlichen Fakultät der
Heinrich-Heine-Universität Düsseldorf

Berichterstatter:

1. Prof. Dr. Jörg Breitkreutz

2. Prof. Dr. Dr. h.c. Peter Kleinebudde

Tag der mündlichen Prüfung: 20.02.2024

Preface

The present work was conducted at the Institute of Pharmaceutics and Biopharmaceutics at Heinrich Heine University Düsseldorf, as part of the ´ProMatLeben-Polymere-PolyPrint' project, which was funded by the German Federal Ministry of Education and Research (BMBF). The project consortium consisted of the companies Merck and Gen-Plus, the Laboratory for Manufacturing Systems of the University of Applied Sciences, Cologne, and the Institute of Pharmaceutics and Biopharmaceutics at Heinrich Heine University Düsseldorf.

Table of contents

List of abbreviations

3D	Three-dimensional
3DP	3D printing
ADR	Adverse drug reaction
Ala	Alanine
AM	Additive manufacturing
ANDA	Abbreviated new drug application
API	Active pharmaceutical ingredient
aPMMA	Ammonio methacrylate copolymer (type A) (Ph. Eur.)
ASD	Amorphous solid dispersion
ASTM	American Society for Testing and Materials
BCS	Biopharmaceutics Classification System
BJ	Binder jetting
BLA	Biologics License Application
BMBF	Bundesministerium für Bildung und Forschung (engl. Federal Ministry of Education and Research)
bPMMA	Basic butylated methacrylate copolymer (Ph. Eur.), Eudragit® E
CAD	Computer-aided design
cGMP	Current Good Manufacturing Practice
CQA	Critical quality attribute
CT	Computed tomography
CU	Content uniformity
DMF	Drug master file
DNA	Deoxyribonucleic acid
DoD	Drop-on-drop
DoS	Drop-on-solid
DPE	Direct powder extrusion
EC	Ethylcellulose (Ph. Eur.)
EM	Enalapril maleate
EMA	European Medicines Agency
ENP	Enalapril
ESC	Escitalopram
ESC-OX	Escitalopram oxalate
EU	European Union
FD&C Act	Federal Food, Drug, and Cosmetic Act
FDA	Food and Drug Administration (U.S.)
FDM™	Fused deposition modeling
FFF	Fused filament fabrication
FIH	First-in-human
GMP	Good Manufacturing Practice
HME	Hot-melt extrusion
HPLC	High-performance liquid chromatography
HPC	Hydroxypropylcellulose (Ph. Eur.)
HPMC	Hydroxypropylmethylcellulose, hypromellose (Ph. Eur.)

ICH	International Council for Harmonisation of Technical Requirements for Pharmaceuticals for Human Use
Imp	Impurity
IND	Investigational New Drug
ISO	International Organisation for Standardisation
K VA 64	Kollidon® VA 64, copovidone (Ph. Eur.)
K 12 PF	Kollidon® 12 PF, povidone (Ph. Eur.) with a K-value of 12
L/D	Length-to-diameter ratio
logP	Decadic logarithm of the octanol-water coefficient
MED™	Melt extrusion deposition
MIR	Mid-infrared spectroscopy
MRI	Magnetic resonance imaging
NDA	New drug application
NGS	Next-generation sequencing
NIR	Near-infrared
ODF	Orodispersible film
ODT	Orodispersible tablet
OoC	Organ-on-chip
PAM	Pressure-assisted microsyringes
PAT	Process analytical technology
PCL	Poly-ε-caprolactone
PEGs	Polyethylene glycols, macrogols (Ph. Eur.)
PEO	Polyethylene oxide
PF	Pyrogen-free
Ph. Eur.	European Pharmacopoeia
Phe	Phenylalanine
PLA	Polylactic acid
PMDA	Pharmaceuticals and Medical Devices Agency (Japan)
PMI	Precision Medicine Initiative
Pro	Proline
PVA	Poly(vinyl alcohol) (Ph. Eur.)
PVP	Polyvinylpyrrolidone, povidone (Ph. Eur.), Kollidon®
SLA	Stereolithography
SLS	Selective laser sintering
sNIR	Short-near-infrared spectroscopy
SOL	Soluplus® (polyvinyl caprolactam-polyvinyl acetate-polyethylene glycol graft copolymer)
SSE	Single-screw extruder
STL	Standard Tessalation Language
TSE	Twin-screw extruder
U.S.	United States
UV	Ultraviolet
UV-VIS	Ultraviolet-visible spectroscopy
WHO	World Health Organisation

List of figures and tables

1 Introduction

1.1 General

The present thesis deals with the investigation of the behaviour of the thermo-sensitive drug substances enalapril maleate (EM) and escitalopram oxalate (ESC-OX) during the two heat-intensive processes of hot-melt extrusion (HME) and subsequent fused deposition modeling (FDM) three-dimensional (3D) printing. High-performance liquid chromatography (HPLC) methods for quantifying the active pharmaceutical ingredients (APIs) and potential degradation products have been developed. Suitable formulations have been evolved and strategies to avoid drug degradation have been designed. The analytical characterisation of extrudates and tablets produced by HME and FDM 3D printing are within the focus of the work.

3D printing (3DP) is an additive manufacturing (AM) technology which is defined by the International Organisation for Standardisation (ISO) as “fabrication of objects through the deposition of a material using a print head, nozzle, or another printing technology“ [1]. Due to the additive deposition of the layers of the 3D printed object, this manufacturing process must be distinguished from subtractive and formative manufacturing methodologies [1].

The basic components of 3DP consist of the hardware, the software as well as the printing materials which are required for the 3DP process [2]. Although there are various 3DP technologies available which differ in the used materials and the manufacturing processes, the working principle of 3DP follows the same procedure from digital design to the production of the 3D printed object [3].

The basic procedure of 3DP is divided into five steps [4] which are shown in Figure 1.

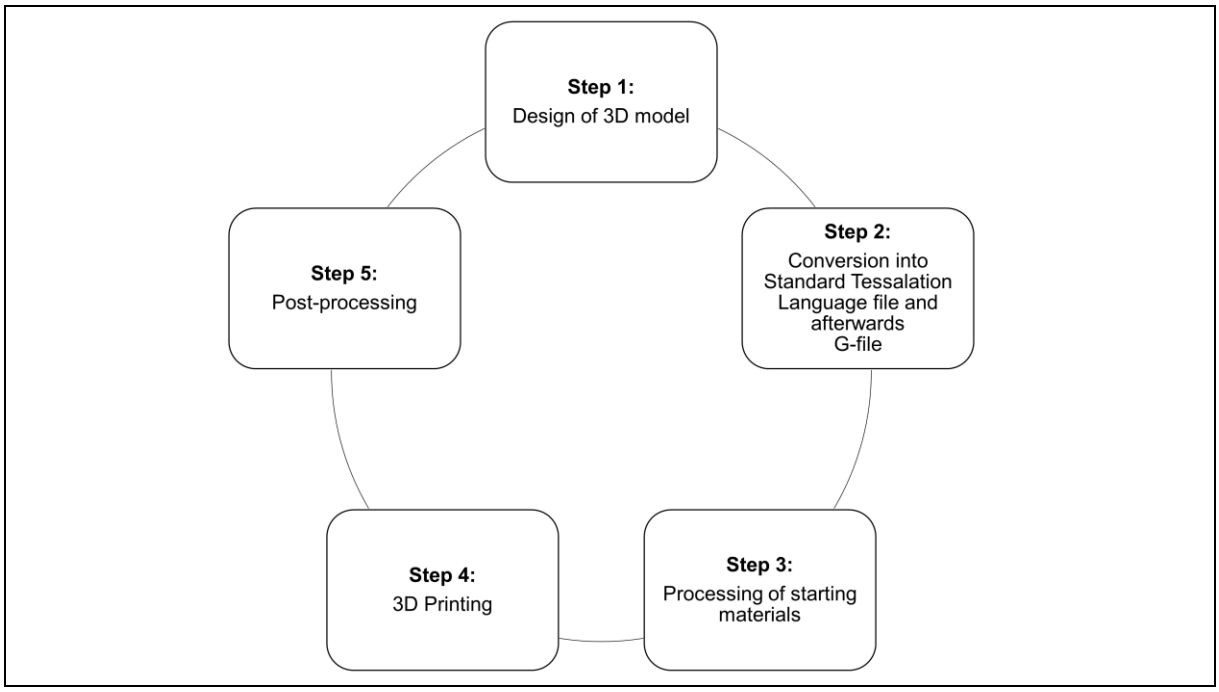

Figure 1. 3D printing procedure.

The first step is to design the desired object with the help of computer-aided design (CAD) software [5]. In the second step, the designed 3D model is converted into a Standard Tessalation Language (STL) file format that can be read by the 3D printer and describes the

surface geometry of a 3D model as a tessellation of triangles [1,5]. The STL file format only defines the surface grid, but does not contain any specifications for the representation of the object, such as colour or texture [6]. The surface of the 3D model is sliced into printable layers using a slicer software and the parameters regarding the designed dosage form (e.g. geometry and internal structure) as well as the printing process (e.g. nozzle temperature, print bed temperature and printing speed) can be set [4,7]. Afterwards, the information is saved as a G-file in the form of a G-code and sent digitally to the 3D printer [3,5]. The third step is the processing of intermediates from starting materials, i.e. the production of granules, extrudates, also known as filaments from solid materials, or binder inks for the 3DP process [3,8]. In the fourth step, the manufactured objects are used for 3DP and the designed 3D model is printed layer by layer. After the 3DP process, evaluation of the 3D printed object according to the product specifications takes place and further post-processing steps in the fifth step may be required, which may include harvesting, drying, sintering, polishing, or recycling [3,8,9].

AM technologies can be divided into seven categories according ISO standard 52900:2021 “Additive manufacturing – General principles – Fundamentals and vocabulary” and ISO standard 17296-2:2015 “Additive manufacturing – General principles – Part 2: Overview of process categories and feedstock“ [1,10,11]. These include vat photopolymerisation, material jetting, binder jetting (BJ), material extrusion, powder bed fusion, sheet lamination and directed energy deposition [1,10,11]. While the first five technologies are widely used in medicine, the two technologies of sheet lamination and directed energy deposition are used less, but beneficially for more specific applications [11]. ISO standard 17296-2:2015 provides more detailed information and requirements about the process, the materials used, the binding mechanism as well as the activation energy and secondary processing [10].

AM technologies are widely used for prototyping, tooling, and production of fully functional end products in the engineering industry as well as in medicine, education, architecture, cartography, toys and entertainment and must be distinguished from additive processes as for example coating, capsule filling and film lamination in the pharmaceutical industry [1,3,10,12].

Fused deposition modeling, which has been trademarked by Stratasys Inc. (FDM™, abbreviated as FDM for convenience), is an extrusion-based 3DP technology and one of the five most important 3DP technologies for pharmaceutical applications, along with stereolithography (SLA), selective laser sintering (SLS), BJ and pressure-assisted microsyringes (PAM) [13-15].

In the healthcare industry, 3DP is used for the production of dosage forms and medical devices, whereas 3D bioprinting offers the opportunity to fabricate artificial tissues and even organs [8].

1.2 Motivation for 3D printing

1.2.1 General

The main motivations for 3DP in the healthcare industry are shown in Figure 2.

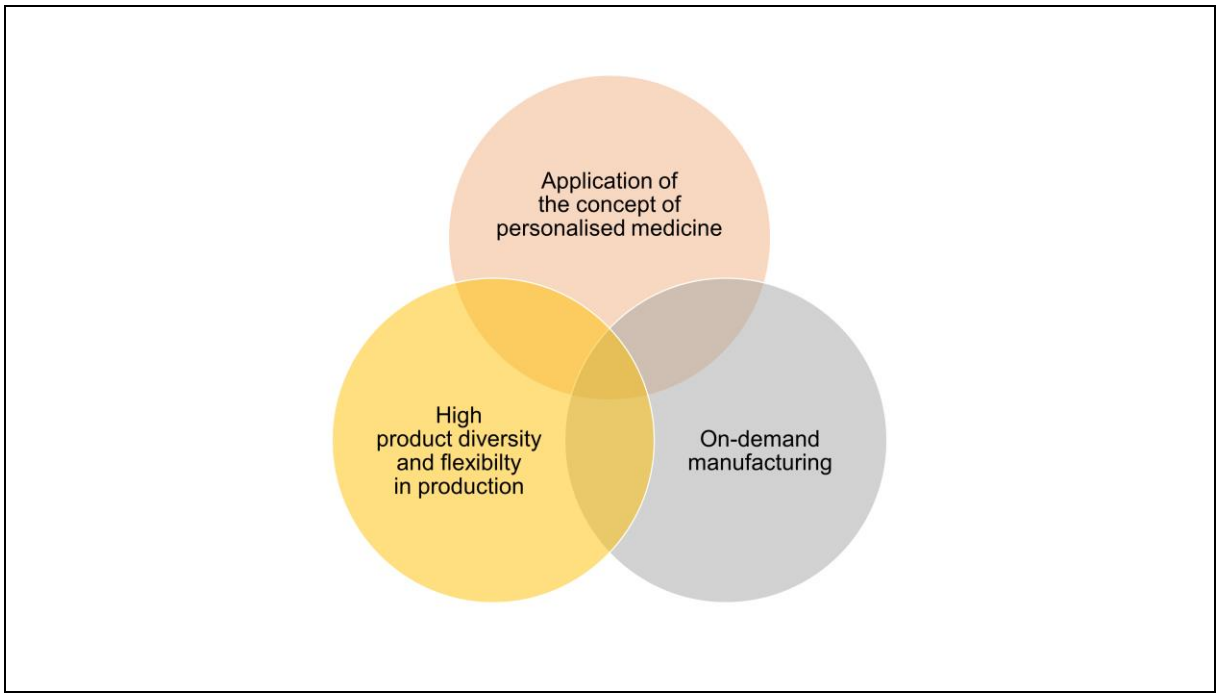

Figure 2. Main motivations for 3D printing in the healthcare industry (modified from [3,9]).

These comprise [3,8,9,15]:

- **application of the concept of personalised medicine:** Provision of dosage forms with APIs in flexible doses for preclinical and clinical applications adapted to the patients need.
- **high product diversity and flexibility in production:** Manufacturing of dosage forms and combination products with different drug delivery concepts for one or multiple APIs, but also for small batches in early-phase drug development, e.g. first-in-human (FIH) trials.
- **on-demand manufacturing:** Decentralised production of dosage forms at point-of-care even under extraordinary circumstances.

1.2.2 Application of the concept of personalised medicine

One of the main motivations for 3DP is the application of the concept of personalised medicine. Although the term "personalised medicine" is often used, there is no commonly accepted definition [16]. The European Union (EU) Health Ministers of the Horizon 2020 Advisory Group defined the term personalised medicine in the Council conclusions on personalised medicine for patients in December 2015 as follows: “A medical model using characterisation of individuals’ phenotypes and genotypes (e.g. molecular profiling, medical imaging, lifestyle data) for tailoring the right therapeutic strategy for the right person at the right time, and/or to determine the predisposition to disease and/or to deliver timely and targeted prevention. Personalised medicine relates to the broader concept of patient-centred care, which takes into account that, in general, healthcare systems need to better respond to patient needs.“ [16]

Furthermore, according to the European Commission, personalised medicine is seen as an evolution of medicine whose application into the healthcare systems still faces a number of challenges [16]. However, new genetic technologies such as pharmacogenomics can drive progress in personalised medicine [16]. Pharmacogenomics is one of the decisive elements in the drug discovery and drug development processes, as it is based on the association between genetic variations and drug response [17,18]. Variability in drug response due to individual differences in metabolic pathways can lead to different reactions and adverse drug reactions (ADRs) [19]. Predictions about diagnoses and prognoses can be made by identifying appropriate biomarkers. Biomarkers are objectively measurable characteristics that can serve as indicators of biological processes or of pharmacological responses to therapeutic interventions [20,21]. Pharmacogenetics, on the other hand, investigates the connection between a deoxyribonucleic acid (DNA) variant and the response to a drug [22].

Personalised medicine can be considered as a further development of intuition medicine and evidence-based medicine, which finds its application in "omics" technologies [16,23]. The suffix "omics" such as genomics, transcriptomics, proteomics and metabolomics encompasses high-throughput experimental technologies that use tools to comprehensively monitor disease processes at the molecular level and rely on big data [23].

In the context of personalised medicine, other terms are precision medicine, stratified medicine, individualised medicine and p4 medicine [23-27]. The term "precision medicine", which is often used synonymously with "personalised medicine", is preferably applied for targeted treatment through the use of biomarkers [28]. The Precision Medicine Initiative (PMI), launched in 2015 by former White House President Barack Obama, defines precision medicine as “an emerging approach for disease prevention and treatment that takes into account people's individual variations in genes, environment, and lifestyle." [26,27] "Stratified medicine" refers to the concept of targeted treatment based on the patient's genes and physical characteristics [23]. The term “stratified medicine“ is to be distinguished from the term "individualised medicine", which involves tailor-made treatments. It describes the medical treatment with products from the patient's own autologous cells [23]. The term p4 medicine was first introduced in the concept of integrating biological data for therapeutic interventions [29]. The concept of p4 medicine, which comprises the features "personalised", “predictive“, “preventive“ and “participatory“ shall apply the “multi-omic“ approach including genomics, transcriptomics and proteomics [23]. Nowadays, the feature "population/public perspective" (5P) has to be incorporated in addition to the other four features [23].

The further development of personalised medicine is being driven by the European Medicines Agency (EMA), the United States (U.S.) Food and Drug Administration (FDA) and the Japanese Pharmaceuticals and Medical Devices Agency (PMDA), which have an interest in investigating the relation between genetic polymorphisms and pharmacodynamic endpoints. EMA has expressed its interest in pharmacogenomics by publishing scientific guidelines [30]. In the U.S., the PMI focused on the paradigm shift from mass production to personalised medicine [19]. PMI sets as its goal for “targeting the right treatments to the right patients at the right time“ [25,26]. This is intended to make the shift from treating the "average patient" with the traditional "one-size-fits-all" approach to treating the "right patient" with the "right drug" in the "right dose" at the "right time" [18,26,27,31]. This new approach assumes that treatment with the right drug will result in the fewest side effects [18]. PMI also supported the FDA in issuing two draft guidance documents on next-generation sequencing (NGS) tests [25]. The NGS tests are intended to help patients learn about their genetic and genomic constitution [25,26]. That the FDA recognises great promise in precision medicine, can be demonstrated in the development of new technologies in the field of pharmacogenomics [26]. The FDA has allocated a cloud-based portal called "precisionFDA" to enable the research and development community to engage in exchange to improve bioinformatics related to NGS processing [26].

Moreover, the FDA is establishing recommendations and databases regarding NGS-based tests [26]. The PMDA incorporates pharmacogenetic information as part of the development process [30].

Within the framework of personalised medicine, there is an effort to integrate new technologies into the healthcare system that enable personalised therapy according to the specific characteristics of each individual. The 3DP technology, which allows the production of personalised 3D printed dosage forms, could make such a contribution. Thus, the FDA tried to promote new innovations such as the 3DP technology and to support pharmaceutical companies in their development.

In August 2015, the first 3D printed drug product Spritam®, manufactured by the company Aprecia Pharmaceuticals, was approved by FDA [32]. In 2017, researchers at the University of Nottingham, together with the company GlaxoSmithKline, conducted a study on "3DP of tablets using inkjet with UV photoinitiation" [33]. For this purpose, 3D printed tablets containing the API ropinirole hydrochloride were produced using a combination of inkjet printing and ultraviolet (UV) curing [33]. In addition, the three products T19, T20 and T21 fabricated with the 3DP technology melt extrusion deposition (MED™) by the company Triastek are in clinical development, which began for the first drug in 2021 [34]. The two medical devices OsteoFab Patient-Specific Facial Device and OsteoFab Patient-Specific Cranial Device manufactured by Oxford Performance Materials Inc., the Unite3D™ Bridge Fixation System commercialised by Zimmer Biomet Holdings and 85 other medical devices have been approved by FDA [8].

Therefore, 3DP has gained interest for its ability to personalise medicines not only in the pharmaceutical industry but also in the hospital and pharmacy, as an easy-to-implement technology in the era of the fourth industrial revolution, also referred to as Industry 4.0 [35]. An important element of Industry 4.0 is the intelligent factory (Smart Factory) with a focus on the production of intelligent products, procedures and processes (Smart Production) [36]. Industry 4.0 is characterised by the individualisation or hybridisation of products as well as the integration of customers and business partners into business processes through digitalisation [37]. 3DP represents one of the main manifestations of the fourth industrial revolution and an important element in telemedicine care [38]. The production of 3D printed dosage forms based on an electronic prescription can make its contribution in digital pharmacy [38]. The 3DP technology is one of the innovative methods of manufacturing dosage forms that is reflected in the drive in the healthcare system to improve drug therapy through systems such as electronic prescribing as well as automated dispensing and compounding systems [19]. 3DP, in combination with digitalisation, can contribute to the rapid development of Industry 4.0 [12].

3D printed medicines can address the problems of patients with pharmacogenetic polymorphisms and adjust the dose to the patient's clinical response [39]. Personalised dosing of low-dose, high-potent drug substances and drugs with narrow therapeutic indices is possible [3,39]. Furthermore, 3DP can address issues such as the processing of poorly soluble drug substances, peptides and peptidomimetic drugs [40]. The production of 3D printed dosage forms according to the patient's anatomy for the treatment of chronic diseases can increase the effectiveness of treatment [3].

3DP is a suitable method for producing medicines in the desired doses and dimensions for all age groups from paediatric to geriatric patients, because future medicine should consider the individual patient profile. An ideal personalised dosing method should be simple and inexpensive, but also accurate and appropriate for a large number of patients [41]. Existing strategies are based on the accumulation of small drug carriers or the partitioning of a defined volume from multi-dose container [41]. Solid dosage forms such as tablets would

have to be divided for personalised dosing [42]. For liquid dosage forms, inaccuracies of the API in the medicinal product may result from volumetric dosing, which may include e.g., counting errors for the dosing of drops or reading errors on the dosing devices for the dosing of syrups [43-46]. Hence, dosage forms that enable personalised dosing represent the dosage form of the future [17]. These include multiparticulate dosage forms such as mini-tablets and pellets, for which, however, a suitable dosing device needs to be developed [41]. Orodispersible dosage forms such as orodispersible tablets (ODTs) and orodispersible films (ODFs) offer suitable dosage forms. ODFs combined with printing technologies provide the possibility to produce multilayer coatings, stacked systems and multi-compartment systems [47,48].

Thus, 3D printed dosage forms show great potential for personalised dosing. 3DP can avoid the need to alter the dosage forms [4]. Tablets would not require to be splitted by healthcare professionals or family members to achieve the desired dose, which can lead to under- or overdose and ADRs due to dose variations in each half [42]. Using 3DP, patient-specific liquid capsules with individualised drug content and release profiles can be produced through coordinated 3DP and liquid dispensing [49].

The development of child-appropriate dosage forms is of huge interest and has been steadily promoted since the implementation of the European Pediatric Regulation in 2007 [50]. The goal was to improve the development and availability of medicines for children in order to be able to administer ethically acceptable and approved medicines of high quality [50]. Incentives for the approval of medicines for children were created to reduce the use of unlicensed and off-label medicines. In addition, the introduction of the Paediatric Committee has forced companies to conduct studies in children as part of the marketing authorisation process by preparing the paediatric investigation plan. For paediatric patients, 3D printed medicines offer the possibility to overcome swallow difficulties and to improve the palatibility due to taske masking of bitter tasting drugs for increased patient safety and acceptance [51-53]. Chewable dosage forms for paediatrics could be printed through embedded 3DP [54]. In addition, dose adjustment for the paediatric patient can be performed for example with respect to greater first-pass metabolism due to higher enzyme activity and enzyme immatury to ensure adequate dosing and dose accuracy, reduce side effects and medication errors [35]. In elderly patients, the choice of drugs and their dosing must consider reduced organ functions i.e. visual, swallowing and motoric functions, increased morbidity and immobility as well as the intake of multiple drugs [35]. 3DP, which enables the production of bilayer tablets and polypills, can reduce the dose frequency as well as the pill burden resulting in reduced mortality [15].

1.2.3 High product diversity and flexibility in production

3DP offers the opportunity to produce dosage forms with new product designs to achieve the desired release profiles, which allows increased flexibility and throughput [3]. Therefore, dosage forms with different shapes and geometries can be printed [55]. 3DP of highly porous structures can enable rapid oral disintegration and fast dissolution [3]. A higher dissolution rate can be achieved by 3DP of dosage forms with a large surface area to volume ratio [3]. In addition, the production of amorphous solid dispersions (ASDs) should improve the dissolution rate for poorly soluble drug substances from extrudates by HME [3]. A variety of different products could be manufactured which include single or bilayer tablets with immediate or modified release, coated tablets with pulsatile release as well as osmotic pumps [3]. Drug-device and drug-biologic combination products that offer new therapeutic options can be produced with the help of a 3D printer and the release of the API can be controlled digitally [3]. Moreover, 3D printed micro- and nanocapsules, nanosuspensions as well as implants and patches can be fabricated [39]. The possibilities in product diversity give the chance to produce

a dosage form tailored to the patient's needs, which increases the effectiveness of the therapy and the patient's associated compliance.

The flexibility and adaptability of this technology make it useful in the early stage of product development in the pharmaceutical industry, when formulations are first developed with minimal effort and then examined with regard to their product specifications e.g. release profiles [56]. The production of small batches allows for the FIH studies and pre-clinical studies the product to be manufactured shortly before use, avoiding transport and storage costs and an accelerated stability study [15]. This results in lower demand for starting materials and lower material and production costs [15]. It also makes orphan drugs affordable to produce without shortages, as they are often expensive drugs and potential instability can be avoided by manufacturing them just before use [56]. In addition, the dose for the preclinical and FIH studies can be flexibly adjusted by three different approaches. This includes dose adjustment by varying the infill, by varying the physical dimensions, and by varying the drug load of the feedstock material such as the extrudates for FDM 3DP.

1.2.4 On-demand manufacturing

The manufacturing on demand can be enabled through decentralised production of pharmaceuticals at the point-of-care [15]. This can be beneficial both in the pharmacy and in the hospital when the 3D printed dosage form shall be printed in time and an immediate application for example for preclinical studies is required [15]. For this purpose, it is required that the patient's data can be sent to the healthcare professionals either physically or digitally and communication between different sectors such as software developers, technical engineers, healthcare professionals and regulatory agencies for standardisation are set [57]. 3DP technology would bring about integration into the healthcare network through on-demand manufacturing, accelerating progress in digital healthcare [32]. The pharmacist would be actively involved in the healthcare network by designing the dosage form according to the patient's needs and tailoring the dose on the 3D printer [32]. The aim is to increase the patient's compliance and avoid ADRs. It may be necessary to produce dosage forms with new designs, e.g. for children. The method of production can be advantageous if shortages are present and there is a need for rapid patient care in resource- or time-constrained settings [3,15]. On-demand manufacturing can be of interest in wound treatment, if fabricated tissue-engineered scaffolds or wound-healing gels shall be applied directly onto the patient [3]. It also plays a major role for low-stability drugs that have a short shelf-life and need a rapid administration [3].

1.3 3D printing in medicine

1.3.1 Medical applications

3DP is frequently used in medicine and encompasses the fields of dentistry, tissue and organs, tissue models as replacement, medical devices, anatomic models, and drug formulation [58]. The production of tissues and organs using 3DP is also known as 3D bioprinting [58]. The biomaterials used are called bio-ink if cells are incorporated [59]. Bio-inks are designed to enable 3D bioprinting of cellular products [8]. The bio-ink can consist of hydrogels composed of natural biopolymers or synthetic polymers, cell suspensions and solutions based on extracellular matrix and is designed to mimic the natural microenvironment of the cells [8]. 3DP has to be distinguished from 4D printing, which includes time as an additional parameter besides the three dimensions [58]. 4D printing thus refers to 3D printed objects in which the printing material used mature over time to various stimuli such as heat, pH, light or magnetic

field, making the objects programmable [60]. 4D bioprinting describes the process of maturation of engineered living cells after the printing process for biomedical applications such as tissue engineering and targeted drug delivery [60].

With respect to the fields presented, dentistry represents one of the most progressive fields in the application of 3DP [58]. It enables the production of restorations such as protheses and dentures, surgical guides and dental models based on medical images obtained using magnetic resonance imaging (MRI) or computed tomography (CT) [58].

In regenerative medicine, biocompatible scaffolds with porous microstructures can be produced which contain growth factors and differentiation factors [9]. They are seeded with stem cells for organ regeneration to restore diseased tissue or replace it with artificial tissue [9]. The scaffold used must therefore meet certain requirements. It must be mechanically strong, porous and have a high pore interconnectivity for the diffusion of cellular and waste products [58]. Furthermore, it must be biocompatible and bioactive as well as biodegradable with controlled degradation in order to replace the scaffold with a newly manufactured artificial tissue [58].

3D printed in vitro disease or tissue models have attracted considerable interest both as a replacement for in vivo animal models and clinical trials on humans in drug and cosmetic development as well as toxicology testing [2]. This was triggered in 2013 by the EMA, which banned the use of animals for testing cosmetic products and accelerated the development of engineered tissue 3D printed in vitro skin models [58]. Further developments in the field of microfabrication were 3D models, so-called organ-on-chip (OoC) systems [58,61]. OoC systems purpose to mimic cellular tissue in the microenvironment and to deliver information about disease progression [61].

The AM of medical devices gives the opportunity to produce surgical instruments, implants, prostheses, and orthoses as well as hearing aids [58]. Surgical instruments can be fabricated and used in the clinical setting for a variety of applications, e.g. orthopaedics and surgery [8]. 3D printed implants can be produced either customised according to the patient´s anatomy by using the patient’s medical image or commercially as implant product, whereas 3D printed prostheses can be patient-specific produced based on medical images including for example radiographs, MRI and CT [62]. 3DP is also extensively used in the hearing aid industry for the fabrication of in-the-ear, in-the-canal and completely-in-the-canal hearing aid models and also hearing shells [58].

Anatomic models are utilised for pre-surgical planning and surgical education and the printing technique and material are selected according to the requirements of the model which include properties such as resolution, accuracy, colour and long-term stability [58].

1.3.2 Pharmaceutical applications

The API can be processed with excipients in a formulation to produce a 3D printed drug product in the form of tablets, films, transdermal drug delivery systems (e.g. patches, microneedles), nanocapsules or implants. There is huge interest in dosage forms intended for oral administration due to their ease of application [63]. Thus, tablets are the most common type of 3D printed dosage forms [64]. 3D printed oral dosage forms with immediate or modified release (extended, delayed, pulsatile), single or bilayer tablets and polypills for personalised therapy can be produced [3,56]. The needs of children can also be addressed through paediatric formulations such as 3D printed chewable tablets. In addition, 3DP offers the possibility of manufacturing abuse-deterrent formulations [4].

1.4 3D printing technologies

The five most commonly used 3DP technologies for pharmaceutical applications are depicted in Figure 3 and can be divided according to their principle into laser-based printing technologies, inkjet-based printing technologies and extrusion-based printing technologies [56].

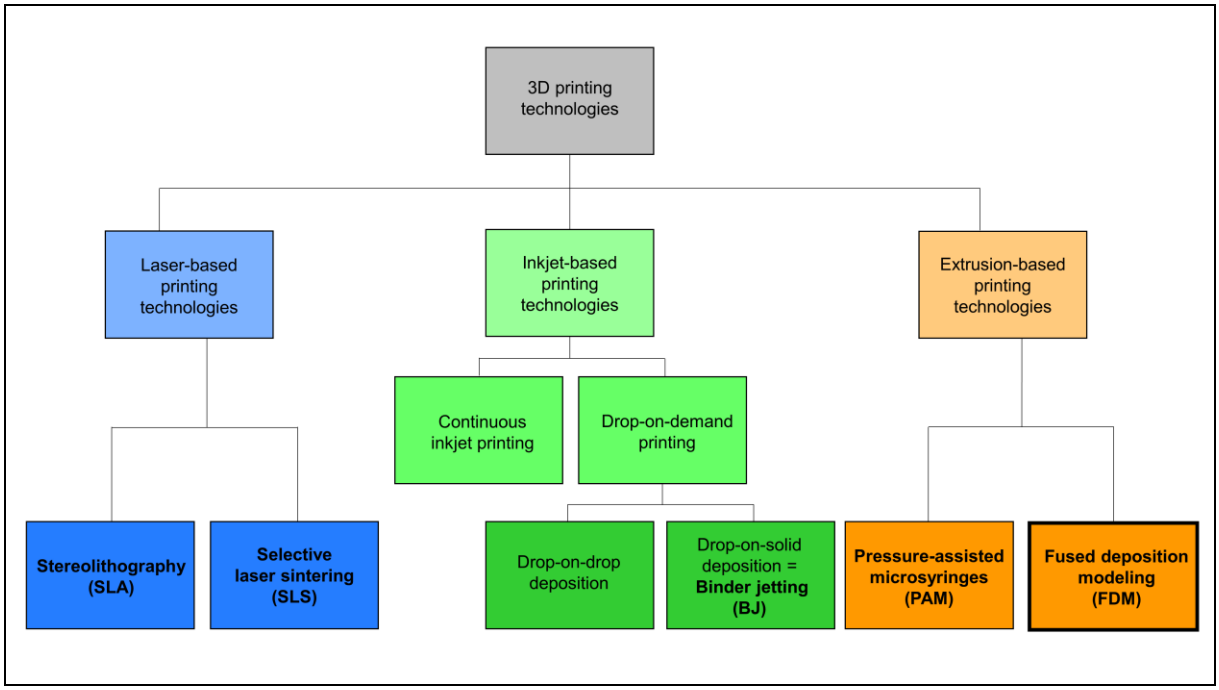

Figure 3. 3D printing technologies for pharmaceutical applications.

Stereolithography (SLA) and selective laser sintering (SLS) belong to the laser-based printing technologies. SLA, also known as photopolymerisation, photo-induced polymerisation or laser-based writing systems, was the first AM technology patented by Charles "Chuck" Hull in 1986 and is used in various fields such as microfluidics, biomedical devices, soft robotics, surgery, tissue engineering, drug delivery and the food industry [65,66]. In medicine, this technology is used to manufacture surgical instruments, hearing aids, knee joints and dental devices [65]. SLA is based on the principle of vat photopolymerisation, a chemical reaction in which UV rays trigger a light-induced polymerisation reaction of a liquid photosensitive thermoset polymer with the aid of a laser, leading to the curing of the vat or resin [11,58]. The light-induced polymerisation reaction can take place according to the mechanism of a radical polymerisation or, as in most cases, according to the mechanism of a cationic polyaddition [5,66]. After the 3DP process, post-processing to fully implement the polymerisation reaction takes place in a UV chamber [11]. The product can be refined by light sanding and a UV-resistant seal [11].

SLS, a powder bed fusion technique, was invented by Carl Deckard and Joe Beaman and patented in 1989 [67-69]. SLS is used in medicine to produce implants, protheses, dental appliances and surgical tools as well as for tissue engineering [58,68]. It is well suited in the pharmaceutical development for tailoring medicine utilising pharmaceutical-grade polymers [69]. Thermoplastic semi-crystalline polymers in the form of powdered materials are used as feedstock material for the printing process [68]. Powdered material is fused layer by layer into a 3D printed object onto a powder bed using a laser beam [70]. The laser beam sinters the

powder and bonds the individual layers [68]. After the printing process the powder bed and the 3D printed object are cooled down before the 3D printed object is removed and can be used [71].

Binder jetting (BJ) represents an inkjet technology which was first developed and patented by Sachs et al. at Massachusetts Institute of Technology in 1993 [72,73]. BJ represents a further development of the 2D inkjet printing technology which can be divided into continuous inkjet printing and drop-on-demand printing [56]. Drop-on-demand printing can be differentiated into drop-on-drop (DoD) and drop-on-solid (DoS) deposition based on the physical principle of droplet generation [74,75]. In DoD deposition, a solid layer based on the binder is formed by the mutual deposition of the droplets [76]. In DoS deposition, droplets of a low melting point binder are deposited on a powder bed containing particles with a high melting point [76]. After Sachs et al. patented the BJ technology, medical and pharmaceutical applications for BJ were licensed through Therics Inc., tradenamed under the TheriForm™ process in 2006 [77]. In medicine, this technology has gained importance in bone tissue engineering and plastic surgery [72]. Furthermore, it has also been applied in engineering and cosmetic industries [72]. In principle, BJ is based on the inkjet printing technology, in which liquid binder is applied to a powder bed to bond the particles [72,75]. For the binder deposition two different kinds of print heads can be used which are piezoelectric and thermal print heads [40].

Extrusion-based printing technologies are pressure-assisted microsyringes (PAM), also referred to semi-solid extrusion, and fused deposition modeling (FDM). The PAM technique was first introduced by Landers and Mülhaupt in 2000 [78,79]. The suitability of the PAM technology for personalised manufacturing was initially demonstrated by Khaled et al. in 2014 and 2015, who produced bilayer tablets with a controlled drug release as well as a polypill containing five different drugs with specific release profiles [80-82]. In addition, both Khaled et al. (2018) as well as El Aita et al. (2019) demonstrated the feasibility of PAM printing for the fabrication of high-dose, immediate release tablets [83,84]. Meanwhile, the PAM process has pharmaceutical applications in the production of chewable dosage forms for paediatric and geriatric patients and in the tissue engineering for the manufacturing of tissue engineered scaffolds [54,85-87]. With the help of PAM technology both single- and bilayer tablets with different dissolution profiles as well as gastro-retentive drug delivery systems and floating dosage forms can be produced [87-89]. The production of ODFs, solid self-emulsifying formulations, rectal suppositories, parenteral formulations including implants, scaffolds and patches and cutaneous formulations become possible [87,88]. In addition to pharmaceutical applications, this technology is most commonly used for bioprinting in medicine [90]. Due to the low printing temperature and the semi-solid starting material, cell-loaded hydrogels can be extruded to produce bones, joints and skeletal muscles as tissue substitutes [87,91]. Medical devices including drug-eluting and bio-absorbable scaffolds, called ‘biopierces’, as well as drug-medical device combination products can be manufactured [87]. The technology also has applications in dentistry from surgical models to dental prostheses [92]. In addition, the PAM technology is suitable in the food industry for the production of candies and for 3DP in electronics and bioelectronics [87,92]. In the PAM process, semi-solid formulations such as gels or pastes are extruded through a syringe in a layer by layer manner onto a print bed [87,88]. The extrusion can be carried out by pneumatic, mechanical and solenoid piston [87,92]. After the 3DP process, post-processing is required for shape fidelity due to the use of heat or solvents which can include cooling, drying or ionic cross-linking [88]. PAM technology offers a huge opportunity for processing cells through 3D printing at room temperature [88].

FDM is the most popular 3D printing technology for pharmaceutical applications [93], which requires extrudates produced by HME as starting material for the FDM 3DP.

HME has its origins in the 1930s in the plastic, rubber and food industries and was first used in the pharmaceutical industry in the early 1970s [94]. The technology shall contribute to the production of APIs as part of formulation and product development, as well as to the improvement of already approved medicinal products on the market [94]. HME is a widely used, versatile technology in the pharmaceutical industry and can be used for the continuous manufacturing production enabling improved product quality and reproducibility compared to batch manufacturing [95-97]. HME finds it application in the solubility and bioavailability enhancement of poorly soluble drugs by the production of ASDs, the taste masking of bitter tasting drugs as well as the manufacture of a variety of different dosage forms including pellets, granules, films, implants, ophthalmic and topical delivery systems [97-100]. These can be produced from obtained extrudates in the form of strands, films, sheets and granules through further processing steps and allows the production of extended release delivery systems, targeted and shaped drug delivery systems as well as abuse deterrence systems [94,101]. New applications related to HME represent co-extrusion and foam extrusion, nanotechnology, co-crystallisation and 3DP [95,101,102]. Additionally, there has been growing interest in processing biological agents such as proteins and peptides alongside small molecule drugs [95]. The fact that the HME technology is suitable for industrial application is shown by the existing approvals of drug products [103].

FDM, also known as fused filament fabrication (FFF), is a widely used, versatile 3DP technique especially in the fields of engineering and medicine, but also in many other fields (Figure 4) [18,104,105].

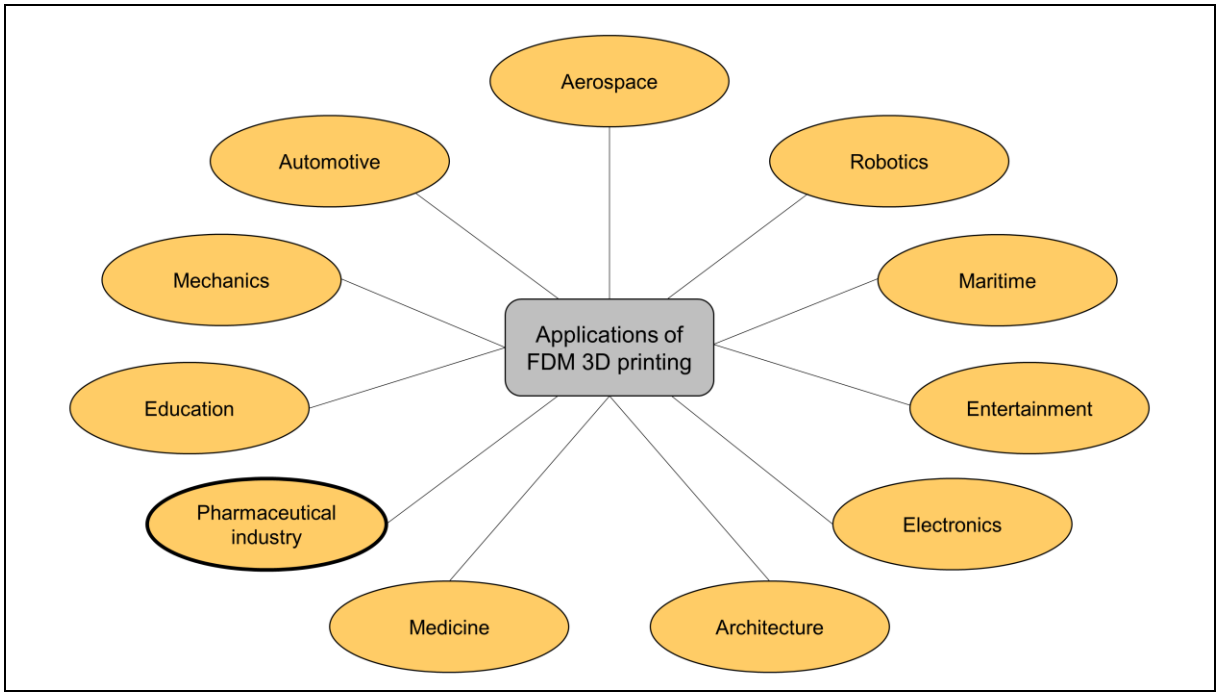

Figure 4. Applications of FDM 3D printing (content from [104]).

In the pharmaceutical industry, FDM is suitable for the fabrication of single-unit dosage forms and follows 3Ds design, develop and dispense [15]. It was first developed by Scott Crump of the Stratasys company in 1988 and commercialised in 1992 [57,104]. While the origins of this technology lay in prototyping in engineering, developments have progressed to consumer products and industrial processing [104]. In pharmaceutical development, coupling HME with

FDM shall enable the continuous production of 3D printed dosage forms with low-dose drugs, but also with enhanced drug load for personalised medicine and telemedicine [97,106]. Another growing research area in the FDM technology is the nanotechnology including polymer-based biomaterials, nanoparticle drug delivery, polymer blends, nanofibers and nanocomposites [107].

1.5 Regulatory considerations

1.5.1 Medical devices

3DP can be considered a suitable technology for the production of patient-specific medical devices which is reflected in more than 85 3D printed medical devices already approved by the FDA [58]. Medical devices are products with a medical purpose intended by the manufacturer for human use. The intended main effect of medical devices is determined physically compared to medicinal products, which have a pharmacological, immunological, and metabolic effect [108].

The first implementations of 3DP took place by medical device manufacturers in 2010, which led to an exponential increase in approved 3D printed medical devices [109]. This allowed experience to be gained which should ensure further progress in the use of 3D printed medical devices. In 2014, the FDA organised a public workshop that addressed the technical challenges and development of assessment standards for AM products [110,111]. Five technical topics were discussed, which included materials; validation of design, printing and post-printing; printing characteristics and parameters; physical and mechanical evaluation of end products; and biological aspects of end products, including cleaning, sterility, and biocompatibility [111]. In 2016, the FDA worked on a draft guidance and could issued the guidance “Technical Considerations for Additive Manufactured Medical Devices“ in 2017 to give considerations regarding the design and manufacturing, device testing as well as labeling of medical devices [112]. Regarding medical device design and manufacturing, the guidance provides information on overall device design, patient-matched device design, software workflow, material controls, post-processing, process validation and acceptance activities, and quality data [112]. In the context of device testing, information is presented on device description, mechanical testing, dimensional measurements, material characterisation, removing manufacturing material residues and sterilisation, and biocompatibility [112]. Device testing must be carried out on the finished product and must demonstrate that the product can be used by the user for its intended purpose [113]. While the FDA has published its considerations on the manufacture of medical devices using AM technology in the aforementioned guidance document, no guidance document has yet been made available to the public by the EMA [113]. The PMDA has issued a technical guidance document for 3D printed medical devices such as orthopaedic surgical implants, but it does not contain information about the regulations of these medical devices [113].

In the U.S., medical devices are divided into three classes according to their intended purpose, based on the risk to health and the degree of control to ensure safety and effectiveness [114,115]. Class I medical devices are low risk and therefore subject to general controls [115]. Therefore, some medical devices can be exempted from pre-market requirements and only need to be registered and listed [109,113,115]. Class II medical devices have moderate risk and require premarket notification, also known as 510(k) process for the approval of medical devices [109,116]. 510(k) refers to the Section in the Federal Food, Drug, and Cosmetic Act (FD&C Act) codified in Chapter 9 of Title 21 of the United States Code [117]. These medical devices must prove substantial equivalence with a predicate [109,116,117]. Besides the general controls, special controls are needed [109]. Class III medical devices demonstrate high

risk and require premarket approval next to general controls [116]. For the approval of medical devices on the U.S. market, the manufacturer must fulfil the requirements of the Code of Federal Regulations [105,109]. Within the framework of an investigational device exemption, clinical studies must be conducted and data collected [109]. Thus, premarket notifications (510(k)), premarket approvals and investigational device exemptions represent the majority of submissions to the Center for Devices and Radiological Health for medical devices [109]. In some cases, it is required to waive medical device approval. This is the case in the presence of a life-threatening condition or in an emergency in the absence of standard treatment [32]. These medical devices receive an exemption and are approved through emergency use [32]. Most 3D printed products have been able to provide sufficient evidence to be cleared through the 510(k) process by demonstrating equivalence to a marketed device [111].

1.5.2 Medicinal products

So far, only one drug, named Spritam® by Aprecia Pharmaceuticals, has been approved by the FDA in 2015 [72,111,118]. Furthermore, the FDA has granted the Chinese company Triastek permission to conduct clinical trials in 2021 and 2022 for three drugs based on Investigational New Drug (IND) applications [34]. No 3D printed drug has yet been approved by the EMA. It is expected that this will be approved as part of a hybrid application [118]. Thereby, a hybrid medicine is defined as a medicine that is similar to an authorised medicine which contains the same active substance but may have differences in dose strength, indication or pharmaceutical form [119].

Medicinal products that contain an active substance and have a pharmacological, immunological, and metabolic effect are subject to higher requirements than medical devices that do not contain an active substance and exert their effect physically [120]. In principle, 3D printed medicinal products can be authorised similarly to conventional medicinal products. Medicines can be approved in the U.S. through one of three approval pathways which are defined in the Sections of the FD&C Act [118,121,122]. New drugs can be approved through the 505b(1) and 505b(2) approval pathways, while generic drugs are approved through the 505(j) approval pathway [122]. The 505b(1) approval pathway represents the traditional approval pathway for new drug applications (NDAs) [122]. This pathway is used to approve products with new APIs that have not yet been approved [122]. Clinical and non-clinical studies must be conducted to provide evidence of the safety and efficacy of the new drug molecule for the therapeutic indication [122]. The 505(b)(2) approval pathway involves the approval of new drug products with already approved APIs [122]. In this application, the applicant refers to one or more studies that "were not conducted by or for the applicant and for which the applicant has not obtained a right or reference or use from the person by or for whom the studies were conducted." [121] For generic drugs, approval is through the 505(j) approval pathway, and an abbreviated new drug application (ANDA) for approval may be submitted [122]. The 505(j) approval pathway does not include clinical or preclinical data to demonstrate safety and efficacy, but requires comparison to the listed reference drug through bioavailability/bioequivalence studies [122]. Products that have been authorised under the ANDA are judged to be equivalent and can be interchanged under the same conditions of use [77]. In addition to the three approval pathways mentioned above, biologics are approved through the biologics license application (BLA) [118].

In order to facilitate and encourage the approval of drug products with new technologies, the FDA published the “Advancement of Emerging Technology Applications for Pharmaceutical Innovation and Modernization” guidance in September 2017 [123]. This was intended to provide the pharmaceutical industry with the opportunity to take part in the Emerging Technology Program [123]. The program was intended to enable collaboration between the

“Emerging Technology Team”, a special group of the FDA, and pharmaceutical companies aiming at the approval of products with new technologies [124,125]. The program can be used by companies engaged in the regulatory submission of an IND, NDA, ANDA, BLA or the drug master file (DMF) [124]. These technologies are reviewed by the Center for Drug Evaluation and Research [124]. In order to enter the program, the applicant must demonstrate that the proposed technology falls within the scope of the program and can enhance product quality. [124]. Thus, the benefits of this new technology program offer the possibility to get early in contact and exchange with the FDA during product development [124]. Questions concerning the product technology, manufacturing process and control strategy can be clarified [124].

Aprecia Pharmaceuticals took the opportunity prior to Spritam®'s approval to engage with the FDA during "lunch-and-learns" to showcase 3DP technology and its application in the pharmaceutical industry [126]. In addition, Aprecia Pharmaceuticals held two formal meetings with the FDA and organised several visits with the FDA to show the manufacturing facility, the equipment as well as the manufacturing process [126,127]. Furthermore, Aprecia Pharmaceuticals was also in exchange with the U.S. Pharmacopoeia to obtain a dosage form designation that could not be replaced by a generic drug to ensure reimbursement by health insurance companies and dispensing in pharmacies [126]. Spritam® was approved through the 505(b)(2) approval pathway, which allowed reference to the safety and efficacy studies of the reference listed drug Keppra® film-coated tablets by UCB, Inc. [126]. Spritam® is a 3D printed drug product manufactured by powder bed 3D inkjet printing based on ZipDose® technology, a drug formulation platform, which enables the production of ODTs with a high drug load of 1,000 mg of the API levetiracetam [74,77]. The characteristic features of dosage forms manufactured using this technology is rapid disintegration, which is due to the highly porous structure and the use of freely soluble mannitol as main excipient as well as the possibility of taste masking [128,129]. The approval of Spritam® has shown that the commercial production of a 3D printed drug product became possible in compliance with current good manufacturing practices (cGMP) regulations [77].

The company Triastek received FDA approval as an IND via 505(b)(2) application in 2021 for its proprietary 3D printed drug T19 for the treatment of rheumatoid arthritis (RA), which was manufactured using MED™ technology [55,129]. MED™ technology was included in the FDA's Emerging Technology Program in 2020, because this technology enables the continuous production of 3D printed modified release oral dosage forms with process analytical technology (PAT) and feedback controls [129,130]. The production of the 3D printed tablets using MED™ technology, also known as direct powder extrusion (DPE), is achieved by directly processing the powder mixture consisting of APIs and excipients after melting from the extruder nozzle, from which continuous extrusion takes place in layers [129-131]. Thus, the preceding production of filaments, which are required for FDM 3DP, can be dispensed with [130]. In order to save time and costs, Triastek has also developed the 3DP Formulation by Design concept for digital formulation development [129]. Through the arrangement of several nozzles, complex structures as well as several APIs can be processed in one dosage form [130]. Tablets can be manufactured in different shapes and geometries to achieve the desired release profile with the resulting pharmacokinetics [55,129,130]. In 2022, Triastek's second 3D printed drug T20 for the therapy of cardiovascular disease and clotting disorders was approved by the FDA as an IND via the 505(b)(2) approval [131]. This was followed by the IND application for Triastek's third 3D printed medicine, T21, targeting ulcerative colitis by the FDA [34]. In addition, other pharmaceutical companies are cooperating with polymer manufacturers to develop 3D printed dosage forms for personalised therapy [129]. Medicinal products produced with the two processes HME and FDM 3D printing are not yet available on the market.

In addition, in the context of personalised medicine, the manufacturing of dosage forms in facilities such as pharmacies and hospitals is of interest, which are regulated under Section 503A of the FD&C Act or “Section 353a – Pharmacy compounding“ and Section 503B of the FD&C Act or “Section 353b – Outsourcing facilities“ of the United States Code [72]. However, 3DP is not yet mentioned in these Sections [72].

1.6 Regulatory challenges

As previously described, numerous 3D printed medical devices and only one 3D printed drug have already been approved by the FDA in the context of industrial manufacturing. Nevertheless, it is obvious that 3DP technology, despite its advantages in personalised manufacturing, needs further regulation by the authorities, especially in the pharmaceutical sector [9,132]. Superiority of 3DP technology in terms of costs and benefits for the pharmaceutical industry compared to conventional manufacturing processes still needs to be demonstrated [133]. 3DP is a time-consuming process compared to direct compression [133]. Due to the various 3DP technologies and associated processes that can be used to manufacture medicinal products, it has been difficult to establish uniform requirements for the manufacturing processes and products [74]. A uniform assessment of the quality of the 3D printed product must be carried out according to predefined specifications [134]. In addition, the critical quality attributes (CQAs) must be examined as with conventional dosage forms and tests must be carried out in accordance with the pharmacopoeias [3,9,74,77,97,133]. If necessary, further tests specific to the 3D printed product must be established [9,19]. Since the properties of the starting materials used and the product depend strongly on the respective printing process, separate guidelines must be created for each printing process, which can be made available to the pharmaceutical companies. In particular, the stability of the starting materials used, including the API and excipients, under the influence of critical process parameters, such as temperature, during the 3DP process must be investigated in order to avoid thermal degradation. One of the biggest challenges is the processing of thermo-sensitive drug substances during the FDM 3DP process due to the high temperature required [18,135]. Since the extrudates produced by HME are used as the starting material for FDM 3DP, the API is exposed to a double temperature load [4,64]. Therefore, sufficient stability of the API in the drug product despite double heat exposure and control of impurities must be ensured.

This is of huge interest as 3DP is also expected to enable on-demand production of personalised dosage forms in hospitals and pharmacies in the future and product quality, including control of impurities, is required to ensure patient safety [72,136]. For the establishment of 3DP technology in hospitals and pharmacies, regulations must define both the prescription of a 3D printed medicinal product by the physician and the production of a formulation with the 3D printer including release in the hospital or pharmacy as well as dispensing to the patient. Therefore, regulations for the quality control of the starting materials as well as the drug product must be defined, which ensures the quality during the entire process and enables the delivery of the final product to the patient. Thus, the quality control is one of the main challenges in hospitals and pharmacies [133]. Further regulations are required that 3D printed medicinal products with prescription drug substances may only be dispensed on the basis of a physician's prescription. Due to the objective of immediate production and administration of 3D printed medicinal products, the collection of long-term stability data might not be mandatory [118]. Rather, the storage stability of starting materials such as extrudates for FDM 3DP must be specified. It must be demonstrated that the storage stability of the extrudates neither influences the API content in the printed dosage form nor the quality and does not lead to quality impairments, e.g. due to deformation or shrinkage of the printed

dosage form [135]. Furthermore, the recycling of intermediate products such as extrudates as well as surplus product must be clarified in terms of patient safety [3]. Furthermore, the liability for the 3D printed product must be regulated [32]. The manufacturer of the 3D printer, the manufacturer of intermediate products, such as the filament manufacturer in FDM printing, as well as the pharmacist can be considered as liable persons.

In the context of Industry 4.0, big data and advancing digitalisation, regulations must ensure the protection of patient-related data and the encrypted transmission of stored medical patient information [17,48]. Validated 3D software design and simulation tools must be developed [75]. In addition, the reimbursement of the 3D printed medicine must be clarified with the health insurance companies in the case of a medical prescription. Thus, it is evident that the production of 3D printed individual dosage forms in the context of personalised medicine will require integration into the healthcare system and further regulation by the authorities [32]. The introduction of 3DP in hospitals and pharmacies will also lead to changes in the supply chain [17].

1.7 Thermo-sensitive drug substances

1.7.1 General

The production of personalised dosage forms with biologically active molecules has gained increased interest, but processing via FDM 3D printing can be challenging due to the thermolability of the thermo-sensitive drug substances [64].

Although there is no uniform definition for thermo-sensitive drugs, the World Health Organisation (WHO) defines a time- and temperature-sensitive pharmaceutical product as "Any pharmaceutical good or product which, when not stored or transported within predefined environmental conditions and/or within predefined time limits, is degraded to the extent that it no longer performs as originally intended", but usually refers to drugs that must be stored in a refrigerator in this definition [137]. Nevertheless, according to Pazo-Oubiña et al. (2021) this definition can also be applied to drugs that degrade during 3DP due to high temperatures or UV light or beams [138].

Due to the challenge of heat exposure twice during HME and FDM, the behaviour of two thermo-sensitive drug substances should be investigated during both processes. Therefore, drug substances that undergo degradation reactions under thermal stress should be considered. For this reason, the two APIs EM and ESC-OX were chosen. Factors affecting the stability of drug substances may generally include chemical, physical, and, in rarer cases, microbiological changes, as the latter generally affect the drug product. When considering the stability of EM and ESC-OX during HME and FDM 3DP, the focus should be placed on the chemical and physical changes in the drug molecules. Chemical changes may include hydrolysis, oxidation, reduction, steric rearrangement, decarboxylation, and polymerisation, whereas physical changes refer to changes in solid state. An important parameter that can affect chemical and physical stability is the solubility of the drug substance, which in turn can influence the absorption of the drug. Therefore, drug substances are classified into one of the four categories based on their solubility and permeability according to the biopharmaceutics classification system (BCS), which is illustrated in Figure 5 and shows the assignment of the two APIs EM and ESC-OX to their BCS class.

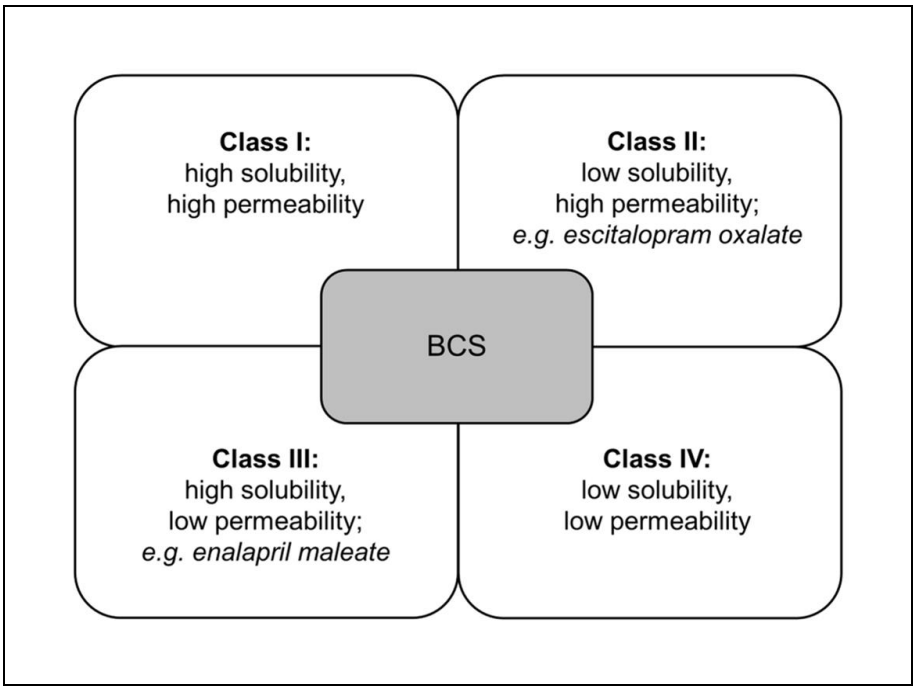

Figure 5. Biopharmaceutics classification system and the assignment for the APIs used in the thesis, enalapril maleate and escitalopram oxalate.

According to the International Council for Harmonisation of Technical Requirements for Pharmaceuticals for Human Use (ICH) M9 guideline, a drug substance is classified as highly soluble if the highest single therapeutic dose is completely soluble in 250 ml or less of an aqueous medium over a pH range of 1.2 – 6.8 at 37 ± 1 °C [139]. The lowest measured solubility in the pH range of 1.2 – 6.8 is used for the classification of the drug substance [139]. A drug substance is classified as having good permeability if the absolute bioavailability is ≥ 85 %. For the assessment of permeability, data on the extent of absorption from pharmacokinetic studies in humans (e.g. absolute bioavailability or mass balance) should preferably be used [139]. In addition, an assessment of permeability based on validated and standardised in vitro methods using Caco-2 cells is possible [139]. In vivo human data from published literature may also be acceptable under certain circumstances [139].

1.7.2 Enalapril maleate

Enalapril maleate (EM) was selected as a model drug substance because it is known for its pronounced thermolability due to its peptidomimetic structure. The API is an angiotensin-converting enzyme inhibitor and has a similar structure to the tripeptide phenylalanine-alanine-proline (Phe-Ala-Pro) (Figure 6) [140].

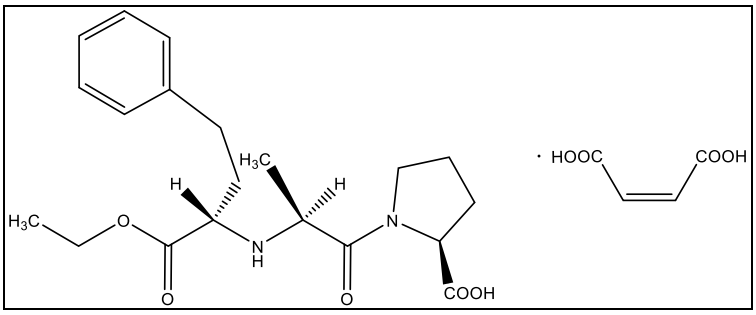

Figure 6. Structural formula of enalapril maleate.

EM is one of the APIs on the WHO list of essential medicines [141]. It is of great interest for the production of oral dosage forms in personalised therapy, especially in paediatrics. This has already been demonstrated with the alternative concept of dose individualisation in the form of low-dose EM orodispersible mini-tablets (ODMTs) which were developed as part of the LENA (labelling enalapril from neonates to adolescents) project [142]. EM is used in particular for heart failure and hypertension [143]. It is administered orally in the form of tablets and the dosage range for adults is between 2.5 mg and 40 mg [143]. With high blood pressure and heart failure therapy, a slow titration of the dose is necessary [143]. For children, the dose should be based on the body weight [143]. Enalapril (ENP) is a prodrug of the active metabolite enalaprilat, which is formed in the liver by cleavage of the ester bond with the help of the hepatic hydrolase carboxylesterase, CES1 [144,145]. The drug belongs to the BCS class III drug substances and therefore has a good solubility but poor permeability (Figure 5) [146]. Both ENP and enalaprilat have a dipeptide (Ala-Pro) structure and bind to intestinal carrier-mediated transporters, but only ENP is selectively transported across the intestinal membrane [147]. This can be explained by the fact that the proline carboxylate moiety is responsible for the recognition of intestinal peptide transporters and the angiotensin-converting enzyme, while the presence of a second carboxylate moiety in enalaprilat has an inhibitory effect on the intestinal transport [147]. Therefore, the presence of the ester group in ENP may increase the affinity for the intestinal peptide transporter and thus increase intestinal absorption [147].

As far as the chemical properties are concerned, ENP is a weak acid with acid constants (pKa values) of 2.97 for the carboxyl group of the substituted proline as well as 5.35 for the protonated secondary aliphatic amine and has a decadic logarithm of the octanol-water coefficient (logP) value of 2.45 [144,148].

With regard to the stability in solution, two main degradation products of ENP are formed depending on pH values. While the cyclisation product enalapril diketopiperazine (DKP), described in the European Pharmacopoeia (Ph. Eur.) as Impurity D (Imp-D), is formed at pH < 2, the hydrolysis product enalaprilat described in the Ph. Eur. as Impurity C (Imp-C), is found at pH > 5 [143,144,146,149]. Regarding the thermal stability, the melting point of EM is given in the literature according to Lin et al. (2002) as an endothermic peak with a maximum at 151 °C [150]. The endothermic event already starts at 147 °C at a heating rate of 3 °C/min and indicates the melting of pure EM [150]. Another partially overlapping endothermic peak is

observed at 163 °C which is related to the thermal decomposition [150]. According to Gómez Pineda et al. (2005), at a heating rate of 10 °C/min and a sample mass of 6.1 mg, an intense and sharp peak was observed at 150 °C and a larger and weaker peak at 170 °C [151]. In agreement with Lin et al. (2002), the first peak is associated with the melting and the second peak with the degradation [150].

1.7.3 Escitalopram oxalate

Escitalopram oxalate (ESC-OX) was selected as the second model drug substance. It is the S-enantiomer of racemic (R,S) citalopram and belongs as an antidepressant to the class of selective serotonin (5-HT) reuptake inhibitor (SSRI) (Figure 7) [152-154]. The thermal stability of this enantiomer is of particular interest, because only the S-enantiomer is therapeutically effective [154]. In addition, the S-enantiomer shows higher efficacy with the same tolerability compared to the racemate [154-157].

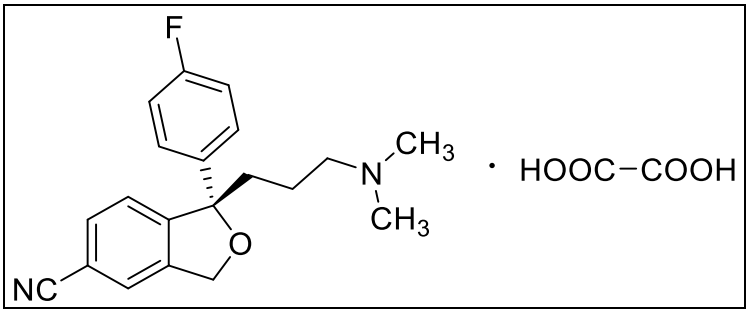

Figure 7. Structural formula of escitalopram oxalate.

It is used for the first-line treatment of major depressive disorder and several anxiety disorders due to its good tolerability resulting in high selectivity and lower interaction potential compared to other antidepressants [158-160]. It also plays a major role in personalised medicine, especially for the geriatric population. It is listed in the WHO Model List of Essential Medicines and commercially available products are Cipralex® and Lexapro® from Lundbeck [141,161]. In the U.S., ESC-OX is one of the most frequently prescribed drug substances [162]. It is available in the form of film-coated tablets and oral solutions and is administered orally [162]. The dosage range is between 5 mg and 20 mg with the dose of ESC-OX in the dosage forms corresponding to the free base [161,162]. A slow titration of the dose is necessary [162]. The antidepressant effect occurs after two to four weeks, while the maximum effect depending on the indication, is reached after several months [162]. Furthermore, a sudden discontinuation of the therapy should be avoided [162].

ESC-OX is a BCS class II drug substance with poor solubility and good permeability compared to EM *(*Figure 5) [161].

Escitalopram (ESC) is a weak base with a pKa value of 9.54 for the tertiary amine and a logP value of 3.63 [162]. A pronounced instability in basic solution has been described for ESC-OX [163,164]. The melting point of ESC-OX has been reported by Pinto et al. (2018) to have an endothermic peak at 153 °C, whereas racemic citalopram oxalate has a melting point of about 165 °C according to De Diego et al. (2011) [154,165].

1.8 Process and quality considerations for fused deposition modeling 3D printing

1.8.1 General

In order to investigate the influence of process parameters, especially temperature, on the degradation of thermo-sensitive drug substances and thus the quality of the finished 3D printed dosage form, a deeper understanding of the two heat-intensive processes HME and FDM is required. Strategies to prevent degradation of the APIs should be devised as part of the process and formulation development.

FDM is a 3D printing technology that is based on extrusion and requires melting, in contrast to the PAM technology (Figure 8) [166].

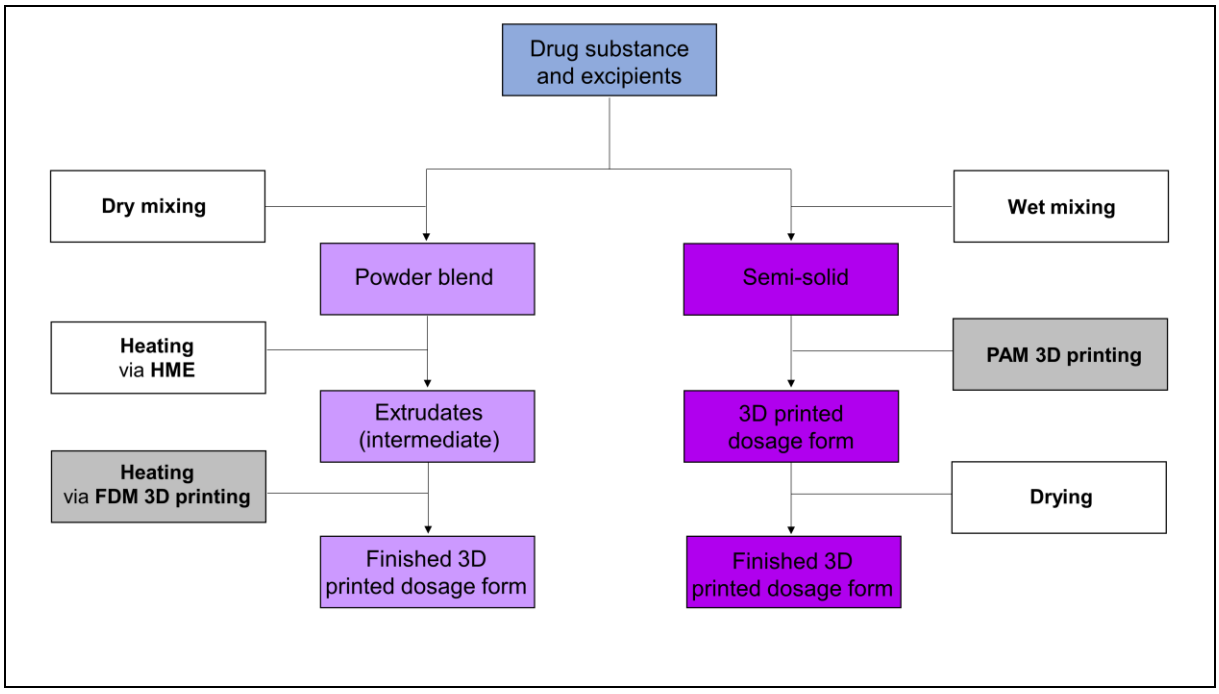

Figure 8. Overview of the extrusion-based printing technologies (modified from [135]).

In PAM technology, the drug substance and excipients are mixed wet and processed into a semi-solid formulation that can be used to produce a 3D printed dosage form. However, this must be dried afterwards to obtain the finished 3D printed dosage form.

For FDM 3DP, the powder mixture is first mixed dry and processed into extrudates or filaments. Extrudates, which are initially produced by HME, serve as starting material for FDM 3DP to receive the finished 3D printed dosage form.

1.8.2 Hot-melt extrusion process

In general, extrusion is a process in which the starting material is forced through a die resulting in a product with a uniform shape and density [98,167]. The process offers the possibility to prepare molten systems through the influence of heat as well as semi-solid viscous systems [98]. In hot-melt extrusion (HME), the application of heat reduces the viscosity of the system and conveys the melt through the die [98]. The equipment for the HME process consists of the

hot-melt extruder, downstream processing equipment and equipment for in-process controls [98]. The hot-melt extruder consists of a feeding system, a barrel, screws, a screw-driving unit and a die [98]. A characteristic criterion of an extruder is the length-to-diameter (L/D) ratio of the screw, which is in the range of 20 to 40:1 or higher [94,168]. Depending on the number of screws used, pharmaceutical extruders can be divided into single-screw, twin-screw and multi-screw extruders [94]. The screws of the twin-screw extruders (TSE) can be co-rotating or counter-rotating and can be further divided in fully intermeshing or non-intermeshing [94,168]. Fully intermeshing twin-screw extruders are proving more popular as they are self-cleaning [94]. This results in better mixing as well as avoidance of local overheating of the starting materials used [94]. Accordingly, the non-intermeshing TSE have a lower mixing performance due to weaker interaction of the screws and are less self-cleaning [94].

Single-screw extruder (SSE) are widely used due to their mechanical simplicity and are composed of one single continuously rotating screw in the barrel, resulting in good product quality and consistent throughput [94,168-170]. Although SSE require little maintenance and are inexpensive, they also have disadvantages [169]. Due to the mode of operation of SSEs, an increase in screw speed leads to increased friction and associated temperature rise, which can cause degradation of thermo-sensitive drug substances [94]. In addition, despite the good product quality, SSE provide high pressures which can cause agglomeration and insufficient mixing [94].

TSE have superior features to SSE in industrial applications, which are shown in Figure 9 [94,98].

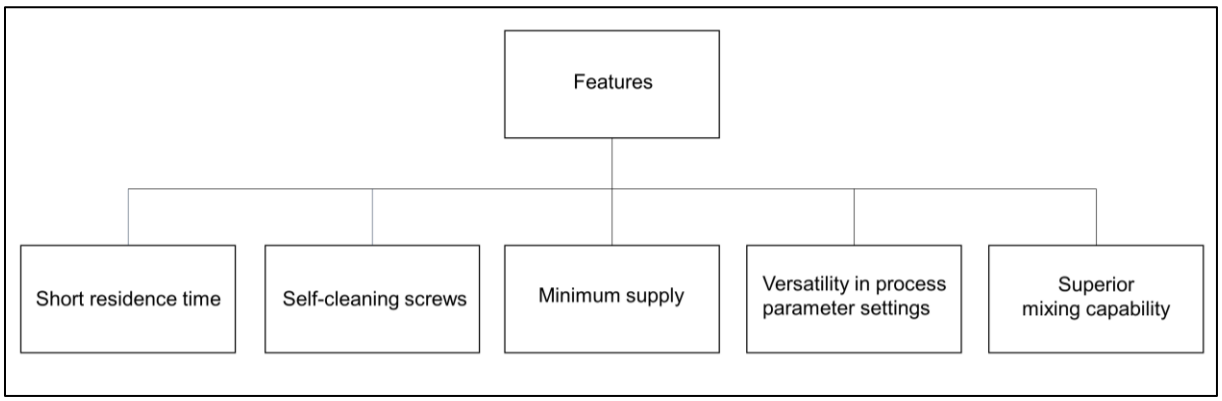

Figure 9. Features of the twin-screw extruder (content from [94,98]).

These properties are coupled with a number of advantages that allow continuous material feeding, higher mixing capacity through dispersive and distributive mixing, lower overheating tendency, higher productivity through shorter residence times as well as higher flexibility and better process controllability [94,98]. In the TSE, heating is controlled externally and independent of the screw speed as the intermeshing screws advance the material from one screw to the other [94]. For the processing of thermo-sensitive drugs substances, it is advantageous that both the screw configuration and the screw speed can be varied. In addition, the use of intermeshing co-rotating screws enables a more homogeneous melt containing the APIs due to the higher mixing capacity and thus a more uniform product temperature, which reduces the risk of local overheating [94]. Furthermore, the screws are most frequently constructed of surface-coated stainless steel to avoid friction and the

occurrence of chemical reactions, which is beneficially for oxidation- and hydrolysis-sensitive drug substances [94].

The HME process for the TSE consists of the following unit operations which are shown in Figure 10 [171].

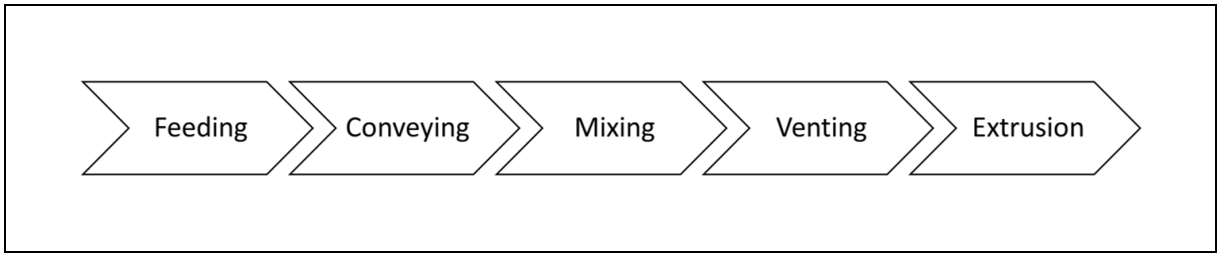

Figure 10. Unit operations of the twin-screw extrusion process (content from [171]).

In the feeding section, the powder mixture is fed with the help of a volumetric or gravimetric feeder [171]. The powder mixture is fed into the barrel at a certain feed rate and conveyed towards the die by the co-rotating screws [171]. In the conveying section, the powder mixture is further conveyed by the use of conveying screw elements and melted due to the energy input and the applied shear forces [171]. In the mixing zone, the powder mixture is mixed depending on the selected design and arrangement of the mixing elements at specific offset angles to produce a well-dispersed and homogeneously distributed dispersion [171]. The stability of the prepared dispersion depends on the physical form in which the drug is embedded in the polymer. The venting zone serves to remove the air present in the powder and venting can generally be accomplished by venting inserts or by applying a vacuum [171]. In the extrusion section, pressure is built up in front of the die to achieve a high degree of filling, which is required for the constant melt flow through the die and shaping of the product [171].

For drug product development the powder mixture for HME can consist of the API, polymers and other excipients. Other excipients may include plasticisers, lubricants, disintegrants, and glidants [94]. During the HME process, the API should exhibit stability in the formulation, in order to have sufficient bioavailability and can unfold its effect [94,95]. In order to be able to assess this, the physical and also the thermal stability of the API must be considered [94,172]. The physical state of the API can influence the stability and dissolution rate of the formulation. Most APIs are initially present as starting materials in a crystalline state which is the preferred form in terms of chemical and physical stability [94]. Nevertheless, it may be advantageous to embed the drug amorphously in a polymer and thus produce ASDs to improve solubility and bioavailability of the drug and to enhance dissolution [173]. This concerns poorly soluble drugs according to BCS classes II and IV [174]. However, since ASDs can also be thermodynamically unstable and tend to recrystallise, strategies must be devised to stabilise the ASDs and thus the shelf-life of a product [97,173,175]. The melting point of the API specifies the processable temperature range in which the drug can be processed [95]. The thermal stability results from the degradation temperature of the API [97]. The degradation of the API can also take place below the degradation temperature, as the set process parameters can also have an influence on the degradation [176]. Besides the API, the polymers are also selected according to their physicochemical properties. The chemical structure and the molecular weight of the polymers can influence the thermal properties as well as the melt behaviour [172,177]. For the processability of the polymers their glass transition temperature or melting temperature should be taken into account [176]. The polymers should be processed at a temperature of 20 °C to 40 °C above their glass transition temperature [97,176]. Furthermore, the melt viscosity of the

polymers has an influence on the torque of the extruder and depends on both the temperature and the shear applied through the design of the screws and the screw speed [176]. For an optimal extrusion process the complex viscosity should be in the range from 800 to 10,000 Pa*s [177,178]. Additionally, an interaction between the polymer and the API can also lead to degradation products and should be excluded [95]. Other additives mentioned besides the polymer matrix are equally selected with regard to their physical and thermal stability as well as compatibility. Plasticisers, which lower the glass transition temperature of the formulation, can be added to reduce the processing temperature and melt viscosity [172,179]. Disintegrants serve to accelerate the disintegration, while glidants improve the feedability of the formulation [172].

Parameters, which can impact the quality and stability of the product manufactured via HME can be categorised as depicted in Figure 11 [171,177].

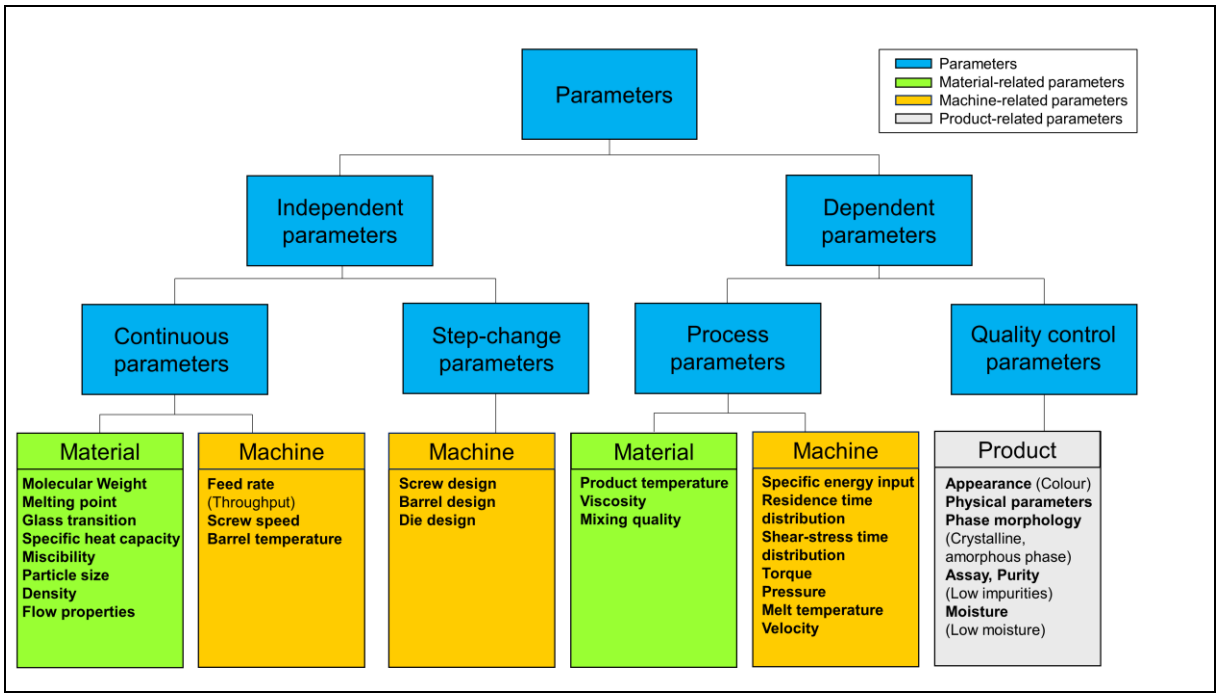

Figure 11. Influence of parameters on the drug product during HME (content and modified from [171,177]).

The parameters can be divided into independent and dependent parameters [171]. Independent parameters are established by the operator, while dependent parameters are parameters that result from the settings [171]. Independent parameters can be further differentiated into continuous parameters and step-change parameters [171]. Continuous parameters are parameters that can be changed and controlled during extrusion [171]. Step-change parameters require an interruption of the extrusion process [171].

Independent, continuous parameters related to the material are the thermal and physical properties of the powder mixture. Thermal properties are the melting point of the API and the melting point or glass transition temperature of the polymers as well as the specific heat capacity [177]. Physical properties include the molecular weight of the polymers as well as the particle size and the density of the powder mixture which influence the overall miscibility and flow properties of the powder blend [177]. In relation to the machine, independent, continuous parameters are the feed rate, the screw speed and the barrel temperature (Figure 11) [171,179]. The feed rate determines the throughput of the entire system [171]. A higher feed

rate leads to a higher throughput and lower melt temperature [171]. The screw speed impacts the conveying and mixing as well as the energy input into the system and can therefore have a major influence on the quality of the product [169,171]. As the screw speed increases, the energy input and also the melt temperature increases. The barrel temperature influences the viscosity and stability of the melt and affects the melt pressure [169]. A lower barrel temperature leads to increased viscosity and shear forces, which leads to a higher product temperature [169,177]. An increased product temperature can in turn lead to an increase in impurities due to degradation of the API in the product, which must be considered when processing thermo-sensitive drug substances [169,177]. This can create a vicious circle for thermo-sensitive drug substances, which is shown in Figure 12 [177].

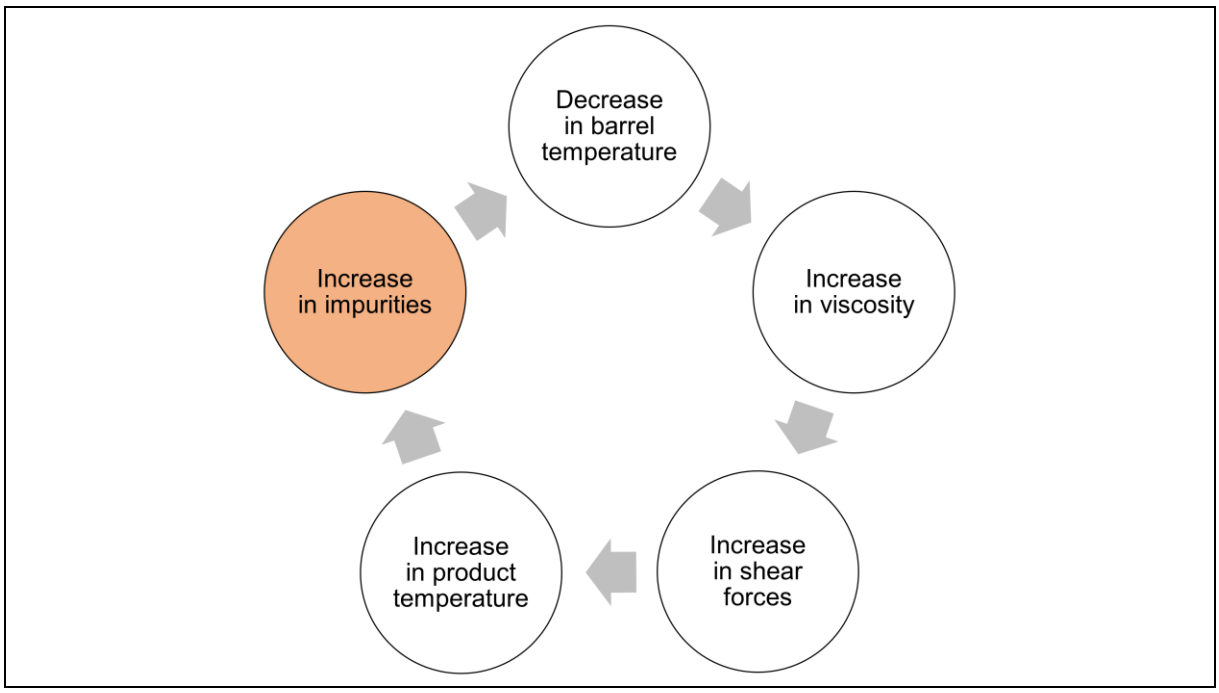

Figure 12. Vicious circle in the processing of thermo-sensitive drug substances (modified from [177]).

Therefore, strategies to avoid thermal degradation of the API include adjusting the feed rate, selecting a suitable screw configuration and screw speed and reducing the process temperature by adding plasticisers. When setting the parameters, the maximum torque of the extruder must also be taken into consideration. Step-change parameters are the screw design, the barrel design and the die design [171].

Dependent and thus influenceable parameters are further subdivided into process parameters and quality control parameters [171]. Material-related process parameters are the product temperature, viscosity and mixing quality, whereas most important machine-related process parameters are the melt temperature, the residence time, respectively residence time distribution and the specific energy input [171,177]. The residence time is influenced by the parameters feed rate and the screw speed [169]. A higher feed rate and a higher screw speed lead to a lower residence time, whereby the feed rate has a greater impact [171]. In conjunction with the feed rate, the residence time also depends on the filling level of the barrel [171]. The higher the filling level, the higher the mixing and the residence time [171]. The residence time is an important parameter that significantly influences the product quality and stability [94,102,169]. Too short a residence time can result in an inhomogeneous product, while too long a residence time can lead to the degradation of the thermo-sensitive API and the

polymers. Besides the residence time, the specific mechanical energy consumption is an important influencing parameter that describes the extrusion process and must also be considered when scaling up the extrusion process, as it should be kept constant [171].

Quality control parameters, on the other hand, are the appearance and physical parameters (e.g. colour, dispersion), as well as moisture [171]. In order to be able to control the process parameters during HME, various approaches are possible. Real-time measurements using PATs can be carried out for continuous monitoring of the extrusion process [171,173]. Optical spectroscopy measurements like ultraviolet-visible spectroscopy (UV-VIS), short-near-infrared spectroscopy (sNIR), near-infrared spectroscopy (NIR), and mid-infrared spectroscopy (MIR) are preferably used for content determination because they are non-destructive and help to increase the process understanding [171]. They can ensure a continuous process resulting in a consistent quality of the product as well as product safety [173].

Thus, HME represents a precise and reproducible, easily scalable process that, once the equipment has been purchased and implemented, is time-saving and economical due to the reduced number of production steps [95,97,99]. Due to the absence of organic solvents as well as water, hydrolysis-sensitive drug substances can be processed [169]. During the processing of thermo-sensitive drug substances, including peptidomimetic drugs and proteins, the heat exposure must be reduced through process and formulation development, as these can otherwise degrade under the influence of heat, shear as well as high energy input [97]. Furthermore, HME offers the possibility of developing new polymers with improved properties during formulation development as performed in the PolyPrint consortium, which may be of interest for the manufacture of products in the context of clinical applications. Therefore, the combination of HME with other technologies such as FDM 3DP opens up new possibilities in the production of dosage forms for personalised therapy [106].

1.8.3 Fused deposition modeling process

The FDM technique is based on fusion of a thermoplastic polymer, which is printed layer by layer through a hot nozzle on a print bed to build a 3D printed object [7,70]. After applying a polymer layer, it hardens due to heat conduction into the previously applied layer and forms another solid layer [7]. The print bed is lowered by the amount of one print layer before the next layer is applied [7]. This is repeated until a complete 3D printed object has been obtained. The FDM 3D printer consists of a hotend, a heatable nozzle and a print bed [35].

Materials used for the FDM 3DP are thermoplastic extrudates which can be extruded through a heatable nozzle [58]. Commercially available filaments are e.g. made of polylactic acid (PLA), acrylonitrile butadiene styrene, polypropylene, poly(vinyl alcohol) and polycarbonate and are available in different filament diameters and different colours [180,181]. Depending on the material used these filaments have different mechanical strength and durability due to different physical properties. Since no drug-loaded extrudates based on pharmaceutical-grade polymers are commercially available, these must first be produced via HME for FDM 3DP. Therefore, the APIs and polymers which are used for HME and subsequent FDM 3DP have to meet certain requirements. The drug substances must have sufficient thermal stability to avoid degradation, as a 40 °C to 50 °C higher temperature is required in FDM compared to HME [182]. The polymers should show thermoplastic behaviour and a glass transition temperature which allows the polymers to soften during FDM 3DP and be deposited on the print bed in the form of polymer strands [169,183]. In addition, the polymers must also have sufficient thermal stability as well as a low melt viscosity [169]. In order to sufficiently embed the drug in the polymer matrix, the polymer must have sufficient solubilisation capacity [169]. For sufficient

storage stability it is important that the polymer has a low hygroscopicity [169]. As part of product development, the polymer should be approved for human use [169]. Polymers can be selected based on their water solubility and pH dependent release behaviour [135,183,184]. Water-soluble polymers represent hydroxypropylcellulose (Ph. Eur., HPC), hypromellose (Ph. Eur., HPMC, AFFINISOL™ HPMC HME), poly-ε-caprolactone (PCL), macrogols (Ph. Eur.; polyethylene glycols, PEGs), poly(vinyl alcohol) (Ph. Eur., PVA), povidone [Ph. Eur.; polyvinylpyrrolidone, PVP such as Kollidon® 12 PF (K 12 PF)], copovidone (Ph. Eur.; Kollidon® VA 64, K VA 64) and polyvinyl caprolactam-polyvinyl acetate-polyethylene glycol graft copolymer (Soluplus®, SOL) [135]. Water-insoluble polymers are ethylcellulose (Ph. Eur., EC), PLA, polyethylene oxide (PEO, POLYOX®) and polymethacrylates as basic butylated methacrylate copolymer (Ph. Eur., bPMMA, Eudragit® E) or ammonio methacrylate copolymer type A (Ph. Eur., aPMMA) [135]. As pH neutral immediate release polymers, PEG, PVA and PVP can be used, while bPMMA shows due to its pH-dependent solubility an immediate release at pH < 5 [135]. HPC, HPMC, PCL, SOL, EC, PLA, PEO and aPMMA serve as pH neutral extended-release polymers [97,135].

As with HME the parameters during FDM 3DP have an influence on the quality and stability of the printed drug product and were also classified into independent and dependent parameters (Figure 13) [185].

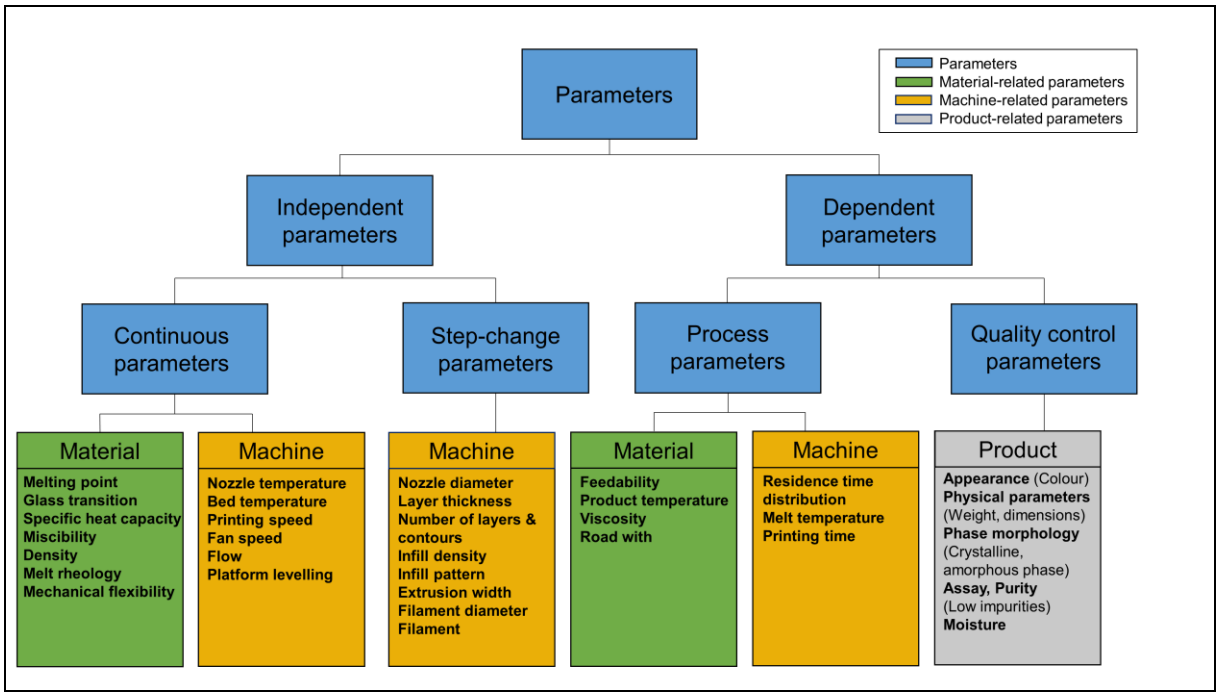

Figure 13. Influence of parameters on the drug product during FDM 3D printing (content and modified from [185]).

The independent parameters can be further divided into continuous and step-change parameters and the continuous parameters can be influenced through the material and the machine [171,185].

Regarding the material the mechanical, rheological and thermal properties of the extrudate used are decisive for the product quality (Figure 13) [4,166,183,185]. The mechanical properties such as stiffness and elasticity can be described by tensile strength and Young's modulus (elastic modulus), whereas the rheological properties can be described by the filament flow index [7,97]. For an extrudate to be printed, it should exhibit a high breaking

stress, high stiffness and a long distance to break [4]. If the extrudate is too brittle, it can break under the force of the drive gears, whereas a soft extrudate can deform between the drive gears and cannot act as a piston [4,7]. The thermal properties can be described by the melting point of the drug and the melting point or the glass transition temperature of the polymers, the degradation temperatures as well as the heat distribution [183]. These properties influence the melting and physical state as well as the thermal stability of the formulation. Thus, drug and polymer should have sufficient miscibility to result in a filament with homogeneous drug distribution and consistent density [186]. For FDM 3DP amorphous polymers are preferred because they have a lower coefficient of thermal expansion and therefore lead to less shrinkage, warpage and distortion [7]. Thermal and rheological properties influence the feeding of the formulation, whereas the rheological properties are mostly described through the viscosity [183]. A high-viscosity formulation may result in tougher extrudates that need to be forced through the die, while a low-viscosity formulation may cause the piston mechanism to fail due to the build-up of molten formulation [183]. Therefore, polymers with a broad processing window should be chosen in order to achieve an optimal feeding [183]. This is mainly because the melt viscosity and thus the printability of the formulation strongly depends on the thermal gradient, as the heat exposure during FDM 3D printing is comparatively short [183]. With regard to the FDM 3D printer used the nozzle and print bed temperature as well as the printing speed can be further adjusted during 3DP and can have a major influence on the product specifications [4]. Thermo-sensitive drug substances can degrade at higher temperatures during FDM 3DP because a printing temperature above the melting point is required, which may be associated with degradation of the drug substance [7]. Therefore, printing at lower temperatures and control of impurities in the finished product are essential. The printing speed affects the printing time and too high a printing speed can negatively affect the quality of the printed object [4,35]. The step-change parameters, which can be adjusted by cancelling the current printing process or after completing the printing process are the nozzle diameter, the layer thickness, the number of layer and contours, the infill density and infill pattern, the extrusion width and the filament diameter and material [4]. The layer thickness will determine the resolution and the accuracy of the printed dosage form [4]. The infill density has an impact on the porosity [4]. 3D printed dosage forms with lower infill results in a higher porosity and surface area, but lower hardness [4]. The infill pattern can also affect the hardness and thus influence the drug release [4].

The most important process parameters as dependent parameters are the product temperature and viscosity in relation to the material and the melt temperature and printing speed as well as the residence time in relation to the machine [185]. Quality control parameters of the product are the appearance, e.g. colour, and the physical parameters including weight and dimensions of the finished product which can be tested during or immediately after production [18,187]. The physical state as well as the moisture provide information about the physical stability, while studies on assay and purity reflect the chemical stability of the drug substance in the dosage form [18,187].

Thus, FDM 3DP is a simple, versatile technology for producing customised dosage forms with uniform drug content and less waste [3,9,188]. Due to its low cost and solvent-free process, it is a sustainable process [64,70,133,189]. However, filaments are required as the starting material for FDM 3DP. The combination of HME and FDM enables the continuous production of personalised dosage forms with no further processing steps due to the absence of organic solvents [106,133]. Furthermore, no preservation of the dosage form is required. It also offers the opportunity of solubilisation and amorphisation of poorly soluble drugs leading to an improved printability of the drug substance as well as improved dissolution rate from the 3D printed dosage form, but may also be associated with stability problems such as recrystallisation [183]. Due to the high temperature and the melting twice during HME and FDM 3DP, the processing of thermo-sensitive drug substances can be challenging compared to the

other 3D printing technologies, which will be shown in Table 1 [10]. The selection of temperature-resistant APIs and polymers during formulation development can help to reduce or even avoid degradation during these two processes [104]. Compared to FDM 3D printing, the heat influence in SLA is minimal and thermal degradation can be avoided [18,65]. SLS can also cause degradation of the API due to the laser beam and heat, however the influence can be reduced by printing at lower temperatures, with lower laser energy, i.e. higher wavelength and lower laser power with multiple scanning, as well as faster scanning speed [68]. In BJ, the influence of heat can be excluded by printing with a piezoelectric print head at room temperature, while degradation can occur by using a thermal print head [40]. The PAM technology also enables 3DP at room temperature due to the underlying principle [88].

Table 1. Overview of pharmaceutical 3D printing technologies and their stability considerations for processing of challenging APIs (content from [10]).

3D printing technology	Binding mechanisms	Activation	Conclusions regarding stability considerations of APIs	
			Advantages	Disadvantages and challenges
Stereolitho-graphy (SLA)	Chemical reaction (Photopolymerisation)	UV radiation from a laser	Processing of thermo-sensitive and hydrolysis-sensitive APIs is feasible.	Unwanted polymerisation reaction between APIs and excipients can occur due to laser beam.
Selective laser sintering (SLS)	Physical reaction	Thermal energy from a laser	Processing of hydrolysis-sensitive APIs is feasible.	Degradation reaction of APIs can occur due to laser beam and heat.
Binder jetting (BJ)	Physical reaction	Physical reaction between the components	Processing of thermo-sensitive APIs by printing at room temperature is feasible.	Degradation of thermo-sensitive APIs can occur by using a thermal print head or during drying.
Pressure-assisted micro-syringes (PAM)	Physical reaction	Physical reaction between the components	Processing of thermo-sensitive APIs is feasible.	Degradation of hydrolysis-sensitive APIs can occur due to drying.
Fused deposition modeling (FDM)	Thermal reaction	Heat from a hot nozzle	Processing of hydrolysis-sensitive APIs is feasible.	Degradation reaction of APIs can occur due to double heat exposure during HME and FDM.

1.8.4 Quality considerations

The quality of a medicinal product as an important core issue in the context of the authorisation of a medicinal product must be demonstrated by conformity with previously defined specifications [40]. Therefore, the ICH, which is a joint initiative of competent authorities and the pharmaceutical industry, strives to promote a worldwide harmonisation of the scientific and technical bases within the framework of the development of a medicinal product up to its authorisation [190]. Thus, the ICH has published guidelines that can be assigned to the topics of quality, safety, efficacy and multidisciplinary [191]. These ICH guidelines, especially quality guidelines, should be applied in the development of a 3D printed dosage form and are designed to enable manufacturing using scientific and risk-based approaches to ensure consistent product quality [3,122]. At the European level, scientific guidelines on quality are provided by the EMA to assist applicants in the submission of medicinal products. These concern guidelines on the topics of active substance; manufacturing; impurities; specifications, analytical procedures and analytical validation; excipients; packaging; stability; pharmaceutical development; quality by design; specific product types and life cycle management [192]. In the context of the development of paediatric formulations the EMA guideline "Guideline on pharmaceutical development of medicines for pediatric use" can assist, although it does not imply 3DP [193]. In addition to the aforementioned guidelines, the specific quality attributes of the 3D printed dosage forms must be considered.

Quality requirements for the development of a FDM 3D printed dosage form especially for paediatrics were developed within the framework of the PolyPrint consortium and beyond as part of this work. The development of a 3D printed dosage form for paediatrics begins with the selection of suitable starting materials [77]. The selected starting materials should each be sourced from the same starting material manufacturer in order to exclude batch variability [122]. APIs and polymers should show sufficient stability. Polymers used should exhibit thermoplastic properties that are required for HME and FDM 3DP [180]. Furthermore, they should be of pharmaceutical grade as well as safe and acceptable for children when developing a child-appropriate dosage form. When selecting excipients, the requirements of EMA, which are specified in the guideline "Excipients in the dossier for application for marketing authorisation of a medicinal product", should be considered [194]. Appropriate starting material specifications should be established and validated analytical test methods should be used [122]. Methods should be verified if necessary. Since FDM 3DP uses the extrudates from HME as an intermediate product, specifications for the intermediate product must also be available. In order to ensure sufficient quality including product homogeneity, physical parameters (mass, dimensions) and content uniformity (CU) can be determined [3]. The quality of the intermediate should be linked to the CQAs of the product [118,122]. For the control of starting materials and intermediates, PAT tools can be used to determine an appropriate control strategy based on the understanding of the 3D printed product and the 3DP process [122]. PAT tools in the context of HME may include filament diameter determination and sphericity using a multiaxial laser system [see Chapter II]. Other non-destructive determinations include in-line spectroscopic methods such as UV-VIS, NIR or Raman measurements, in-line rheometric measurements, and optical coherence tomography [195]. Verification of the quality of the 3D printed product should be done by comparison with previously defined specifications. For 3D printed dosage forms, as for conventional dosage forms, specifications must be set up according to the compendial pharmacopoeias, which include the CQAs of the dosage form [195]. Release testing for 3D printed tablets may include the uniformity of mass of single-dose preparations as well as destructive tests such as assay, purity, CU, dissolution, disintegration, and microbial contamination [3,9,118]. In addition, further physical tests may be required due to the physical properties of the 3D printed tablets compared to conventionally compressed tablets [122]. Once a formulation has been shown to be suitable, scale-up trials must be carried out which demonstrate large-scale manufacture

and define the critical process parameters [122]. A suitable packaging material must be selected that does not compromise the stability of the printed drug product. In addition to the requirements for the starting materials as well as the finished product, there are also requirements for the equipment, especially the FDM 3D printer [195]. Within the framework of an Impact Assessment for the qualification of the FDM 3D printer, it must be checked, whether the FDM 3D printer to be used must be qualified according to the good manufacturing practice (GMP) requirements or can be operated at the status of a good engineering practice [196]. GMP regulations must always be complied with for production in the pharmaceutical industry. Besides the qualification of the equipment, the 3DP process and the software used must be validated as well as the cleaning process [196]. Deviations from the process should be documented and corrective and preventive actions should be implemented.

When processing thermo-sensitive drug substances during HME and FDM, which is the focus of the work, attention must be paid to the stability of the drugs including chemical and physical stability. An influence on the stability of the active substance can negatively affect the product quality. Therefore, with regard to chemical stability control of impurities is essential and an effective quality assurance tool to ensure patient safety. Impurities must be identified and quantified [197]. In order to be able to control impurities in the drug product, suitable analytical methods must be established. Suitable methods for the identification and quantification of impurities represent chromatographic methods, such as HPLC and spectroscopic methods, such as mass spectrometry or nuclear magnetic resonance spectroscopy. In addition, the use of several methods or the coupling of two methods e.g. HPLC with mass spectrometry or nuclear magnetic resonance spectroscopy may be required to elucidate unknown impurities [198]. The stability of the 3D printed product must be demonstrated until the end of its shelf-life. Therefore, stability studies should be performed and stability-indicating methods should be developed to quantify the impurities [198]. In addition to chemical stability, solid state studies are required as part of the investigation of the physical stability of the APIs in the 3D printed tablets. The solid state can therefore be investigated using the well-established complementary methods differential scanning calorimetry and X-ray powder diffraction. ASDs produced using 3DP technology offer advantages of increased solubility and improved dissolution rate but are prone to recrystallisation due to kinetic stabilisation. Instabilities resulting from changes in the solid phase state can significantly affect the quality of the product and its stability and dissolution rate.

1.9 Aims of the thesis

Due to the increasing importance of 3DP of medicines in the context of personalised medicine, there is a great interest in processing of thermo-sensitive drug substances with different polymers into 3D printed oral dosage forms. Therefore, the aim of the thesis "3D printing of thermo-sensitive drug substances via Fused Deposition Modeling (FDM™)" was to investigate and quantify the degradation of the two thermo-sensitive drug substances EM and ESC-OX during the two heat-intensive processes HME and FDM 3DP.

More specific aims of the presented investigations were:

- To generate a current overview of the required quality aspects of FDM 3D printed medicines for paediatrics regarding formulation development, filament extrusion, printing process and printer design (Chapter II).
- To investigate and quantify the chemical degradation of the drug EM and degradation products during HME (Chapter III).
- To elucidate the reasons for the polymer dependent degradation (Chapter III).

- To optimise the HME process and to develop formulations that enable HME of EM at lower temperatures with reduced or no degradation (Chapter III).
- To investigate and quantify the chemical degradation of the peptidomimetic drug substance EM and degradation products during FDM 3DP (Chapter IV).
- To optimise the FDM 3DP process and develop strategies to reduce thermal degradation of EM during FDM 3DP (Chapter IV).
- To characterise the solid state of produced extrudates and 3D printed tablets as well as the release profile from 3D printed tablets with EM (Chapter IV).
- To produce oral solid dosage forms with EM (Chapter IV).
- To investigate and quantify the chemical degradation of ESC-OX and degradation products during HME and FDM 3DP (Chapter V).
- To investigate a potential conversion of ESC-OX into the R-enantiomer during HME and FDM 3DP (Chapter V).
- To develop strategies to reduce the thermal stress of ESC-OX during HME and FDM 3DP (Chapter V).
- To characterise the solid state and release profile of produced extrudates and 3D printed tablets with ESC-OX (Chapter V).
- To produce oral solid dosage forms with ESC-OX (Chapter V).

The procedure and methodology of the research concept of the doctoral thesis are presented graphically in Figure 14.

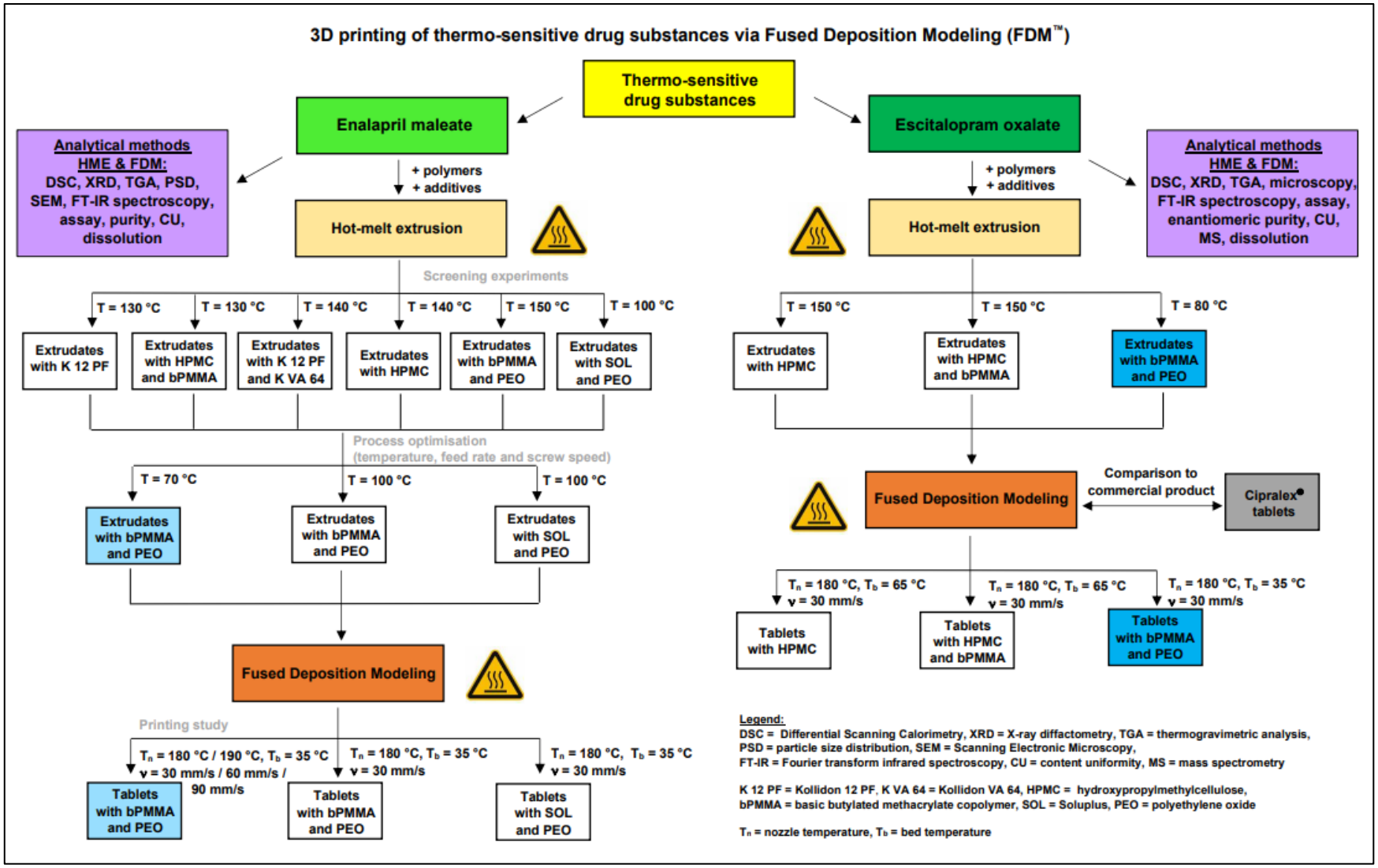

Figure 14. Research concept of the doctoral thesis.

1.10 Outline of the thesis

A current overview over the quality considerations of FDM 3D printed medicines for paediatrics is presented in the second chapter of this thesis in the form of a review article. The view on the quality aspects regarding the formulation development, the printing process and the 3D printed dosage forms are described by the PolyPrint consortium. The requirements for the pharmaceutical excipients used are outlined and the relevant parameters of the polymers for HME and FDM 3DP are presented. The different analytical tools for the in-line and off-line characterisation of the extrudates as well as for the characterisation of the 3D printed dosage forms are depicted. The stricter requirements for a GMP compliant 3D printer regarding dosing precision and quality control are pointed out. Furthermore, 3D printed dosage forms, which are accepted in children due to their appearance and taste, are highlighted.

The third chapter focuses on HME of the thermo-sensitive peptidomimetic drug substance EM and the production of extrudates for the treatment of hypertension and heart failure. The chemical degradation of the drug substance EM and its degradation products during HME was examined and quantified. For this purpose, a fast HPLC method has been developed. In order to investigate the extent of degradation of EM, screening experiments with six different formulations were conducted. From these screening experiments suitable process conditions for the HME process and two formulations were found which enabled the extrusion at reduced temperatures. In order to investigate possible interactions between EM and the polymers, FT-IR spectroscopy measurements were performed. Lastly, dissolution studies for the optimised formulations were carried out to study the release profile of EM from the extrudates. Thus, the aim of this research article was to minimise or avoid the degradation of EM during HME.

Chapter IV deals with the production of 3D printed tablets with EM via FDM 3DP. Therefore, extrudates from the optimised formulations served as feedstock material for the consecutive FDM 3DP process. Solid state analysis of the 3D printed tablets was performed in comparison to the extrudates, in order to explore possible differences. Again, the thermal degradation of EM and its degradation product was studied during the second melting process and determined by HPLC. Furthermore, the aim of this research article was to examine the nozzle diameter, the printing temperature and the printing speed as factors to reduce thermal stress as much as possible during FDM 3DP. Finally, the influence of a reduced infill on the content of EM should also be investigated. The dissolution behaviour from the optimised formulation was also assessed.

Chapter V depicts the thermal degradation of ESC-OX and its degradation products during HME and FDM 3DP and the formulation development to reduce thermal degradation. The influence of different polymer matrices on the degradation of the API was investigated and compared to the instability of ESC-OX in solution. In addition, a potential conversion of the S-enantiomer to the R-enantiomer on a chiral column was also examined during the two heat-intensive processes as well as in solution. Furthermore, the solid state of ESC-OX in the extrudates and the 3D printed tablets was analysed and the release behaviour was studied. Comparative studies were conducted with the Cipralex® film coated tablets available on the market.

Chapter VI contains the discussion of the thesis.

Finally, in Chapter VII, the thesis is concluded and future perspectives are discussed.

1.11 References

[1] ISO/ASTM 52900:2021. 2021. Additive manufacturing – General principles – Fundamentals and vocabulary.

[2] Roopavath, U. K., Kalaskar, D. M. 2017. 1 - Introduction to 3D printing in medicine. In: Kalaskar, D. M. (Ed.), 3D Printing in Medicine. Woodhead Publishing, 1-20. https://doi.org/10.1016/B978-0-08-100717-4.00001-6

[3] Norman, J., Madurawe, R. D., Moore, C. M. V., Khan, M. A., & Khairuzzaman, A. 2017. A new chapter in pharmaceutical manufacturing: 3D-printed drug products. Adv. Drug Deliv. Rev. 108, 39-50. https://doi.org/https://doi.org/10.1016/j.addr.2016.03.001

[4] Dumpa, N., Butreddy, A., Wang, H., Komanduri, N., Bandari, S., & Repka, M. A. 2021. 3D printing in personalized drug delivery: an overview of hot-melt extrusion-based fused deposition modeling. Int. J. Pharm. 600, 120501. https://doi.org/10.1016/j.ijpharm.2021.120501

[5] Ali, A., Ahmad, U., & Akhtar, J. 2020. 3D Printing in pharmaceutical sector: an overview. In: Pharmaceutical Formulation Design - Recent Practices. IntechOpen. http://dx.doi.org/10.5772/intechopen.90738

[6] ISO/ASTM 52915:2020. 2020. Specification for additive manufacturing file format (AMF) Version 1.2.

[7] Kafle, A., Luis, E., Silwal, R., Pan, H. M., Shrestha, P. L., Bastola, A. K. 2021. 3D/4D printing of polymers: Fused deposition modelling (FDM), selective laser sintering (SLS), and stereolithography (SLA). Polymers. 13, 3101. https://doi.org/10.3390/polym13183101

[8] Pravin, S., & Sudhir, A. 2018. Integration of 3D printing with dosage forms: a new perspective for modern healthcare. Biomed. 107, 146-154. https://doi.org/10.1016/j.biopha.2018.07.167

[9] Gupta, D. K., Ali, M. H., Ali, A., Jain, P., Anwer, M. K., Iqbal, Z., Mirza, M. A. 2022. 3D printing technology in healthcare: applications, regulatory understanding, IP repository and clinical trial status. J. Drug. Target. 30 (2), 131-150. https://doi.org/10.1080/1061186X.2021.1935973

[10] ISO 17296-2:2015. 2015. Additive manufacturing – General principles – Part 2: Overview of process categories and feedstock.

[11] Mitsouras, D., Liacouras, P. C. 2017. 3D printing technologies. In: Rybicki, F. J., Grant, G. T. (Eds.), 3D Printing in Medicine. A Practical Guide for Medical Professionals. Springer, Cham, 5-22. http://dx.doi.org/10.1007/978-3-319-61924-8_2

[12] Fischer, A., Gebauer, S., Khavkin, E. 2018. 3D-Druck im Unternehmen. Entscheidungsmodelle, Best Practices und Anwendungsbeispiele. Am Beispiel Fused Layer Modeling (FLM).1st ed. Carl Hanser Verlag, Munich.

[13] El Aita, I., Ponsar, H., Quodbach, J. 2018. A critical review on 3D-printed dosage forms. Curr. Pharm. Des. 24, 4957-4978. https://doi.org/10.2174/1381612825666181206124206

[14] Manini, G., Benali, S., Mathew, A., Napolitano, S., Raquez, J.-M., Goole, J. 2022. Paliperidone palmitate as model of heat-sensitive drug for long-acting 3D printing application. Int. J. Pharm. 618, 121662. https://doi.org/10.1016/j.ijpharm.2022.121662

[15] Trenfield, S. J., Awad, A., Goyanes, A., Gaisford, S., Basit, A. W. 2018. 3D printing pharmaceuticals: drug development to frontline care. Trends Pharmacol. Sci. 39 (5), 440-451. https://doi.org/10.1016/j.tips.2018.02.006

[16] Council of the European Union. 2015. Personalised medicine for patients – Council conclusions. https://health.ec.europa.eu/medicinal-products/personalised-medicine_en (Accessed 29 Sep 2023).

[17] Rantanen, J., & Breitkreutz, J. 2017. Drivers for a change – Manufacturing of future medicines for personalized drug therapies. In: Kleinebudde, K., Khinast, J., Rantanen, J. (Eds.), Continuous Manufacturing of Pharmaceuticals. John Wiley & Sons Ltd, Chichester, 507-523. https://doi.org/https://doi.org/10.1002/9781119001348.ch15

[18] Amekyeh, H., Tarlochan, F., Billa, N. 2021. Practicality of 3D printed personalized medicines in therapeutics. Front Pharmacol. 12, 646836. https://doi.org/10.3389/fphar.2021.646836

[19] Algahtani, M. S. 2021. Assessment of pharmacist's knowledge and perception toward 3D printing technology as a dispensing method for personalized medicine and the readiness for implementation. Pharmacy. 9 (1), 68. https://doi.org/10.3390/pharmacy9010068

[20] André, A., Vignaux, J.-J. 2019. Precision medicine. In: André, A. (Ed.), Digital Medicine. Health Informatics. Springer, Cham, 49-58. https://doi.org/10.1007/978-3-319-98216-8_5

[21] Vignaux, J.-J., & André, A. 2019. Biomarkers in precision medicine: the era of omics. In: André, A. (Ed.), Digital Medicine. Springer, Cham, 59-69. https://doi.org/10.1007/978-3-319-98216-8_6

[22] European Medicines Agency. 2006. ICH E15 Definitions for genomic biomarkers, pharmacogenomics, pharmacogenetics, genomic data and sample coding categories – Step 4. https://www.ema.europa.eu/en/documents/scientific-guideline/ich-e-15-definitions-genomic-biomarkers-pharmacogenomics-pharmacogenetics-genomic-data-sample-coding_en.pdf (Accessed 29 Sep 2023).

[23] Larijani, B., Aghaei Meybodi, H. R., Sarhangi, N., Hasanzad, M. 2022. Principles of precision medicine. In: Hasanzad, M. (Ed.), Precision Medicine in Clinical Practice. Springer, Singapore, 1-11. https://doi.org/10.1007/978-981-19-5082-7_1

[24] Brew-Sam, N., Parkinson, A., Lueck, C., Brown, E., Brown, K., Bruestle, A., Chisholm, K., Collins, S., Cook, M., Daskalaki, E., Drew, J., Ebbeck, H., Elisha, M., Fanning, V., Henschke, A., Herron, J., Matthews, E., Murugappan, K., Neshev, D., Nolan, C.-J., Pedley, L., Phillips, C., Suominen, H., Tricoli, A., Wright, K. Desborough, J. 2022. The current understanding of precision medicine and personalised medicine in selected research disciplines: study protocol of a systematic concept analysis. BMJ Open. 12 (9), e060326. https://doi.org/10.1136/bmjopen-2021-060326

[25] FDA news release. 2016. FDA advances Precision Medicine Initiative by issuing draft guidances on next generation sequencing-based tests. https://www.fda.gov/news-events/press-announcements/fda-advances-precision-medicine-initiative-issuing-draft-guidances-next-generation-sequencing-based (Accessed 29 Sep 2023).

[26] FDA. Precision Medicine. https://www.fda.gov/medical-devices/in-vitro-diagnostics/precision-medicine (Accessed 29 Sep 2023).

[27] THE PRECISION MEDICINE INITIATIVE. https://obamawhitehouse.archives.gov/precision-medicine (Accessed 29 Sep 2023).

[28] Slikker, W. Jr. 2018. Biomarkers and their impact on precision medicine. Exp. Biol. Med. (Maywood). 243 (3), 211-212. https://doi.org/10.1177%2F1535370217733426

[29] Alonso, S. G., de la Torre Díez, I. & Zapiraín, B. G. 2019. Predictive, personalized, preventive and participatory (4P) medicine applied to telemedicine and eHealth in the literature. J. Med. Syst. 43, 140. https://doi.org/10.1007/s10916-019-1279-4

[30] Hasanzad, M., Sarhangi, N., Hashemian, L., Sarrami, B. 2022. Principles of pharmacogenomics and pharmacogenetics. In: Hasanzad, M. (Ed.), Precision Medicine in Clinical Practice. Springer, Singapore, 13-32. https://doi.org/10.1007/978-981-19-5082-7_2

[31] Piquette-Miller, M., & Grant, D. M. 2007. The art and science of personalized medicine. Clin. Pharmacol. Ther. 81 (3), 311-315. https://doi.org/https://doi.org/10.1038/sj.clpt.6100130

[32] Mahmood, A., Singhvi, G., Manchanda, P., Pandey, M. M., Dubey, S. K., Gupta, G., Chellappan, D. K., Seyfoddin, A., Dua, K. 2020. 2 - Applications of 3D printing for the advancement of oral dosage forms. In: du Toit, L. C., Kumar, P., Choonara, Y. E., Pillay, V. (Eds.), Woodhead Publishing Series in Biomaterials, Advanced 3D-Printed Systems and Nanosystems for Drug Delivery and Tissue Engineering. Elsevier, 39-57. https://doi.org/10.1016/B978-0-12-818471-4.00002-9

[33] Clark, E. A., Alexander, M. R., Irvine, D. J., Roberts, C. J., Wallace, M. J., Sharpe, S., Yoo, J., Hague, R. J. M, Tuck, C. J., Wildman, R. D. 2017. 3D printing of tablets using inkjet with UV photoinitiation. Int. J. Pharm. 529 (1-2), 523-530. https://doi.org/10.1016/j.ijpharm.2017.06.085

[34] Triastek, Inc. 2022. Triastek receives FDA IND clearance for 3D printed medicine for the treatment of ulcerative colitis. https://www.prnewswire.com/news-releases/triastek-receives-fda-ind-clearance-for-3d-printed-medicine-for-the-treatment-of-ulcerative-colitis-301682515.html (Accessed 29 Sep 2023).

[35] Joo, Y., Shin, I., Ham, G., Abuzar, S. M., Hyun, S.-M., Hwang, S.-J. 2020. The advent of a novel manufacturing technology in pharmaceutics: superiority of fused deposition modeling 3D printer. J. Pharm. Investig. 50, 131-145. https://doi.org/10.1007/s40005-019-00451-1

[36] Hellinger, A., Stumpf, V., Kobsda, C. 2013. Deutschlands Zukunft als Produktionsstandort sichern, Umsetzungsempfehlungen für das Zukunftsprojekt Industrie 4.0, Abschlussbericht des Arbeitskreises Industrie 4.0. https://www.bmbf.de/bmbf/shareddocs/downloads/files/umsetzungsempfehlungen_industrie4_0.pdf?__blob=publicationFile&v=2 (Accessed 29 Sep 2023).

[37] Gabler Wirtschaftslexikon: Industrie 4.0 https://wirtschaftslexikon.gabler.de/definition/industrie-40-54032 (Accessed 29 Sep 2023).

[38] Araújo, R. M., Sa-Barreto, L. L., Gratieri, T., Gelfuso, M. G., & Cunha-Filho, M. 2019. The digital pharmacies era: how 3D printing technology using fused deposition modeling can become a reality. Pharmaceutics. 11 (3), 128. https://doi.org/10.3390/pharmaceutics11030128

[39] Kotta, S., Nair, A., Alsabeelah, N. 2018. 3D printing technology in drug delivery: recent progress and application. Curr. Pharm. Des. 24 (42), 5039-5048. https://doi.org/10.2174/1381612825666181206123828

[40] Desu, P. K., Maddiboyina, B., Vanitha, K., Rao Gudhanti, S. N. K, Anusha, R., Jhawat, V. 2012. 3D printing technology in pharmaceutical dosage forms: advantages and challenges. Curr. Drug Targets. 22 (16), 1901-1914. https://doi.org/10.2174/1389450122666210120142416

[41] Wening, K., Breitkreutz, J. 2011. Oral drug delivery in personalized medicine: unmet needs and novel approaches. Int. J. Pharm. 404, 1-9. https://doi.org/10.1016/j.ijpharm.2010.11.001

[42] Hill, S. W., Varker, A. S., Karlage, K., Myrdal, P. B. 2009. Analysis of drug content and weight uniformity for half-tablets of 6 commonly split medications. J. Manag. Care Pharm. 15, 253-261. https://doi.org/10.18553/jmcp.2009.15.3.253

[43] Brown, D., Ford, J. L., Nunn, A. J., Rowe, P. H. 2004. An assessment of dose-uniformity of samples delivered from paediatric oral droppers. J. Clin. Pharm. Ther. 29, 521-529. https://doi.org/10.1111/j.1365-2710.2004.00595.x

[44] Grießmann, K., Breitkreutz, J., Schubert-Zsilavecz, M., Abdel-Tawab, M. 2007. Dosing accuracy of measuring devices provided with antibiotic oral suspensions. Paediatr. Perinat. Drug Ther. 8, 61-70. http://dx.doi.org/10.1185/146300907X178950

[45] Walsh, J., Bickmann, D., Breitkreutz, J., Chariot-Goulet, M. 2011. Delivery devices for the administration of paediatric formulations: overview of current practice, challenges and recent developments. Int. J. Pharm. 415, 221-231. https://doi.org/10.1016/j.ijpharm.2011.05.048

[46] Yin, H. S., Mendelsohn, A. L., Wolf, M. S., Parker, R. M., Fierman, A., van Schaick, L., Bazan, I. S., Kline, M. D., Dreyer, B. P. 2010. Parents' medication administration errors: role of dosing instruments and health literacy. Arch. Paediatr. Adolesc. Med. 164, 181-186. https://doi.org/10.1001/archpediatrics.2009.269

[47] Preis, M., Breitkreutz, J., Sandler, N. 2015. Perspective: concepts of printing technologies for oral film formulations. Int. J. Pharm. 494, 578-584. https://doi.org/10.1016/j.ijpharm.2015.02.032

[48] Öblom, H., Sjöholm, E., Rautamo, M., Sandler, N. 2019. Towards printed pediatric medicines in hospital pharmacies: comparison of 2D and 3D-printed orodispersible warfarin films with conventional oral powders in unit dose sachets. Pharmaceutics. 11 (7), 334. https://doi.org/10.3390/pharmaceutics11070334

[49] Okwuosa, T. C., Soares, C., Gollwitzer, V., Habashy, R., Timmins, P., & Alhnan, M. A. 2018. On demand manufacturing of patient-specific liquid capsules via co-ordinated 3D printing and liquid dispensing. Eur. J. Pharm. Sci. 118, 134-143. https://doi.org/10.1016/j.ejps.2018.03.010

[50] European Medicines Agency. Paediatric regulation. https://www.ema.europa.eu/en/human-regulatory/overview/paediatric-medicines/paediatric-regulation (Accessed 29 Sep 2023).

[51] Goyanes, A., Scarpa, M., Kamlow, M., Gaisford, S., Basit, A.W., Orlu, M. 2017. Patient acceptability of 3D printed medicines. Int. J. Pharm. 530 (1-2), 71-78. https://doi.org/10.1016/j.ijpharm.2017.07.064

[52] Goyanes, A., Madla, C. M., Umerji, A., Duran Piñeiro, G., Giraldez Montero, J. M., Lamas Diaz, M. J., Gonzalez Barcia, M., Taherali, F., Sánchez-Pintos, P., Couce, M. L., Gaisford, S., Basit, A. W. 2019. Automated therapy preparation of isoleucine formulations using 3D printing for the treatment of MSUD: first single-centre, prospective, crossover study in patients. Int. J. Pharm. 567, 118497. https://doi.org/10.1016/j.ijpharm.2019.118497

[53] Scoutaris, N., Ross, S. A., & Douroumis, D. 2018. 3D printed "Starmix" drug loaded dosage forms for paediatric applications. Pharm. Res. 35, 34. https://doi.org/10.1007/s11095-017-2284-2

[54] Rycerz, K., Stepien, K. A., Czapiewska, M., Arafat, B. T., Habashy, R., Isreb, A., Peak, M., Alhnan, M. A. 2019. Embedded 3D printing of novel bespoke soft dosage form concept for pediatrics. Pharmaceutics. 11 (12), 630. https://doi.org/10.3390/pharmaceutics11120630

[55] Wang, S., Chen, X., Han, X., Hong, X., Li, X., Zhang, H., Li, M., Wang, Z., Zheng, A. 2023. A review of 3D printing technology in pharmaceutics: technology and applications, now and future. Pharmaceutics. 15, 416. https://doi.org/10.3390/pharmaceutics15020416

[56] Mohammed, A. A., Algahtani, M. S., Ahmad, M. Z., Ahmad, J., Kotta, S. 2021. 3D printing in medicine: technology overview and drug delivery applications. Annals of 3D Printed Medicine. 4, 100037. https://doi.org/10.1016/j.stlm.2021.100037

[57] Awad, A., Trenfield, S. J., Gaisford, S., Basit, A. W. 2018. 3D printed medicines: a new branch of digital healthcare. Int. J. Pharm. 548 (1), 586-596. https://doi.org/10.1016/j.ijpharm.2018.07.024

[58] Liaw, C. Y., Guvendiren, M. 2017. Current and emerging applications of 3D printing in medicine. Biofabrication. 9 (2), 024102. https://doi.org/10.1088/1758-5090/aa7279

[59] Groll, J., Burdick, J. A., Cho, D. W., Derby, B., Gelinsky, M., Heilshorn, S. C., Jüngst, T., Malda, J., Mironov, V. A., Nakayama, K., Ovsianikov, A., Sun, W., Takeuchi, S., Yoo, J. J., Woodfield, T. B. F. 2018. A definition of bioinks and their distinction from biomaterial inks. Biofabrication. 11 (1), 013001. https://doi.org/10.1088/1758-5090/aaec52

[60] Jadhav, R. G., Das, A. K. 2017. 10 - Four dimensional printing in healthcare. In: Kalaskar, D. M. (Ed.), 3D Printing in Medicine, Woodhead Publishing, 207-218. https://doi.org/10.1016/B978-0-08-100717-4.00010-7

[61] Kassem, T., Sarkar, T., Nguyen, T., Saha, D., Ahsan, F. 2022. 3D printing in solid dosage forms and organ-on-chip applications. Biosensors. 12 (4), 186. https://doi.org/10.3390/bios12040186

[62] Xia, R.-Z., Zhai, Z.-J., Chang, Y.-Y., & Li, H.-W. 2019. Clinical applications of 3-dimensional printing technology in hip joint. Orthop. Surg, 11, 533-544. https://doi.org/10.1111/os.12468

[63] Alhnan, M. A., Okwuosa, T. C., Sadia, M., Wan, K. W., Ahmed, W., Arafat, B. 2016. Emergence of 3D printed dosage forms: opportunities and challenges. Pharm. Res. 33 (8), 1817-1832. https://doi.org/10.1007/s11095-016-1933-1

[64] Abdella, S., Youssef, S. H., Afinjuomo, F., Song, Y., Fouladian, P., Upton, R., & Garg, S. 2021. 3D printing of thermo-sensitive drugs. Pharmaceutics. 13 (9), 1524. https://doi.org/10.3390/pharmaceutics13091524

[65] Deshmane, S., Kendre, P., Mahajan, H., Jain, S. 2021. Stereolithography 3D printing technology in pharmaceuticals: a review. Drug. Dev. Ind. Pharm. 47 (9), 1362-1372. https://doi.org/10.1080/03639045.2021.1994990

[66] Bongiovanni, R., Vitale, A. 2022. Vat photopolymerization. In: Marasso, S. L., & Cocuzza, M. (Eds.), High Resolution Manufacturing from 2D to 3D/4D Printing: Applications in Engineering and Medicine. Springer, Cham, 17-46. https://doi.org/10.1007/978-3-031-13779-2_2

[67] Ibrahimovic, E. 2018. The Application of Advanced Technologies in Industrial Practice. In: Hadžikadić, M., Avdaković, S. (Eds.), Advanced Technologies, Systems, and Applications II. IAT 2017. Lecture Notes in Networks and Systems, 28. Springer, Cham, 1137-1146. https://doi.org/10.1007/978-3-319-71321-2_97

[68] Charoo, N. A., Barakh Ali, S. F., Mohamed, E. M., Kuttolamadom, M. A., Ozkan, T., Khan, M. A., Rahman, Z. 2020. Selective laser sintering 3D printing - An overview of the technology and pharmaceutical applications. Drug. Dev. Ind. Pharm. (6), 869-877. https://doi.org/10.1080/03639045.2020.1764027

[69] Awad, A., Fina, F., Goyanes, A., Gaisford, S., Basit, A. W. 2020. 3D printing: principles and pharmaceutical applications of selective laser sintering. Int. J. Pharm. 586, 119594. https://doi.org/10.1016/j.ijpharm.2020.119594

[70] Chandekar, A., Mishra, D. K., Sharma, S., Saraogi, G. K., Gupta, U, Gupta, G. 2019. 3D printing technology: a new milestone in the development of pharmaceuticals. Curr. Pharm. Des. 25 (9), 937-945. https://doi.org/10.2174/1381612825666190507115504

[71] Badini, C., & Padovano, E. 2022. Powder bed fusion. In: Marasso, S. L., & Cocuzza, M. (Eds.), High Resolution Manufacturing from 2D to 3D/4D Printing: Applications in Engineering and Medicine. Springer, Cham, 81-103. https://doi.org/10.1007/978-3-031-13779-2_4

[72] Sen, K., Mehta, T., Sansare, S., Sharifi, L., Ma, A. W. K., Chaudhuri, B. 2021. Pharmaceutical applications of powder-based binder jet 3D printing process - A review. Adv. Drug. Deliv. Rev. 177, 113943. https://doi.org/10.1016/j.addr.2021.113943

[73] Trenfield, S. J., Madia, C. M., Basit, A. W., Gaisford, S. 2018. Binder jet printing in pharmaceutical manufacturing. In: Basit, A., & Gaisford, S. (Eds.), 3D Printing of Pharmaceuticals. AAPS Advances in the Pharmaceutical Sciences Series AAPS, 31. Springer, Cham, 41-54. https://doi.org/10.1007/978-3-319-90755-0_3

[74] Warsi, M. H., Yusuf, M., Al Robaian, M., Khan, M., Muheem, A., Khan, S. 2018. 3D printing methods for pharmaceutical manufacturing: opportunity and challenges. Curr. Pharm. Des. 24 (42), 4949-4956. http://dx.doi.org/10.2174/1381612825666181206121701

[75] Jose, P., & Christoper, P. 2018. 3D printing of pharmaceuticals – A potential technology in developing personalized medicine. Asian J. Pharm. Res. Dev. 6 (3), 46-54. https://doi.org/https://doi.org/10.22270/ajprd.v6i3.375

[76] Afsana, Vineet, J., Nafis, H., Keerti, J. 2018. 3D printing in personalized drug delivery. Curr. Pharm. Des. 24 (42), 5062-5071. https://doi.org/10.2174/1381612825666190215122208

[77] West, T. G., & Bradbury, T. J. 2019. 3D Printing: A case of ZipDose® technology – World‘s first 3D printing platform to obtain FDA approval for a pharmaceutical product. In: Maniruzzaman, M. (Ed.), 3D and 4D Printing in Biomedical Applications. Wiley-VCH, Weinheim, 53-79. https://doi.org/https://doi.org/10.1002/9783527813704.ch3

[78] Landers, R., Mülhaupt, R. 2000. Desktop manufacturing of complex objects, prototypes and biomedical scaffolds by means of computer-assisted design combined with computer-guided 3D plotting of polymers and reactive oligomers. Macromol. Mater. Eng. 282, 17-21. https://doi.org/10.1002/1439-2054(20001001)282:1%3C17::AID-MAME17%3E3.0.CO;2-8

[79] Mülhaupt, R., Landers, R., John, H. 2001. Device and methods for the production of three-dimensional objects, WO 01/78968 A1.

[80] Khaled, S. A., Burley, J. C., Alexander, M. R., Roberts, C. J. 2014. Desktop 3D printing of controlled release pharmaceutical bilayer tablets. Int. J. Pharm. 461 (1-2), 105-111. https://doi.org/10.1016/j.ijpharm.2013.11.021

[81] Khaled, S. A., Burley, J. C., Alexander, M. R., Yang, J., Roberts, C. J. 2015. 3D printing of tablets containing multiple drugs with defined release profiles. Int. J. Pharm. 494, 643-650. https://doi.org/10.1016/j.ijpharm.2015.07.067

[82] Khaled, S. A., Burley, J. C., Alexander, M. R., Yang, J., Roberts, C. J. 2015. 3D printing of five-in-one dose combination polypill with defined immediate and sustained release profiles. J. Control. Release. 217, 308-314. https://doi.org/10.1016/j.jconrel.2015.09.028

[83] Khaled, S. A., Alexander, M. R., Wildman, R. D., Wallace, M. J., Sharpe, S., Yoo, J., Roberts, C. J. 2018. 3D extrusion printing of high drug loading immediate release paracetamol tablets. Int. J. Pharm. 538 (1-2), 223-230. https://doi.org/10.1016/j.ijpharm.2018.01.024

[84] El Aita, I., Breitkreutz, J., Quodbach, J. 2019. On-demand manufacturing of immediate release levetiracetam tablets using pressure-assisted microsyringe printing. Eur. J. Pharm. Biopharm. 134, 29-36. https://doi.org/10.1016/j.ejpb.2018.11.008

[85] Tagami, T., Ito, E., Kida, R., Hirose, K., Noda, T., Ozeki, T. 2021. 3D printing of gummy drug formulations composed of gelatin and an HPMC-based hydrogel for pediatric use. Int. J. Pharm. 594, 120118. https://doi.org/10.1016/j.ijpharm.2020.120118

[86] Karavasili, C., Gkaragkounis, A., Moschakis, T., Ritzoulis, C., Fatouros, D. G. 2020. Pediatric-friendly chocolate-based dosage forms for the oral administration of both hydrophilic and lipophilic drugs fabricated with extrusion-based 3D printing. Eur. J. Pharm. Sci. 147, 105291. https://doi.org/10.1016/j.ejps.2020.105291

[87] Seoane-Viaño, I., Januskaite, P., Alvarez-Lorenzo, C., Basit, A. W., Goyanes, A. 2021. Semi-solid extrusion 3D printing in drug delivery and biomedicine: personalised solutions for healthcare challenges. J. Control. Release. 332, 367-389. https://doi.org/10.1016/j.jconrel.2021.02.027

[88] Rahman, J., Quodbach, J. 2021. Versatility on demand - The case for semi-solid micro-extrusion in pharmaceutics. Adv. Drug Deliv. Rev. 172, 104-126. https://doi.org/10.1016/j.addr.2021.02.013

[89] Auriemma, G., Tommasino, C., Falconem G., Esposito, T., Sardo, C., Aquino, R. P. 2022. Additive manufacturing strategies for personalized drug delivery systems and medical devices: fused filament fabrication and semi solid extrusion. Molecules. 27 (9), 2784. http://dx.doi.org/10.3390/molecules27092784

[90] Zhang, Y. S., Haghiashtiani, G., Hübscher, T., Kelly, D. J., Lee, J. M., Lutolf, M., McAlpine, M. C., Yeong, W. Y., Zenobi-Wong, M., Malda, J. 2021. 3D extrusion bioprinting. Nat. Rev. Methods Primers. 1, 75. https://doi.org/10.1038/s43586-021-00073-8

[91] Pavan Kalyan, B. G., Kumar, L. 2022. 3D Printing: applications in tissue engineering, medical devices, and drug delivery. AAPS PharmSciTech. 23 (4), 92. https://doi.org/10.1208/s12249-022-02242-8

[92] Firth, J., Basit, A. & Gaisford, S. 2018. The role of semi-solid extrusion printing in clinical practice. In: Basit, A., & Gaisford, S. (Eds.), 3D Printing of Pharmaceuticals. AAPS Advances in the Pharmaceutical Sciences Series AAPS, 31. Springer, Cham, 133-151. https://doi.org/10.1007/978-3-319-90755-0_7

[93] Dave, H. K., Patel, S. T. 2021. Introduction to fused deposition modeling based 3D printing process. In: Dave, H. K., Davim, J. P. (Eds.), Fused Deposition Modeling Based 3D Printing. Materials Forming, Machining and Tribology. Springer, Cham, 1-21. https://doi.org/10.1007/978-3-030-68024-4_1

[94] Patil, H., Tiwari, R. V., Repka, M. A. 2016. Hot-melt extrusion: from theory to application in pharmaceutical formulation. AAPS PharmSciTech. 17 (1), 20-42. https://doi.org/10.1208/s12249-015-0360-7

[95] Ren, Y., Mei, L., Zhou, L., Guo, G. 2019. Recent perspectives in hot melt extrusion-based polymeric formulations for drug delivery: applications and innovations. AAPS PharmSciTech. 20 (3), 92. https://doi.org/10.1208/s12249-019-1300-8

[96] Simões, M., Pinto, R., & Simões, S. 2021. Hot-melt extrusion: A roadmap for product development. AAPS PharmSciTech. 22, 184. https://doi.org/10.1208/s12249-021-02017-7

[97] Nashed, N., Lam, M., Nokhodchi, A. 2021. A comprehensive overview of extended release oral dosage forms manufactured through hot melt extrusion and its combination with 3D printing. Int. J. Pharm. 596, 120237. https://doi.org/10.1016/j.ijpharm.2021.120237

[98] Chokshi, R., & Zia, H. 2010. Hot-melt extrusion technique: a review. Iran. J. Pharm. Res. 3 (1), 3-16. https://doi.org/10.22037/ijpr.2010.290

[99] Maniruzzaman, M., Boateng, J. S., Snowden, M. J., Douroumis, D. 2012. A review of hot-melt extrusion: process technology to pharmaceutical products. ISRN Pharm. 436763. https://doi.org/10.5402/2012/436763

[100] Sarabu, S., Bandari, S., Kallakunta, V. R., Tiwari, R., Patil, H., & Repka, M. A. 2019. An update on the contribution of hot-melt extrusion technology to novel drug delivery in the twenty-first century: part II. Expert Opin. Drug Deliv. 16 (6), 567-582. https://doi.org/10.1080/17425247.2019.1614912

[101] Tiwari, R. V., Patil, H., Repka, M. A. 2016. Contribution of hot-melt extrusion technology to advance drug delivery in the 21st century. Expert Opin. Drug Deliv.13 (3), 451-464. https://doi.org/10.1517/17425247.2016.1126246

[102] Repka, M. A., Bandari, S., Kallakunta, V. R., Vo, A. Q., McFall, H., Pimparade, M. B., Bhagurkar, A. M. 2018. Melt extrusion with poorly soluble drugs - An integrated review. Int. J. Pharm. 535 (1-2), 68-85. https://doi.org/10.1016/j.ijpharm.2017.10.056

[103] Simões, M., Pinto, R., & Simões, S. 2019. Hot-melt extrusion in the pharmaceutical industry: toward filing a new drug application. Drug Discov. Today. 24 (9), 1749-1768. https://doi.org/10.1016/j.drudis.2019.05.013

[104] Awad, A., Gaisford, S., Basit, A. W. 2018. Fused deposition modelling: advances in engineering and medicine. In: Basit, A., Gaisford, S. (Eds.), 3D Printing of Pharmaceuticals. AAPS Advances in the Pharmaceutical Sciences Series, 31. Springer, Cham, 107-132. https://doi.org/10.1007/978-3-319-90755-0_6

[105] Stratasys. Reaching across industries. https://www.stratasys.com/en/industries-and-applications/3d-printing-industries/ (Accessed 29 Sep 2023).

[106] Bandari, S., Nyavanandi, D., Dumpa, N., Repka, M. A. 2021. Coupling hot melt extrusion and fused deposition modeling: critical properties for successful performance. Adv. Drug Deliv. Rev. 172, 52-63. https://doi.org/10.1016/j.addr.2021.02.006

[107] Bhatt, A., & Anbarasu, A. 2017. Nanoscale biomaterials for 3D printing. IOSR J. Pharm. Biol. Sci. 12, 80-86. https://doi.org/10.9790/3008-1203068086

[108] BfArM. Federal Institute for Drugs and Medical Devices. Medicinal devices. https://www.bfarm.de/EN/Medical-devices/_node.html (Accessed 29 Sep 2023).

[109] Coburn, J. C., & Grant, G. T. 2017. FDA Regulatory pathways and technical considerations for the 3D printing of medical models and devices. In: Rybicki, F. J., Grant, G. T. (Eds.), 3D Printing in Medicine: A Practical Guide for Medical Professionals. Springer, Cham, 97-111. https://doi.org/10.1007/978-3-319-61924-8_10

[110] Administration USFDA. Public Workshop – Additive manufacturing of medical devices: An interactive discussion on the technical considerations of 3D printing 2014. https://www.govinfo.gov/content/pkg/FR-2014-05-19/pdf/2014-11513.pdf (Accessed 29 Sep 2023).

[111] Di Prima, M., Coburn, J., Hwang, D., Kelly, J., Khairuzzaman, A., Ricles, L. 2016. Additively manufactured medical products - The FDA perspective. 3D Print. Med. 2,1. https://doi.org/10.1186/s41205-016-0005-9

[112] FDA guidance document. 2017. Technical Considerations for Additive Manufactured Medical Devices. Guidance for Industry and Food and Drug Administration Staff. https://www.fda.gov/media/97633/download (Accessed 29 Sep 2023).

[113] McDonald, J. 2019. Regulatory considerations for devices manufactured using additive manufacturing technologies. In: Devine, D. M. (Ed.), Polymer Based Additive Manufacturing – Biomedical Applications. Springer, Cham, 243-254. https://doi.org/10.1007/978-3-030-24532-0_11

[114] FDA. Overview of Medical Device Classification and Reclassification. https://www.fda.gov/about-fda/cdrh-transparency/overview-medical-device-classification-and-reclassification (Accessed 29 Sep 2023).

[115] FDA. Classify Your Medical Device. https://www.fda.gov/medical-devices/overview-device-regulation/classify-your-medical-device (Accessed 29 Sep 2023).

[116] FDA guidance document. 2014. The 510(k) Program: Evaluating Substantial Equivalence in Premarket Notifications [510(k)]. Guidance for Industry and Food and Drug Administration Staff. https://www.fda.gov/media/82395/download (Accessed 29 Sep 2023).

[117] FDA. Premarket Notification 510(k). https://www.fda.gov/medical-devices/premarket-submissions-selecting-and-preparing-correct-submission/premarket-notification-510k (Accessed 29 Sep 2023).

[118] Mirza, M., & Iqbal, Z. 2018. 3D printing in pharmaceuticals: regulatory perspective. Curr. Pharm. Des. 24 (42), 5081-5083. https://doi.org/10.2174/1381612825666181130163027

[119] European Medicines Agency. Generic and hybrid medicines. https://www.ema.europa.eu/en/human-regulatory/marketing-authorisation/generic-hybrid-medicines (Accessed 29 Sep 2023).

[120] BfArM. Federal Institute for Drugs and Medical Devices. Medicinal products. https://www.bfarm.de/DE/Arzneimittel/_artikel.html#:~:text=BfArM%20-%20Arzneimittel%20-%20Arzneimittel%20Unter%20Arzneimitteln%20versteht,die%20Anwendung%20beim%20Menschen%20als%20auch%20beim%20Tier (Accessed 29 Sep 2023).

[121] FDA guidance document. 1999. Applications Covered by Section 505(b)(2) – draft. https://www.fda.gov/media/72419/download (Accessed 29 Sep 2023).

[122] Khairuzzaman, A. 2018. Regulatory perspectives on 3D printing in pharmaceuticals. In: Basit, A., & Gaisford, S. (Eds.), 3D printing of Pharmaceuticals. AAPS Advances in the Pharmaceutical Sciences Series AAPS, 31. Springer, Cham, 215-236. https://doi.org/10.1007/978-3-319-90755-0_11

[123] FDA guidance document. 2017. Advancement of Emerging Technology Applications for Pharmaceutical Innovation and Modernization Guidance for Industry. https://www.fda.gov/media/95444/download (Accessed 29 Sep 2023).

[124] Jain, M., & Rana, S. 2018. Emerging Technology Integration in FDA's Drug Approval Process. https://www.ppd.com/wp-content/uploads/2018/06/2018-June-Regulatory-Focus-Emerging-Tech.pdf (Accessed 29 Sep 2023).

[125] FDA. Emerging Technology Program. https://www.fda.gov/about-fda/center-drug-evaluation-and-research-cder/emerging-technology-program (Accessed 29 Sep 2023).

[126] Reddy, C. V., Balamuralidhara, V., Venkatesh, M. P., & Pramod Kumar, T. M. 2020. First FDA approved 3D printed drug paved new path for increased precision in patient care. Appl. Clin. Res. Clin. Trials Regul. Aff. 7, 93-103. https://doi.org/10.2174/2213476X07666191226145027

[127] FDA guidance document. 2017. Formal meetings between the FDA and Sponsors or Applicants of PDUFA products Guidance for Industry – draft. https://www.fda.gov/media/109951/download (Accessed 29 Sep 2023).

[128] Kim, J. H., Kim, K., & Jin, H. E. 2022. Three-dimensional printing for oral pharmaceutical dosage forms. J. Pharm. Investig. 52, 293-317. https://doi.org/10.1007/s40005-022-00561-3

[129] Everett, H. 2021. Triastek receives FDA IND clearance for 3D printed drug to treat rheumatoid arthritis-3D printing industry. https://3dprintingindustry.com/news/triastek-receives-fda-ind-clearance-for-3d-printed-drug-to-treat-rheumatoid-arthritis-184159/ (Accessed 29 Sep 2023).

[130] Zheng, Y., Deng, F., Wang, B., Wu, Y., Luo, Q., Zuo, X., Liu, X., Cao, L., Li, M., Lu, H., Cheng, S., Li, X. 2021. Melt extrusion deposition (MEDTM) 3D printing technology – A paradigm shift in design and development of modified release drug products. Int. J. Pharm. 602, 120639. https://doi.org/10.1016/j.ijpharm.2021.120639

[131] Triastek, Inc. 2022. Triastek receives FDA IND clearance for 3D printed product of blockbuster molecule. https://www.prnewswire.com/news-releases/triastek-receives-fda-ind-clearance-for-3d-printed-product-of-blockbuster-molecule-301519962.html (Accessed 29 Sep 2023).

[132] Bhattacharya, S., Singh, S., Shrestha, S., Baghel, Y., Maity, D., Kumar, A., Gupta, G., Narang, R., Kosey, S. 2019. Recent findings and development of 3D printing technology in pharmaceutical formulation development: an extensive review. Int. J. Drug Dev. Res. 11, 1-14. http://dx.doi.org/10.36648/0975-9344.11.4.142

[133] Wallis, M., Al-Dulimi, Z., Tan, D. K., Maniruzzaman, M., Nokhodchi, A. 2020. 3D printing for enhanced drug delivery: current state-of-the-art and challenges. Drug Dev. Ind. Pharm. 46 (9), 1385-1401. https://doi.org/10.1080/03639045.2020.1801714

[134] Melocchi, A., Briatico-Vangosa, F., Uboldi, M., Parietti, F., Turchi, M., von Zeppelin, D., Maroni, A., Zema, L., Gazzaniga, A., Zidan, A. 2021. Quality considerations on the pharmaceutical applications of fused deposition modeling 3D printing. Int. J. Pharm. 592, 119901. https://doi.org/10.1016/ j.ijpharm.2020.119901

[135] Azad, M. A., Olawuni, D., Kimbell, G., Badruddoza, A. Z. M, Hossain, M. S., Sultana, T. 2020. Polymers for extrusion-based 3D printing of pharmaceuticals: a holistic materials-process perspective. Pharmaceutics. 12 (2), 124. https://doi.org/10.3390/pharmaceutics12020124

[136] Bhattacharjee, D., Srivastava, V. 2020. Aspects of 3D printed drugs. J. Med. Eng. Technol. 44 (8), 472-480. https://doi.org/10.1080/03091902.2020.1822942

[137] World Health Organization. WHO Technical Report Series, No. 961. 2011. Annex 9 Model guidance for the storage and transport of time- and temperature-sensitive pharmaceutical products. https://www.who.int/docs/default-source/medicines/norms-and-standards/guidelines/distribution/trs961-annex9-modelguidanceforstoragetransport.pdf?sfvrsn=b80e925f_2 (Accessed 29 Sep 2023).

[138] do Pazo-Oubiña, F., Alorda-Ladaria, B., Gomez-Lobon, A., Boyeras-Vallespir, B., Santandreu-Estelrich, M. M., Martorell-Puigserver, C., Gomez-Zamora, M., Ventayol-Bosch, P., Delgado-Sanchez, O. 2021. Thermolabile drug storage in an ambulatory setting. Sci. Rep. 11, 5959. https://doi.org/10.1038/s41598-021-85413-0

[139] European Medicines Agency. 2020. ICH M9 guideline on biopharmaceutics classification system-based biowaivers – Step 5. https://www.ema.europa.eu/en/documents/scientific-guideline/ich-m9-biopharmaceutics-classification-system-based-biowaivers-step-5_en.pdf (Accessed 29 Sep 2023).

[140] Steinhilber, D., Schubert-Zsilavecz, M., Roth, H. J. 2010. Medizinische Chemie: Targets, Arzneistoffe, Chemische Biologie. Deutscher Apotheker Verlag, Stuttgart.

[141] WHO Model List of Essential Medicines – 23nd list. 2023. https://www.who.int/publications/i/item/WHO-MHP-HPS-EML-2023.02 (Accessed 29 Sep 2023).

[142] Thabet, Y., Walsh, J., Breitkreutz, J. 2018. Flexible and precise dosing of enalapril maleate for all paediatric age groups utilizing orodispersible minitablets. Int. J. Pharm. 541(1-2), 136-142. https://doi.org/10.1016/j.ijpharm.2018.02.037

[143] Neubeck, M. Commentary on Ph. Eur. 9.0, 2017. 57th supply, enalapril maleate. In: Commentary on the European Pharmacopoeia. Wissenschaftliche Verlagsgesellschaft, Stuttgart.

[144] Ip, D. P., Brenner, G. S. 1987. Enalapril maleate. In: Florey, K. (Ed.), Analytical profiles of drug substances. Academic Press, Cambridge, MA, USA. 16, 207-243.

[145] Her, L. H., Wang, X., Shi, J., Choi, H. J., Jung, S. M., Smith, L. S., Wu, A. H., Bleske, B. E., Zhu, H. J. 2021. Effect of CES1 genetic variation on enalapril steady-state pharmacokinetics and pharmacodynamics in healthy subjects. Br. J. Clin. Pharmacol. 87 (12), 4691-4700. https://doi.org/10.1111/bcp.14888

[146] Verbeeck, R. K., Kanfer, I., Löbenberg, R., Abrahamsson, B., Cristofoletti, R., Groot, D. W., Langguth, P., Polli, J. E., Parr, A., Shah, V. P., Mehta, M., Dressman, J. B. 2017. Biowaiver monographs for immediate-release solid oral dosage forms: enalapril. J. Pharm. Sci. 106, 1933-1943. https://doi.org/10.1016/j.xphs.2017.04.019

[147] Dhareshwar, S. S. 2007. Case study: Enalapril: A prodrug of enalaprilat. In: Stella, V. J., Borchardt, R. T., Hageman, M. J., Oliyai, R., Maag, H., Tilley, J. W. (Eds.), Prodrugs. Biotechnology: Pharmaceutical Aspects, V. Springer, New York, 1221-1229. https://doi.org/10.1007/978-0-387-49785-3_39

[148] Moffat, A. C., Osselton, M. D., Widdop, B. 2004. Clarke's Analysis of Drugs and Poisons. Pharmaceutical Press, London. 2, 971-973.

[149] Lick, I. D., Villalba, M. L., Gavernet, L. 2012. Synthesis of diketopiperazine: a kinetic study by means of thermoanalytical methods. Thermochim. Acta. 527, 143-147. https://doi.org/10.1016/j.tca.2011.10.020

[150] Lin, S.-Y., Wang, S.-L., Chen, T.-F., Hu, T.-C. 2002. Intramolecular cyclization of diketopiperazine formation in solid-state enalapril maleate studied by thermal FT-IR microscopic system. Eur. J. Pharm. Biopharm. 54, 249-254. https://doi.org/10.1016/S0939-6411(02)00053-X

[151] Gómez Pineda, E. A., Martins Ferrarezi, A. D., Ferrarezi, J. G., Winkler Hechenleitner, A. A. 2005. Thermal decomposition of enalapril maleate studied by dynamic isoconversional method. J. Therm. Anal. Calorim. 79, 259-262. https://doi.org/10.1007/s10973-005-0045-7

[152] Jagtap, A., Bhaskar, M. 2013. Evaluation of antidepressant and antinociceptive activity of escitalopram. Ind. J. Pharm. Edu. Res. 47, 97-102.

[153] Burke, W. J. 2002. Escitalopram. Expert. Opin. Investig. Drugs. 11 (10), 1477-1486. https://doi.org/10.1517/13543784.11.10.1477

[154] Pinto, B. V., Ferreira, A. P. G., Cavalheiro, E. T. G. 2018. Thermal degradation mechanism for citalopram and escitalopram. J. Therm. Anal. Calorim. 133 (3), 1509-1518. https://doi.org/10.1007/s10973-018-7226-7

[155] Cipriani, A., Furukawa, T. A., Salanti, G., Geddes, J. R., Higgins, J. P. T., Churchill, R., Watanabe, N., Nakagawa, A., Omori, I. M., McGuire, H., Tansella, M., Barbui, C. 2009. Comparative efficacy and acceptability of 12 new-generation antidepressants: a multiple-treatments meta-analysis. Lancet 373 (9665), 746-758. https://doi.org/10.1016/S0140-6736(09)60046-5

[156] Cipriani, A., Santilli, C., Furukawa, T. A., Signoretti, A., Nakagawa, A., McGuire, H., Churchill, R., Barbui, C. 2009. Escitalopram versus other antidepressive agents for depression. Cochrane Database Syst. Rev. (2), CD006532.

[157] Gartlehner, G., Hansen, R. A., Morgan, L. C., Thaler, K., Lux, L., Van Noord, M., Mager, U., Thieda, P., Gaynes, B. N., Wilkins, T., Strobelberger, M., Lloyd, S., Reichenpfader, U., Lohr, K. N. 2011. Comparative benefits and harms of second-generation antidepressants for treating major depressive disorder: an updated meta-analysis. Ann. Intern. Med. 155 (11), 772-785.

[158] Waugh, J., Goa, K. L. 2003. Escitalopram: a review of its use in the management of major depressive and anxiety disorders. CNS Drugs. 17, 343-362. https://doi.org/10.2165/00023210-200317050-00004

[159] Kirino, E. 2012. Escitalopram for the management of major depressive disorder: a review of its efficacy, safety, and patient acceptability. Patient Prefer. Adher. 6, 853-861. https://doi.org/10.2147/ppa.s22495

[160] O'Donnell, J. M., Shelton, R. C. 2015. Drug therapy of depression and anxiety disorders. In: Brunton, L. L., Chabner, B. A., Knollmann, B. C. (Eds.), Goodman & Gilman's: The Pharmacological Basis of Therapeutics, 12th ed. McGraw Hill. https://accesspharmacy.mhmedical.com/content.aspx?bookid=1613&sectionid=102158640 (Accessed 29 Sep 2023).

[161] Akay, S., Yang, Y., Kayan, B. 2021. Investigation on the solubility of the antidepressant drug escitalopram in subcritical water. J. Chem. Eng. Data. 66 (6), 2550-2560. https://doi.org/10.1021/acs.jced.1c00148

[162] Neubeck, M. 2017. Commentary on Ph. Eur. 8.8. 2017. 56th supply, escitalopram oxalate. In: Commentary on the European Pharmacopoeia. Wissenschaftliche Verlagsgesellschaft, Stuttgart.

[163] Rao, R. N., Raju, A. N., Narsimha, R. 2008. Isolation and characterization of degradation products of citalopram and process-related impurities using RP-HPLC. J. Sep. Sci. 31 (10), 1729-1738. https://doi.org/10.1002/jssc.200700410

[164] Dhaneshwar, S. R., Mahadik, M. V., Kulkarni, M. J. 2008. Column liquid chromatography-ultraviolet and column liquid chromatography/mass spectrometry evaluation of stress degradation behavior of escitalopram oxalate. J. AOAC Int. 92, 138-147. https://dx.doi.org/10.1093/jaoac/92.1.138

[165] De Diego, H. L., Bond, A. D., Dancer, R. J. 2011. Formation of solid solutions between racemic and enantiomeric citalopram oxalate. Chirality. 23 (5), 408-416. https://doi.org/10.1002/chir.20943

[166] Mohammed, A. A., Algahtani, M. S., Ahmad, M. Z., Ahmad, J. 2021. Optimization of semisolid extrusion (pressure-assisted microsyringe)-based 3D printing process for advanced drug delivery application. Annals of 3D Printed Medicine. 2, 100008. https://doi.org/10.1016/j.stlm.2021.100008

[167] Rauwendaal, C. 2014. 1 – Introduction. In: Rauwendaal, C. (Ed.), Polymer extrusion. 5th ed. Carl Hanser Verlag, Munich, 1-10. https://doi.org/10.3139/9781569905395.001

[168] Wilson, M., Williams, M. A., Jones, D. S., Andrews, G. P. 2012. Hot-melt extrusion technology and pharmaceutical application. Ther. Deliv. 3 (6), 787-97. https://doi.org/10.4155/tde.12.26

[169] Deshkar, S., Rathi, M., Zambad, S., Gandhi, K. 2021. Hot melt extrusion and its application in 3D printing of pharmaceuticals. Curr. Drug Deliv. 18 (4), 387-407. https://doi.org/10.2174/1567201817999201110193655

[170] Luker, K. 2012. Single-screw extrusion: principles. In: Douroumis, D. (Ed.), Hot-melt extrusion: Pharmaceutical applications. John Wiley & Sons Ltd, Chichester, 1-21. https://doi.org/10.1002/9780470711415.ch1

[171] Leister, D., Geilen, T., & Geissler, T. 2012. Twin-screw extruders for pharmaceutical hot-melt extrusion: technology, techniques and practices. In: Douroumis, D. (Ed.), Hot-Melt Extrusion: Pharmaceutical Applications. John Wiley & Sons Ltd, Chichester, 23-42. https://doi.org/10.1002/9780470711415.ch2

[172] Almeida, A., Claeys, B., Remon, J. P., & Vervaet, C. 2012. Hot-melt extrusion developments in the pharmaceutical industry. In: Douroumis, D. (Ed.), Hot-Melt Extrusion: Pharmaceutical Applications. John Wiley & Sons Ltd, Chichester, 43-69. https://doi.org/10.1002/9780470711415.ch3

[173] Hitzer, P., Bäuerle, T., Drieschner, T., Ostertag, E., Paulsen, K., van Lishaut, H., Lorenz, G., Rebner, K. 2017. Process analytical techniques for hot-melt extrusion and their application to amorphous solid dispersions. Anal. Bioanal. Chem. 409, 4321-4333. https://doi.org/10.1007/s00216-017-0292-z

[174] Nair, A. R., Lakshman, Y. D., Anand, V. S. K, Sree, K. S. N., Bhat, K., Dengale, S. J. 2020. Overview of extensively employed polymeric carriers in solid dispersion technology. AAPS PharmSciTech. 21 (8), 309. https://doi.org/10.1208/s12249-020-01849-z

[175] Bhujbal, S. V., Mitra, B., Jain, U., Gong, Y., Agrawal, A., Karki, S., Taylor, L. S., Kumar, S., Tony Zhou, Q. 2021. Pharmaceutical amorphous solid dispersion: a review of manufacturing strategies. Acta Pharm. Sin. B. 11 (8), 2505-2536. https://doi.org/10.1016/j.apsb.2021.05.014

[176] Thakkar, R., Thakkar, R., Pillai, A., Ashour, E. A., Repka, M. A. 2020. Systematic screening of pharmaceutical polymers for hot melt extrusion processing: a comprehensive review. Int. J. Pharm. 576, 118989. https://doi.org/10.1016/j.ijpharm.2019.118989

[177] Kolter, K., Karl, M., Gryczke, A. 2012. Hot-melt extrusion with BASF Pharma polymers. Ludwigshafen, Germany: BASF SE 2012.

[178] Aho, J., Edinger, M., Botker, J., Baldursdottir, S., Rantanen, J. 2016. Oscillatory shear rheology in examining the drug-polymer interactions relevant in hot melt extrusion. J. Pharm. Sci. 105, 160-167. http://dx.doi.org/10.1016/j.xphs.2015.11.029

[179] Repka, M. A., Shah, S., Lu, J., Maddineni, S., Morott, J., Patwardhan, K., Mohammed N. N. 2012. Melt extrusion: process to product. Expert Opin. Drug Deliv. 9 (1), 105-125. https://doi.org/10.1517/17425247.2012.642365

[180] Konta, A. A., García-Piña, M., Serrano, D. R. 2017. Personalised 3D printed medicines: which techniques and polymers are more successful? Bioengineering. 4, 79. https://doi.org/10.3390/bioengineering4040079

[181] Khinast, J., Rantanen, J., Sandler, N., & Ihalainen, P. 2017. Perspectives of printing technologies in continuous drug manufacturing. In: Kleinebudde, P., Khinast, J., Rantanen, J. (Eds.), Continuous Manufacturing of Pharmaceuticals. John Wiley & Sons Ltd, Chichester, 525-549. https://doi.org/10.1002/9781119001348.ch16

[182] Pietrzak, K., Isreb, A., Alhnan, M. A. 2015. A flexible-dose dispenser for immediate and extended release 3D printed tablets. Eur. J. Pharm. Biopharm. 96, 380-387. https://doi.org/10.1016/j.ejpb.2015.07.027

[183] Govender, R., Kissi, E. O., Larsson, A., Tho, I. 2021. Polymers in pharmaceutical additive manufacturing: a balancing act between printability and product performance. Adv. Drug Deliv. Rev. 177, 113923. https://doi.org/10.1016/j.addr.2021.113923

[184] Pereira, G. G., Figueiredo, S., Fernandes, A. I., Pinto, J. F. 2020. Polymer selection for hot-melt extrusion coupled to fused deposition modelling in pharmaceutics. Pharmaceutics. 12 (9), 795. https://doi.org/10.3390/pharmaceutics12090795

[185] Alhijjaj, M., Nasereddin, J., Belton, P., Qi, S. 2019. Impact of processing parameters on the quality of pharmaceutical solid dosage forms produced by fused deposition modeling (FDM). Pharmaceutics. 11 (12), 633. https://doi.org/10.3390/pharmaceutics11120633

[186] Jamróz, W., Szafraniec, J., Kurek, M., Jachowicz, R. 2018. 3D printing in pharmaceutical and medical applications - Recent achievements and challenges. Pharm. Res. 35 (9), 176. https://doi.org/10.1007/s11095-018-2454-x

[187] Ameeduzzafar, Nabil K. A., Md, R., Syed Nasir, A. B., Mohd, A., Muhammad Masood, A., Mohammad, F. 2018. 3D printing technology in design of pharmaceutical products. Curr. Pharm. Des. 24 (42), 5009-5018. https://doi.org/10.2174/1381612825666190116104620

[188] Skowyra, J., Pietrzak, K., Alhnan, M. A. 2015. Fabrication of extended-release patient-tailored prednisolone tablets via fused deposition modelling (FDM) 3D printing. Eur. J. Pharm. Sci. 68, 11-17. https://doi.org/10.1016/j.ejps.2014.11.009

[189] Repka, M. A., Battu, S. K., Upadhye, S. B., Thumma, S., Crowley, M. M., Zhang, F., Martin, C., & McGinity, J. W. 2007. Pharmaceutical applications of hot-melt extrusion: part II. Drug Dev. Ind. Pharm. 33 (10), 1043-1057. https://doi.org/10.1080/03639040701525627

[190] International Council for Harmonisation of Technical Requirements for Pharmaceuticals for Human Use. https://www.ich.org/ (Accessed 29 Sep 2023).

[191] International Council for Harmonisation of Technical Requirements for Pharmaceuticals for Human Use. ICH Guidelines. https://www.ich.org/page/ich-guidelines (Accessed 29 Sep 2023).

[192] European Medicines Agency. Quality guidelines. https://www.ema.europa.eu/en/human-regulatory/research-development/scientific-guidelines/quality-guidelines (Accessed 29 Sep 2023).

[193] European Medicines Agency. 2013. Guideline on pharmaceutical development of medicines for paediatric use. https://www.ema.europa.eu/en/documents/scientific-guideline/guideline-pharmaceutical-development-medicines-paediatric-use_en.pdf (Accessed 29 Sep 2023).

[194] European Medicines Agency. 2007. Guideline on excipients in the dossier for application for marketing authorisation of a medicinal product – Revision 2. https://www.ema.europa.eu/en/documents/scientific-guideline/guideline-excipients-dossier-application-marketing-authorisation-medicinal-product-revision-2_en.pdf (Accessed 29 Sep 2023).

[195] Quodbach, J., Bogdahn, M., Breitkreutz, J., Chamberlain, R., Eggenreich, K., Elia, A. G., Gottschalk, N., Gunkel-Grabole, G., Hoffmann, L., Kapote, D. Kipping, T., Klinken, S., Loose, F., Marquetant, T., Windolf, H., Geißler, S., Spitz, T. 2021. Quality of FDM 3D printed medicines for pediatrics: considerations for formulation development, filament extrusion, printing process and printer design. Ther. Innov. Regul. Sci. 56 (6), 910-928. https://doi.org/10.1007/s43441-021-00354-0

[196] European Medicines Agency. 2017. 2000. ICH Q 7 Good manufacturing practice for pharmaceutical ingredients – Step 5. https://www.ema.europa.eu/en/documents/scientific-guideline/ich-q-7-good-manufacturing-practice-active-pharmaceutical-ingredients-step-5_en.pdf (Accessed 29 Sep 2023).

[197] European Medicines Agency. 2006. ICH Q 3B (R2) Impurities in new drug products – Step 5. https://www.ema.europa.eu/en/documents/scientific-guideline/ich-q-3-b-r2-impurities-new-drug-products-step-5_en.pdf (Accessed 29 Sep 2023).

[198] European Medicines Agency. 1995. ICH Q 2 (R1) Validation of analytical of analytical procedures: Text and Methodology – Step 5. https://www.ema.europa.eu/en/documents/scientific-guideline/ich-q-2-r1-validation-analytical-procedures-text-methodology-step-5_en.pdf (Accessed 29 Sep 2023).

2 Publication 1: Quality of FDM 3D Printed Medicines for Pediatrics

Pretext

It has been shown in literature that 3D printed dosage forms can be produced in the context of personalised therapy using the fused deposition modeling (FDM) 3D printing process and that the dose can be adjusted to the individual needs of the patient. FDM 3D printing thus enables the production of 3D printed dosage forms for paediatric patients, but still leaves open considerations regarding the assessment of the quality of the 3D printed dosage forms. Due to the lack of understanding of critical quality attributes and process parameters in the production of 3D printed medicines for paediatrics, the review will provide an overview of the quality aspects and measures related to the manufactured extrudates as well as the 3D printed dosage forms from the perspective of the PolyPrint consortium. In addition, approaches for quality assurance during the printing process and for the printed dosage form will be presented and requirements for a GMP-compliant printer will be outlined.

Evaluation of authorship

The following research paper has been published in Therapeutic Innovation & Regulatory Science in 2022. Julian Quodbach, Malte Bogdahn, Karin Eggenreich, Thomas Kipping and Simon Geißler were responsible for conceptualisation, writing, editing. Jörg Breitkreutz, Rebecca Chamberlain, Alessandro Giuseppe Elia, Nadine Gottschalk, Gesine Gunkel-Grabol, Lena Hoffmann, Dnyaneshwar Kapote, Stefan Klinken, Fabian Loose, Tristan Marquetant and Hellen Windolf were responsible for writing. Dnyaneshwar Kapote and Tilmann Spitz were responsible for writing, editing.

author/co-author	idea [%]	study design [%]	experimental [%]	evaluation [%]	manuscript [%]
Julian Quodbach	12.5	5.9	0	5.9	15
Malte Bogdahn	5	5.9	0	5.9	5
Jörg Breitkreutz	5	5.9	0	5.9	5
Rebecca Chamberlain	5	5.9	100	5.9	5
Karin Eggenreich	5	5.9	0	5.9	5
Alessandro-Guiseppe Elia	5	5.9	0	5.9	5
Nadine Gottschalk	5	5.9	0	5.9	5
Gesine Gunkel-Grabole	5	5.9	0	5.9	5
Lena Hoffmann	5	5.9	0	5.9	5
Dnyanshewar Kapote	5	5.9	0	5.9	5
Thomas Kipping	5	5.9	0	5.9	5
Stefan Klinken	5	5.9	0	5.9	5
Fabian Loose	5	5.9	0	5.9	5
Tristan Marquetant	5	5.9	0	5.9	5
Hellen Windolf	5	5.9	0	5.9	5
Simon Geißler	12.5	5.9	0	5.9	5
Tilman Spitz	5	5.9	0	5.9	10

Quality of FDM 3D Printed Medicines for Pediatrics: Considerations for Formulation Development, Filament Extrusion, Printing Process and Printer Design

Julian Quodbach[1] · Malte Bogdahn[2] · Jörg Breitkreutz[1] · Rebecca Chamberlain[1] · Karin Eggenreich[4] · Alessandro Giuseppe Elia[3] · Nadine Gottschalk[2] · Gesine Gunkel-Grabole[3] · Lena Hoffmann[1] · Dnyaneshwar Kapote[4] · Thomas Kipping[3] · Stefan Klinken[1] · Fabian Loose[5] ·Tristan Marquetant[3] · Hellen Windolf[1] · Simon Geißler[2] · Tilmann Spitz[5]

[1]Institute of Pharmaceutics and Biopharmaceutics,
Heinrich Heine University Düsseldorf, Düsseldorf, Germany

[2]Merck Healthcare KGaA, Darmstadt, Germany

[3]Merck Life Science KGaA, Darmstadt, Germany

[4]Gen-Plus GmbH & Co. KG, München, Germany

[5]Laboratory for Manufacturing Systems,
University of Applied Sciences Cologne, Cologne, Germany

Ther. Innov. Regul. Sci. 56 (2022) 910-928

Abstract

3d printing is capable of providing dose individualization for pediatric medicines and translating the precision medicine approach into practical application. In pediatrics, dose individualization and preparation of small dosage forms is a requirement for successful therapy, which is frequently not possible due to the lack of suitable dosage forms. For precision medicine, individual characteristics of patients are considered for the selection of the best possible API in the most suitable dose with the most effective release profile to improve therapeutic outcome. 3d printing is inherently suitable for manufacturing of individualized medicines with varying dosages, sizes, release profiles and drug combinations in small batch sizes, which cannot be manufactured with traditional technologies. However, understanding of critical quality attributes and process parameters still needs to be significantly improved for this new technology. To ensure health and safety of patients, cleaning and process validation needs to be established. Additionally, adequate analytical methods for the in-process control of intermediates, regarding their printability as well as control of the final 3d printed tablets considering any risk of this new technology will be required. The PolyPrint consortium is actively working on developing novel polymers for fused deposition modeling (FDM) 3d printing, filament formulation and manufacturing development as well as optimization of the printing process, and the design of a GMP-capable FDM 3d printer. In this manuscript, the consortium shares its views on quality aspects and measures for 3d printing from drug-loaded filaments, including formulation development, the printing process, and the printed dosage forms. Additionally, engineering approaches for quality assurance during the printing process and for the final dosage form will be presented together with considerations for a GMP-capable printer design.

Article available online at:

https://doi.org/10.1007/s43441-021-00354-0

Introduction

The general principle of pharmaceutical 3d printing, or additive manufacturing, renders this approach a promising candidate for the automated manufacturing of solid pediatric medicines [1]. Solid medicines have significant benefits over the use of liquids for the treatment of children. They provide a high microbial stability, good chemical and physical stability, enable controlled release properties and demonstrate high dosing accuracy [2]. With common manufacturing approaches, dosages can be varied only incrementally in certain ranges. 3d printing enables manufacturing of medicines with precise and fully variable dosing. Dosage forms are printed layer-by-layer in a shape predefined in a computer aided design (CAD) software. In theory, every imaginable size and shape can be printed. A direct consequence of this approach is the ability to modify the dosage simply and conveniently, a lack of which is widely recognized as a major hurdle in pediatric therapy [3]. Besides the inherently possible size adaption, which is key to improve acceptability [4], 3d printing techniques also allow the manufacturing of small batches down to a single individual dosage form for a given patient.

While several 3d printing techniques exist and are investigated for pharmaceutical use [5], *fused deposition modeling (FDM)* emerges as one of the most interesting technologies for the manufacturing of pediatric medicines. In FDM, filaments, drug loaded polymer wires, are fed into the printhead of the 3d printer. In the printhead, the filament is heated and extruded through a nozzle on a temperature-controlled print bed. A kinematic system allows movement of the printhead in x-, y-, and z-direction respective to the printhead, enabling the layer-wise deposition of the polymer-drug matrix until the dosage form is printed. Filaments are manufactured in a hot-melt extrusion (HME) step, which has to be performed industrially due to the required equipment, environment, and process understanding. This results in two main advantages. Firstly, a properly developed formulation and hot-melt extrusion process result in a high-quality intermediate that undergoes proper quality testing. Secondly, the active pharmaceutical ingredient (API) is bound in a polymer matrix within the filament, significantly reducing the risk of drug exposure for the professional operating the printer. The combination of these advantages makes FDM the most promising candidate for manufacturing of (pediatric) medicines also in decentralized settings, e.g., hospitals, compounding centers and community pharmacies. Other technologies require either the manufacturing of aqueous intermediates that cannot be prepared easily industrially due to the risk of contamination during storage [6] or the handling of powders in the final printing step, e.g., binder jetting and selective laser sintering [5], which bears a high risk of operator exposure. If a semi-solid formulation is prepared in decentralize settings, proper quality control of the API distribution within the semi-solid and printed dosage forms requires a significant analytical effort that cannot be performed for individual batches.

While many publications cover proof-of-concept studies of novel dosage form designs and approaches to formulation and process development [7,8] quality consideration of excipients, formulations, processes, filaments and medicines are frequently mentioned but rarely formalized. This lack was recognized by the United States Pharmacopeia (USP) and the International Association for Pharmaceutical Technology (APV) who co-organized a 4-day workshop on quality and standards considerations of 3d printed medicines (Homepage workshop). Even though quality aspects are mentioned for dosage forms for adult drug therapy, no publications about the quality of pediatric 3d printing are available until now.

This publication aims to remedy this issue. The authors are members of the PolyPrint project [9] a project funded by the German Federal Ministry of Education and Research (BMBF). The project consortium exists of the companies Merck KGaA and Gen-Plus, the Laboratory for Manufacturing Systems of the University of Applied Sciences Cologne and the Institute of

Pharmaceutics and Biopharmaceutics at Heinrich Heine University Düsseldorf. In the project, novel polymers for pharmaceutical FDM 3d printing are developed and thoroughly tested and benchmarked. Additionally, a novel type of FDM printer is developed to enable high-quality and cGMP compliant 3d printing of medicines. Here, we reflect on the status of the complete manufacturing process of 3d printed pediatric medicines beginning with the raw materials and ending with the final dosage form. We highlight existing shortcomings and provide guidance based on the experience gathered in the PolyPrint project.

Key Attributes of Raw Materials

Quality Aspects of Pharmaceutical Excipients

Pediatric formulation developments are obliged to follow the guidance of the EMA ensuring the overarching goal: “The development of pediatric formulations and presentations is necessary to ensure that children of all ages and their caregivers have access to safe and accurate dosage forms of medicines.”[10]

More detailed information is provided in the “Guideline on pharmaceutical development of medicines for pediatric use” [11]. In general, solid oral dosage forms such as tablets and capsules can offer advantages of greater stability, accuracy of dosing and improved portability over liquid formulations. To assure suitable swallowability the size of tablets and capsules should be kept as small as possible [2].

The choice of excipients plays an important role in pediatric formulation development, both for safety and acceptability of the resulting dosage forms. The physiology of neonates and infants differs considerably from that of adults. They exhibit significantly different clearance and volume of distribution as well as differences in the metabolic profile [12]. Prominent excipient examples for the resulting challenges and issues are propylene glycol or sorbitol in infants. Also, polyethylene glycol (PEG) - a useful additive for filament plasticity and solubility enhancement – needs careful consideration regarding maximum intake. While studies confirm safe use of, e.g., PEG 3350-4000 as laxative, undesired laxative effects and potential gastroinstestinal disorders limit the use of PEG to 10 mg/kg/d [13].

Looking at FDM based 3d printed formulations, usually the polymer makes up more than 50% of the formulation. Given the comparatively high intake of these excipients, the safety of polymers and additives (glidants, plasticizers) in pediatric formulations is a very important factor, especially if (partial) degradation of the polymer in the GIT is to be expected. Therefore, not only polymer but also degradants and synthesis constituents of the polymer need to be carefully integrated into the safety assessment for pediatric medications. To date, several pharmaceutical polymers, such as methacrylates and ethylcellulose, are commercialized in pediatric products. Unfortunately, most polymers are used in comparatively low amounts as coating agents for taste masking and release modification [14]. Little information is available for polymers used as matrix agent and related high daily intake. Although observed adverse reactions from coated formulations might be used to prevent further incompatibilities, the maximum acceptable intake for children is critical and not easily derived from toxicological studies performed in adults. An important tool for assessing the safety of relevant excipients is the STEP database (Safety and Toxicity of Excipients for Pediatrics) [15].

In addition to safety, the taste sensation of excipients needs to be carefully considered. Polymers and additives should be taste- and odorless and ideally offer opportunities for obscuration of taste (see subsection on taste masking). The important decision factors affecting the use of excipients are summarized by Yochana et al.: “Excipients for pediatric formulations should be carefully selected with reference to the age of the pediatric population,

ADME developmental changes, and duration of treatment to ensure safety and efficacy of such formulations in pediatric population." [16]

Polymer Requirements – Limitations in FDM

In recent years, the application of thermoplastic polymers in pharmaceutical development of 3d printed products via FDM has gained increasing interest. A multitude of different material requirements need to be fulfilled by the polymer for these applications, as illustrated in Fig. 1 (further details on these parameters can be found in the supplementary information in Table S1). Here, we summarized relevant properties and parameters which influence the suitability of given polymers or APIs, respectively. For an overview of different polymer families and a selection of marketed products in the field of hot-melt extrusion, the reader is referred to Simoes et al. [17,18]. 3d printing using the FDM technique requires further polymer prerequisites [19] in addition to the parameters important in HME development, which typically depend on the product properties and the utilized API. During an FDM 3d printing process, the polymeric filament is subject to significant mechanical forces. A specific mechanical profile is required due to "pinching" of these filaments between two feeding gears in the printhead. Filaments carrying a high Young's modulus (> 300 N/mm^2, depending on printhead) can be conveyed without breakage or deformation [20,21]. At the same time, the tensile strength and the brittleness of the extrudates are crucial parameters for successful printing [19,21–28]. The latter of which may be assessed using the three-point bending test (breaking distance > 1 mm – 1.5 mm [21,22] and breaking stress > 2941 – 3126 g/mm^2 [22]). Nasereddin et al. evaluated a selection of the most commonly used polymers in FDM and developed a screening method to assess their brittleness including these parameters and thus evaluate printability [24].

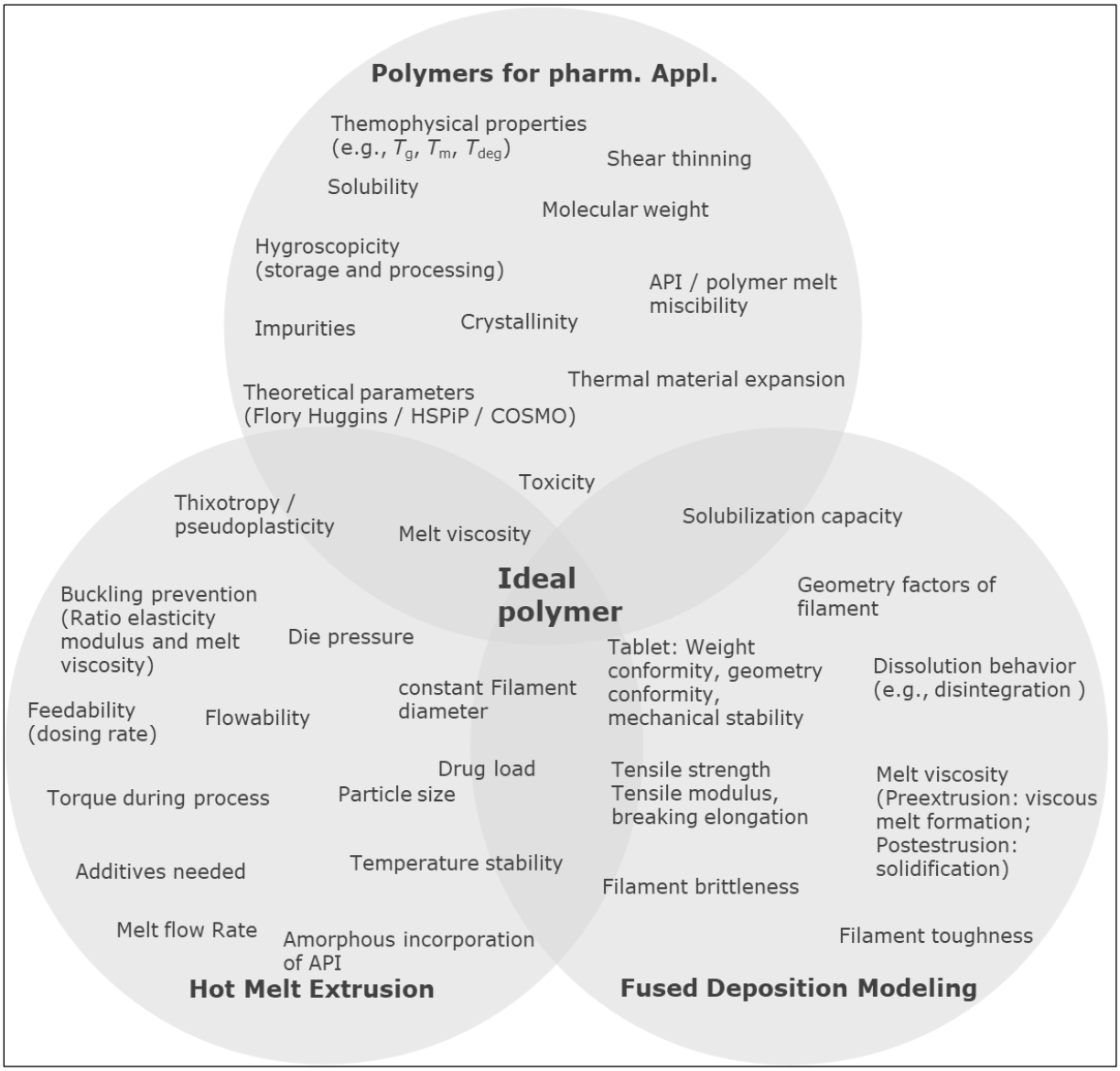

Figure 1 Selection of Parameters That are Relevant for Pharmaceutical Application of Polymers, Particularly in HME and FDM.

Taste Masking

Taste is an important sensation to be considered in pharmaceutical development. Taste aversiveness might impact patients' compliance and medication adherence. Sensory components of both the olfactory and the gustatory sensations have to be distinguished. Whereas substances which should develop the smell as an olfactory signal need to be volatile under the conditions of drug administration, the gustatory system is directly based on the tongue comprising different types of taste buds and papillae where the sensory receptors and ion channels for salty, sour, sweet, bitter, and umami taste are located. Depending on the properties of the poorly tasting components, various taste-masking techniques are available [14]. In pharmaceutical printing technologies, most of the proposed taste-masking approaches can be applied although scientific papers or patents are scarce:

(a) One obvious approach is to mask the unpleasant taste of a printed object by the addition of differently tasting excipients, e.g., sweet carbohydrates (sucrose, fructose, glucose), sugar alcohols (mannitol, xylitol, sorbitol) or artificial sweeteners (saccharine,

aspartame, cyclamate or acesulfame). An olfactory signal can be added to the printing formulation using volatile substances such as menthol or more complex organic or synthetic flavors [29]. However, it should be noted that one or more components of these mixtures will partly evaporate during the manufacturing and over storage time changing taste sensation as a key property to be controlled in stability studies.

(b) Unpleasant tasting ingredients can be physically bound within inclusion complexes, e.g., by use of cyclodextrins, or to polyelectrolytes (anionic or cationic polymers) which can also be part of the solid matrix. Entrapping by the printed polymers may be sufficient for taste masking of bitter compounds [30,31].

(c) High viscosity hydrophilic polymers may prevent fast hydration and dissolution of the dosage form, thereby reducing the migration to the taste receptors on the tongue and the resulting taste sensation.

(d) Barriers inside or outside the printed dosage form may shield against quick dissolution and saliva contact.

The taste-masking effect of the applied pharmaceutical measures are usually demonstrated by using advanced dissolution setups [30] or electronic tongues in vitro [32], and human taste panels [31] or animal experiments like the BATA (brief-access taste aversion) model in vivo [33].

Hot-Melt Extrusion of Intermediates for Pediatric 3d Printing

Filament Extrusion – a Question of Homogeneity

The filament required for FDM 3d printing is generated as endless strand via twin-screw hot-melt extrusion. Filament extrusion comprises multiple individual unit operations and processes that must be considered to obtain an overview of relevant quality attributes. To meet quality attributes of products and establish robust processes, the Food and Drug Administration (FDA) recommends quality-by-design (QbD) approaches for formulation and process development [34]. This led to different implementations of QbD in pharmaceutical melt-extrusion processes [34–36]. As mentioned in the section on polymer requirements, the mechanical properties of filaments must allow proper feeding and extrusion from the printhead. Additionally, diameter homogeneity and API distribution are much more important compared to regular hot-melt extrusion processes. Usually, the obtained extrudate is milled or pelletized and a subsequent homogenization of the individual particles is performed. In FDM, the filament is commonly kept intact and printed as it exited the extrusion die. This means that diameter and API distribution inhomogeneities directly reflect in the printed amount of filament and API. This can be an issue for regularly sized dosage forms [37] and even more so for pediatric medicines of lower dose and mass. In this case, even small variations of diameter and API distribution can lead to non-compliance with monographs on the uniformity of dosage units and must be avoided. The API distribution is influenced primarily by the powder feeding process and hot-melt extrusion, the diameter homogeneity by the hot-melt extrusion process.

Powder Feeding

In twin-screw filament extrusion processes feeding of polymers, solid additives and APIs is a critical aspect. Unlike single-screw extruders, twin-screw extruders are run partially filled. Thus, the material flow inside the extruder depends on the flow rate of the feeder used.

Process parameters like the specific feed load (SFL) and residence time distribution (RTD) are directly influenced by the feeding [38]. In Fig. 2 left, a typical residence time distribution curve of a filament extrusion process is shown. On the right, feeding fluctuations are shown in black and the resulting output fluctuations after extrusion are shown in red. The reduction in fluctuations demonstrates the mixing and homogenizing abilities of extruders. As the reduction is not absolute, feeding should be as homogeneous as possible, to reduce output variations.

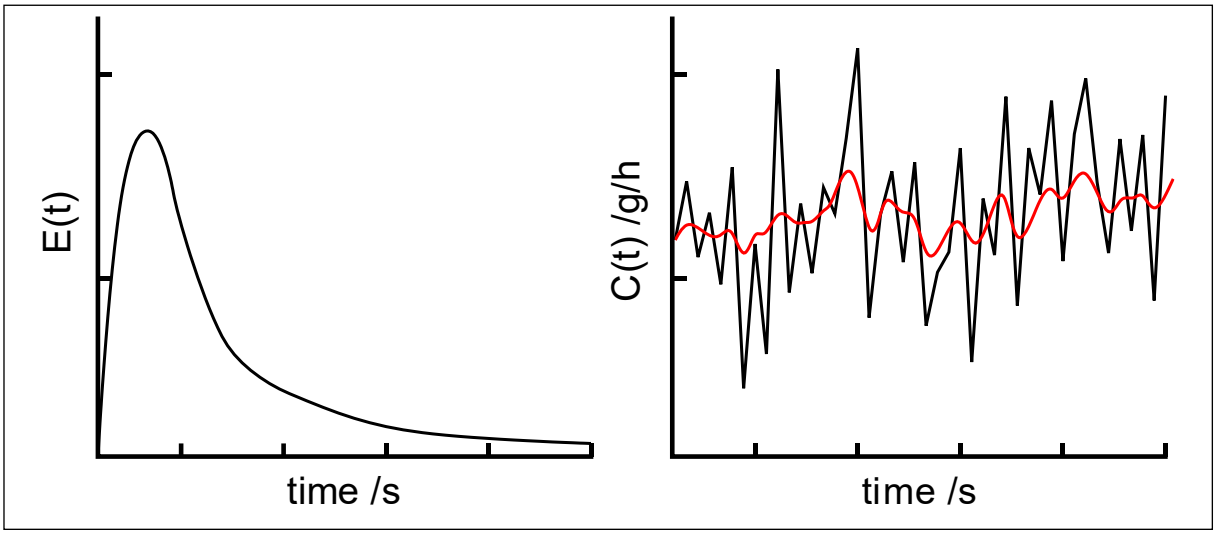

Figure 2 Exemplary Drawing of: (left) a Typical Residence Time Distribution Function of a Hot-Melt Extrusion Process; (right) Fluctuations of the Feed Rate (Black) and Output Fluctuations After Extruder (Red).

Several types of dispensing devices are available for feeding bulk solids. Vibrating trays or screws are a widespread method of conveying the material [39]. Simple devices feed in volumetric mode at a constant actuating variable. In contrast, loss-in-weight or gravimetric feeders are equipped with an integrated load cell that detects fluctuations in the feed rate. The actuating variable is adjusted via a control mechanism, leading to a compensation of fluctuations [40]. Material properties as well as the target feed rate must be considered in selection of the most suitable dosing device [41]. Low dosing rates and poor flow properties result in particularly high demands on equipment attributes [42]. Matarazzo et al. has provided a checklist to assist in the selection of proper feeder equipment [43].

Bulk solid feed is evaluated in several studies usually by using an external scale where the fed material is collected. Data analysis of the dosing curve or its integral can be conducted using statistic parameters like measure of dispersion or target-actual-ratio of moving measures of central tendency [44,45]. Another way is using discrete Fourier transform of dosing fluctuations, which provides information about the materials dosed [46].

Extruding Filaments as Intermediates

The efficiency of the melting process of polymers in HME depends on the properties of the excipients and the extruder design. In general, polymers with low melt viscosities and high thermal conductivities exhibit a more efficient melting process. Changes in the screw design are often necessary to improve the melting process of the powders and to improve mass flow of the melt through the extruder. Otherwise, solid material may block the screws transiently, which can result in increased torque if the melting process is incomplete.

Ponsar et al. highlighted the effect of the extruder barrel fill level on filament homogeneity. The higher the fill level, the lower are the fluctuation of the mean diameter (Fig. 3 left) [37].

Frequently, as diameter fluctuations are not necessarily normal distributed, the inter quartile range of the diameter is used to describe fluctuations. Besides having a measure for fluctuations, it is as important to set limitations for said variations. Usually, deviations of ± 0.02 mm or 0.05 mm from the set value are considered tolerable. By varying the temperature, the polymers, the process setting and the screw configuration in an extruder, the limits are met with varying degrees of success. In Fig. 3 right, the same formulation was extruded at different temperatures and with different screw designs (no kneading zones or two kneading zones). The best batch was extruded at a high temperature of 225°C with no kneading zone and the worst at the same temperature with two kneading zones. These data show the decrease of filament diameter within the ± 0.02 mm or 0.05 mm specification when adding two kneading zones.

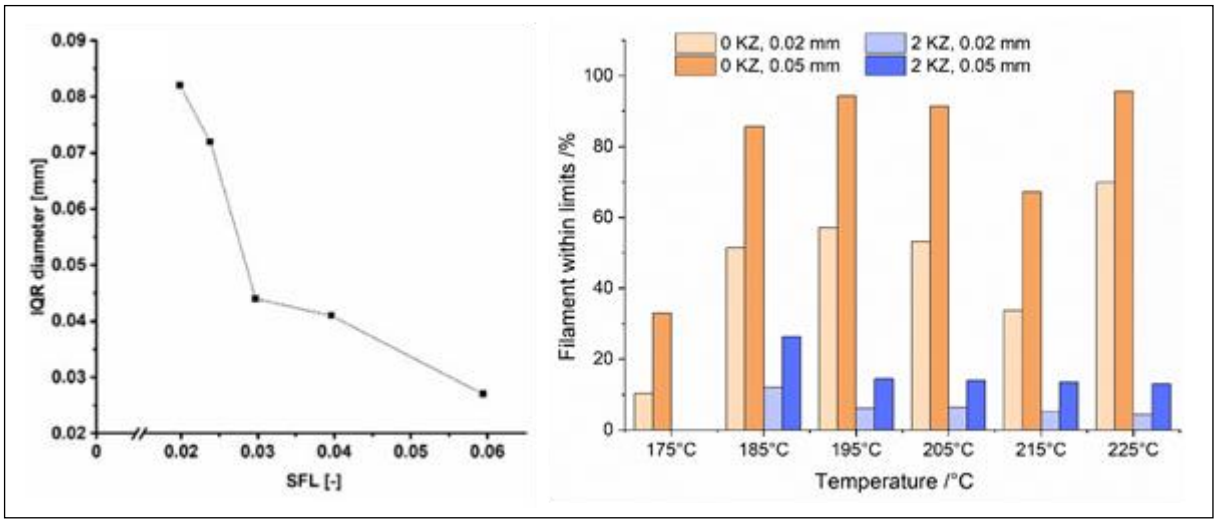

Figure 3 (Left) Interquartile Ranges of Diameter Measurements During Extrusion Correlated with SFL of the Extrusion Process [37], (Right) Amount of Filament Within ± 0.02 and 0.05 mm Specification With or Without Two Kneading Zones (KZ 1: 4x90°,4x60°, 2x30°, KZ 2: 8x60°, Unpublished data).

This observation indicates the importance of a continuous melt flow in the extruder, which is better provided by a screw configuration of only conveying elements. When adding kneading elements, the melt is retained before the kneading zones until enough pressure is build up by the following melt. To increase the homogeneity of the filament diameter further, a melt pump can be attached between the end of the extruder barrel and the die. The purpose of this attachment is to stabilize inevitable melt fluctuations that occur within the hot-melt extrusion process. The pump aligns those fluctuations by metering the melt flow to a very constant rate and therefore a very constant pressure level [47]. This leads to an increase of filament homogeneity since the fluctuations mentioned before are reduced drastically. This was shown by in-process monitoring of filament diameters [48].

After extrusion, it must be considered how to properly cool down the obtained filament. Commercial FDM filaments such as acrylonitrile butadiene styrene copolymer (ABS) or polyether ether ketone (PEEK) are not water soluble and can therefore be cooled down in a water bath. Polymers for pharmaceutical FDM applications are frequently at least partially water soluble and they contain one or more APIs. Consequently, cooling in a water bath cannot be performed, even though it is a highly effective and efficient cooling process. For pharmaceutical applications, proper cooling can only be achieved by either passive cooling on a conveyor belt at atmospheric conditions or by using an air ring or air tunnel [49].

While polymer melt is being pushed out of the nozzle, a phenomenon can occur known in HME as “die swell”. Die swell is the expansion of molten polymer to a larger diameter than determined by the die itself, resulting in a filament thicker than desired. This effect is mainly related to the energy preserved by compression and force alignment of polymer chains being forced through the die, followed by the relaxation of those chains when exiting the die again [50]. The viscoelastic behavior of the melt as well as process parameters are major factors when die swell shall be reduced [37,51]. A reduction of die swell can be achieved by increasing the temperature at the die. Even with thorough optimization, a larger mean diameter than desired will frequently result. To further adjust the mean diameter after extrusion, a pulling unit, e.g., a conveyor belt or the haul- off unit of a winder [37] can be implemented. The speed of haul-off units is variable and defines the final mean diameter of the filament, which can be wound or used as individual strands. Commercial filament diameters are typically 1.75 or 2.85 mm. For pharmaceutical purposes, a lower diameter is beneficial, as potential inhomogeneities of diameter and content will have less of an impact relatively.

In Fig. 4, two prototype extrusion lines are shown. They consist of gravimetric powder feeders, twin-screw hot-melt extruders, cooling units (conveyor belt or cooling line with ring air-knives), laser-based diameter measurement system and optionally a filament winder.

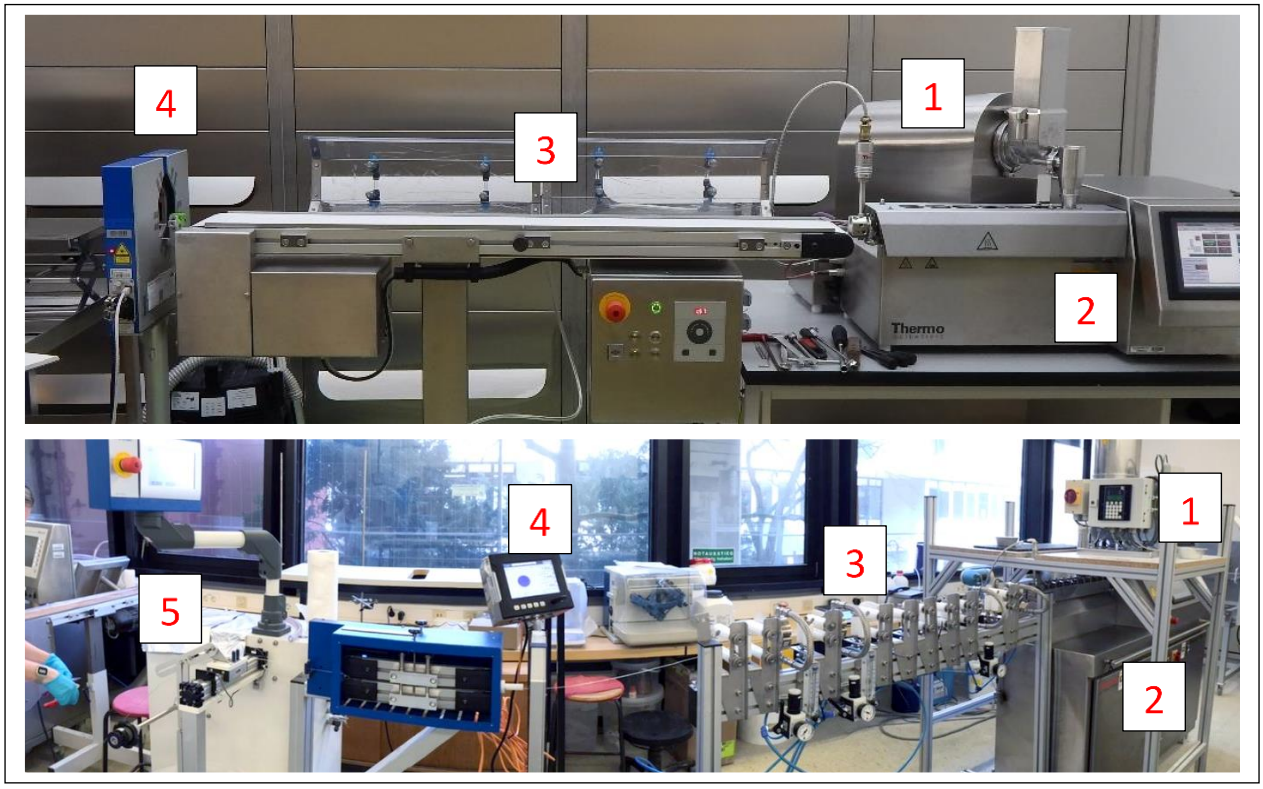

Figure 4 Two Filament Production Lines. (1) Gravimetric Feeders, (2) Twin-Screw Extruders, (3) Cooling Via Conveyor Belt (Top) and Ring Air-Knives (Bottom), (4) Three-Axes Laser Micrometers, (5) Winding Unit.

Characterization of Filaments

To evaluate, optimize and monitor the process of filament production, different analytical tools can be used off-line and in-line.

Off-line Characterization

A simple and useful approach is the visual assessment of API-loaded filaments. This way it is frequently possible to initially assess potential degradation via color changes and possible recrystallization of the active ingredient(s) especially for higher drug loadings and APIs that exhibit thermal sensitivity. As already discussed in the section on polymer requirements, the mechanical properties of filaments are an important factor for the feedability of the formulation that must be analyzed. The mechanical properties of filaments may change over time due to enthalpy relaxation [21] or because the included excipients are hygroscopic. Water absorbed during processing or storage is a powerful plasticizer that lowers the glass transition temperature. Is does not only affect the mechanical properties and appearance, but also drug stability, may induce degradation, and needs to be quantified for this reason [52,53]. In vitro dissolution as per compendial monographs is used to determine the amount of drug dissolved over time and thereby to assess the performance of the formulation (filament/tablet) in regard to release behavior [54]. For the content determination and examination of homogeneous drug distribution as well as characterization of related substances within filaments and tablets, most frequently HPLC analysis is used [55].

In-line Characterization of Filaments via PAT

The physicochemical properties of filaments produced by HME are crucial for the 3d printing process. Quality and performance of the 3d printed tablet and can be examined with PAT tools like spectroscopy, rheometry and optical coherence tomography (OCT) [56]. These tools enable capturing real-time information of process and filament properties during HME non-destructively. Some of the data can be easy to interpret, e.g., diameter and sphericity of filaments determined via multi-axes laser scanning modules (see Fig. 4). Some can be difficult to interpret and may require the preparation of multivariate, quantitative models, for example spectral information. Independent of the data complexity, it can be utilized to monitor the process and initiate corrective actions to reach a desired state and potentially to allow real time release [57]. In the following, relevant technologies are listed.

In-line Spectroscopy

UV-vis spectroscopy has been used and established as PAT tool in HME. Spoerk et al. used in-line UV-vis spectroscopy as an analytical tool for characterizing of active ingredients (Estradiol, Estriol, Ibuprofen) and polymer matrices (ethylene vinyl acetate, Eudragit RL-PO). The studies focused on the quantification of the drug for cleaning-in-place strategies [58]. Wesholowski et al. have investigated in-line UV-vis spectroscopy as a PAT tool for preparing solid dispersions of two APIs (carbamazepine and theophylline) with one polymer (copovidone) [59]. The obtained results revealed the suitability of the implemented PAT tool to quantify the drug load in a typical range for pharmaceutical applications. The range of linearity differed with different formulation and was 5-30% for carbamazepine, whereas that for the theophylline formulations was 2.5-10%. They reported that the efforts to evaluate data was minimal due to univariate data analysis in combination with a measurement frequency of 1 Hz, the system is sufficient for the real-time data acquisition. In-line near infrared (NIR) spectroscopy has also been used to investigate drug–polymer interactions and to validate a method for continuous API quantification during HME processing [60]. Vo et al. demonstrated the use of Fourier transform NIR spectroscopy in conjunction with multivariate analysis (MVA) for in-line API concentration monitoring during a HME process [61]. In this study, they used ketoprofen as model drug, Eudragit L100-55 as matrix polymer and stearic acid as processing aid. A principal component analysis (PCA) model was used to monitor the process state shift in

response to disturbances, such as temperature and material feed rate. Thus, an NIR based quality monitoring methodology can be easily transferred from process development to manufacturing. Saerens et al. evaluated the suitability of Raman spectroscopy as PAT tool for the in-line determination of API concentration and the polymer-drug solid state during HME process [60]. They used different concentration of metoprolol tartrate (10%, 20%, 30%, and 40%) with Eudragit RL PO mixtures, which were extruded and monitored in-line in the die using Raman spectroscopy. A PLS model was developed and validated, which allowed the real-time API concentration determination. They also investigated application of Raman spectroscopy in solid state characterization and found that the mixtures containing solid solution showed broadened Raman peak compared with the solid dispersion.

In-line Rheometry

In-line measurements of the rheological characteristics play an important role in real-time monitoring of torque, influence of drug load, and effect of formulation ingredients on the process. The real time evaluation of rheology data in the extrusion process can be determined by pressure drop inside an extruder die connected to suitable instruments. In-line rheological characterization can enhance process control and understanding [62].

Optical Coherence Tomography (OCT)

OCT, a non-invasive method, is used as an off-line tool for semi-transparent and turbid media. It can be applied to measure parameters such as surface properties of filaments and layer thicknesses, e.g., of coating layers or filaments produced in hot-melt co-extrusion, and uniformity [63]. Koutsamanis and Eggenreich et al. reported the application of OCT to evaluate the integrity of the core/membrane interface and membrane thickness of vacuum compression molding formulations containing progesterone with ethylene vinyl acetate polymer [64].

Characterization of the Solid State

Even though some of the above-mentioned analytical tools can determine certain aspects of solid-state properties, other approaches are commonly used that provide a better understanding of materials. The solid state of an API incorporated in a polymer matrix can have a large impact on the performance of the final dosage form in terms of dissolution rate and bioavailability [65]. Poorly soluble APIs, which make up a large proportion of potential drug candidates [66], can be formulated as amorphous solid dispersions (ASD) where the crystalline structure of the API is broken up and the resulting molecular dispersions are stabilized by a polymer matrix. In contrast, an API can be incorporated into filaments maintaining a crystalline structure [67,68]. The presence or absence of crystalline structures strongly influences printability, such as mechanical [69] and rheological properties of filaments [70]. Consequently, the assessment of crystallinity in filaments is important in process development, quality control and stability studies. Even though this assessment can be supported by in-line measurements, traditional techniques are more widespread.

The formation and stability of the ASD is influenced by solubility and miscibility of the API and the polymer matrix [71]. Thermal and mechanical energy uptake during manufacturing facilitates the dispersion and reduces the number and size of crystal nuclei, which may lead to premature precipitation of API in vivo or reduce physical stability during storage. To maintain the solid state during shipment and storage is important for the ASD itself, but for FDM the second heating cycle during printing needs to be considered, additionally. The thermal impact

may not only impair the chemical stability of the formulation but can also lead to recrystallisation of API [28].

Several techniques can be applied to determine the solid state. Differential scanning calorimetry (DSC) as well as well as X-ray powder diffraction (XRPD) are well-established analytical methods to investigate the solid state of API dispersed in polymer matrices [72]. One caveat is the limit of detection of crystalline fractions in mostly amorphous systems [73]. The detection of small traces of crystalline fraction is possible by the use of polarized light microscopy [74]. However, this method lacks quantitative determination and selectivity.

In regard to the assessment of crystallinity in intermediate and final product the manufacturing process should be considered end to end for FDM printed solid dosage forms.

FDM Printing at Site of Care – Stricter Requirements for Dose Precision and Quality Control

3d printing based on FDM has been state of the art for years and is used primarily in the consumer sector but also in industrial environments. Particularly in industry, a quality demand is placed on the products to be printed from the ground up. Unlike in pharmaceutical industry, however, the focus is primarily on geometric aspects.

Different consumer 3d printers are already being used in pharmaceutical research. One of several issues with off-the-shelf printers is that the amount of active ingredient processed cannot be verified. Thus, the quality of the pharmaceutical products is not verifiable. In contrast to classical manufacturing methods, 3d manufacturing is slow and only few dosage forms are printed [5]. Therefore, destructive quality control approaches are not profitable and in-line testing is unavoidable. Furthermore, there is hardly any system on the market that meets the cleaning requirements of pharmaceutical equipment [75].

In addition to the common requirements of mechanical engineering for the development and market placement of production machines, special requirements are part of the GMP guidelines [76]. For these reasons, it is imperative to rethink 3d printer design and adapt it to the needs of pharmaceutical manufacturing. The following sections highlight some of the most critical components.

Motion System and Overall Printer Design

The most common design in FDM 3d printing is the Cartesian printer, but other forms like the delta printer and the polar printer exist [77]. Cartesian printers operate by linear movement of the printhead in x-, y-, and z-direction respective to the print bed. In most cases, the axes, motors, and drives are designed for general industrial and mechanical engineering purposes and the requirements of the pharmaceutical industry are not considered. For example, many of the moving parts, which are usually lubricated, are not encapsulated and are, therefore, exposed to potential contaminants from filament and product. Since it is required for pharmaceutical production, that all surfaces in contact with the product are cleanable, these elements do not meet the GMP standard [78].

During the development of new machines all requirements for the system are defined beforehand. In addition to the basic functions for a 3d printer almost all machines are designed to be as compact and as inexpensive as possible. To achieve this, many functions are implemented in a small space. When looking at existing printing systems under the prerequisites of the GMP guideline, several problems become apparent. In regular 3d printing

systems, all subsystems such as material handling, material processing, build plate, and motions system are implemented openly in a very confined space. For a GMP-compliant implementation, however, it is recommended to separate all elements and to design individual and well controlled areas (Fig. 5).

For industrial and non-pharmaceutical applications, the print chamber usually does not have to be kept particle-free or sanitized. Axis systems for moving print head or print bed can be placed directly in the printing space. Since outgassing, particle detachment and other sources for (cross-) contamination must be contained or avoided during the print job, this arrangement is not applicable for GMP printers. The printing chamber should be as isolated as possible from all moving elements. In addition, surfaces should not have complex geometries or sharp angles to ensure cleanability.

In addition to the risk of contamination of the printer parts, attention must also be paid to the safety of the operator. During the processing of API's, the user may be exposed to harmful chemicals. For example, in the case of outgassing, it must be ensured that substances cannot endanger the user. For this purpose, the printer should be equipped with appropriate protective devices such as air filters. In the pharmaceutical sector, little research has been done on the possible safety aspects of using 3d printing for the manufacture of pharmaceutical products [78].

Here, it is advisable to use approaches from industrial 3D printing as a starting point. Powder-based printing technologies in particular place great emphasis on user safety. The GMP guidelines stipulate that all surfaces in contact with the product must be made of approved and cleaning-resistant materials, and that these must not have any edges, joints, undercuts or similar [79]. For this reason, all elements should be milled or machined from a single piece of material, if possible.

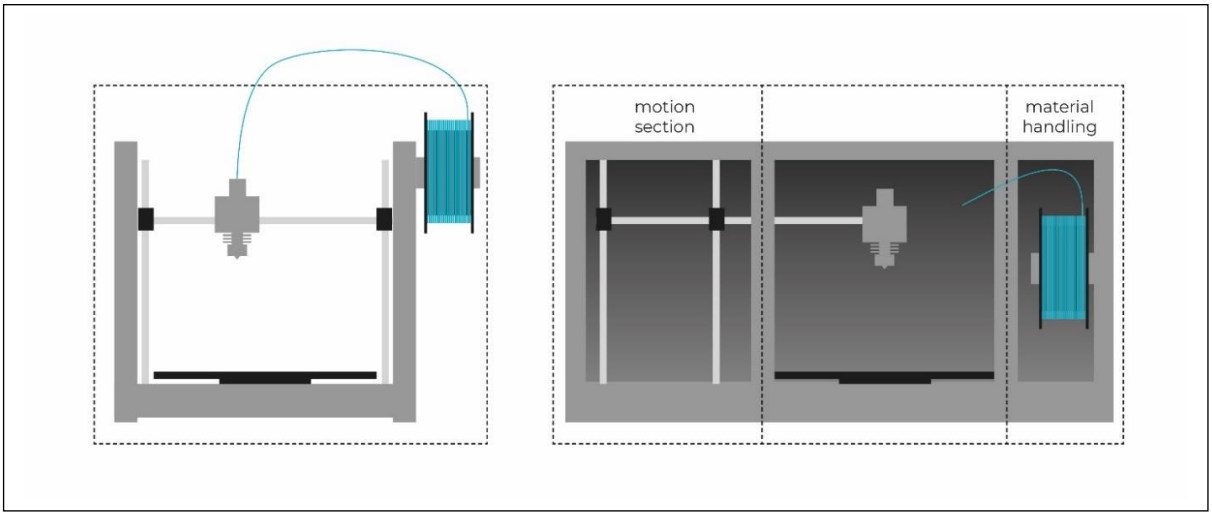

Figure 5 Schematic of an Off-the-Shelf 3D printer (Left) and a 3D printer With Separate Build, Motion, and Material Handling Section (Right).

Feeding Mechanism, Filament, and Filament Storage

In commercially available printers, filament is conveyed in the extruder by two counter-rotating rollers. To increase the conveying force, at least one of the rollers is a gear wheel. This approach to filament transport is not suitable for pharmaceutical materials. The force exerted on the filament might become too high, resulting in slippage. Slippage, in turn, leads to small, usually statically charged filament grains that accumulate in the cavities of the feed roller and on other elements in the printhead. At high conveying resistances, i.e., high melt viscosities, this effect can even lead to breakage and creation of dislodged filament pieces. The consequence of this behavior is that the extruder must be cleaned extensively to avoid cross-contamination. In particular, the complex geometry of the gear wheel(s) with its many cavities prevents efficient cleaning. In addition, damage to the material leads to an undefined geometry of the filament and, thus, to an uncontrolled quantity of deposited material. Breakage of the filament will lead to printing process failure and manual intervention will be required to restart the process.

Traditional FDM 3D printing is based on a spool-based filament supply system. Technical polymers for classical FDM printing are designed and manufactured to display sufficient flexibility to be wound on a spool, but also enough stiffness to be processed by a standard feeding mechanism. As described in the section on key attributes of excipients, pharmaceutical polymers often do not allow reliable feeding and printing easily due to their brittleness or undesirable deformation behavior. A filament provision and supply system must be developed that can handle a greater diversity of mechanical properties. To achieve this, both the bearing and the extruder technology must be completely revised.

Up to 450 m of filament can be wound onto a spool. When printing multiple large components, this is an advantage. For the production of small dosage forms in lower quantities this is not necessary. If a lower amount of material is required, a smaller filament supply that is used up quicker reduces potential issues with the storage stability. Particularly in view of the API cost, smaller units of filaments are to be preferred. In addition, cross-contamination of filament must be avoided during handling so that encapsulation of the filament is necessary. For this reason, the currently selected filament geometry (“endless”) and the bearing units (coils) must be questioned.

The material storage, commonly designed as filament reel, should also be redesigned as part of a separate area. This is realized by some commercial printers that have cartridge systems, but large amounts of material are still wound on spools. We recommended to reduce the amount of material stored in or on the material accumulator. With reduced material amounts, coiled-up, long filaments strands that require feeding rollers or gears are not necessary, solving multiple issues with the current printer design. Omitting spools enables a new design of the storage system which can offer hermetic encapsulation of the filament. This would allow filament storage and transport under controlled conditions, similar to a tablet in a blister. Initial approaches can already be found in printers from the company Stratasys [80]. Yet, these are not suitable for pharmaceutical manufacturing machines without significant modifications.

If filaments are not a continuous long strand anymore and new bearing units are designed, the conveying mechanism needs to be revised, too. Roller or gear-based feeding mechanisms should not be used for this purpose as they facilitate cross-contamination. Piston based mechanisms similar to those already used in certain bioprinters [81,82] would be a superior approach, as slippage and breakage could be prevented.

Hotend and Coldend

One of the most central parts in a 3d printer is the hotend. With the help of electrical heating, the polymer is melted and extruded through a nozzle. Conventional hotends are optimized for high throughput and printing speeds. Technical polymers allow processing at temperatures well above the melting or glass transition temperature to reduce duration of melt formation. The result is a high temperature gradient from the core to the edge of the filament [83]. The use of additive manufacturing in the pharmaceutical environment, on the other hand, requires processing that is particularly gentle on the material, as many APIs are thermo-labile. Nevertheless, high printing speeds must still be achieved for a productive process. It is necessary to optimize the hotend in terms of uniform heat input to reduce the heat strain put on pharmaceutical filaments.

The other components of a common printhead are also not suitable for use in the pharmaceutical manufacturing. To compensate for the high temperatures, the upper parts of the printing core, the coldend, are cooled to prevent or reduce softening of the filament before the actual hotend. Commonly, active air cooling with cooling fins is used. Due to their complex and fine geometry these parts are particularly difficult to clean and increase the risk of cross-contamination. As the hotend is located directly above the product, evaporation of residual solvents, plasticisers and other volatile components is to be expected. They will be distributed in the printing chamber via the cooling air, further increasing the risk of cross-contamination and reducing cleanability. Pharmaceutical print heads must be completely cleanable. Purging with cleaning filaments, what is the common procedure in research, will not suffice to prevent cross-contamination. Since the material is fed through coldend and hotend, all elements that come into contact with the product must be cleaned without residues after each use and before each material change. To avoid changing the complete print head, a system design similar to the design of hot-melt extruders is recommended. Similar to the barrels, the printhead should be demountable and the material touching parts easily accessible [58]. The coldend of the printhead is placed in the print chamber as well and its cooling fins cannot be cleaned properly. Switching to water cooling would solve this issue and provide a more accurate control of the temperature. This has been realized in some non-pharmaceutical systems such as the x500pro from German RepRap [84].

Sensors and Quality Control

A few years ago, 3d printing gained a detrimental reputation of being usable only for prototyping, due to frequent print failures, limited resolution, anisotropic mechanical properties, low production speeds and rough surface finish [85]. The reason for this is a lack of process and quality control. Even though the implementation of in-line quality is beginning in some 3d printing technologies, in FDM such methods are still at the experimental or research stage. The focus is mostly on thermal monitoring (melt pool analysis in selective laser sintering / melting) and layer monitoring [86]. Even though some of these approaches can also be used in a pharmaceutical context, they focus mostly on quality attributes for other manufacturing industries. Relevant pharmaceutical quality attributes cannot be captured with such systems. The use of the sensors applied for control issues only allows accurate control and regulation of the process. However, a quality statement regarding the solid state, API content or printed quantity is not possible. For 3D printers to be used for pharmaceutical manufacturing in the future, additional measures must be undertaken in addition to adapting the mechanical components. A major point is the quality control of the printed product.

Various types of defects in 3d printed parts are described in the literature [86,87]. While structural integrity is key for technical applications of FDM, the doses of incorporated API in the final dosage form is the crucial parameter for medication manufactured by FDM. Especially medications to be used by children need to be manufactured in an accurate way, because the doses for children are typically lower and small deviations in the content of a dosage form result in higher relative over or underdosing potentially harming the patient.

To improve the quality of dosage forms, process control has to be improved as well. In general, three groups of parameters can be identified for in process control.

1. Machine parameters derived from the control electronics. For example, motor and heater current, temperature of nozzle and cooling zone, vibrations etc.

2 Monitoring of the extruded volume or mass of the filament, either derived from measurements described in 1. or measured by dedicated sensors attached to the printer.

3. Non-destructive chemical analysis of the raw material and / or intermediate and final printed product.

The monitoring of machine parameters can be implemented in industrial control systems and do not necessarily rely on additional sensors which might lead to higher machine costs in the end. It has been described in literature to use the current of the feeding motor to detect a blocked nozzle [87,88]. Chemical degradation and under-extrusion related to blocked nozzles is a major concern for the quality and accurate dosing of pharmaceutical dosage forms. In another example, Becker [87,89] used accelerometers to monitor the state of the printer and detect fluctuations in the flow of extruded raw material during the printing process. These substitute parameters can only be used if comparative data are available of the printing process for a specific raw material on a specific printer limiting the application to well understood processes. To circumvent these issues, dedicated sensors can be introduced into the printing system to directly measure the extruded volume or mass. Calculation of the printed dosage may act as a valuable in-process control, assuming that the active ingredient is homogenously distributed in the raw material.

Optical systems were described to measure the distance between printed object and nozzle detecting under-extrusion [90,91] providing error detection during a print process. It is also possible to monitor the movement and quality of filament by a camera [92]. Dosage forms with defects can then be discarded after the printing process and documented in a batch report for documentation. Of course, specialized sensors as well as integrated balances measuring the actual printed mass of filament could be an option to further improve the accuracy of 3d printed oral dosage forms, assuring the quality. For printing at the site of care, implementation of feedback loops based of the obtained data to automatically adjust the printing process of each individual dosage form will enable to meet the claimed dose and lead to an efficient manufacturing process with reduced waste and higher yields resulting in fast supply of high-quality medication to the patients.

Focusing more on the final product than the process itself, chemical analysis of the API incorporated in the printed dosage form could enable real-time release in a clinical printing setup. Different spectroscopic methods were described in the literature to analyze pharmaceutical dosage forms without destroying the samples. It was shown that NIR-chemical imaging of 3d printed objects can be used to measure the amount of printed API [93]. Transmission Raman measurements were reported in literature to investigate the amorphous and crystalline fraction of fenofibrate in solid oral dosage forms [94]. Such methods could be used in future pharmaceutical 3D printers to assure the quality of amorphous solid dispersions. Chemical analysis of printed objects can lead to full batch real-time release of medications

printed at site of care ensuring that the quality of the final product was not negatively influenced by the printing process. Downsides of non-destructive chemical imaging are high costs and large equipment, which might not be easily integrated in the printing platform.

Still, FDM as a digitally controlled manufacturing process opens the opportunity to integrate multiple sensors to not only monitor the quality of the printing process and product but furthermore adjusting critical process parameter on the fly to resemble a true rapid manufacturing process.

3d printed Dosage Forms for Pediatric Use

General Consideration

Only few solid dosage forms have been investigated for their acceptability in children [95]. Of those, even less can be manufactured by 3d printing: minitablets, orodispersible films, (orodispersible) tablets, and capsules. A definite advantage of 3d printing is a freedom of design previously not possible. This is demonstrated by many novel dosage form designs [7,96]. It is likely that such novel designs will also demonstrate high acceptability in children, e.g., because of more appealing coloring and dimensions. However, this has not been demonstrated in clinical trials and this section will focus mostly on the above-mentioned dosage forms. As the resolution of FDM printing is limited, small capsules suitable for pediatric treatment are not sensible to manufacturing via this route. Similarly, printing of orodispersible tablets and minitablets has not been established, yet.

Minitablets and Small Oblong Tablets

Tablets of < 4 mm diameter are usually considered to be minitablets [97]. As they have demonstrated acceptability in neonates, infants and children [2,98] minitablets of 2 mm diameter are considered more frequently than larger ones. Accurate printing of small objects is challenging in general. A typical nozzle diameter is 0.4 mm and tablets with a diameter of 2 mm are only five times larger than the nozzle diameter. These small geometries are on the lower limit of what is possible with the FDM process [99] and dimensional accuracy is difficult to achieve. Due to the small surface area of a single layer the cool down period of the material before the nozzle passes an area a second time is short, which may lead to insufficient mechanical stability of already printed layer. Several strategies are suitable to circumvent such issues. Reduction of print speed is generally associated with higher dimensionally accuracy and improved surface quality. However, throughput and productivity will decrease with lower print speed. The manufacturing order of objects on one build plate can also be changed from sequential printing (complete all layers of one object, then moving on to the next object) to layer-wise printing where the printing layer is changed after the specific layer of all objects is completed. While cooling time per object layer is associated with beneficial effects on dimensional accuracy, frequent changes between objects may introduce additional classes of printing errors like stringing and blobs [100]. Every additional travel movement comes with the risk of oozing filament and therefore inaccuracy of dose. The dosing of smaller tablets is even more challenging than with larger objects because the relative change of incorporated API due to printing defects is more significant. Krause et al. printed objects with a diameter of 4 mm, 3 mm, 2mm and 1.5 mm with decreasing tablet mass and calculated the acceptance value according to Ph. Eur. 2.9.40. While the standard deviation of tablet mass was higher for the largest objects, their acceptance value was lower compared to smaller tablets. These results show that dosing accuracy is especially important for mini tablets and low dose drug forms [99].

Ayyoubi et al. printed spherical tablets with a diameter of 6 mm with channels to improve dissolution rate [101]. Small oblong tablets (9 mm x 5 mm x 4 mm (width x length x height)) were manufactured for children > 6 years old by Fanous et al [102].

Another aspect besides the dimensionally accuracy is the geometric flexibility. Geometrical flexibility offers the opportunity to increase the compliance in pediatric patient as well as to reduce the resistance of taking medication in children. The reason lies in the possibility of 3d printing for personalized medicine to choose the color, shape and design of the tablet according to the child's wishes [103]. Scoutaris et al. imitated chewable STARMIX® sweets by printing objects in the shape of a heart, ring, bottle, bear and lion which contained the model substance indomethacin, hypromellose acetate succinate (HPMCAS) and polyethylene glycol (PEG) as polymers. The aim for the development of this pediatric dosage forms with the STARMIX® design via hot-melt extrusion (HME) and FDM 3d printing was also to enhance the palatability [104].

Besides the flexibility in geometry FDM can also be used to manufacture layer-wise polypills [105]. Multiple APIs were printed into one solid oral dosage form. In case of the layer-based FDM process, chemical compatibility of these APIs is not as limiting as in traditional manufacturing processes since the compounds are separately printed into different compartments of the dosage form. The flexibility of a computer-controlled manufacturing process opens the possibilities to match the exact needs for pediatric patients, but deep understanding of the underlaying processes and optimized print settings are necessary to ensure high quality of the final product.

Orodispersible Films

Orodispersible films are accepted by infants and children [95,106,107] and are dosage forms of choice for patient centric applications. The European Pharmacopoeia defines orodispersible films as solid oromucosal preparations intended for the administration in the mouth, where they disperse rapidly to deliver active substances (Ph. Eur. Monograph “Oromucosal preparations”). Dose adaption is possible by (1) modifying the API concentration in the formulation, (2) adapting the film thickness, and (3) by cutting films to the desired size, as both thickness and size defines the amount of incorporated API. However, the cutting approach can be accompanied by material waste and is prone to human errors.

Manufacturing routes of orodispersible films include solvent casting [108–110] and 2d and 3d printing technologies. In 2D printing [111,112], the printing fluid consists of the drug dissolved in a suitable solvent or dispersed in a dispersant, which is printed onto a substrate which contains polymer(s) and additives (e.g., plasticizers, flavors) and is made in a separate manufacturing step. As for the solvent casting technique, the process parameters (drying temperature, humidity) need to be precisely controlled, as they significantly influence the final film properties [113,114].

3d printing offers a waste-less route of precise manufacturing medicines for children. Jamróz and colleagues accurately printed orodispersible films containing aripripazole [115], whereas Ethezazi et al. printed multi-layered films containing individual layers with paracetamol, ibuprofen and a taste masking agent [29]. Cho et al. applied a variation of FDM printing to prepare an orodispersible film containing the poorly water-soluble drug olanzapine [116]. They heated a polymer-API mixture until it melted and used pneumatic extrusion to drive the printing process, an approach similar to the one published by Musazzi et al. [108]. In another study, a bi-layer film was FDM printed with a mucoadhesive chitosan and drug containing layer and an ethyl cellulose backing layer that formed a permeation barrier, thus creating a unidirectional drug release [117].

Even though none of these studies directly investigated the suitability of FDM 3d printing to individualize the dose, they demonstrated sufficient mechanical properties to enable robust handling and acceptable accuracy that strongly hints at technological proficiency to produce pediatric orodispersible films. However, acceptability of orodispersible films was assessed with solvent-casted films and the different appearance of FDM printed films will have to be investigated separately in future studies.

Dosage Form Characterization

To ensure that printed dosage forms meet the requirements, physical properties need to be characterized, and the homogeneous distribution of the API can be controlled to guarantee that patients receive the necessary therapeutical amount of API. For physical characterization, various tests are listed in the pharmacopoeia: test for friability (Ph. Eur. 2.9.7), crushing strength (Ph. Eur. 2.9.8) and disintegration (Ph. Eur. 2.9.1). To check the homogeneity of the drug distribution, the content of the API in the tablets is determined via the uniformity of the mass or content (Ph. Eur. 2.9.5 / 2.9.6). In addition, it is tested how the drug is released from the tablet over time (Ph. Eur. 2.9.3).

However, FDM printed tablets have different physical properties than compressed tablets, so further methods have been developed for physical characterization. Often, the printed tablets are less porous than the pressed ones, due to the individual layers fused together [118,119]. Depending on the polymers used, the tablets cannot be crushed, do not disintegrate, or disintegrate very slowly, and do not exhibit abrasion [101,120]. The porosity of the tablets can be easily controlled by the pattern and percentage of the infill of the design [120,121]. To check the accuracy of the printing, as well as to determine the porosity of the printed tablets, µCT measurements are often used [102, 122]. The visualization of the internal structure of dosage forms reveals the structural quality, how well the layers adhere to each other, and how well the geometry matches the desired design without destruction of the tablet [123,124]. In a study by Alhijjaj et al., it was shown that the printing speed, printing temperature, build plate leveling and polymer viscosity (melt flow index) have a high influence on the precision of the print, weight of the object and print reproducibility [125]. The effects of these parameters can be registered in the µCT and contribute to the improvement of the process.

As 3d printing is suitable for small, personalized batches, and produces a smaller throughput than industrial tablet machines, non-destructive methods are advantageous for this process. In addition, for the determination of the mass or CU, the tablets must be dissolved, or the API must be extracted from the matrix. Therefore, there is also a growing interest in non-destructive content analysis, which is possible using NIR and Raman technology [102,104]. This technique enables in-line and off-line implementation [126]. To verify the release of the API from the dosage form, in vitro studies must be performed. Here, the ingestion of the tablet, the residence time in the stomach and GIT are simulated. For children the dissolution studies were often adapted. For example, Starmix® candy-like dosage forms were dissolved in 2 ml saliva for 2 min, because children often are expected to chew the tablets [104,127]. In addition, volumes and dwell times can also be adjusted for the specific patient group. Accurate dosing is especially important for children, which can be easily realized with FDM printing. The individually produced batch can be adapted to the needs of the children. Not only the dose, but also the release behavior can be varied. This is possible with the choice of polymer, as well as with the SA/V ratio, which can be implemented with the choice of geometry [99, 128, 129]. Various approaches are also currently being pursued to predict release curves using ANNs so that non-destructive methods can be established here as well [130–132]. These predictions are based, among other things, on the infill pattern of the tablets

and their influences on the release pattern. In the study of Obeid et al. the influence of the SA/V ratio was used to predict the resulting release profile of the printed tablet [131].

Outlook

This manuscript aims to provide an overview of pharmaceutical as well as engineering considerations for FDM printed medication for children. We reflected on current liabilities and intended to depict ways for further innovation in the engineering of unit operations to enhance suitability of equipment and dosage forms. As for 3d printing of solid dosage forms in general, formulation and print technology need to be considered in a holistic manner taking into account all aspects from raw materials to final dosage forms. We conclude that there is strong need to advance FDM printing technologies and excipients to accommodate for pharmaceutical needs – with even more elevated quality requirements for pediatric patients especially in the fields of excipient safety and acceptability and printing control and accuracy. Good news is that remedy is underway with commercial start-ups (e.g. Triastek) as well es public-private consortia such as PolyPrint actively working on the necessary technical innovation to meet pharma requirements. Also, the pediatric patient population will benefit from future capabilities of individualized therapy with precise dose adjustment and possibilities to enhance compliance via tablet morphology and size. First small clinical trials on medications for children applying other additive manufacturing techniques clearly demonstrated the future potential of the tech field [133] and we speculate that FDM – due to its technical maturity and accessibility - will be one of the key enabling technologies to advance and establish pharmaceutical 3d printing for individualized and decentralized production of dosage forms - for adults as well as children.

Author contributions

JQ: conceptualization, writing, editing; MB: conceptualization, writing, editing; JB: writing; RC: writing; KE: conceptualization, writing, editing; A-GE: writing; NG: writing; GG-G: writing; LH: writing; DK: writing, editing; TK: conceptualization, writing, editing; SK: writing; FL: writing; TM: writing; HW: writing; SG: conceptualization, writing, editing; TS: writing, editing.

Funding

Open Access funding enabled and organized by Projekt DEAL. The PolyPrint project is funded by the German Federal Ministry of Education and Research—project ‘ProMat Leben - Polymere’ ‘PolyPrint’ (Project No.: 13XP5064).

Declarations

Conflict of interest

The authors declare that they have no conflict of interest.

Open Access

Supplementary Information

The online version contains supplementary material available at https://doi.org/10.1007/s43441-021-00354-0.

References

1. Moreira M, Sarraguça M. How can oral paediatric formulations be improved? A challenge for the XXI century. *Int J Pharm*. 2020. https://doi.org/10.1016/J.IJPHARM.2020.119905.
2. Klingmann V, Spomer N, Lerch C. Favorable acceptance of minitablets compared with syrup: a randomized controlled trial in infants and preschool children. *J Pediatr*. 2013. https://doi.org/10.1016/J.JPEDS.2013.07.014.
3. Breitkreutz J, Boos J. Paediatric and geriatric drug delivery. *Expert Opin Drug Deliv*. 2007;4:37–45. https://doi.org/10.1517/17425247.4.1.37.
4. Liu F, Ranmal S, Batchelor HK. Patient-centered pharmaceutical design to improve acceptability of medicines: similarities and differences in paediatric and geriatric populations. *Drugs*. 2014;74:1871–89. https://doi.org/10.1007/S40265-014-0297-2.
5. el Aita I, Ponsar H, Quodbach J. A critical review on 3D-printed dosage forms. *Curr Pharm Des*. 2018;24:4957–78. https://doi.org/10.2174/1381612825666181206124206.
6. el Aita I, Breitkreutz J, Quodbach J. Investigation of semi-solid formulations for 3D printing of drugs after prolonged storage to mimic real-life applications. *Eur J Pharm Sci*. 2020;146: 105266. https://doi.org/10.1016/J.EJPS.2020.105266.
7. Melocchi A, Uboldi M, Cerea M. A graphical review on the escalation of fused deposition modeling (FDM) 3D printing in the pharmaceutical field. *J Pharm Sci*. 2020;109:2943–57. https://doi.org/10.1016/J.XPHS.2020.07.011.
8. Shaqour B, Samaro A, Verleije B. Production of drug delivery systems using fused filament fabrication: a systematic review. *Pharmaceutics*. 2020;12:517. https://doi.org/10.3390/PHARMACEUTICS12060517.
9. PolyPrint | ProMatLeben - Polymere n.d. https://promatleben.de/de/projekte/projekte-alphabetisch/polyprint/. Accessed 2 Sep 2021.
10. Paediatric formulations | European Medicines Agency n.d. https://www.ema.europa.eu/en/human-regulatory/research-development/paediatric-medicines/paediatric-investigation-plans/paediatric-formulations. Accessed 2 Sep 2021.
11. Reflection paper: formulations choice paediatric population n.d. https://www.ema.europa.eu/en/documents/scientific-guideline/reflection-paper-formulations-choice-paediatric-population_en.pdf. Accessed 2 Sep 2021.
12. Thabet Y, Klingmann V, Breitkreutz J. Drug formulations: standards and novel strategies for drug administration in pediatrics. *J Clin Pharmacol*. 2018;58:S26-35. https://doi.org/10.1002/JCPH.1138.
13. Rouaz K, Chiclana-Rodríguez B, Nardi-Ricart A. Excipients in the paediatric population: a review. *Pharmaceutics*. 2021. https://doi.org/10.3390/PHARMACEUTICS13030387.
14. Walsh J, Cram A, Woertz K. Playing hide and seek with poorly tasting paediatric medicines: do not forget the excipients. *Adv Drug Deliv Rev*. 2014;73:14–33. https://doi.org/10.1016/J.ADDR.2014.02.012.
15. STEP Database – EuPFI n.d. http://www.eupfi.org/step-database-info/. Accessed 2 Sep 2021.
16. Yochana S, Yu M, Alvi M. Pharmaceutical excipients and pediatric formulations. *Chim Oggi*. 2012;30:56–61.

17. Simões MF, Pinto RMA, Simões S. Hot-melt extrusion in the pharmaceutical industry: toward filing a new drug application. *Drug Discov Today*. 2019;24:1749–68. https://doi.org/10.1016/J.DRUDIS.2019.05.013.

18. Simões MF, Pinto RMA, Simões S. Hot-melt extrusion: a roadmap for product development. *AAPS PharmSciTech*. 2021. https://doi.org/10.1208/S12249-021-02017-7.

19. Bandari S, Nyavanandi D, Dumpa N. Coupling hot melt extrusion and fused deposition modeling: critical properties for successful performance. *Adv Drug Deliv Rev*. 2021;172:52–63. https://doi.org/10.1016/J.ADDR.2021.02.006.

20. Melocchi A, Parietti F, Maroni A. Hot-melt extruded filaments based on pharmaceutical grade polymers for 3D printing by fused deposition modeling. *Int J Pharm*. 2016;509:255–63. https://doi.org/10.1016/j.ijpharm.2016.05.036.

21. Korte C, Quodbach J. Formulation development and process analysis of drug-loaded filaments manufactured via hot-melt extrusion for 3D-printing of medicines. *Pharm Dev Technol*. 2018;23:1117–27. https://doi.org/10.1080/10837450.2018.1433208.

22. Zhang J, Feng X, Patil H. Coupling 3D printing with hot-melt extrusion to produce controlled-release tablets. *Int J Pharm*. 2017;519:186–97. https://doi.org/10.1016/j.ijpharm.2016.12.049.

23. Fuenmayor E, Forde M, Healy AV. Material considerations for fused-filament fabrication of solid dosage forms. *Pharmaceutics*. 2018;10:44. https://doi.org/10.3390/PHARMACEUTICS10020044.

24. Nasereddin JM, Wellner N, Alhijjaj M. Development of a simple mechanical screening method for predicting the feedability of a pharmaceutical FDM 3D printing filament. *Pharm Res*. 2018;35:1–13. https://doi.org/10.1007/S11095-018-2432-3.

25. Zhang J, Xu P, Vo A. Development and evaluation of pharmaceutical 3D printability for hot melt extruded cellulose-based filaments. *J Drug Deliv Sci Technol*. 2019;52:292. https://doi.org/10.1016/J.JDDST.2019.04.043.

26. Azad MA, Olawuni D, Kimbell G. Polymers for extrusion-based 3D printing of pharmaceuticals: a holistic materials-process perspective. *Pharmaceutics*. 2020;12:124. https://doi.org/10.3390/PHARMACEUTICS12020124.

27. Thakkar R, Thakkar R, Pillai A. Systematic screening of pharmaceutical polymers for hot melt extrusion processing: a comprehensive review. *Int J Pharm*. 2020;576: 118989. https://doi.org/10.1016/J.IJPHARM.2019.118989.

28. Gottschalk N, Bogdahn M, Harms M. Brittle polymers in fused deposition modeling: an improved feeding approach to enable the printing of highly drug loaded filament. *Int J Pharm*. 2021;597: 120216. https://doi.org/10.1016/J.IJPHARM.2021.120216.

29. Ehtezazi T, Algellay M, Islam Y. The application of 3D printing in the formulation of multilayered fast dissolving oral films. *J Pharm Sci*. 2018;107:1076–85. https://doi.org/10.1016/J.XPHS.2017.11.019.

30. Boniatti J, Januskaite P, da Fonseca LB. Direct powder extrusion 3D printing of praziquantel to overcome neglected disease formulation challenges in paediatric populations. *Pharmaceutics*. 2021. https://doi.org/10.3390/PHARMACEUTICS13081114.

31. Wang H, Dumpa N, Bandari S. Fabrication of taste-masked donut-shaped tablets via fused filament fabrication 3D printing paired with hot-melt extrusion techniques. *AAPS PharmSciTech.* 2020. https://doi.org/10.1208/S12249-020-01783-0.

32. Woertz K, Tissen C, Kleinebudde P. Taste sensing systems (electronic tongues) for pharmaceutical applications. *Int J Pharm*. 2011;417:256–71. https://doi.org/10.1016/J.IJPHARM.2010.11.028.

33. Soto J, Keeley A, Keating AV. Rats can predict aversiveness of active pharmaceutical ingredients. *Eur J Pharm Biopharm*. 2018;133:77–84. https://doi.org/10.1016/J.EJPB.2018.09.027.

34. Patwardhan K, Asgarzadeh F, Dassinger T. A quality by design approach to understand formulation and process variability in pharmaceutical melt extrusion processes. *J Pharm Pharmacol*. 2015;67:673–84. https://doi.org/10.1111/JPHP.12370.

35. Islam MT, Maniruzzaman M, Halsey SA. Development of sustained-release formulations processed by hot-melt extrusion by using a quality-by-design approach. *Drug Deliv Transl Res*. 2014;4:377–87. https://doi.org/10.1007/S13346-014-0197-8.

36. Agrawal A, Dudhedia M, Deng W. Development of tablet formulation of amorphous solid dispersions prepared by hot melt extrusion using quality by design approach. *AAPS PharmSciTech*. 2016;17:214–32. https://doi.org/10.1208/S12249-015-0472-0.

37. Ponsar H, Wiedey R, Quodbach J. Hot-melt extrusion process fluctuations and their impact on critical quality attributes of filaments and 3D-printed dosage forms. *Pharmaceutics*. 2020;12:511. https://doi.org/10.3390/pharmaceutics12060511.

38. Kohlgrüber K. *Co-rotating twin-screw extruders: fundamentals | Hanser-Fachbuch*. Munich: Hanser; 2008.

39. Coperion Download Center n.d. https://download.coperion.com/index_html?download=111413. Accessed 2 Sep 2021.

40. Hopkins M. LOSS in weight feeder systems. *Meas Control*. 2006;39:237–40. https://doi.org/10.1177/002029400603900801.

41. Schulze D. *Powders and Bulk Solids - Behavior, Characterization, Storage and Flow | Dietmar Schulze* | Springer. vol. 22. Springer; 2008.

42. Fahlenbock TD. Selecting a screw feed device for low-rate lossin-weight feeding. *Powder Bulk Eng*. 2007;21(12):27–31.

43. Matarazzo P. Checklist for selecting a volumetric or gravimetric feeder. *Powder Bulk Eng*. 2010.

44. NAMUR. *Dosiergenauigkeit von kontinuierlichen Waagen*. 2006.

45. Meier R, Thommes M, Rasenack N. Granule size distributions after twin-screw granulation—do not forget the feeding systems. *Eur J Pharm Biopharm*. 2016;106:59–69. https://doi.org/10.1016/J.EJPB.2016.05.011.

46. Engisch WE, Muzzio FJ. Method for characterization of loss-in-weight feeder equipment. *Powder Technol.* 2012;228:395–403. https://doi.org/10.1016/J.POWTEC.2012.05.058.

47. Bruce C, Manning M. *Melt extruded thin strips containing coated pharmaceutical actives*, 2011.

48. Merck KGAA. *Shaping the Future of Formulation Development with Melt-based 3d printing Technologies [White Paper]*. 2021. https://www.pharmaexcipients.com/wp-content/uploads/2021/06/Shaping-the-Future-of-Formulation-Development-with-Melt-based-3D-Printing-Technologies.pdf. Accessed Sept 21, 2021.

49. Vynckier A-K, Dierickx L, Voorspoels J. Hot-melt co-extrusion: requirements, challenges and opportunities for pharmaceutical applications. *J Pharm Pharmacol*. 2014;66:167–79. https://doi.org/10.1111/JPHP.12091.

50. Crowley MM, Zhang F, Repka MA. Pharmaceutical applications of hot-melt extrusion: part I. *Drug Dev Ind Pharm*. 2008;33:909–26.https://doi.org/10.1080/03639040701498759.

51. Liang JZ. Effects of extrusion conditions on die-swell behavior of polypropylene/diatomite composite melts. *Polym Test*. 2008;27:936–40. https://doi.org/10.1016/J.POLYMERTESTING.2008.08.001.

52. Öblom H, Zhang J, Pimparade M. 3D-printed isoniazid tablets for the treatment and prevention of tuberculosis—personalized dosing and drug release. *AAPS PharmSciTech*. 2019. https://doi.org/10.1208/S12249-018-1233-7.

53. Xie T, Taylor LS. Effect of temperature and moisture on the physical stability of binary and ternary amorphous solid dispersions of celecoxib. *J Pharm Sci*. 2017;106:100–10. https://doi.org/10.1016/J.XPHS.2016.06.017.

54. Awad A, Fina F, Trenfield SJ. 3D printed pellets (miniprintlets): a novel, multi-drug, controlled release platform technology. *Pharmaceutics*. 2019;11:148. https://doi.org/10.3390/PHARMACEUTICS11040148.

55. Eggenreich K, Windhab S, Schrank S. Injection molding as a one-step process for the direct production of pharmaceutical dosage forms from primary powders. *Int J Pharm*. 2016;505:341–51. https://doi.org/10.1016/J.IJPHARM.2016.03.034.

56. Repka M, Bandari S, Kallakunta V. Melt extrusion with poorly soluble drugs—an integrated review. *Int J Pharm*. 2018;535:68– 85. https://doi.org/10.1016/J.IJPHARM.2017.10.056.

57. Saerens L, Vervaet C, Remon JP. Process monitoring and visualization solutions for hot-melt extrusion: a review. *J Pharm Pharmacol*. 2014;66:180–203. https://doi.org/10.1111/JPHP.12123.

58. Spoerk M, Koutsamanis I, Matic J. Novel cleaning-in-place strategies for pharmaceutical hot melt extrusion. *Pharmaceutics*. 2020;12:1–21. https://doi.org/10.3390/PHARMACEUTICS12060588.

59. Wesholowski J, Prill S, Berghaus A. Inline UV/Vis spectroscopy as PAT tool for hot-melt extrusion. *Drug Deliv Transl Res*. 2018;8:1595–603. https://doi.org/10.1007/S13346-017-0465-5.

60. Saerens L, Dierickx L, Lenain B. Raman spectroscopy for the in-line polymer–drug quantification and solid state characterization during a pharmaceutical hot-melt extrusion process. *Eur J Pharm Biopharm*. 2011;77:158–63. https://doi.org/10.1016/J.EJPB.2010.09.015.

61. Vo AQ, He H, Zhang J. Application of FT-NIR analysis for in-line and real-time monitoring of pharmaceutical hot melt extrusion: a technical note. *AAPS PharmSciTech*. 2018;19:3425. https://doi.org/10.1208/S12249-018-1091-3.

62. Kallakunta VR, Sarabu S, Bandari S. An update on the contribution of hot-melt extrusion technology to novel drug delivery in the twenty-first century: part I. *Expert Opin Drug Deliv*. 2019;16:539. https://doi.org/10.1080/17425247.2019.1609448.

63. Kim EJ, Kim JH, Kim M-S. Process analytical technology tools for monitoring pharmaceutical unit operations: a control strategy for continuous process verification. *Pharmaceutics*. 2021;13:919. https://doi.org/10.3390/PHARMACEUTICS13060919.

64. Koutsamanis I, Paudel A, Nickisch K. Controlled-release from high-loaded reservoir-type systems—a case study of ethylenevinyl acetate and progesterone. *Pharmaceutics*. 2020. https://doi.org/10.3390/PHARMACEUTICS12020103.

65. Auch C, Harms M, Mäder K. How changes in molecular weight and PDI of a polymer in amorphous solid dispersions impact dissolution performance. *Int J Pharm*. 2019;556:372–82. https://doi.org/10.1016/J.IJPHARM.2018.12.012.

66. Ting J, William W, Porter I, Mecca JM. Advances in polymer design for enhancing oral drug solubility and delivery. *Bioconjug Chem*. 2018;29:939–52. https://doi.org/10.1021/ACS.BIOCONJCHEM.7B00646.

67. Đuranović M, Obeid S, Madžarevic M, et al. Paracetamol extended release FDM 3D printlets: evaluation of formulation variables on printability and drug release. *Int J Pharm*. 2021. https://doi.org/10.1016/J.IJPHARM.2020.120053.

68. Gorkem Buyukgoz G, Soffer D, Defendre J. Exploring tablet design options for tailoring drug release and dose via fused deposition modeling (FDM) 3D printing. *Int J Pharm*. 2020. https://doi.org/10.1016/J.IJPHARM.2020.119987.

69. Prasad E, Islam MT, Goodwin DJ. Development of a hot-melt extrusion (HME) process to produce drug loaded Affinisol™ 15LV filaments for fused filament fabrication (FFF) 3D printing. *Addit Manuf*. 2019. https://doi.org/10.1016/J.ADDMA.2019.06.027.

70. Aho J, van Renterghem J, Arnfast L. The flow properties and presence of crystals in drug-polymer mixtures: rheological investigation combined with light microscopy. *Int J Pharm*. 2017;528:383–94. https://doi.org/10.1016/J.IJPHARM.2017.06.012.

71. Qian F, Huang J, Hussain M. Drug-polymer solubility and miscibility: stability consideration and practical challenges in amorphous solid dispersion development. *J Pharm Sci*. 2010;99:2941–7. https://doi.org/10.1002/JPS.22074.

72. Baird J, van Eerdenbrugh B, Taylor L. A classification system to assess the crystallization tendency of organic molecules from undercooled melts. *J Pharm Sci*. 2010;99:3787–806. https://doi.org/10.1002/JPS.22197.

73. Dedroog S, Pas T, Vergauwen B. Solid-state analysis of amorphous solid dispersions: why DSC and XRPD may not be regarded as stand-alone techniques. *J Pharm Biomed Anal*. 2020. https://doi.org/10.1016/J.JPBA.2019.112937.

74. Ma X, Williams RO III. Characterization of amorphous solid dispersions: an update. *J Drug Deliv Sci Technol*. 2019;50:113–24. https://doi.org/10.1016/j.jddst.2019.01.017.

75. Wadher K, Trivedi R, Wankhede N. 3D printing in pharmaceuticals: an emerging technology full of challenges. *Ann Pharm Fr*. 2021;79:107–18. https://doi.org/10.1016/J.PHARMA.2020.08.007.

76. Hauser G. *Hygienegerechte apparate und anlagen*, vol. 1. 1st ed. Weinheim: Wiley; 2008.

77. Kampker A, Triebs J, Kawollek S. Review on machine designs of material extrusion based additive manufacturing (AM) systems—status-Quo and potential analysis for future AM systems. *Procedia CIRP*. 2019;81:815–9. https://doi.org/10.1016/J.PROCIR.2019.03.205.

78. Melocchi A, Briatico-Vangosa F, Uboldi M. Quality considerations on the pharmaceutical applications of fused deposition modeling 3D printing. *Int J Pharm*. 2021. https://doi.org/10.1016/J.IJPHARM.2020.119901.

79. Leitlinien - EHEDG n.d. https://www.ehedg.org/germany. Accessed 2 Sep 2021.

80. Fortus 450mc | StratasysTM Support Center n.d. https://support.stratasys.com/en/printers/fdm/fortus-450mc. Accessed 2 Sep 2021.

81. BIO X Syringe Pump Printhead - CELLINK n.d. https://www.cellink.com/product/syringe-pump-printhead/ Accessed 2 Sep 2021.

82. SDS-5 3d printer Extruder| Hyrel3D n.d. https://www.hyrel3d.com/portfolio/sds-5-extruder/. Accessed 2 Sep 2021.

83. Serdeczny MP, Comminal R, Mollah MT. Numerical modeling of the polymer flow through the hot-end in filament-based material extrusion additive manufacturing. *Addit Manuf*. 2020. https://doi.org/10.1016/J.ADDMA.2020.101454.

84. x500pro | German RepRap GmbH n.d. https://www.germanreprap.com/printer/x500pro.aspx. Accessed 2 Sep 2021

85. van Bracht R, Piller FT, Marquardt E. Das Potenzial der additiven Fertigung: digitale Technologien im Unternehmenskontext : Auswert 2019.

86. Kim H, Lin Y, Tseng TLB. A review on quality control in additive manufacturing. *Rapid Prototyping* J. 2018;24:645–69. https://doi.org/10.1108/RPJ-03-2017-0048.

87. Becker P, Gebert J, Roennau A et al. Online error detection in additive manufacturing: a review. In: *Proceedings of the 2021 IEEE 8th International Conference on Industrial Engineering and Applications, ICIEA 2021*, pp. 167–75. https://doi.org/10.1109/ICIEA52957.2021.9436729.

88. Tlegenov Y, Lu WF, Hong GS. A dynamic model for current-based nozzle condition monitoring in fused deposition modelling. *Progress Addit Manuf*. 2019;4:211–23. https://doi.org/10.1007/S40964-019-00089-3.

89. Rao P, Liu J, Mathew Roberson D, et al. Online real-time quality monitoring in additive manufacturing processes using heterogeneous sensors additive manufacturing view project fatigue life prediction from defect criticality for L-PBF parts view project online real-time quality monitoring in additive manufacturing processes using heterogeneous sensors. *J Manuf Sci Eng*. 2014. https://doi.org/10.1115/1.4029823.

90. Baumann F, Roller D. Vision based error detection for 3D printing processes. *MATEC Web Conf*. 2016;59:1–7. https://doi.org/10.1051/conf/2016.

91. Becker P, Spielbauer N, Roennau A. Real-time in-situ process error detection in additive manufacturing. In: *Proceedings of the 4th IEEE International Conference on Robotic Computing, IRC 2020*, 2020, pp 426–427. https://doi.org/10.1109/IRC.2020.00077.

92. Greeff GP, Schilling M. Closed loop control of slippage during filament transport in molten material extrusion. *Addit Manuf*. 2017;14:31–8. https://doi.org/10.1016/j.addma.2016.12.005.

93. Khorasani M, Edinger M, Raijada D, et al. Near-infrared chemical imaging (NIR-CI) of 3D printed pharmaceuticals. *Int J Pharm*. 2016;515:324–30. https://doi.org/10.1016/j.ijpharm.2016.09.075.

94. Theil F, Milsmann J, Anantharaman S, et al. Manufacturing amorphous solid dispersions with a tailored amount of crystallized API for biopharmaceutical testing. *Mol Pharm*. 2018;15:1870–7. https://doi.org/10.1021/acs.molpharmaceut.8b00043.

95. Alessandrini E, Brako F, Scarpa M. Children's Preferences for Oral Dosage Forms and Their Involvement in Formulation Research via EPTRI (European Paediatric Translational Research Infrastructure). *Pharmaceutics*. 2021;13:730. https://doi.org/10.3390/PHARMACEUTICS13050730.

96. Jamróz W, Szafraniec J, Kurek M. 3D printing in pharmaceutical and medical applications – recent achievements and challenges. *Pharm Res*. 2018. https://doi.org/10.1007/S11095-018-2454-X.

97. Lennartz P, Mielck JB. Minitabletting: improving the compactability of paracetamol powder mixtures. *Int J Pharm*. 1998;173:75–85. https://doi.org/10.1016/S0378-5173(98)00206-3.

98. Klingmann V, Seitz A, Meissner T. Acceptability of uncoated mini-tablets in neonates – a randomized controlled trial. *J Pediatr*. 2015;167:893-896.e2. https://doi.org/10.1016/J.JPEDS.2015.07.010.

99. Krause J, Müller L, Sarwinska D. 3D printing of mini tablets for pediatric use. *Pharmaceuticals*. 2021;14:1–16. https://doi.org/10.3390/PH14020143.

100. Parhi R. A review of three-dimensional printing for pharmaceutical applications: quality control, risk assessment and future perspectives. *J Drug Deliv Sci Technol*. 2021. https://doi.org/10.1016/J.JDDST.2021.102571.

101. Ayyoubi S, Cerda JR, Fernández-García R. 3D printed spherical mini-tablets: geometry versus composition effects in controlling dissolution from personalised solid dosage forms. *Int J Pharm*. 2021. https://doi.org/10.1016/J.IJPHARM.2021.120336.

102. Fanous M, Bitar M, Gold S. Development of immediate release 3D-printed dosage forms for a poorly water-soluble drug by fused deposition modeling: study of morphology, solid state and dissolution. *Int J Pharm*. 2021;599: 120417. https://doi.org/10.1016/J.IJPHARM.2021.120417.

103. Vijayavenkataraman S, Fuh JYH, Lu WF. 3D printing and 3D bioprinting in pediatrics. *Bioengineering*. 2017. https://doi.org/10.3390/BIOENGINEERING4030063.

104. Scoutaris N, Ross S, Douroumis D. 3D printed "Starmix" drug loaded dosage forms for paediatric applications. *Pharm Res*. 2018. https://doi.org/10.1007/S11095-017-2284-2.

105. Pereira BC, Isreb A, Forbes RT. 'Temporary Plasticiser': a novel solution to fabricate 3D printed patient-centred cardiovascular 'Polypill' architectures. *Eur J Pharm Biopharm*. 2019;135:94– 103. https://doi.org/10.1016/J.EJPB.2018.12.009.

106. Klingmann V, Pohly CE, Meissner T. Acceptability of an orodispersible film compared to syrup in neonates and infants: a randomized controlled trial. *Eur J Pharm Biopharm*. 2020;151:239–45. https://doi.org/10.1016/J.EJPB.2020.03.018.

107. Orlu M, Ranmal SR, Sheng Y. Acceptability of orodispersible films for delivery of medicines to infants and preschool children. Drug Deliv. 2017;24:1243–8. https://doi.org/10.1080/10717544.2017.1370512.

108. Musazzi UM, Selmin F, Ortenzi MA. Personalized orodispersible films by hot melt ram extrusion 3D printing. *Int J Pharm*. 2018;551:52–9. https://doi.org/10.1016/J.IJPHARM.2018.09.013.

109. Liu C, Chang D, Zhang X. Oral fast-dissolving films containing lutein nanocrystals for improved bioavailability: formulation development, in vitro and in vivo evaluation. AAPS PharmSciTech. 2017;18:2957–64. https://doi.org/10.1208/S12249-017-0777-2.

110. Foo WC, Khong YM, Gokhale R. A novel unit-dose approach for the pharmaceutical compounding of an orodispersible film. *Int J Pharm*. 2018;539:165–74. https://doi.org/10.1016/J.IJPHARM.2018.01.047.

111. Huanbutta K, Sriamornsak P, Singh I. Manufacture of 2D-printed precision drug-loaded orodispersible film prepared from tamarind seed gum substrate. *Appl Sci*. 2021;11:5852. https://doi.org/10.3390/APP11135852.

112. Öblom H, Sjöholm E, Rautamo M. towards printed pediatric medicines in hospital pharmacies: comparison of 2D and 3D-printed orodispersible warfarin films with conventional oral powders in unit dose sachets. *Pharmaceutics*. 2019. https://doi.org/10.3390/PHARMACEUTICS11070334.

113. Landová H, Vetchý D. Evaluation of the influence of formulation and process variables on mechanical properties of oral mucoadhesive films using multivariate data analysis. *BioMed Res Int*. 2014. https://doi.org/10.1155/2014/179568.

114. Evans SE, Harrington T, Rodriguez Rivero MC, et al. 2D and 3D inkjet printing of biopharmaceuticals – a review of trends and future perspectives in research and manufacturing. *Int J Pharm*. 2021;599: 120443. https://doi.org/10.1016/J.IJPHARM.2021.120443.

115. Jamróz W, Kurek M, Łyszczarz E, et al. 3D printed orodispersible films with Aripiprazole. *Int J Pharm*. 2017;533:413–20. https://doi.org/10.1016/J.IJPHARM.2017.05.052.

116. Cho HW, Baek SH, Lee BJ, et al. Orodispersible polymer films with the poorly water-soluble drug, olanzapine: hot-melt pneumatic extrusion for single-process 3D printing. *Pharmaceutics*. 2020;12:1–16. https://doi.org/10.3390/PHARMACEUTICS12080692.

117. Eleftheriadis GK, Ritzoulis C, Bouropoulos N, et al. Unidirectional drug release from 3D printed mucoadhesive buccal films using FDM technology: In vitro and ex vivo evaluation. *Eur J Pharm Biopharm*. 2019;144:180–92. https://doi.org/10.1016/J.EJPB.2019.09.018.

118. Than YM, Titapiwatanakun V. Tailoring immediate release FDM 3D printed tablets using a quality by design (QbD) approach. *Int J Pharm*. 2021;599: 120402. https://doi.org/10.1016/J.IJPHARM.2021.120402.

119. Nukala PK, Palekar S, Patki M, et al. Abuse deterrent immediate release egg-shaped tablet (Egglets) using 3D printing technology: quality by design to optimize drug release and extraction. *AAPS PharmSciTech*. 2019. https://doi.org/10.1208/S12249-019-1298-Y.

120. Zhang J, Thakkar R, Zhang Y. Structure-function correlation and personalized 3D printed tablets using a quality by design (QbD) approach. *Int J Pharm*. 2020. https://doi.org/10.1016/J.IJPHARM.2020.119945.

121. Palekar S, Nukala P, Mishra S. Application of 3D printing technology and quality by design approach for development of age-appropriate pediatric formulation of baclofen. *Int J Pharm*. 2019;556:106–16. https://doi.org/10.1016/J.IJPHARM.2018.11.062.

122. Goyanes A, Fina F, Martorana A, et al. Development of modified release 3D printed tablets (printlets) with pharmaceutical excipients using additive manufacturing. *Int J Pharm*. 2017;527:21–30. https://doi.org/10.1016/J.IJPHARM.2017.05.021.

123. Markl D, Zeitler JA, Rasch C. Analysis of 3D prints by X-ray computed microtomography and terahertz pulsed imaging. *Pharm Res*. 2016;34:1037–52. https://doi.org/10.1007/S11095-016-2083-1.

124. Gioumouxouzis CI, Katsamenis OL, Fatouros DG. X-ray microfocus computed tomography: a powerful tool for structural and functional characterisation of 3D printed dosage forms. J Microsc. 2019. https://doi.org/10.1111/JMI.12798.

125. Alhijjaj M, Nasereddin J, Belton P. Impact of processing parameters on the quality of pharmaceutical solid dosage forms produced by fused deposition modeling (FDM). *Pharmaceutics*. 2019;11:633. https://doi.org/10.3390/PHARMACEUTICS11120633.

126. Trenfield SJ, Goyanes A, Telford R, et al. 3D printed drug products: non-destructive dose verification using a rapid point-and-shoot approach. *Int J Pharm*. 2018;549:283–92. https://doi.org/10.1016/J.IJPHARM.2018.08.002.

127. Rachid O, Rawas-Qalaji M, Estelle F. Dissolution testing of sublingual tablets: a novel in vitro method. *AAPS PharmSciTech*. 2011;2011(12):544–52. https://doi.org/10.1208/s12249-011-9615-0.

128. Reynolds TD, Mitchell SA, Balwinski KM. Investigation of the effect of tablet surface area/volume on drug release from hydroxypropylmethylcellulose controlled-release matrix tablets. *Drug Dev Ind Pharm*. 2002. https://doi.org/10.1081/DDC-120003007.

129. Goyanes A, Robles Martinez P, Buanz A, et al. Effect of geometry on drug release from 3D printed tablets. *Int J Pharm*. 2015. https://doi.org/10.1016/j.ijpharm.2015.04.069.

130. Madzarevic M, Medarevic D, Vulovic A. Optimization and prediction of ibuprofen release from 3D DLP printlets using artificial neural networks. *Pharmaceutics*. 2019. https://doi.org/10.3390/PHARMACEUTICS11100544.

131. Obeid S, Madžarević M, Krkobabić M, et al. Predicting drug release from diazepam FDM printed tablets using deep learning approach: Influence of process parameters and tablet surface/ volume ratio. *Int J Pharm*. 2021;601: 120507. https://doi.org/10.1016/J.IJPHARM.2021.120507.

132. Novák M, Boleslavská T, Grof Z, et al. Virtual prototyping and parametric design of 3D-printed tablets based on the solution of inverse problem. *AAPS PharmSciTech*. 2018;19:3414–24. https://doi.org/10.1208/s12249-018-1176-z.

133. Goyanes A, Madla CM, Umerji A, et al. Automated therapy preparation of isoleucine formulations using 3D printing for the treatment of MSUD: First single-centre, prospective, crossover study in patients. *Int J Pharm*. 2019;567: 118497. https://doi.org/10.1016/J.IJPHARM.2019.118497.

Supplementary Information

Table S1: Overview of polymer requirements for the pharmaceutical application of polymers processed by HME and FDM. The authors make no claim on completeness.

Parameter / Technique	Range / Value	Relevance Polymer / HME / FDM / Application
Amorphous or semi-crystalline	Amorph: High solidification time with less shrinking	Polymer[1]
API / polymer miscibility	amorphous state of API	Polymer[2] / HME[3] / FDM[2] / Application[2]
Brittleness (three point bending test)	breaking distance > 1 mm - 1.5 mm [3,4] breaking stress > 2941 – 3126 g/mm [2 3-5]	FDM[3,4,6]
Degradation temperature T_{deg}	T_{deg} of polymer matrix has to fit thermal properties of API	Polymer[2,4,7,8] / HME[2,4,8] / FDM[7,8] / Application[7]
Feedability of powder	Powder in HME Filament in FDM and for Application	HME[7] / FDM[9,10] / Application[9,10]
Filament Diameter	Extrudate uniformity 1.75 mm	HME[11] / FDM[11]
Glass transition temperature T_g	$\frac{T_m}{T_g}$ < 1.3 preferred[8] $T_g - T_{storage} \geq 50$ °C [12] 50-180 °C for commonly used polymer/API combinations[2]	Polymer[2,4,7,8] / HME[2,4,8] / FDM[7,8] / Application[7]
HME Temperature	Extrusion 20-30 °C below degradation temperature T_{deg}[4]	HME[13] / FDM
HME Temperature range	100 - 170 °C, depending on API stability	Polymer / HME[3]
Low hygroscopicity	Prevents crystallization	HME[2] / FDM[2] / Application[2]
Melt flow rate	10 g per 10 min through heated capillary→ ISO 1133[3]	HME[3] / FDM[14]
Melt viscosity η_{melt}	$1000 < \eta_{melt} < 10000$ Pa·s [2,15] viscous melt formation preextrusion[11] solidification postextrusion[11]	Polymer / HME[11,16] / FDM[11,16] / Application[11]
Melting temperature T_m	$\frac{T_m}{T_g}$ < 1.3 preferred[8] Depends on API/polymer combination e.g. T_m (Polylactic acid) = 170 – 180 °C;[17] T_m (Polycaprolactone) = 57 °C.[17]	Polymer[2,4,7,8,17] / HME[2,4,8,17] / FDM[7,8] / Application[7]
Molecular weight		Polymer[2] / HME[2] / FDM[2] / Application
No toxicity	Application of large amounts	Application[2]
Particle Size		HME[2]
Printability		FDM[9,10,18] / Application[9,10,18]
ratio of the elastic modulus to the viscosity of the polymer melt $\frac{\delta E}{\eta_{melt}}$	Material to be functional in FDM process with no buckling, when ratio above $\frac{\delta E}{\eta_{melt}} \geq [3 \cdot 10^5\ s^{-1}$ to $5 \cdot 10^5\ s^{-1}]$ [19]	Polymer / HME[19,20] / FDM[19,20]
Shear thinning / thixotropy	favored	HME[3] / FDM
Theoretical parameters **Flory Huggins** **Hansen** **PC-SAFT** **COSMO**	Interaction parameter (Flory-Huggins Theory): χ <0 for strong miscibility concerning Polymer melt / API[21] Hansen solubility parameter δ: $\delta^2 \leq 7$ MPa^{½} indicates miscibility API/polymer[21,22] $\delta^2 > 10$ MPa^{½} indicates immiscibility[21,22]	Polymer[21,22] / HME[21,22] / FDM[21,22]
Toughness	> 80 g/mm^2	FDM[4]
Polymer Solubility	Solvents required for processing	Polymer[23]
Youngs Modulus (Tensile Test)	Youngs Modulus > 300 N/mm [2 4,5] distance at break > 1.125 mm [5] Thermoplastic behavior[2]	FDM[4,5,24,25]

1. Penumakala PK, Santo J, Thomas A. A critical review on the fused deposition modeling of thermoplastic polymer composites. *Composites Part B: Engineering.* 2020;201.

2. K.Kolter, Karl M, Grycke A. Hot-Melt Extrusion with BASF Pharma Polymers. In: *Extrusion Compendium.* 2nd Revised and Enlarged ed.: BASF SE; 2012.

3. Cailleaux S, Sanchez-Ballester NM, Gueche YA, Bataille B, Soulairol I. Fused Deposition Modeling (FDM), the new asset for the production of tailored medicines. *J Control Release.* 2021;330:821-841.

4. Bandari S, Nyavanandi D, Dumpa N, Repka MA. Coupling hot melt extrusion and fused deposition modeling: Critical properties for successful performance. *Adv Drug Deliv Rev.* 2021;172:52-63.

5. Korte C, Quodbach J. Formulation development and process analysis of drug-loaded filaments manufactured via hot-melt extrusion for 3D-printing of medicines. *Pharm Dev Technol.* 2018;23(10):1117-1127.

6. Zhang J, Feng X, Patil H, Tiwari RV, Repka MA. Coupling 3d printing with hot-melt extrusion to produce controlled-release tablets. *Int J Pharm.* 2017;519(1-2):186-197.

7. Alshehri S, Imam SS, Hussain A, et al. Potential of solid dispersions to enhance solubility, bioavailability, and therapeutic efficacy of poorly water-soluble drugs: newer formulation techniques, current marketed scenario and patents. *Drug Deliv.* 2020;27(1):1625-1643.

8. Simoes MF, Pinto RMA, Simoes S. Hot-Melt Extrusion: a Roadmap for Product Development. *AAPS PharmSciTech.* 2021;22(5):184.

9. Nasereddin JM, Wellner N, Alhijjaj M, Belton P, Qi S. Development of a Simple Mechanical Screening Method for Predicting the Feedability of a Pharmaceutical FDM 3d printing Filament. *Pharm Res.* 2018;35(8):151.

10. Zhang J, Xu P, Vo AQ, et al. Development and evaluation of pharmaceutical 3D printability for hot melt extruded cellulose-based filaments. *J Drug Deliv Sci Technol.* 2019;52:292-302.

11. Procopio A, Tewari D. Opportunities and challenges of 3D-printed pharmaceutical dosage forms. In: *Drug Delivery Trends.*2020:15-44.

12. Agrawal AM, Dudhedia MS, Zimny E. Hot Melt Extrusion: Development of an Amorphous Solid Dispersion for an Insoluble Drug from Mini-scale to Clinical Scale. *AAPS PharmSciTech.* 2016;17(1):133-147.

13. Breitenbach J. Melt extrusion: from process to drug delivery technology. *Eur J Pharm Biopharm.* 2002;54(2):107-117.

14. Fuenmayor E, Forde M, Healy AV, et al. Material Considerations for Fused-Filament Fabrication of Solid Dosage Forms. *Pharmaceutics.* 2018;10(2).

15. Gupta SS, Solanki N, Serajuddin ATM. Investigation of Thermal and Viscoelastic Properties of Polymers Relevant to Hot Melt Extrusion, IV: Affinisol HPMC HME Polymers. *AAPS PharmSciTech.* 2016;17(1):148-157.

16. Repka MA, Bandari S, Kallakunta VR, et al. Melt extrusion with poorly soluble drugs - An integrated review. *Int J Pharm.* 2018;535(1-2):68-85.

17. Mohd Pu'ad NAS, Abdul Haq RH, Mohd Noh H, Abdullah HZ, Idris MI, Lee TC. Review on the fabrication of fused deposition modelling (FDM) composite filament for biomedical applications. *Materials Today: Proceedings.* 2020;29:228-232.

18. Korte C, Quodbach J. 3D-Printed Network Structures as Controlled-Release Drug Delivery Systems: Dose Adjustment, API Release Analysis and Prediction. *AAPS PharmSciTech.* 2018;19(8):3333-3342.

19. Venkataraman N, Rangarajan S, Matthewson MJ, et al. Feedstock material property – process relationships in fused deposition of ceramics (FDC). *Rapid Prototyping Journal.* 2000;6(4):244-253.

20. Rahim TNAT, Abdullah AM, Md Akil H. Recent Developments in Fused Deposition Modeling-Based 3d printing of Polymers and Their Composites. *Polymer Reviews.* 2019;59(4):589-624.

21. Butreddy A, Bandari S, Repka MA. Quality-by-design in hot melt extrusion based amorphous solid dispersions: An industrial perspective on product development. *Eur J Pharm Sci.* 2021;158:105655.

22. Thakkar R, Thakkar R, Pillai A, Ashour EA, Repka MA. Systematic screening of pharmaceutical polymers for hot melt extrusion processing: a comprehensive review. *Int J Pharm.* 2020;576:118989.

23. Simoes MF, Pinto RMA, Simoes S. Hot-melt extrusion in the pharmaceutical industry: toward filing a new drug application. *Drug Discov Today.* 2019;24(9):1749-1768.

24. Çevik Ü, Kam M. A Review Study on Mechanical Properties of Obtained Products by FDM Method and Metal/Polymer Composite Filament Production. *Journal of Nanomaterials.* 2020;2020:1-9.

25. Samy AA, Golbang A, Harkin-Jones E, Archer E, McIlhagger A. Prediction of part distortion in Fused Deposition Modelling (FDM) of semi-crystalline polymers via COMSOL: Effect of printing conditions. *CIRP Journal of Manufacturing Science and Technology.* 2021;33:443-453.

3 Publication 2: HME of Formulations with Enalapril Maleate

Pretext

Following the presentation of quality requirements for extrudates and 3D printed dosage forms for children in Chapter 2, the thermo-sensitive drug enalapril maleate (EM), which is relevant for paediatrics, was processed into extrudates using hot-melt extrusion (HME) and its stability during HME was investigated. First, six different formulations consisting of EM with a drug load of 10 % and various polymers were extruded at temperatures of 100 °C to 150 °C as part of a polymer screening and the content of enalapril (ENP) and its degradation products in the extrudates was determined. The polymers used were Kollidon® 12 PF, Kollidon® VA 64, hydroxypropylmethylcellulose, Eudragit® E PO (bPMMA) and Soluplus® (SOL), while the plasticisers were polyethylene glycol 6,000 and polyethylene oxide with a molecular weight of 100,000. After successful process optimisation, two optimised formulations containing the polymers Soluplus and bPMMA were found, which were fed at a higher feed rate of 100 g/h and extruded at lower temperatures. The optimised formulations allowed extrusion at 100 °C, whereas the formulation with bPMMA could be extruded at 70 °C. Polymer-related differences with regard to the physical and chemical properties of the extrudates were elaborated. A fast HPLC method was developed to determine the content of ENP and possible degradation products.

Evaluation of authorship

The following research paper has been published in Pharmaceutics in 2022. Lena Hoffmann was responsible for conceptualisation, methodology, formal analysis, investigation, writing – original draft preparation, writing – review and editing, visualisation. Jörg Breitkreutz was responsible for conceptualisation, methodology, supervision, funding acquisition. Julian Quodbach was responsible for conceptualisation, writing – review and editing, project administration, funding acquisition.

author/co-author	idea [%]	study design [%]	experimental [%]	evaluation [%]	manuscript [%]
Lena Hoffmann	85	80	100	100	85
Jörg Breitkreutz	10	10	0	0	5
Julian Quodbach	5	10	0	0	10

Hot-Melt Extrusion of the Thermo-Sensitive Peptidomimetic Drug Enalapril Maleate

Lena Hoffmann[1], Jörg Breitkreutz[1] and Julian Quodbach[1,2]

[1]Institute of Pharmaceutics and Biopharmaceutics,

Heinrich Heine University, Düsseldorf, Germany

[2]Department of Pharmaceutics,

Utrecht University, Utrecht, The Netherlands

Pharmaceutics 14(10) (2022) 2091

Abstract

The aim of this research was the production of extrudates for the treatment of hypertension and heart failure and the investigation of the degradation of the peptidomimetic drug enalapril maleate (EM) during hot-melt extrusion (HME). A fast HPLC method was developed to quantify enalapril maleate and possible degradation products. Screening experiments revealed that the diketopiperazine derivative (Impurity D) was the main degradation product. Hot-melt extrusion of enalapril maleate with the polymer Soluplus® enabled extrusion at 100 °C, whereas a formulation with the polymer Eudragit® E PO could be extruded at only 70 °C. Extrusion at 70 °C prevented thermal degradation. A stabilizing molecular interaction between enalapril maleate and Eudragit® E PO was identified via FT-IR spectroscopy. Dissolution studies were carried out to study the influence of the formulation on the dissolution behavior of enalapril maleate. These promising results can be transferred to other thermo-sensitive and peptidomimetic drugs to produce extrudates which can be used, for instance, as feedstock material for the production of patient-specific dosage forms via Fused Deposition Modeling (FDM) 3D printing.

Keywords: hot-melt extrusion; peptidomimetic drug; thermal degradation; analytics of extrudates; HPLC method development; content uniformity; personalized medicine; treatment of hypertension and heart failure

Article available online at:

https://doi.org/10.3390/pharmaceutics14102091

1. Introduction

The peptidomimetic drug enalapril maleate is an angiotensin-converting enzyme inhibitor (ACEI), which is one of the active ingredients on the World Health Organization (WHO) model list of essential medicines and is used, in particular, for heart failure and hypertension in both adults and children [1,2]. Enalapril maleate is the prodrug of the active metabolite enalaprilat and has a similar structure to the tripeptide phenylalanine (Phe)-alanine (Ala)-proline (Pro) [3]. The active pharmaceutical ingredient belongs to the biopharmaceutics classification system (BCS) class III with high solubility and low permeability [4]. In an aqueous solution, two main degradation products, enalaprilat and a diketopiperazine derivative (DKP), have been identified which are described in the European Pharmacopoeia as Impurities C (Imp-C) and D (Imp-D) of the starting material besides the other Pharmacopoeial Impurities. The rate and pathways of the degradation are pH-dependent. Below pH 2, the main degradation product is DKP and above pH 5, the main degradation product is enalaprilat (Figure 1) [5]. Whereas the formation of DKP is an intramolecular cyclization typically observed for peptides, the formation of enalaprilat is a hydrolysis reaction [4,6].

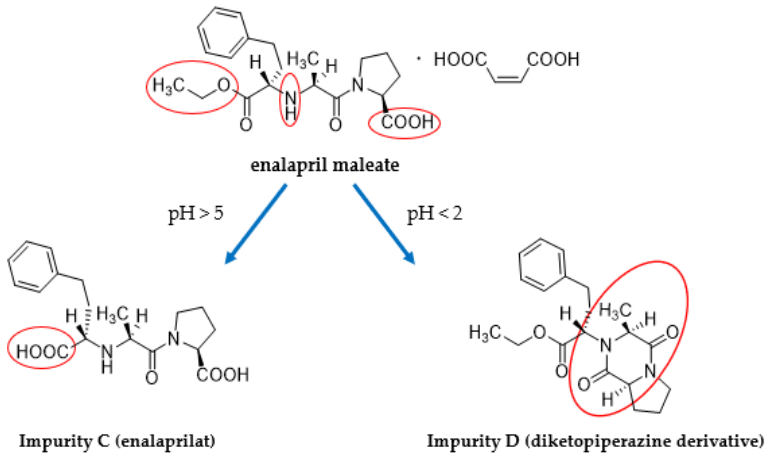

Figure 1. Illustration of the main degradation products of enalapril maleate [5].

Due to the instability of peptidomimetic drugs in an aqueous solution, hot-melt extrusion (HME) can be a preferred method for the preparation of solid dispersions because of the lack of solvents [7–10].

HME is frequently used for the production of formulations with desired release characteristics, for the taste masking of bitter-tasting drugs and especially for solubility enhancement of poorly soluble drugs [8–15]. Furthermore, HME is a continuous process, which can be easily scaled up [16]. Nevertheless, HME also shows some drawbacks. Thermally unstable drugs may degrade at elevated temperatures and under shear forces present during hot-melt extrusion [17,18]. Therefore, attempts were made to overcome this problem, which also refer to the improvement of solubility or bioavailability of the model drug. Liu et al. (2013) prepared solid dispersions with the thermally unstable drug carbamazepine and used polymer combinations of Kollidon® VA 64 (Ludwigshafen, Germany), Soluplus® (Ludwigshafen, Germany) and Eudragit E® PO (Essen, Germany) as carriers to improve the drug-polymer miscibility and decrease the process temperature [8]. Huang et al. (2017) prepared amorphous solid dispersions of the thermally labile drug gliclazide with the polymer hydroxypropyl methyl cellulose (HPMC) and investigated the degradation kinetics depending on the different

polymorphs of gliclazide. From the study, the authors concluded that the degradation of the drug could be influenced by the applied temperature, the unstable nature of the amorphous form of the drug and the mechanical energy input. Optimization of these parameters led to an improved recovery rate of the drug [19]. DiNunzio et al. (2010) produced solid dispersions containing the heat-sensitive active ingredient hydrocortison by hot-melt extrusion and Kinetisol® dispersing. The authors demonstrated that the choice of a suitable carrier for processing at lower temperatures and a reduced residence time could improve product potency [18]. Huang et al. (2019) worked with the heat-sensitive and high-melting drug tadalafil and tried to inhibit the recrystallization of produced amorphous solid dispersions to improve bioavailability [20]; whereas, Kulkarni et al. (2018) applied hot-melt extrusion for the improvement of the bioavailability of the thermolabile drug artemisinin. The degradation could be reduced by producing a solid dispersion with the polymer Soluplus® and the addition of 5% citric acid [21].

The focus of this work was to investigate and quantify the chemical degradation of the model peptidomimetic drug enalapril maleate during hot-melt extrusion in the absence of water. Further, formulations should be developed that enable extrusion with reduced or no degradation. Different polymers were screened for their suitability and the most promising formulations were further optimized. Not only the content of enalapril in the extrudates, but also the dissolution behavior for the optimized formulations was investigated.

2. Materials and Methods

2.1. Materials

Enalapril maleate was purchased from Azelis (Sankt Augustin, Germany) ex Zhejiang Huahai Pharmaceutical Industry Co. (Zhejiang, China). Hypromellose (HPMC, AFFINISOL™ HPMC HME 15 LV) and POLYOX™ WSR N10 (PEO, Mw 100,000) were kindly provided by DuPont Nutrition & Biosciences (Neu-Isenburg, Germany). Kollidon® 12 PF (K 12 PF), Kollidon® VA 64 fine (K VA 64 fine) and Soluplus® (SOL) were kindly provided by BASF (Ludwigshafen, Germany). Basic butylated methacrylate copolymer (bPMMA, Eudragit® E PO) and fumed silica (SiO2, Aerosil 200 V/V Pharma) were kindly provided by Evonik (Essen, Germany). Polyethylene glycol (PEG) 6.000 (Polyglykol® 6000 P) was kindly provided by Clariant (Frankfurt, Germany). Enalapril maleate chemical reference standard (CRS), enalapril for system suitability CRS (containing EM and Impurity A), enalaprilat dihydrate CRS, enalapril impurity G CRS and enalapril impurity mixture A CRS (containing Impurity C and Impurity H) (all European Pharmacopoeia Reference Standards) were purchased at the European Directorate for the Quality of Medicine & Healthcare (Strasbourg, France). Enalapril maleate United States Pharmacopoeia (USP) Reference Standard wase purchased by Eurofins PHAST GmbH (Homburg, Germany). Impurity B and enalapril diketopiperazine were purchased from LGC Standards GmbH (Wesel, Germany). Other chemicals such as solvents and buffering materials were of reagent grade.

2.2. Screening Experiments for HME

For the polymer screening, six different formulations with a drug load of 10% enalapril maleate were investigated (Table 1).

Table 1. Composition of HME formulations for screening experiments (*w/w*).

Formulation	Matrix (%)				Plasticizer (%)		Glidant (%)	
F1	K 12 PF	74.5			PEG 6.000	15	SiO_2	0.5
F2	HPMC	74.5	bPMMA	10	PEG 6.000	5	SiO_2	0.5
F3	K 12 PF	30	K VA 64	30	PEG 6.000	29.5	SiO_2	0.5
F4	HPMC	84.5			PEG 6.000	5	SiO_2	0.5
F5	bPMMA	44			PEO	44	SiO_2	2.0
F6	SOL	44.75			PEO	44.75	SiO_2	0.5

To destroy and remove agglomerates, enalapril maleate and the polymers were separately sieved and mixed for 15 min in a turbula mixer (T2F, Willy A. Bachofen, Switzerland).

The powder blends of each formulation were fed with a flat-bottom powder feeder (ZD 5 FB, Three-Tec, Seon, Switzerland) and dosed at a feed rate of 50 g/h or 100 g/h into a co-rotating twin screw extruder Leistritz ZSE12 HP-PH extruder (Leistritz, Nürnberg, Germany) with a screw diameter of 12 mm and a screw length to diameter ratio of 40:1. Screws with two kneading zones and a die with a diameter of 2 mm were used. Different temperatures and process parameters as detailed in Table 2 were applied for the formulations.

Table 2. Process parameters for HME for the different formulations.

Formulation	Powder Feed Rate (g/h)	Screw Speed (1/min)	Temperature (°C)
F1	50	50	130
F2	50	25	130
F3	50	25	140
F4	50	35	140
F5	100	35	150
F6	100	25	100

2.3. Formulations for HME at Reduced Temperatures

HME was carried out again with formulations F5 and F6 for the production of extrudates at reduced temperatures.

Both formulations were fed either with a flat-bottom powder feeder (ZD 5 FB, Three-Tec, Seon, Switzerland) or a volumetric feeder (Brabender MT-S-HYD, Brabender, Duisburg, Germany) at a feed rate of 100 g/h into a co-rotating twin screw extruder (ZSE12 HP-PH, Leistritz, Germany) with a screw diameter of 12 mm and a screw length to diameter ratio of 40:1. Screws with two kneading zones and a die with a diameter of 2 mm were used. The temperature profiles at a constant screw speed of 25 rpm are shown in Table 3.

Table 3. Temperature profiles across the different zones of the extruder barrel (°C).

Formulation	Zone 1	2	3	4	5	6	7	8	Die
F5	20	20	100	100	100	100	100	100	100
F5	20	20	70	70	70	70	70	70	70
F6	20	20	100	100	100	100	100	100	100

Following extrusion, the extruded strand was cooled and transported with a conveyor belt (model 846102.001, Brabender, Germany). The desired diameter of the extrudates of 1.75 mm was achieved using a belt haul-off unit of a winder (Brabender, Duisburg, Germany). Extrudates were collected over the whole extrusion process and used for the content determination.

2.4. Particle Size Distribution

The particle size distributions were determined via laser diffraction (Mastersizer 3000, Malvern Instruments, UK) with dry dispersion using Fraunhofer approximation for data evaluation (n = 3). The dispersion pressure was adjusted to 0.8 bar.

2.5. Scanning Electron Microscopy (SEM) Imaging

Morphology of both powder mixtures and extrudates were examined using Zeiss scanning electron microscope Leo 1430 VP (Zeiss, Germany). Samples were sputter coated with a thin gold layer. The working voltage ranged from 5 to 10 kV.

2.6. Thermal Analysis

Thermo analysis of enalapril maleate starting material and the reference standards of the degradation products were performed using dynamic scanning calorimetry (DSC, DSC 1, Mettler-Toledo, Giessen, Germany). Samples were heated at 10 °C/min from 20 °C to 200 °C. For thermogravimetric analysis (TGA) and derivative thermogravimetric analysis (DTG), enalapril maleate was measured using a NETZSCH TG 209F1 Libra (NETZSCH, Selb, Germany). The sample was placed in an 85 µL aluminium pan and was then heated from 35 °C to 500 °C using 10 °C/min as a heating rate. The thermal decomposition was analyzed using NETZSCH Proteus Software. The experiments were carried out under a nitrogen gas flow of 20 mL/min.

2.7. Drug Content of Extrudates

2.7.1. Screening Experiments

Sections of drug-loaded extrudates (approximately 0.1 g), with the exception of formulation F6, were placed in a 100 mL volumetric flask and dissolved in 100 mL 0.1 N hydrochloric acid. Samples of the solutions were then filtered through a 0.20 µm polypropylene filter. The content of enalapril (ENP) and degradation products in the extrudates was determined by high-performance liquid chromatography (HPLC) analysis. An Elite LaChrom system consisting of an L-2200 automatic sampler, L-2130 high pressure pump, L-2300 column oven and L-2400 UV detector was used (all Hitachi-VWR). A Eurospher II 100-5 C18A column (125 mm × 4.6 mm, 5 µm) with integrated precolumn (Knauer, Germany) served as the stationary phase. The mobile phase was composed of acetonitrile and 1 mM potassium dihydrogen phosphate buffer (pH 3.0, adjusted with orthophosphoric acid 85%). The flow rate was 1 mL/min and the column temperature was 50 °C. Detection was performed at a wavelength of 215 nm. After injection of 10 µL of the sample solution samples were separated under gradient conditions (Table 4).

Table 4. Gradient conditions for the separation of enalapril and its related substances.

Time [min]	Acetonitrile (% *v/v*)	Buffer (% *v/v*)
0–5.0	5	95
5.0–8.0	5 → 25	95 → 75
8.0–16.0	25	75
16.0–24.0	25 → 55	75 → 45
24.0–26.0	55	45
26.0–26.1	55 → 95	45 → 5
26.1–28.0	95	5
28.0–28.1	95 → 5	5 → 95
28.1–30.0	5	95

For formulation F6, a section of a drug-loaded extrudate (approximately 0.1 g) was placed in a 100 mL volumetric flask and was dissolved in 100 mL of a mixture of acetonitrile and 1 mM potassium dihydrogen phosphate buffer pH 3.0 (50/50, *v/v*). Samples of the solutions were then filtered through a 0.45 µm nylon filter. The content of enalapril and degradation products in the extrudates were determined by HPLC analysis with an optimized gradient (Table 5).

Table 5. Optimized gradient for the separation of enalapril and its related substances.

Time [min]	Acetonitrile (% *v/v*)	Buffer (% *v/v*)
0–1.0	2	98
1.0–1.2	2 → 25	98 → 75
1.2–5.0	25	75
5.0–7.5	25 → 40	75 → 60
7.5–9.0	40 → 75	60 → 25
9.0–11.0	75 → 95	25 → 5
11.0–12.5	95	5
12.5–12.6	95 → 2	5 → 98
12.6–15.0	2	98

2.7.2. Samples from Extrusion at Reduced Temperatures

The HPLC method with the gradient shown in Table 5 was further used for the quantification of the drug content of formulations F5 extruded at optimized conditions and F6.

Extrudate samples were collected and analyzed at the beginning, the middle and end of extrusion (n = 10, mean ± SD). Therefore, sections of a drug-loaded extrudate (approximately 0.1 g) were placed in a 100 mL volumetric flask and dissolved in 100 mL of a mixture of acetonitrile and 1 mM potassium dihydrogen phosphate buffer pH 3.0 (50/50, v/v). Samples of the solutions were then filtered through a 0.45 µm nylon filter. An Elite LaChrom system (VWR, Darmstadt, Germany) consisting of an L-2200 automatic sampler, L-2130 high pressure pump, L-2300 column oven and L-2400 UV detector was used.

Compared to the originally developed method and, also, already published methods, the separation of enalapril and possible degradation products with the optimized gradient was carried out on an XBridge C18 column (3.0 × 150 mm, 3.5 µm) at a temperature of 65 °C and an injection volume of 30 µL [22,23]. The temperature increase leads to an improved peak shape of enalapril [24] and a higher separation efficacy between enalapril and pharmacopoeial Impurity A. Furthermore, the method allows on the one hand the complete separation of maleic acid and enalaprilate (Imp-C), which makes the quantification of this possible main degradation product more reliable (Figure 2a). On the other hand, the separation of enalapril and the known pharmacopoeial impurities A, B, C, D, G and H is possible in a single run time of 15 min (Figure 2b–d).

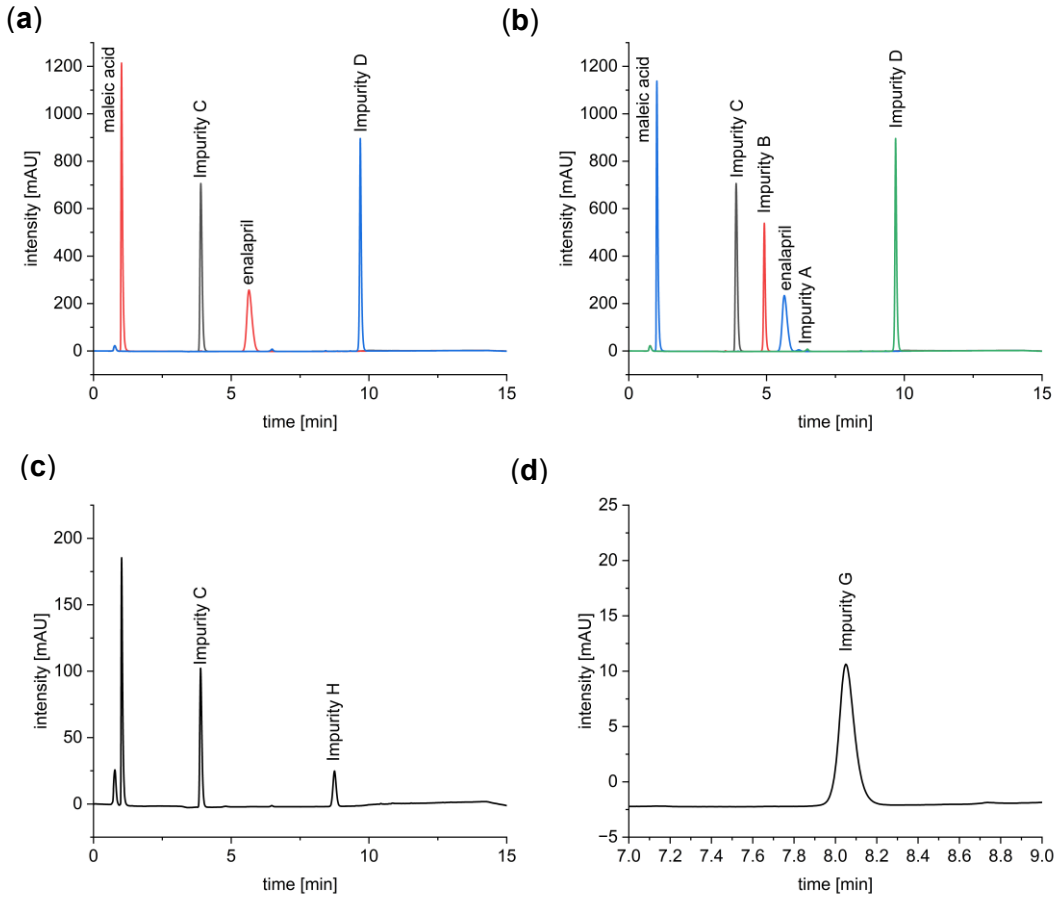

Figure 2. HPLC chromatograms of EM and the main degradation products Imp-C and Imp-D (**a**), of EM and Imp-A, Imp-B, Imp-C and Imp-D (**b**), of Imp-C and Imp-H (**c**) and of Imp-G (**d**).

The identification of the related substances was done with solutions of each standard. For the selectivity of the developed HPLC method, the enalapril maleate CRS solution was spiked with the other related substances. The determination of the limit of detection (LOD) and the limit of quantification (LOQ) for enalapril resulted in concentrations of 19.4 ng/mL and 58.7 ng/mL. Linearity was given for the content uniformity of enalapril in the extrudates in the concentration range of 60 to 140 µg/mL and for the dissolution in a concentration range of 0.2 to 12 µg/mL with a correlation coefficient of $R^2 > 0.999$. The accuracy of the content in the samples was ensured by using the enalapril maleate USP reference standard and enalapril diketopiperazine standard with a known content. The calibration for enalapril diketopiperazine was always performed with the external standard. Precision was determined in terms of repeatability for enalapril, where the coefficient of variation (CV) was 0.74%.

2.8 FT-IR Spectra Measurements

FT-IR spectra measurements were made to investigate possible interactions between enalapril maleate and the polymers. Therefore, infrared spectra were recorded with a Shimadzu IR Affinity-1 with ATR sampling technique (Shimadzu, Duisburg, Germany).

2.9. Dissolution

In vitro drug release studies were carried out using dissolution tester AT7 Smart (Sotax, Aesch, Switzerland) with USP type I apparatus (basket apparatus) at 37 °C ± 0.5 °C with a rotating speed of 50 rpm in 900 mL phosphate buffer at pH 6.8 or in 0.1 N hydrochloric acid. Extrudates were taken from the lowest possible extrusion temperature. The amount of EM was quantified by HPLC.

3. Results and Discussion

3.1. Raw Material Properties

3.1.1. Particle Size Distribution

The determination of the median particle size x50 of the raw materials showed large differences between the polymers bPMMA and SOL (Table 6). The median particle size of bPMMA was 9.7 µm ± 0.1 µm and 308 µm ± 6.1 µm for SOL. PEO had a median particle size of 111 ± 8.6. In contrast, the median particle size of the active ingredient enalapril maleate was 47.2 ± 1.3 µm.

Table 6. Particle size of raw materials (*n* = 3, mean ± SD).

Substance	x_{10} (µm)	x_{50} (µm)	x_{90} (µm)
Enalapril maleate	6.2 ± 0.1	47.2 ± 1.3	181 ± 6.9
bPMMA	3.8 ± 0.1	9.7 ± 0.1	37.3 ± 26.9
SOL	191 ± 4.6	308 ± 6.1	483 ± 5.6
PEO	14 ± 0.6	111 ± 8.6	320 ± 15.6

3.1.2. Scanning Electron Microscopy (SEM) Imaging

SEM images showed that enalapril maleate was present in crystalline form as platelets in both physical mixtures. In formulation F5, the small particles of bPMMA adhered to the larger particles of enalapril maleate, resembling a dry coating. Formulation F6 does not display any kind of interaction between SOL and enalapril maleate. In the SEM images of both extrudates, crystalline parts of the semi-crystalline PEO could be observed on the surface, as previously described by Tidau et al. (2019) for PEO-based extrudates [25] (Figure 3).

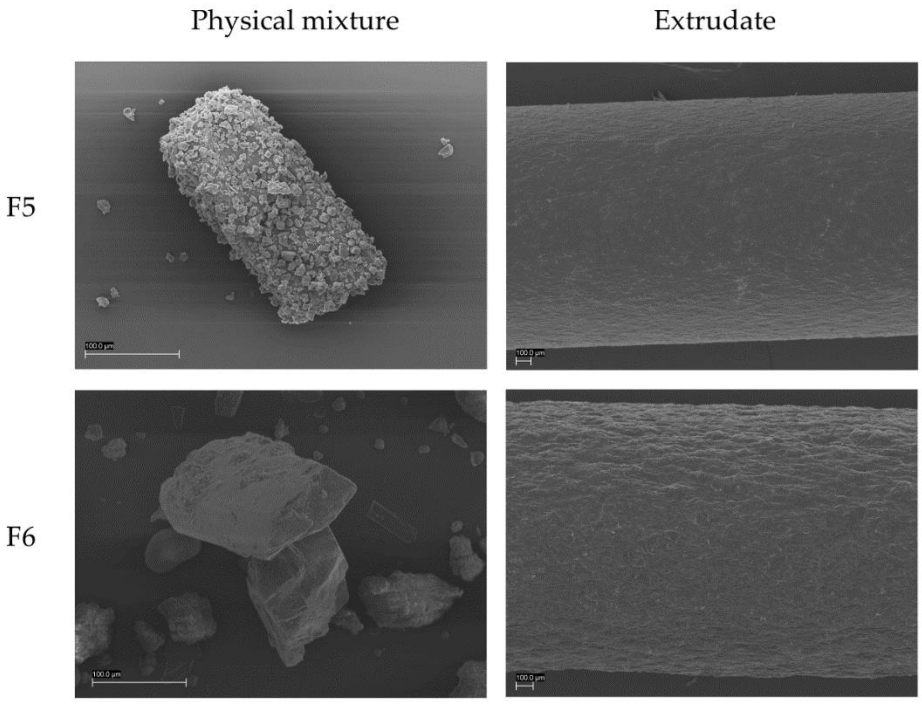

Figure 3. SEM images of the physical mixtures and extrudates of formulation 5 and 6 (Scale: 100 µm).

3.1.3. Thermal Analysis

DSC analysis of enalapril maleate starting material showed two superimposed peaks in the range from 150 °C to 200 °C, as previously described by Lin et al. (2002) [26,27]. The intense and sharp peak at approximately 153 °C was caused by melting and the broad thermal event at 163 °C was caused by thermal decomposition (Figure 4). The degradation product enalaprilat showed an endothermic peak at 151 °C and a second peak at 173 °C, whereby the second thermal event started at 165 °C (Figure 5a). The thermogram of the degradation product DKP showed a minimal first endothermic event at 78 °C and a second endothermic peak at 95 °C, which was associated with the melting of the substance (Figure 5b).

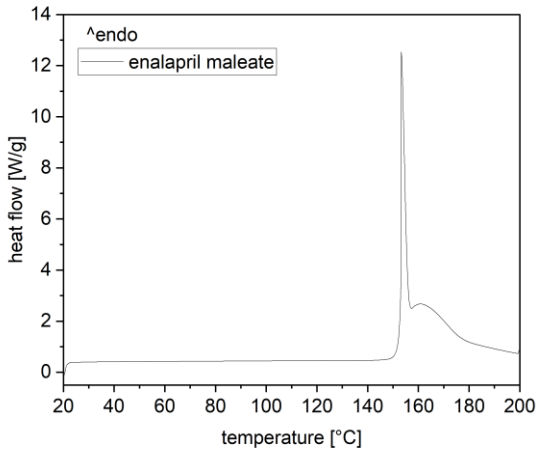

Figure 4. DSC thermogram of enalapril maleate starting material.

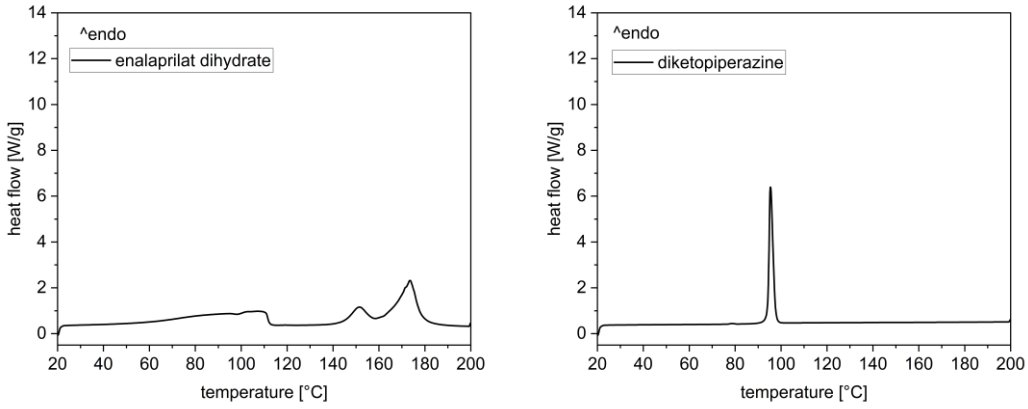

(**a**) (**b**)

Figure 5. DSC thermograms of the main degradation products enalaprilat as dihydrate (**a**) and enalapril diketopiperazine derivative (**b**).

Thermogravimetric analysis (TGA) confirmed the decomposition of enalapril maleate as observed in the DSC data. TGA showed an onset at a temperature of approximately 154 °C and a mass loss of approximately 27% up to a temperature of 220 °C (Figure 6a) [27,28]. The derivative thermogravimetric curve showed the maximum of the initial decomposition at a temperature of approximately 168 °C (Figure 6b).

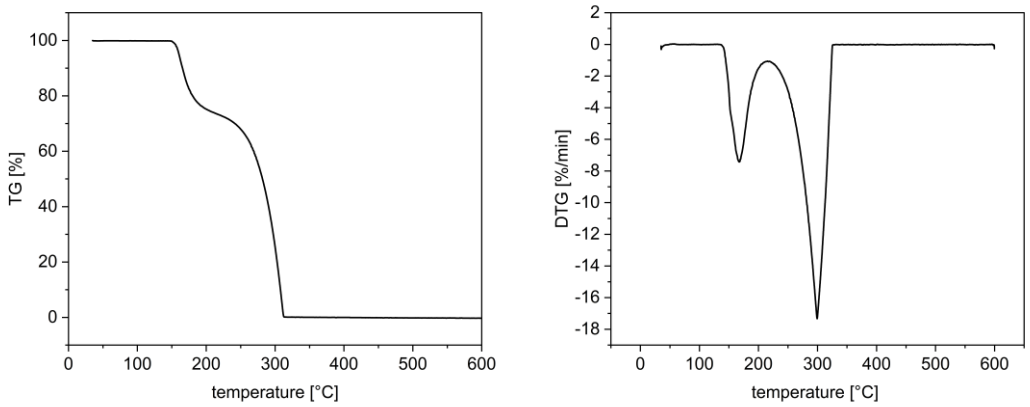

(**a**) (**b**)

Figure 6. TG (**a**) and DTG curves (**b**) of enalapril maleate.

Consequently, extrusion must take place below the melting temperature of enalapril maleate, since melting was accompanied by decomposition.

3.2. Polymer Selection for HME

3.2.1 Screening Experiments

Obtained extrudates from screening experiments differed in their properties. Formulation F1 with the polymer K 12 PF could be extruded between 120 °C and 130 °C. While extrudates at 120 °C exhibited a rough surface, likely due to the glass transition temperature (Tg) of K 12 PF at 90 °C being close to the extrusion temperature [29,30], extrudates processed at a temperature of 130 °C showed a smooth surface and were collected for further analysis.

Formulation F2 with the polymers HPMC and bPMMA were extruded at 130 °C because the polymer HPMC has a higher Tg of 115 °C compared to the polymer bPMMA with a lower Tg of 57 °C [31–33]. Extrudates from formulation F2 appeared orange and had a smooth surface.

Formulation F3 with the polymers K 12 PF and K VA 64 could be extruded at a temperature of 140 °C as the lowest extrusion temperature. The reason for this is the higher glass transition temperature of the polymer K VA 64 with a Tg of 101 °C [29,30]. Extrusion of both formulations was not possible at lower temperatures, although Kempin et al., (2018) and Kollamaram et al., (2018) could extrude these polymers below 100 °C with a self-constructed extruder [34] and with a single screw extruder [35].

Extrudates from formulations F1 and F3, which contained either K 12 PF alone or a combination of K 12 PF and K VA 64 appeared milky-white and sticky. The extrudates of both formulations were smooth, but brittle despite a high plasticizer content.

Formulation F4 with the polymer HPMC could be extruded at a temperature of 140 °C, which is considered a suitable process temperature for HPMC in literature and can be explained by the higher proportion of this polymer in the formulation [25,32,36–39]. The extrudates from formulation F4 appeared orange similar to formulation F2. This could be explained by the formation of the diketopiperazine derivative. The extrudates with HPMC had a rough surface in comparison to the smooth surface of the extrudates of formulation F2.

Formulation F5 and F6, unlike the previous formulations, were extruded at a feed rate of 100 g/h.

Compared to 50 g/h, 100 g/h was used to investigate the influence of the feed rate on the degradation of enalapril maleate. Formulation F5 was extruded at a temperature above the melting point of enalapril maleate at 150 °C [40], whereas formulation F6 was extruded at a temperature of 100 °C. The extrudates of F5 appeared yellowish and the extrudates of F6 slightly yellowish. Both filaments had a smooth surface.

3.2.2 Optimized Process Conditions

Due to their low glass transition temperatures, bPMMA (Tg = 57 °C) and SOL (Tg = 70 °C) in formulations F5 and F6 were identified as suitable formulations for extrusion at lower temperatures [33,41]. The extrusion of F5 with the polymers bPMMA and PEO was performed under optimized conditions at temperatures of 70 °C and 100 °C [7], whereas the extrusion of F6 with the two polymers SOL and PEO was repeated at a temperature of 100 °C, identified as lowest possible process temperature. Lightly yellowish-colored extrudates obtained from the extrusion process had a smooth surface and were flexible.

3.3. Drug Content of Extrudates

3.3.1 Content Uniformity of the Extrudates of the Screening Experiments

The results of the content uniformity showed that in all formulations, besides the active ingredient enalapril maleate, the diketopiperazine derivative (DKP, Imp-D) occurred as the main thermal degradation product in the extrudates (Figure 7). Formulation F1 with K 12 PF showed the highest content of enalapril. In the extrudates, 72.88 ± 6.42% enalapril was found, whereas 29.50 ± 6.97% Imp-D were determined. Formulation F2 with the polymers HPMC and bPMMA also extruded at a temperature of 130 °C showed a higher degradation. 38.05 ± 1.00% enalapril and 59.84 ± 1.98% Imp-D were recovered. Formulation F3 with the polymers K 12 PF and K VA 64 was extruded at 140 °C and showed a further decrease in the content of enalapril. 34.01 ± 3.09% enalapril and 76.05 ± 6.74% Imp-D were determined. Formulation F4 with the polymer HPMC showed an almost complete degradation of enalapril and only 0.74 ± 0.10% was found. 74.18± 3.05% Imp-D and further unidentified impurities could be detected.

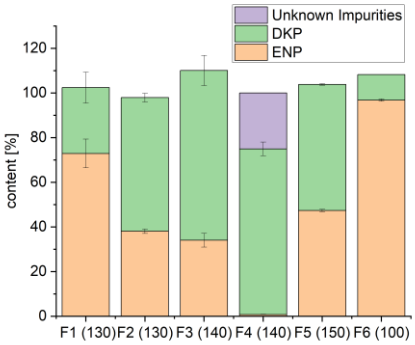

Figure 7. Content uniformity of the extrudates of the screening experiments (*n* = 6, mean ± SD).

From the extrusion of these four formulations, which were all fed at a feed rate of 50 g/h, it could be observed that not only the temperature but also the used polymers have an influence on enalapril maleate degradation. The formulations F2 and F4, which both contained the polymer HPMC showed, due to a higher melt viscosity, a higher pressure at the die during extrusion [37,42]. This could explain the higher amount of degradation of enalapril in formulation F2 and especially in formulation F4 (Figure 7), which was also observed during hot-melt extrusion of gliclazide with HPMC in a previous publication by Huang et al. (2017) [19]. Formulation F5 was fed with the higher feed rate of 100 g/h into the extruder and the extrusion was performed at a temperature of 150 °C. In the extrudates, 47.33 ± 0.50% enalapril and 56.44 ± 0.34% Imp-D were determined. The results showed that also the feed rate had an impact on the degradation. Despite the higher extrusion temperature of 150 °C, more enalapril was found compared to formulations F2, F3 and F4. For formulation F6 with the polymer SOL and PEO, which was also fed with a feed rate of 100 g/h and extruded at a temperature of 100 °C, the highest amount of enalapril could be found. 96.78 ± 0.54% enalapril was recovered and 11.43 ± 0.05% Imp-D.

The process temperature and also the applied shear forces had a great impact on enalapril maleate degradation. A higher feed rate could shorten the residence time, and thus, reduce the amount of degradation. Process conditions and formulations were optimized since degradation of enalapril maleate already takes place below the melting temperature contrary

to DSC and TG measurements. The optimized formulations F5 and F6 containing the polymers bPMMA and SOL were extruded again at reduced temperatures and with a higher feed rate of 100 g/h into the extruder.

3.3.2. Content Uniformity for the Formulations under Optimized Conditions

For formulation F5 with bPMMA extruded at 100 °C, it was observed that the content of enalapril remained constant over the extrusion and was 98.44 ± 0.30% versus 2.83 ± 0.09% Imp-D in the middle of the run (Figure 8a). For formulation F6 with the polymer SOL also extruded at 100 °C it was observed that the content of enalapril decreased to a greater degree during extrusion. In the middle, the content of enalapril was 94.83 ± 1.72% and 7.54 ± 0.24% Imp-D (Figure 8b). The larger decrease in the content of enalapril could be due to an inhomogeneous powder mixture which could be explained by a larger particle size of SOL (308 ± 6.1 µm) compared to bPMMA (9.7 ± 0.1 µm). The x50 of enalapril maleate is 47.2 ± 1.3 µm. By comparing the two formulations, a lower content was found for formulation F6 under the same process conditions.

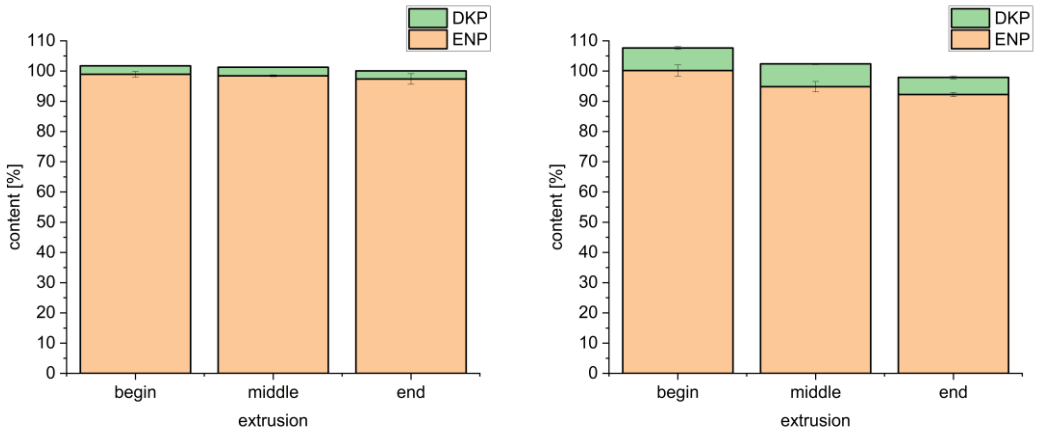

Figure 8. Enalapril and diketopiperazine derivative contents over the extrusion processes at 100 °C of formulation 5 (**a**) and formulation 6 (**b**) (*n* = 10, mean ± SD).

The lowest possible extrusion temperature for F6 was 100°C, whereas F5 could be extruded at 70 °C. The content of enalapril was 101.72 ± 1.65% and no degradation products were found (Figure 9). The different recovered enalapril concentrations after extrusion at 100 °C imply a potentially stabilizing interaction between enalapril maleate and bPMMA.

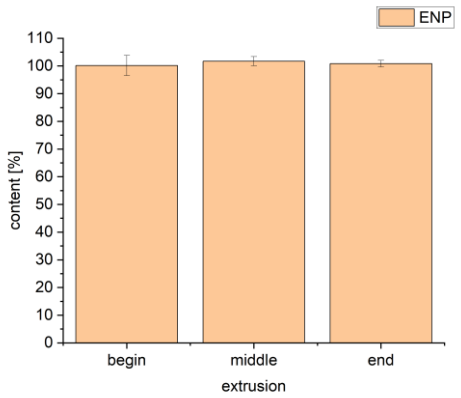

Figure 9. Content uniformity over the entire extrusion for formulation 5 at 70 °C (*n* = 10, mean ± SD).

3.4. FT-IR Spectra Measurements

FT-IR spectroscopy was used to investigate interactions between enalapril maleate and the polymers. The structures of the basic polymer bPMMA and the neutral polymer SOL are shown in Figure 10.

The FT-IR spectrum of enalapril maleate showed characteristic bands at 1749 cm^{-1} (C=O of the carboxylic group), 1645 cm^{-1} (C=O of the tertiary amide), 1578 cm^{-1} (C=O of the carboxylic acid of monohydrogen maleate) and 1225 cm^{-1} (C-C-O of acetate and ester) [43,44]. Characteristic bands for the dimethylamino groups of bPMMA could be found at 2822 cm^{-1} and 2770 cm^{-1}. FT-IR spectrum of bPMMA showed further characteristic peaks for the ester groups at 1144 cm^{-1}, 1238 cm^{-1} and 1267 cm^{-1} and the C = O ester vibration at 1724 cm^{-1} [43,45]. FT-IR spectrum of SOL showed characteristic bands at 2922 cm^{-1} (C-H), 2857 cm^{-1} (C-H), 1740 cm^{-1} (C=O of the carboxylic group) and 1633 cm^{-1} (C=O of the amide group) [46,47]. FT-IR spectrum of PEO showed characteristic bands at 2888 cm^{-1} (C-H), 1240 cm^{-1} (O-H), 1093 cm^{-1} (C-O) and 1059 cm^{-1} (C-O) [48].

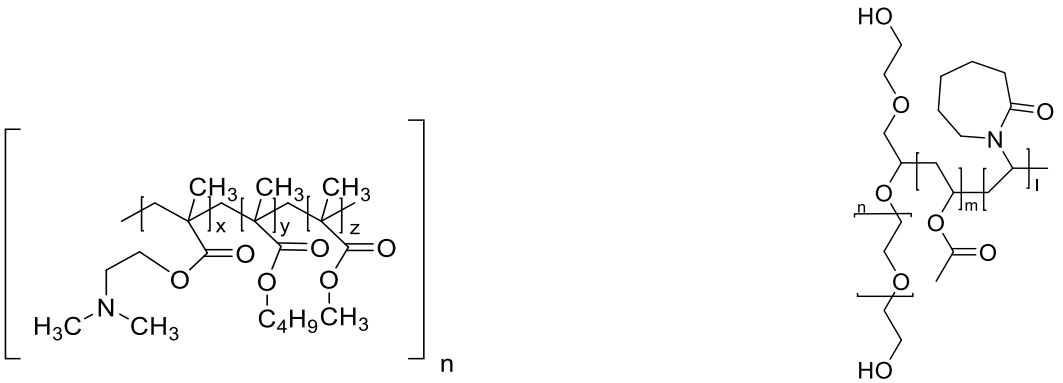

(**a**) (**b**)

Figure 10. Structural formulas of bPMMA (**a**) and SOL (**b**) [41,45].

For the filament of F6 containing the polymer SOL no interaction could be observed as peak shifts or loss of disappearance of peaks. (Figure 11b), whereas for the filament of formulation F5 containing the polymer bPMMA differences in the spectra could be detected (Figure 11a).

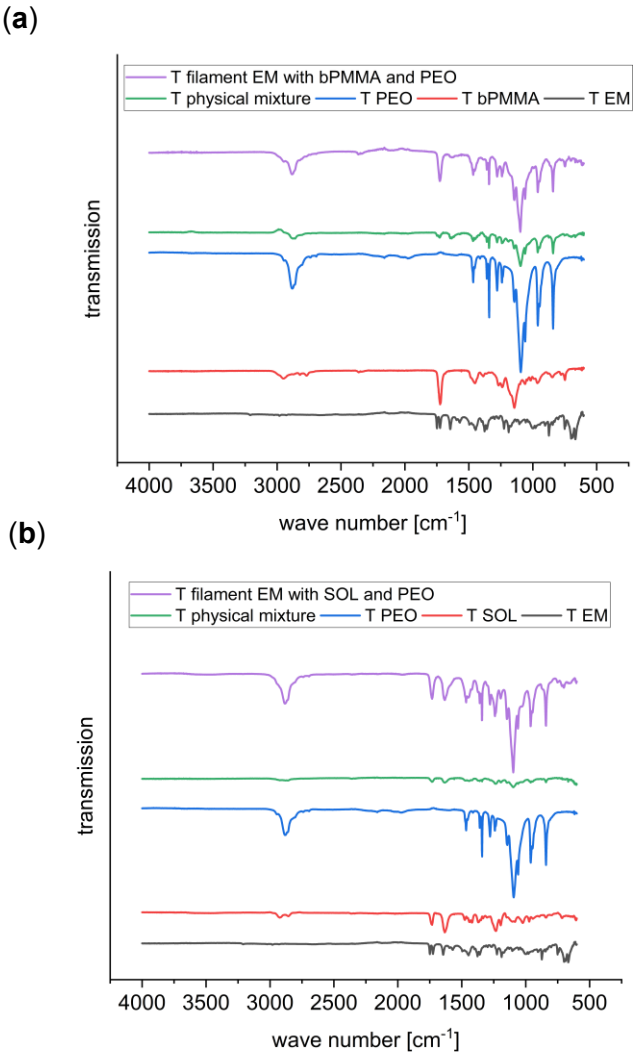

Figure 11. FT-IR spectra for formulations 5 (**a**) and 6 (**b**).

For formulation F5, the absence of characteristic bands for the spectrum of enalapril maleate at 1740 cm^{-1} and 1578 cm^{-1}, and also, for dimethylamino groups of the bPMMA at 2822 cm^{-1} and 2770 cm^{-1} indicates a cation-anion interaction between the carboxylic groups of enalapril maleate and the dimethylamino groups of bPMMA (Figure 11a) [7,49]. Wang et al. (2004) investigated this phenomenon in casted films with enalapril maleate and bPMMA and postulated that one carboxylic group of maleic acid could interact with the amino group of enalapril and the other carboxylic group of maleic acid and/or the carboxylic group of enalapril could interact with the dimethylamino groups of bPMMA [50,51]. This effect could explain the stabilizing effect when enalapril maleate is hot-melt extruded with bPMMA as a polymer [52]. No changes were observed in the spectra due to the use of PEO.

3.5. Dissolution

The release profile of enalapril from the extrudates containing SOL and bPMMA was also investigated.

The US Pharmacopeia (USP) monograph for enalapril maleate tablets specifies that at least 80% enalapril has to be released after 30 min in the paddle apparatus (USP II method) in phosphate buffer pH 6.8 at a rotational speed of 50 rpm [53]. However, during previous dissolution studies, it was observed that extrudates wrapped around the paddle and this phenomenon influenced the dissolution behavior. Therefore, investigations were made with the basket apparatus (USP I method).

In the basket apparatus formulation F6 with SOL released 25.81 ± 0.53% enalapril after 30 min and 91.74 ± 4.72% after 150 min (Figure 12a). After 180 min 96.44 ± 2.16% enalapril was released. Alongside the dissolution of extrudates with SOL in phosphate buffer pH 6.8, the dissolution behavior of enalapril in 0.1 N hydrochloric acid in the basket apparatus was investigated. Of enalapril, 29.52 ± 0.57% was released after 30 min and 88.53 ± 1.60% enalapril was released after 120 min and after 180 min 96.55 ± 1.73% enalapril was released. In comparison to the dissolution in phosphate buffer pH 6.8 the criterion of Q = 80% is reached earlier but, nevertheless, after 180 min approximately the same amount of enalapril is released (96.44 ± 2.16% vs. 96.55 ± 1.73%) (Figure 12a). These results indicate the pH-independent dissolution of enalapril from the extrudates with SOL.

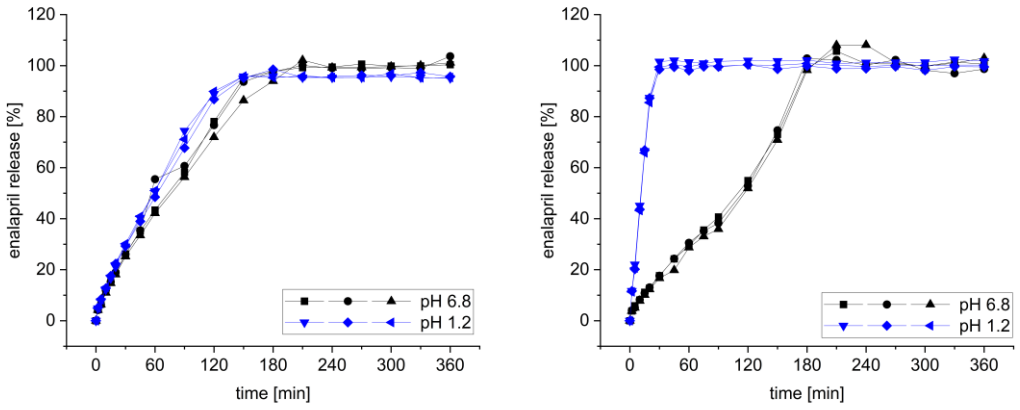

Figure 12. Dissolution behaviour of extrudates with SOL (**a**) and bPMMA (**b**) in basket apparatus in phosphate buffer pH 6.8 and 0.1 N hydrochloric acid (*n* = 3).

Formulation F5 with bPMMA extruded at 70 °C released 17.39 ± 0.57% after 30 min and 100% after 180 min in phosphate buffer pH 6.8 (100.19 ± 2.47%). However, when released in 0.1 N hydrochloric acid, 99.87 ± 1.56% enalapril was released after 30 min (Figure 12b).

As expected, the formulation composition has a decisive influence on the release of the active ingredient. Since bPMMA is a pH-dependent polymer that dissolves at a pH below 5.5, the release of enalapril from the bPMMA extrudates is prolonged at higher pH compared to the extrudates with the polymer SOL. However, a fast drug release from the extrudates with bPMMA in 0.1 N hydrochloric acid could be observed. Thus, the criterion of Q = 80% after 30 min could be fulfilled. Depending on the intended target profile, a suitable formulation has to be identified.

4. Conclusions

The obtained results showed that the peptidomimetic drug enalapril maleate could degrade during the hot-melt extrusion process at temperatures above 120 °C, more than 30 °C below the degradation temperature identified via thermo analysis. The main thermal degradation product formed during this process was the cyclization product enalapril diketopiperazine (Imp-D). Extrusion with bPMMA and SOL at 100 °C revealed a higher drug content in the formulation containing bPMMA. FT-IR data hints towards a cation-anion interaction with the basic bPMMA and enalapril maleate, which might have a stabilizing effect. Further formulation development and optimization of the process conditions during hot-melt extrusion could completely avoid the degradation of the drug enalapril maleate.

Our study demonstrates that by selecting suitable polymers and extrusion conditions, thermo-sensitive drugs can be hot-melt extruded and the formation of degradation products can be avoided. The question to what extent other even more thermo-sensitive compounds, such as proteins and peptides, can also be stabilized by melt extrusion remains to be clarified in the future. Furthermore, it should be noted that the formulation, in particular the polymers used, can have a decisive influence on the properties of the extrudate, such as the physical properties, the content as well as the release of the active ingredient. This work highlights the importance for formulation scientists to first know the properties of the active ingredient in order to select suitable polymers for melt extrusion.

Author Contributions: Conceptualization, L.H., J.Q. and J.B.; methodology, L.H. and J.B.; formal analysis, L.H.; investigation, L.H.; writing—original draft preparation, L.H.; writing—review and editing, L.H. and J.Q.; visualization, L.H.; supervision, J.Q. and J.B.; project administration, J.Q.; funding acquisition, J.Q. and J.B. All authors have read and agreed to the published version of the manuscript.

Funding: This research was funded by the German Federal Ministry of Education and Research—project ‘ProMat Leben-Polymere-PolyPrint’ (project no.: 13XP5064B).

Institutional Review Board Statement: Not applicable.

Informed Consent Statement: Not applicable.

Data Availability Statement: The data presented in this study are available upon request from the corresponding author.

Acknowledgments: The authors want to thank Tom Kunde for conducting the FT-IR spectra measurements. This work is associated with the German Federal Ministry of Education and Research—project ‘ProMat Leben-Polymere-PolyPrint’ (project no.: 13XP5064B).

Conflicts of Interest: The authors 1,3 declare that they have no conflicts of interest. Jörg Breitkreutz is a minority shareholder of Ethicare GmbH, a small company developing a pediatric drug with enalapril.

Abbreviations

ACEI	angiotensin-converting enzyme inhibitor
Ala	alanine
BCS	Biopharmaceutics Classification System
bPMMA	basic butylated methacrylate copolymer
CRS	chemical reference standard
CV	coefficient of variation
DKP	diketopiperazine derivative
DSC	Dynamic Scanning Calorimetry
DTG	Derivative Thermogravimetric Analysis
EM	enalapril maleate
ENP	enalapril
FDM	Fused Deposition Modeling
FT-IR	Fourier transform-infrared spectroscopy
HME	hot melt extrusion
HPLC	High Performance Liquid Chromatography
HPMC	hydroxypropyl methyl cellulose, hypromellose
Imp	impurity
K	Kollidon
LOD	limit of detection
LOQ	limit of quantification
PF	Pyrogen-free
Phe	phenylalanine
Pro	proline
SD	standard deviation
SEM	Scanning Electron Microscopy
SiO_2	fumed silica
SOL	Soluplus
Tg	glass transition temperature
TGA	thermogravimetric analysis
VA	poly(vinylpyrrolidone-vinyl acetate)-copolymer
WHO	World Health Organization

References

1. WHO Model List of Essential Medicines – 22nd list, 2021. Available online: https://www.who.int/publications/i/item/WHO-MHP-HPS-EML-2021.02 (accessed on 24 July 2022).
2. Ip, D.P.; Brenner, G.S. Enalapril maleate. In *Analytical Profiles of Drug Substances*; Florey, K., Ed.; Academic Press: Cambridge, MA, USA, 1987, Volume 16, pp. 207–243.
3. Steinhilber, D.; Schubert-Zsilavecz, M.; Roth, H.J. *Medizinische Chemie: Targets, Arzneistoffe, Chemische Biologie*; Deutscher Apotheker Verlag: Stuttgart, Germany, 2010; pp. 214–253.
4. Verbeeck, R.K.; Kanfer, I.; Löbenberg, R.; Abrahamsson, B.; Cristofoletti, R.; Groot, D.W.; Langguth, P.; Polli, J.E.; Parr, A.; Shah, V.P.; et al. Biowaiver monographs for immediate-release solid oral dosage forms: Enalapril. *J. Pharm. Sci*. **2017**, *106*, 1933–1943. [CrossRef]
5. Commentary on Ph. Eur. 9.0, 2017. 57th supply, enalapril maleate. In *Commentary on the European Pharmacopoeia*; Wissenschaftliche Verlagsgesellschaft mbH: Stuttgart, Germany; Govi-Verlag: Eschborn, Germany, 2017.
6. Lick, I.D.; Villalba, M.L.; Gavernet, L. Synthesis of diketopiperazine: A kinetic study by means of thermoanalytical methods. *Thermochim. Acta*. **2012**, *527*, 143–147. [CrossRef]
7. Sadia, M.; Isreb, A.; Abbadi, I.; Isreb, M.; Aziz, D.; Selo, A.; Timmins, P.; Alhnan, M.A. From 'fixed dose combinations' to 'a dynamic dose combiner': 3D printed bi-layer antihypertensive tablets. *Eur. J. Pharm. Sci*. **2018**, *123*, 484–494. [CrossRef] [PubMed]

8. Liu, J.; Cao, F.; Zhang, C.; Ping, Q. Use of polymer combinations in the preparation of solid dispersions of a thermally unstable drug by hot-melt extrusion. *Acta Pharm. Sin. B*. **2013**, *3*, 263–272. [CrossRef]

9. Simões, M.F.; Pinto, R.M.A.; Simões,S. Hot-Melt Extrusion: A roadmap for product development. *AAPS PharmSciTech* **2021**, *22*, 184. [CrossRef]

10. Breitenbach, J. Melt extrusion: From process to drug delivery technology. *Eur. J. Pharm. Biopharm*. **2002**, *54*, 107–117. [CrossRef]

11. Almeida, A.; Possemiers, S.; Boone, M.; De Beer, T.; Quinten, T.; Van Hoorebeke, L.; Remon, J.P.; Vervaet, C. Ethylene vinyl acetate as matrix for oral sustained release dosage forms produced via hot-melt extrusion. *Eur. J. Pharm. Biopharm*. **2011**, *77*, 297–305. [CrossRef]

12. Verhoeven, E.; De Beer, T.; Schacht, E.; Van den Mooter, G.; Remon, J.; Vervaet, C. Influence of polyethylene glycol/polyethylene oxide on the release characteristics of sustained-release ethylcellulose mini-matrices produced by hot-melt extrusion: In vitro and in vivo evaluations. *Eur. J. Pharm. Biopharm*. **2009**, *72*, 463–470. [CrossRef] [PubMed]

13. Gryczke, A.; Schminke, S.; Maniruzzaman, M.; Beck, J.; Douroumis, D. Development and evaluation of orally disintegrating tablets (ODTs) containing Ibuprofen granules prepared by hot melt extrusion. *Colloids Surf. B*. **2011**, *86*, 275–284. [CrossRef] [PubMed]

14. Witzleb, R.; Kanikanti, V.-R.; Hamann, H.-J.; Kleinebudde, P. Solid lipid extrusion with small die diameters—Electrostatic charging, taste masking and continuous production. *Eur. J. Pharm. Biopharm*. **2011**, *77*, 170–177. [CrossRef] [PubMed]

15. Ma, D.; Djemai, A.; Gendron, C.M.; Xi, H.; Smith, M.; Kogan, J.; Li, L. Development of a HPMC-based controlled release formulation with hot melt extrusion (HME). *Drug Dev. Ind. Pharm*. **2013**, *39*, 1070–1083. [CrossRef] [PubMed]

16. Crowley, M.M.; Zhang, F.; Repka, M.A.; Thumma, S.; Upadhye, S.B.; Kumar Battu, S.; McGinity, J.W.; Martin, C. Pharmaceutical Applications of Hot-Melt Extrusion: Part I. *Drug Dev. Ind. Pharm*. **2007**, *33*, 909–926. [CrossRef]

17. Ghosh, I.; Vippagunta, R.; Li, S.; Vippagunta, S. Key considerations for optimization of formulation and melt-extrusion process parameters for developing thermosensitive compound. *Pharm. Dev. Technol*. **2012**, *17*, 502–510. [CrossRef] [PubMed]

18. DiNunzio, J.C.; Brough, C.; Hughey, J.R.; Miller, D.A.; Williams, R.O.; McGinity, J.W. Fusion production of solid dispersions containing a heat-sensitive active ingredient by hot melt extrusion and Kinetisol® dispersing. *Eur. J. Pharm. Biopharm*. **2010**, *74*, 340–351. [CrossRef]

19. Huang, S.; O'Donnell, K.P.; Delpon de Vaux, S.M.; O'Brien, J.; Stutzman, J.; Williams, R.O. Processing thermally labile drugs by hot-melt extrusion: The lesson with gliclazide. *Eur. J. Pharm. Biopharm*. **2017**, *119*, 56–67. [CrossRef] [PubMed]

20. Huang, D.; Xie, Z.; Rao, Q.; Liamas, E.; Pan, P.; Guan, S.; Zhang, Z.J.; Lu, M.; Li, Q. Hot melt extrusion of heat-sensitive and high melting point drug: Inhibit the recrystallization of the prepared amorphous drug during extrusion to improve the bioavailability. *Int. J. Pharm*. **2019**, *565*, 316–324. [CrossRef]

21. Kulkarni, C.; Kelly, A.L.; Gough, T.; Jadhav, V.; Singh, K.; Paradkar, A. Application of hot melt extrusion for improving bioavailability of artemisinin a thermolabile drug. *Drug Dev. Ind. Pharm*. **2018**, *44*, 206–214. [CrossRef]

22. Bhardwaj, S.P.; Singh, S. Study of forced degradation behavior of enalapril maleate by LC and LC–MS and development of a validated stability-indicating assay method. *J. Pharm. Biomed. Anal*. **2008**, *46*, 113–120. [CrossRef]

23. Koppala, S.; Ranga Reddy, V.; Anireddy, S. User-Friendly HPLC Method Development and Validation for Determination of Enalapril Maleate and Its Impurities in Enalapril Tablets. *J. Chromatogr. Sci*. **2017**, *55*, 979–988. [CrossRef] [PubMed]

24. Šalamoun, J.; Šlais, K. Elimination of peak splitting in the liquid chromatography of the proline-containing drug enalapril maleate. *J. Chromatogr. A*. **1991**, *537*, 249–257. [CrossRef]

25. Tidau, M.; Kwade, A.; Finke, J.H. Influence of High, Disperse API Load on Properties along the Fused-Layer Modeling Process Chain of Solid Dosage Forms. *Pharmaceutics* **2019**, *11*, 194. [CrossRef]

26. Lin, S.-Y.; Wang, S.-L.; Chen, T.-F.; Hu, T.-C. Intramolecular cyclization of diketopiperazine formation in solid-state enalapril maleate studied by thermal FT-IR microscopic system. *Eur. J. Pharm. Biopharm*. **2002**, *54*, 249–254. [CrossRef]

27. Gómez Pineda, E.A.; Martins Ferrarezi, A.D.; Ferrarezi, J.G.; Winkler Hechenleitner, A.A. Thermal decomposition of enalapril maleate studied by dynamic isoconversional method. *J. Therm. Anal. Calorim*. **2005**, *79*, 259–262. [CrossRef]

28. de Souza, S.M.M.; e Melo Franco, P.I.B.; Leles, M.I.G.; da Conceição, E.C. Evaluation of thermal stability of enalapril maleate tablets using thermogravimetry and differential scanning calorimetry. *J. Therm. Anal. Calorim*. **2016**, *123*, 1943–1949. [CrossRef]

29. BASF, Meeting Formulation Challenges for Poorly Soluble Drugs. Available online: https://ipecamericas.org/sites/default/files/ef12april24-hall.b%233-nigel.langley(basf).pdf (accessed on 24 July 2022).

30. Gupta, S.S.; Meena, A.; Parikh, T.; Serajuddin, A.T.M. Investigation of thermal and viscoelastic properties of polymers relevant to hot melt extrusion – I: Polyvinylpyrrolidone and related polymers. *J. Excip. Food Chem*. **2014**, *5*, 32–45.

31. O'Donnell, K.P.; Woodward, W.H.H. Dielectric spectroscopy for the determination of the glass transition temperature of pharmaceutical solid dispersions. *Drug Dev. Ind. Pharm*. **2015**, *41*, 959–968. [CrossRef] [PubMed]

32. Ilyés, K.; Kovács, N.K.; Balogh, A.; Borbás, E.; Farkas, B.; Casian, T.; Marosi, G.; Tomuță, I.; Nagy, Z.K. The applicability of pharmaceutical polymeric blends for the fused deposition modelling (FDM) 3D technique: Material considerations–printability–process modulation, with consecutive effects on in vitro release, stability and degradation. *Eur. J. Pharm. Sci*. **2019**, *129*, 110–123. [CrossRef]

33. Parikh, T.; Gupta, S.S.; Meena, A.; Serajuddin, A.T. Investigation of thermal and viscoelastic properties of polymers relevant to hot melt extrusion-III: Polymethacrylates and polymethacrylic acid based polymers. *J. Excip. Food Chem*. **2016**, 5, 1003.

34. Kempin, W.; Domsta, V.; Grathoff, G.H.; Brecht, I.; Semmling, B.; Tillmann, S.; Weitschies, W.; Seidlitz, A. Immediate Release 3D-Printed Tablets Produced Via Fused Deposition Modeling of a Thermo-Sensitive Drug. *Pharm. Res*. **2018**, *35*, 124. [CrossRef]

35. Kollamaram, G.; Croker, D.M.; Walker, G.M.; Goyanes, A.; Basit, A.W.; Gaisford, S. Low temperature fused deposition modeling (FDM) 3D printing of thermolabile drugs. *Int. J. Pharm. Pharm. Sci*. **2018**, *545*, 144–152. [CrossRef] [PubMed]

36. Ghosh, I.; Snyder, J.; Vippagunta, R.; Alvine, M.; Vakil, R.; Tong, W.-Q.; Vippagunta, S. Comparison of HPMC based polymers performance as carriers for manufacture of solid dispersions using the melt extruder. *Int. J. Pharm. Pharm. Sci*. **2011**, *419*, 12–19. [CrossRef]

37. Gupta, S.S.; Solanki, N.; Serajuddin, A.T.M. Investigation of Thermal and Viscoelastic Properties of Polymers Relevant to Hot Melt Extrusion, IV: Affinisol™ HPMC HME Polymers. *AAPS PharmSciTech* **2016**, *17*, 148–157. [CrossRef] [PubMed]

38. Huang, S.; O'Donnell, K.P.; Keen, J.M.; Rickard, M.A.; McGinity, J.W.; Williams, R.O. A New Extrudable Form of Hypromellose: AFFINISOL™ HPMC HME. *AAPS PharmSciTech* **2016**, *17*, 106–119. [CrossRef] [PubMed]

39. Prasad, E.; Islam, M.T.; Goodwin, D.J.; Megarry, A.J.; Halbert, G.W.; Florence, A.J.; Robertson, J. Development of a hot-melt extrusion (HME) process to produce drug loaded Affinisol™ 15LV filaments for fused filament fabrication (FFF) 3D printing. *Addit. Manuf.* **2019**, *29*, 100776. [CrossRef]

40. Gültekin, H.E.; Tort, S.; Acartürk, F. An Effective Technology for the Development of Immediate Release Solid Dosage Forms Containing Low-Dose Drug: Fused Deposition Modeling 3D Printing. *Pharm. Res*. **2019**, *36*, 128. [CrossRef]

41. BASF, Technical Information Soluplus®. Available online: https://pharma.basf.com/products/soluplus (accessed on 24 July 2022).

42. Meena, A.; Parikh, T.; Gupta, S.S.; Serajuddin, A.T. Investigation of thermal and viscoelastic properties of polymers relevant to hot melt extrusion-II: Cellulosic polymers. *J. Excip. Food Chem*. **2016**, *5*, 1002.

43. Bhattarai, P.; Katuwal, T. Spectroscopic study of Enalapril Maleate and Hydrochlorothiazide. *Int. J. Phys. Appl*. **2021**, *9*, 11–14.

44. Widjaja, E.; Lim, G.H.; Chow, P.S.; Tan, S. Multivariate data analysis as a tool to investigate the reaction kinetics of intra-molecular cyclization of enalapril maleate studied by isothermal and non-isothermal FT-IR microscopy. *Eur. J. Pharm. Sci*. **2007**, *32*, 349–356. [CrossRef]

45. Evonik, Technical Information EUDRAGIT® E 100, EUDRAGIT® E PO and EUDRAGIT® E 12,5. Available online: www.pharmaexcipients.com/wp-content/uploads/attachments/TI-EUDRAGIT-E-100-E-PO-E-12-5-EN.pdf?t=1508413942 (accessed on 24 July 2022).

46. Liu, J.; Zou, M.; Piao, H.; Liu, Y.; Tang, B.; Gao, Y.; Ma, N.; Cheng, G. Characterization and pharmacokinetic study of aprepitant solid dispersions with Soluplus®. *Molecules* **2015**, *20*, 11345–11356. [CrossRef] [PubMed]

47. BASF; Yidan, L.; Shaukat, A.; Nigel, L. Characterization of Soluplus® by FTIR and Raman Spectroscopy. In Proceedings of the CRS 2010 Annual Conference, Portland, USA, 10.07.-14-07.2010.

48. Joshi, Y.; Muppalaneni, S.; Omidian, A.; Mastropietro, D.J.; Omidian, H. Determining abuse deterrence performance of poly (ethylene oxide) using a factorial design. *Adv. Pharm. Bull*. **2018**, *8*, 495. [CrossRef]

49. Ramírez-Rigo, M.V.; Olivera, M.E.; Rubio, M.; Manzo, R.H. Enhanced intestinal permeability and oral bioavailability of enalapril maleate upon complexation with the cationic polymethacrylate Eudragit E100. *Eur. J. Pharm. Sci*. **2014**, *55*, 1–11. [CrossRef] [PubMed]

50. Wang, S.-L.; Lin, S.-Y.; Chen, T.-F.; Cheng, W.-T. Eudragit E accelerated the diketopiperazine formation of enalapril maleate determined by thermal FTIR Microspectroscopic technique. *Pharm. Res*. **2004**, *21*, 2127–2132. [CrossRef] [PubMed]

51. Lin, S.-Y.; Wang, S.-L. Advances in simultaneous DSC–FTIR microspectroscopy for rapid solid-state chemical stability studies: Some dipeptide drugs as examples. *Adv. Drug Deliv. Rev*. **2012**, *64*, 461–478. [CrossRef] [PubMed]

52. Li, Y.; Pang, H.; Guo, Z.; Lin, L.; Dong, Y.; Li, G.; Lu, M.; Wu, C. Interactions between drugs and polymers influencing hot melt extrusion. *J. Pharm. Pharmacol*. **2014**, *66*, 148–166. [CrossRef]

53. Lima, D.M.; dos Santos, L.D.; Lima, E.M. Stability and in vitro release profile of enalapril maleate from different commercially available tablets: Possible therapeutic implications. *J. Pharm. Biomed. Anal*. **2008**, *47*, 934–937. [CrossRef]

4 Publication 3: FDM 3D Printing of Filaments with Enalapril Maleate

Pretext

The extrudates of the two optimised formulations prepared in Chapter 3 were then processed into 3D printed tablets using a FDM 3D printer with a target dose of 10 mg EM at a nozzle temperature of 180 °C and a print bed temperature of 35 °C at a printing speed of 30 mm/s. The content of ENP and potential degradation products in the 3D printed tablets with SOL and bPMMA from the extrusion at 100 °C was also determined and polymer-related differences were analysed. In addition, the extrudates of the optimised formulation with bPMMA from extrusion at 70 °C were used to investigate the nozzle diameter, printing temperature and printing speed as critical process parameters in a printing study. 3D printed bPMMA tablets were produced using a 0.4 mm and a 0.6 mm diameter nozzle with a nozzle temperature of 180 °C and 190 °C and a print bed temperature of 35 °C, as well as a printing speed of 30 mm/s, 60 mm/s and 90 mm/s. The aim was to investigate the influence of the critical process parameters on the stability of ENP during FDM 3D printing and to determine the effect on the content of ENP and degradation products.

Evaluation of authorship

The following research paper has been published in Pharmaceutics in 2022. Lena Hoffmann was responsible for conceptualisation, methodology, formal analysis, investigation, writing – original draft preparation, writing – review and editing, visualisation. Jörg Breitkreutz was responsible for conceptualisation, supervision, funding acquisition. Julian Quodbach was responsible for conceptualisation, writing – review and editing, project administration, funding acquisition.

author/co-author	idea [%]	study design [%]	experimental [%]	evaluation [%]	manuscript [%]
Lena Hoffmann	85	80	100	100	85
Jörg Breitkreutz	10	10	0	0	5
Julian Quodbach	5	10	0	0	10

Fused Deposition Modeling (FDM) 3D Printing of the Thermo-Sensitive Peptidomimetic Drug Enalapril Maleate

Lena Hoffmann[1], Jörg Breitkreutz[1] and Julian Quodbach[1,2]

[1]Institute of Pharmaceutics and Biopharmaceutics,

Heinrich Heine University, Düsseldorf, Germany

[2]Department of Pharmaceutics,

Utrecht University, Utrecht, The Netherlands

Pharmaceutics 14(11) (2022) 2411

Abstract

Fused deposition modeling (FDM) 3D printing was used to produce 3D printed tablets with the thermo-sensitive model peptidomimetic drug enalapril maleate (EM). Two different formulations were prepared to investigate the degradation of enalapril maleate during the FDM 3D printing process. Soluplus® and Eudragit® E PO were chosen as polymers. After hot-melt extrusion (HME) and FDM 3D printing, both formulations were characterised regarding their solid-state properties using DSC and XRD. The degradation of the drug was analysed by determination of the content in the extrudates and 3D printed tablets, and dissolution was assessed. Various approaches have been attempted to prevent degradation of enalapril maleate, including utilization of a larger nozzle diameter and higher printing speeds to reduce heat exposition. None of these approaches were successful in preventing drug degradation. However, significant differences in the amount of degradation between the two formulations with different polymers could be observed. Thus, the FDM 3D printing process was not feasible without any degradation for the thermo-sensitive drug enalapril maleate. A maximum of 85.55 ± 1.48% enalapril was recovered in Eudragit® E PO tablets printed with a 0.4 mm nozzle at a temperature of 180 °C and with a speed of 30 mm/s.

Keywords: hot-melt extrusion; FDM 3D printing; thermo-sensitive drug; decomposition; analytics of extrudates and 3D printed tablets; oral dosage form; personalized medicine

Article available online at:

https://doi.org/10.3390/pharmaceutics14112411

1. Introduction

Nowadays, personalized medicine is gaining increasing interest in the health care sector. The conventional drug treatment approach is based on a "one size fits all" principle where most patients receive the same drug at the same dosages and administration frequencies [1]. This can lead to varying responses and can also be associated with adverse drug reactions [1]. In personalized medicine medical treatments are tailored to patients based on genetic profile, concurrent medicines, and disease state [2,3]. The most promising technology that can drive the paradigm shift to personalized medicine is 3D printing [4]. 3D printing provides the possibility of producing 3D objects layer by layer with the aid of appropriate computer software [4]. 3D printing technologies offer a broad range of applications in the pharmaceutical field. Binder Jetting (BJ), Stereolithography (SLA), Selective Laser Sintering (SLS), Semi-solid extrusion (SSE) and Fused Deposition Modeling (FDM) are researched for pharmaceutical applications [5,6]. The production of 3D printed dosage forms offers several advantages compared to the conventional manufacturing process which includes, for example, the following aspects: customization, polypharmacy, flexible design, point of care production and waste minimization [7]. 3D printing affords us the possibility to precisely producing customised dosage forms for different patient groups, including pediatric and geriatric patients and also patients with pharmacogenetic polymorphism. Furthermore, it can address the needs of these patient groups in terms of swallowability and taste. Besides other benefits, 3D printing can also be considered environmentally friendly due to low amounts of waste [7].

Among the above-mentioned 3D printing techniques, FDM 3D printing is the most widely explored technology for the production of patient-specific dosage forms due to the relatively straightforward, solvent free procedure, its versatility and speed, and also the inexpensive equipment [7-9]. Prefabricated extrudates processed by hot-melt extrusion serve as feedstock material for the 3D printing process (Figure 1) [5,10].

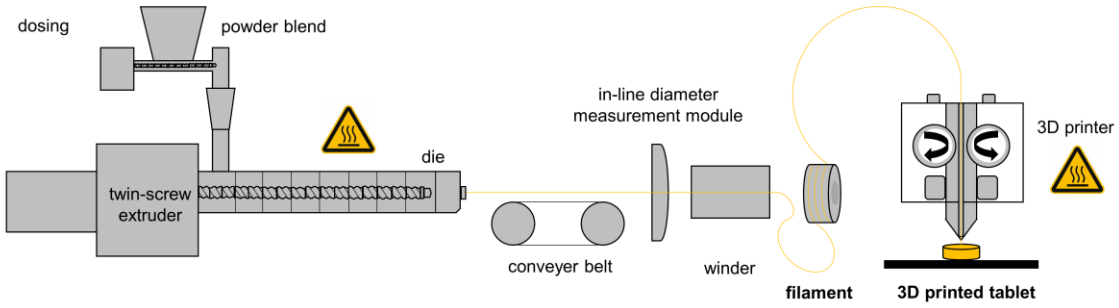

Figure 1. Illustration of the two heat-intensive processes for the manufacturing of 3D printed tablets by HME and FDM (modified from [9]).

Previous publications have demonstrated that thermally stable drugs could be extruded into extrudates with different polymers and processed into 3D printed dosage forms using FDM 3D printers. Due to the increased interest in 3D printed dosage forms, the behavior of thermo-sensitive drugs, including biological agents, during the 3D printing process warrants attention [7]. The world health organization (WHO) defines a time- and temperature-sensitive pharmaceutical product (TTSPP) as “Any pharmaceutical good or product which, when not stored or transported within predefined environmental conditions and/or within predefined time limits, is degraded to the extent that it no longer performs as originally intended.“ [11]. Although this definition usually refers to the storage in a refrigerator, do Pazo-Oubiña et al. (2021) stated

that this definition can also be applied to drugs which degrade during the 3D printing process due to the high printing temperature or UV light/beams [12].

Reduction in hot-melt extrusion and 3D printing temperatures is the most promising approach to reduce drug degradation. So far, the following efforts have been made on the fabrication of 3D printed tablets at lower temperatures. Okwuosa et al. (2016) produced patient-specific immediate release tablets with either the active ingredient theophylline or dipyridamole. Besides the active ingredients, the polymer polyvinylpyrrolidone (PVP), the plasticizer triethyl citrate and the filler talc were used to achieve a lower FDM 3D printing at a temperature of 110 °C [13]. Kempin et al. (2018) also printed immediate release tablets with the model drug pantoprazole sodium at temperatures below 100 °C. Five different pharmaceutical grade polymers, poly vinylpyrrolidone (PVP K12), polyethylene glycol 6000 (PEG 6000), Kollidon® VA 64, polyethylene glycol 20,000 (PEG 20,000) and poloxamer 407, were hot-melt extruded and then printed to tablets at lower temperatures [14]. Kollamaram et al. (2018) investigated the two immediate release polymers, Kollidon® VA 64 and Kollidon® 12 PF, for the FDM 3D printing of ramipril at lower temperatures. It could be extruded at 70 °C and printed into tablets at a temperature of 90 °C. Kollidon® VA 64 and Kollidon® 12 PF were also demonstrated to be suitable for printing the drug 4-aminosalicylic acid (4-ASA), which shows degradation in FDM 3D printing in previous studies [15]. Manini et al. (2022) created long-acting implantable dosage forms with the heat-sensitive drug paliperidone palmitate. Different formulations consisting of polylactic acid (PLA) and poloxamer 188, PLA and PEG 2.000 or PLA and ethylene-vinyl acetate (EVA) were extruded at 180 °C and printed at 150 °C [6]. Sadia et al. (2018) produced 3D printed bilayer antihypertensive tablets with the active ingredient hydrochlorothiazide and enalapril maleate and combined both in a single bilayer tablet by using a dual FDM 3D printer [16].

For the present study, we selected enalapril maleate, an angiotensin-converting enzyme inhibitor (ACEI), as model drug for the investigations of thermal stress during the 3D printing process. Enalapril maleate has a peptidomimetic structure and is therefore highly thermo-sensitive. Additionally, antihypertensive substances like enalapril maleate are of particular importance for the use in personalized medicine because a slow titration of the dosage is frequently necessary [17]. Antihypertensives are among the most commonly used drugs in 3D printing formulations, along with anti-inflammatory and analgesic drugs [18]. Regarding the therapeutic regimen for the active ingredient enalapril maleate, the dosage range for the treatment of hypertension in adults is between 2.5 mg and 40 mg. For children, the dose should be adjusted to the body weight [17].

In a previous publication, suitable process conditions and formulations with the polymers Soluplus® and Eudragit® E PO were investigated for hot-melt extrusion of enalapril maleate. At certain suitable process conditions, it showed minimal to no degradation of the active ingredient compared to other polymers. An interaction between drug and Eudragit® E PO let to stabilization of the drug [19].

Therefore, the aim of this work is to investigate the consecutive drug printing of the HME filaments via FDM. The nozzle diameter, the printing temperature, and the printing speed were examined as factors to keep thermal degradation of the peptidomimetic drug enalapril maleate as minimal as possible.

2. Materials and Methods

2.1. Materials

Enalapril maleate was purchased from Azelis (Sankt Augustin, Germany) and manufactured by Zhejiang Huahai Pharmaceutical Industry (Zhejiang, China). Polyethylene oxide (PEO) Mw 100,000 (POLYOX™ WSR N10) was kindly provided by DuPont Nutrition & Biosciences (Neu-Isenburg, Germany). Soluplus® (SOL) was kindly provided by BASF (Ludwigshafen, Germany). Basic butylated methacrylate copolymer (bPMMA, Eudragit® E PO) and fumed silica (SiO_2, Aerosil® 200 V/V Pharma) were kindly provided by Evonik (Essen, Germany). Enalapril maleate United States Pharmacopoeia (USP) Reference Standard were purchased by Eurofins PHAST GmbH (Homburg, Germany). Enalapril diketopiperazine (DKP) was purchased from LGC Standards GmbH (Wesel, Germany). Other chemicals were of reagent grade.

2.2. Preparation of Drug Loaded Extrudates

Hot-melt extrusion was carried out in our previous paper for the production of extrudates with the preferred formulations with a drug load of 10 % enalapril maleate at reduced temperature of 100 °C and additionally for formulation F2 at 70 °C (Table 1) [19]. HME was repeated for formulation F2 at 70 °C as the lowest possible extrusion temperature for the production of a sufficient number of 3D printed tablets for the printing study.

Table 1. Formulation composition for the production of HME extrudates.

Formulations	API (%)		Matrix (%)		Plasticizer (%)		Glidant (%)	
F1	EM	10	SOL	44.75	PEO	44.75	SiO_2	0.5
F2	EM	10	bPMMA	44	PEO	44	SiO_2	2.0

Briefly, a Leistritz ZSE 12 extruder was used with either a ZD 5 FB gravimetric feeder (Three-Tec, Seon, Switzerland) or a volumetric feeder (Brabender MT-S-HYD, Brabender, Duisburg, Germany). Both formulations were dosed with a feed rate of 100 g/h.

2.3. 3D Printing of Enalapril Maleate Tablets

The drug-loaded extrudates used as a substrate for FDM printing were printed into tablets using an i3 Mk3 printer (Prusa Research; Czech Republic). The tablet geometry was designed using Autodesk Fusion 360 (Mill Valley, CA, USA) and then sliced using the PrusaSlicer (PRUSA Research; Hradec Králové; Czech Republic). The extrudates were printed with two different nozzle diameters of 0.4 mm and 0.6 mm at nozzle temperatures of 180 °C and 190 °C and a print bed temperature of 35 °C with printing speeds of 30 mm/s, 60 mm/s and 90 mm/s. A cylindrical geometry (diameter: 6.8 mm and height: 2.4 mm) was selected to obtain tablets with a dose of 10 mg with a drug loading of 10% enalapril maleate in the extrudates.

2.4. Scanning Electron Microscopy (SEM) Imaging

Morphology of extrudates and 3D printed tablets of formulation F2 based on bPMMA extruded at 70 °C was examined using Zeiss Scanning Electron Microscope Leo 1430 VP (Zeiss, Germany). Samples were sputtered with a thin gold layer. The measurements were done under vacuum at a working voltage of 5–10 kV. The surface of the extrudates and tablets as well as the surface side view of 3D printed tablets were visualized.

2.5. Solid State Analysis

2.5.1. DSC Analysis

Thermo analysis of starting materials, physical mixtures as well as extrudates and tablets was performed using differential scanning calorimetry (DSC) (DSC 1, Mettler-Toledo, Giessen, Germany). Samples were heated at 10 °C / min over the temperature range of 20 °C to 200 °C for the active ingredient enalapril maleate and of 20 °C to 160 °C for the physical mixtures, extrudates and tablets.

2.5.2. X-ray Diffractometer (XRD)

XRD analysis was carried out for starting materials, extrudates and tablets using a Rigaku Miniflex diffractometer in Θ/2Θ geometry at ambient temperature using Cu-Kα radiation (Θ = 1.54182 Å). Scans were performed from 2θ = 2° to 50° in 0.01° steps.

2.6. Drug Content of Extrudates and 3D Printed Tablets

A 3D printed tablet or a section of a drug-loaded extrudate (approximately 0.1 g) was placed in a 100 mL volumetric flask and dissolved in 100 mL of a mixture of acetonitrile and 1 mM potassium dihydrogen phosphate buffer (50/50, *v/v*). Samples of the solutions were then filtered through a 0.45 µm nylon filter. An Elite LaChrom system consisting of L-2200 automatic sampler, L-2130 high pressure pump, L-2300 column oven and L-2400 UV detector was used (all Hitachi-VWR, Darmstadt, Germany). Chromatographic separation of enalapril maleate and possible degradation products were carried out on a XBridge C18 column [3.0 x 150 mm, 3.5 µm (Waters, Germany)]. After injection of 30 µL sample solution the samples were separated with the aid of a gradient using a mobile phase of acetonitrile and 1 mM potassium dihydrogen phosphate buffer pH 3.0 (Table 2). The flow rate was 1.0 mL/min and the column temperature was maintained at 65 °C. The eluent was screened at a wavelength of 215 nm. The run time was set to 15 min. n = 10 samples were measured and mean ± SD are shown in the discussion. As described in [19], the identification and quantification of enalapril maleate and related substances was ensured with the help of reference standards. Selectivity was achieved by spiking enalapril maleate CRS solution with the other related substances. The limit of detection (LOD) was determined to be 19.4 ng/mL and the limit of quantification (LOQ) to be 58.7 ng/mL. Linearity was demonstrated in each case with an $R^2 > 0.999$ for the content uniformity in a concentration range from 60 to 140 µg/mL and for the dissolution study in a concentration range of 0.2 to 12 µg/mL. The accuracy of the content determination in the samples was verified by using enalapril maleate USP reference standard and enalapril diketopiperazine standard with known contents. The determination of the content of enalapril diketopiperazine was done by external calibration and was freshly prepared for the analyses. Precision, determined as repeatability, for enalapril was ensured with a coefficient of variation (CV) of 0.74 %.

Table 2. Gradient for the separation of enalapril and related substances.

Time (min)	Acetonitrile (% *v/v*)	Buffer (% *v/v*)
0 – 1.0	2	98
1.0 – 1.2	2 → 25	98 → 75
1.2 – 5.0	25	75
5.0 – 7.5	25 → 40	75 → 60
7.5 – 9.0	40 → 75	60 → 25
9.0 – 11.0	75 → 95	25 → 5
11.0 – 12.5	95	5
12.5 – 12.6	95 → 2	5 → 98
12.6 – 15.0	2	98

2.7. Dissolution

An in vitro drug release study was carried out using USP type I apparatus (AT7 Smart, Sotax, Aesch, Switzerland) at 37 °C ± 0.5°C with rotating speed of 50 rpm in 900 mL 0.1 N hydrochloric acid (n = 3, mean ± SD). The amount of ENP and DKP was quantified by HPLC.

3. Results

3.1. Hot-Melt Extrusion and 3D Printing of Tablets

A thorough discussion of the formulation composition and adjusting the critical process parameters of the extrusion process can be found in our previous paper [19]. The obtained extrudates from formulations made from SOL and bPMMA are looking flexible for the subsequent 3D printing process. Cylindrical tablets were printed at nozzle temperatures of 180 °C and 190 °C and a print bed temperature of 35 °C.

3.2. Scanning Electron Microscopy (SEM) Imaging

SEM images of formulation F2 extruded at 70 °C are shown in Figure 2a,b and display the surface of an extrudate and a 3D printed tablet. The layer-by-layer structure and the texture of the 3D printed tablet can be seen in Figure 2c,d. Tidau et al. (2019) investigated the surface of PEO-based extrudates and described the surface appearance as an octagonal structuring [20]. This structuring indicated the crystalline part of the semi-crystalline polymer PEO of which the crystal structure was investigated by Takahashi et al. (1973) [21].

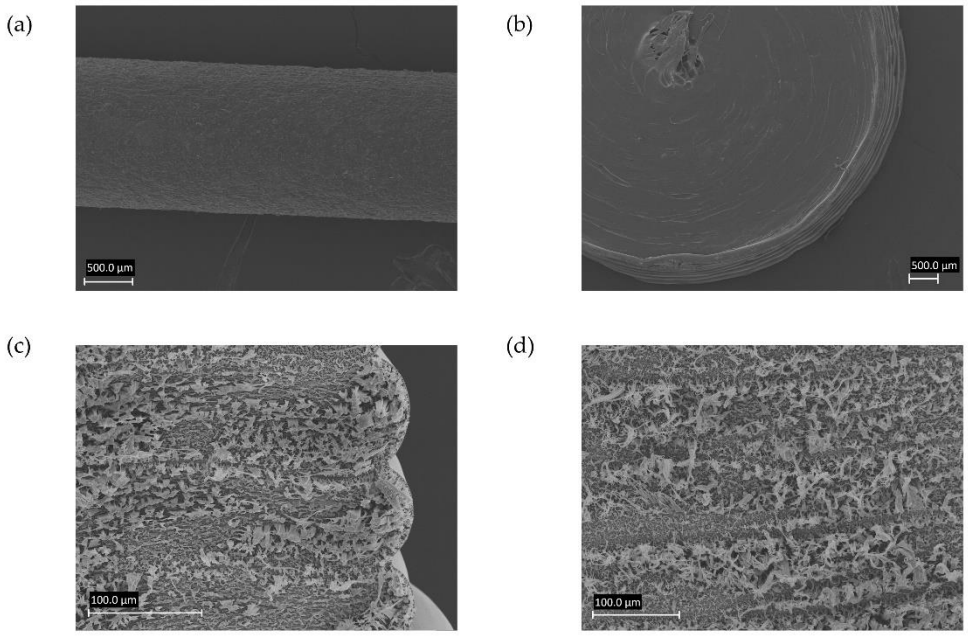

Figure 2. SEM images of the extrudate surface (**a**), tablet surface (**b**) and tablet side view (**c,d**) of the formulation containing bPMMA extruded at 70 °C.

3.3. Solid State Analysis

3.3.1. Thermo Analysis

Differential scanning calorimetry (DSC) analysis of enalapril maleate starting material and physical mixtures showed an endothermic peak at 153 °C (Figure 3a) [22,23]. However, the peak was not present in the extrudates and 3D printed tablets of the two different formulations indicating the absence of crystalline enalapril maleate. Therefore, enalapril maleate or its degradation product seems to be in an amorphous state in the extrudates and 3D printed tablets [16]. The semi-crystalline PEO also depicts an endothermic event with an onset at approximately 62 °C and a peak at 68 °C which can be seen in the physical mixture, extrudates and tablets (Figure 3b-d) [20].

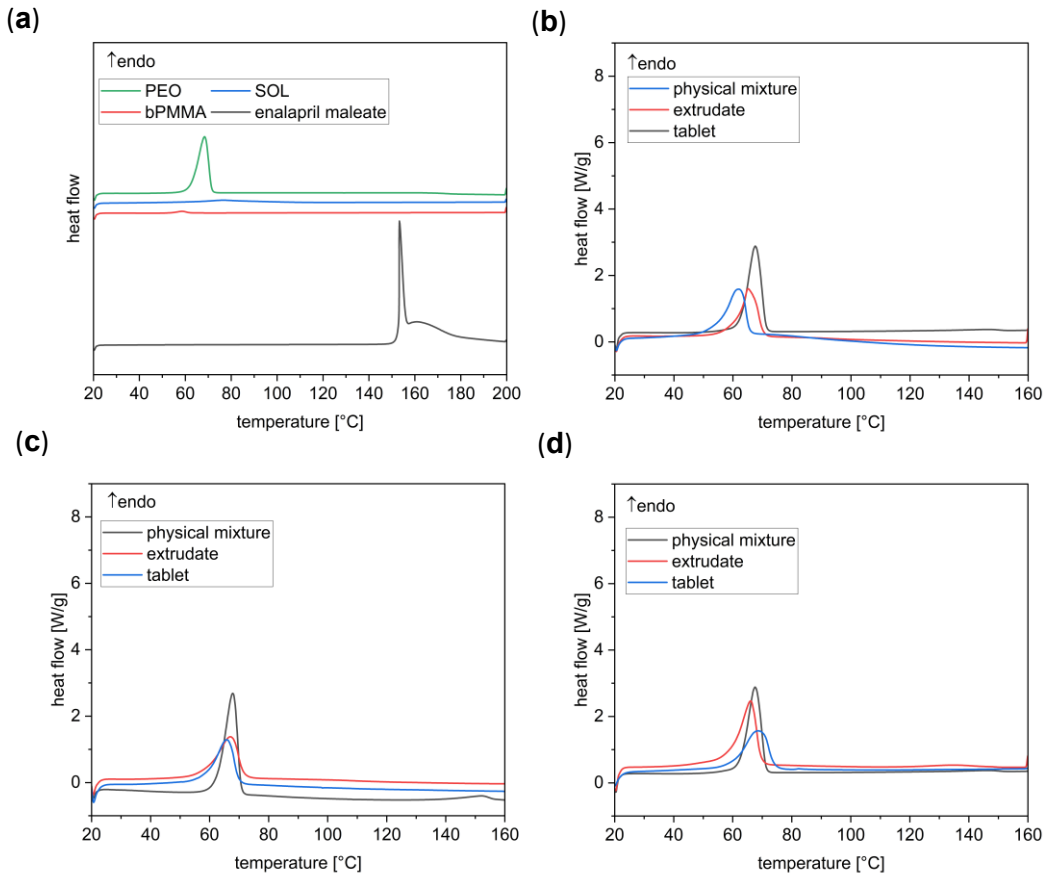

Figure 3. DSC thermograms of the starting materials (**a**), the formulation containing SOL extruded at 100 °C (**b**) and the formulation containing bPMMA extruded at 100 °C (**c**) and at 70 °C (**d**), respectively.

3.3.2. X-ray Diffractometer (XRD)

In addition to the DSC analysis, XRD analysis was performed to investigate changes in the crystallinity of enalapril maleate starting material and the physical mixtures in comparison to the extrudates and 3D printed tablets for both formulations.

Enalapril maleate showed a crystalline structure with characteristic peaks at 5.3°, 8.1°, 10.5°, 15.7°, 21.5°, 24.9° and 31.6° as previously described by Ramírez-Rigo et al. (2014) [24] (Figure 4a,b). For the polymers SOL (Figure 4a) and bPMMA (Figure 4b) no peaks were present due to the amorphous nature of these polymers. Polyethylene oxide exhibited two diffraction peaks at 19.0° and 23.2° (Figure 4a,b) [25]. In the physical mixtures of both formulations the characteristic peaks from enalapril maleate could be observed. The examined extrudates and 3D printed tablets revealed no crystalline active ingredient, only the crystalline parts of PEO were visible in the diffractograms. Furthermore, no differences in the physical state were found between the two formulations with SOL (Figure 4a) and bPMMA (Figure 4b) after extrusion at 100 °C [19] and FDM 3D printing at 180 °C. Reducing the extrusion temperature of the bPMMA formulation to 70 °C was also sufficient to fully convert enalapril maleate to the amorphous state (Figure 4b).

DSC and XRD measurements both demonstrate that enalapril maleate is in amorphous form in the extrudates and 3D printed tablets of both formulations.

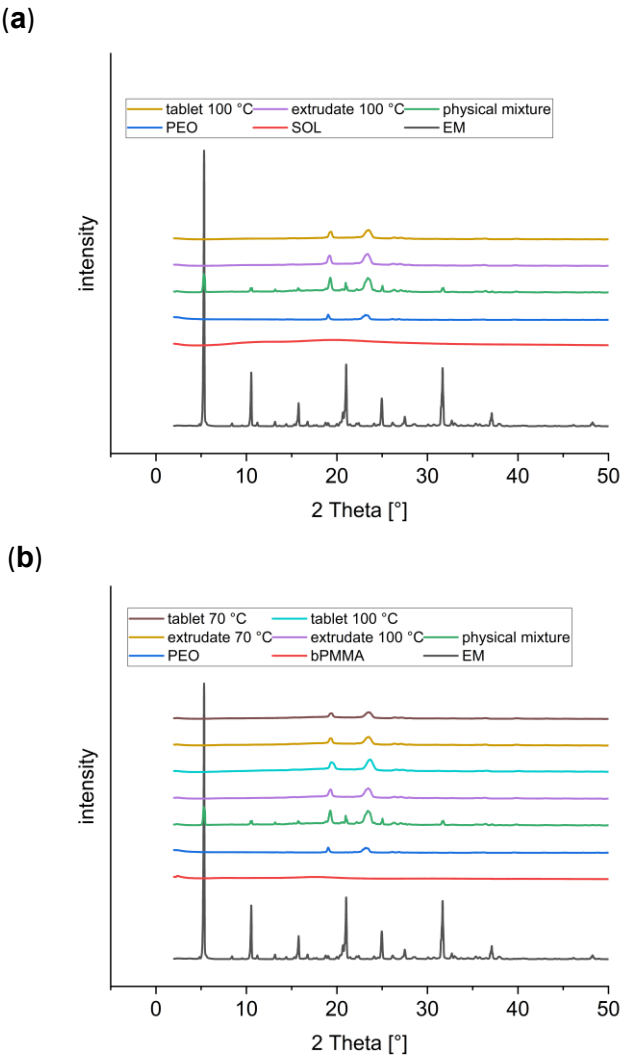

Figure 4. X-ray diffractograms of the formulation containing SOL extruded at 100 °C (**a**) and the formulation containing bPMMA extruded at 100 °C and 70 °C (**b**), respectively.

3.4. Drug Content of Extrudates and 3D Printed Tablets

The content of enalapril and degradation products in extrudates and 3D printed tablets were analysed as described in Section 2.6. The diketopiperazine derivative (DKP, Impurity D), which is described as the intramolecular cyclization product of enalapril [19], was found to be the main and the only degradation product in both the extrudates and the 3D printed tablets of the formulations (Figure 5).

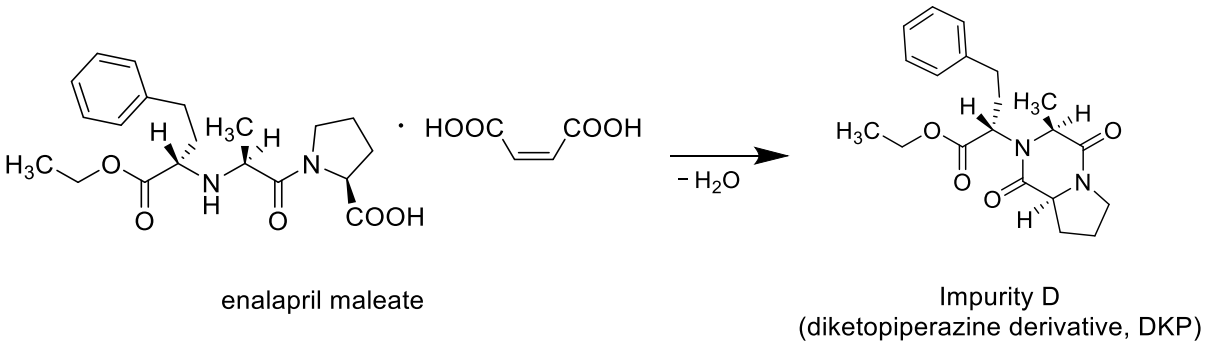

Figure 5. Illustration of the conversion of enalapril maleate to Impurity D at elevated temperatures.

Content data after extrusion has been discussed in our paper [19]. For formulation F1 it was observed that the content of enalapril in the extrudates extruded at 100 °C was 94.83 ± 1.72% after extrusion [19] and decreased after the FDM 3D printing process to 48.34 ± 2.69% (Figure 6). DKP was formed during both heat-intensive processes. A content of 7.54 ± 0.24% DKP was determined in the extrudates [19] and 46.84 ± 4.65% in the 3D printed tablets (Figure 6).

For formulation F2 extruded at a temperature of 100 °C, the content of enalapril was 98.44 ± 0.30% [19]. After 3D printing, the content of enalapril decreased to 73.01 ± 1.91% (Figure 6). Again, the degradation of enalapril is accompanied by an increase in the content of the DKP. A total of 2.83 ± 0.09% DKP was found in the extrudates [19], whereas 26.48 ± 0.92% DKP was formed during the FDM 3D printing process (Figure 6).

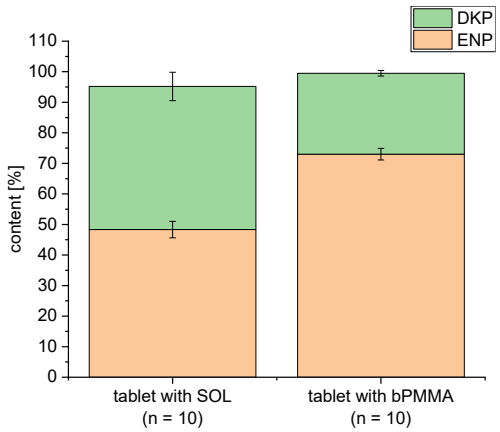

Figure 6. Illustration of the enalapril and diketopiperazine derivative contents after 3D printing for the formulation containing SOL and the formulation containing bPMMA extruded at 100 °C and printed at 180 °C (*n* = 10, mean ± SD).

Comparing both formulations, a higher drug content was found for formulation F2 with the polymer bPMMA under the same process conditions during hot-melt extrusion and FDM 3D printing. This could be explained with the stabilizing effect of the basic polymer bPMMA in comparison to the neutral polymer SOL as described in [19]. This demonstrates the impact formulation constituents may have on the degradation of drugs. Formulation F2, which was also extruded at a temperature of 70 °C and repeated again, revealed an enalapril content of 99.75 ± 0.32% compared to 101.72 ± 1.65% as already has been shown in our previous paper

[19]. After 3D printing, 82.21 ± 1.21% enalapril was recovered (Figure 7). A small amount with 0.68 ± 0.03% DKP was found in the extrudates and 17.86 ± 0.77% in the 3D printed tablets. Thus, FDM 3D printing at 180 °C had the main influence on the degradation of the active ingredient. However, printing at lower temperatures was not possible, most likely due to high melt viscosity of both formulations.

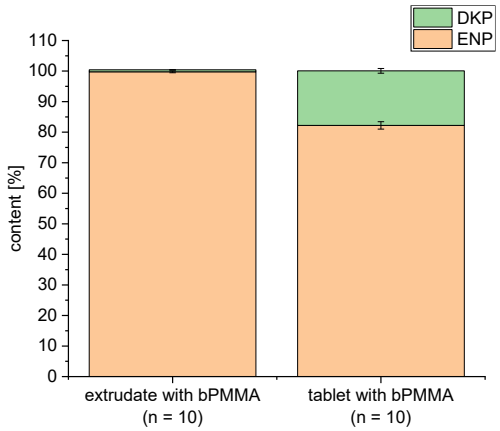

Figure 7. Illustration of the enalapril and diketopiperazine derivative contents after extrusion and 3D printing for the formulation containing bPMMA extruded at 70 °C and printed at 180 °C (*n* = 10, mean ± SD).

Different strategies to reduce degradation were investigated. Tablets were originally printed at a printing speed of 30 mm/s and higher printing speeds were used to investigate if shorter residence times had an influence on degradation, as an exponential decrease in printing time with higher printing speed has been reported [26]. A larger nozzle diameter should enable higher material flow while reducing shear forces, potentially resulting in shorter residence times and less degradation. Tablets were also printed at a higher nozzle temperature of 190 °C to investigate if decreased melt viscosity would allow for higher printing speeds and shorten the residence time. Lastly it was investigated, if lower infill levels enabled quicker cooling and reduced degradation.

Therefore, ten tablets were printed with nozzle diameters of 0.4 mm and 0.6 mm at temperatures of 180 °C and 190 °C and 35 °C print bed temperature with printing speeds of 30 mm/s, 60 mm/s, and 90 mm/s and the content of enalapril and the diketopiperazine derivative was determined.

Surprisingly, a slight decrease of enalapril content was observed with a nozzle diameter of 0.4 mm and increasing printing speed. This was observed at printing temperatures of 180 °C and 190 °C (Table 3). At 180 °C and a printing speed of 30 mm/s, 85.55 ± 1.48% enalapril were recovered whereas the content of enalapril at the highest printing speed of 90 mm/s was 79.97 ± 1.80%. Tablets printed at 190 °C and 30 mm/s had a drug content of 78.47 ± 0.77%. At a printing speed of 90 mm/s, only 74.98 ± 1.47% enalapril was found. The decrease in the content of enalapril for the 0.4 mm nozzle at higher printing speeds may be explained with increased back pressure during 3D printing at the same temperature, which might lead to more back-mixing. Furthermore, it could be observed that a higher nozzle temperature always led to a higher degradation of enalapril in the 3D printed tablets (Table 3).

Table 3. Enalapril (ENP) and diketopiperazine derivative (DKP) contents in the FDM printed tablets with a nozzle diameter of 0.4 mm printed at 180 °C (a) and 190 °C (b) with different printing speeds (*n* = 10, mean ± SD).

Temperature [°C]	Printing speed [mm/s]					
	30		60		90	
	ENP	DKP	ENP	DKP	ENP	DKP
180	85.55 ± 1.48%	15.55 ± 0,87%	82.83 ± 1.58%	16.33 ± 0.94%	79.97 ± 1.80%	19.89 ± 1.12%
190	78.47 ± 0.77%	21.55 ± 0.75%	77.02 ± 0,89%	22.11 ± 0.59%	74.98 ± 1.47%	24.37 ± 0.99%

Using a nozzle diameter of 0.6 mm resulted in a small increase of enalapril content at a printing temperature of 180 °C with increasing printing speed (Table 4). A total of 79.40 ± 0.64% enalapril was found in the 3D printed tablets at 30 mm/s and 84.41 ± 1.30% at 90 mm/s. This could be explained due to a shorter residence time and heat exposure during printing. At 190 °C, 79.27 ± 1.36% enalapril was found at 30 mm/s and 79.24 ± 0.98% at 90 mm/s. No increase in the content could be observed at a temperature of 190 °C. At a printing speed of 60 mm/s, a lower content of 75.32 ± 1.53% was observed. Comparable to printing with the 0.4 mm nozzle, a lower content was found for all printing speeds at a higher temperature.

Table 4. Enalapril (ENP) and diketopiperazine derivative (DKP) contents in the FDM printed tablets with a nozzle diameter of 0.6 mm printed at 180 °C (a) and 190 °C (b) with different printing speeds (*n* = 10, mean ± SD).

Temperature [°C]	Printing speed [mm/s]					
	30		60		90	
	ENP	DKP	ENP	DKP	ENP	DKP
180	79.40 ± 0.64%	18.39 ± 0.54%	79.91 ± 0.81%	18.69 ± 0.60%	84.41 ± 1.30%	15.10 ± 0.71%
190	79.27 ± 1.36%	21.43 ± 0.66%	75.32 ± 1.53%	24.66 ± 1.28%	79.24 ± 0.98%	21.63 ± 0.54%

F- and t-tests (α = 0.05) were performed for recovery rates of enalapril printed at 30 mm/s and 90 mm/s to explore whether differences were significant at both temperatures, both nozzle diameters and between the highest printing speed at 190 °C. The analysis showed that for the 0.4 mm nozzle, there were significant differences in the content between the printing speeds 30 mm/s and 90 mm/s at both temperatures. For the 0.6 mm nozzle, the differences were significantly different only at a temperature of 180 °C. A comparison between the two nozzles for the highest printing speed of 90 mm/s also showed significant differences.

In summary, the investigations into the influence of the nozzle diameter and the printing speed showed that the highest amount of enalapril was found for the 0.4 mm nozzle at a nozzle temperature of 180 °C and a printing speed of 30 mm/s (85.55 ± 1.48%). Nonetheless, utilizing a larger nozzle diameter of 0.6 mm and a printing speed of 90 mm/s, printing times were reduced without sacrificing accuracy, as demonstrated by the not significantly lower but uniform drug content of 84.41 ± 1.30%.

In addition to 3D printing of tablets with 100% infill, the influence of reduced infill and other contours on content of enalapril should also be investigated. Tablets were printed with a nozzle diameter of 0.4 mm. Therefore, besides the cylindrical tablets with 100% infill (Figure 8a),

tablets were printed with reduced infill (25% and 20%) and only one contour (*n* = 3, mean ± SD) (Figure 8b,c). Infills appear to deviate more than 5% in Figure 8 because of the visualization in the slicer software.

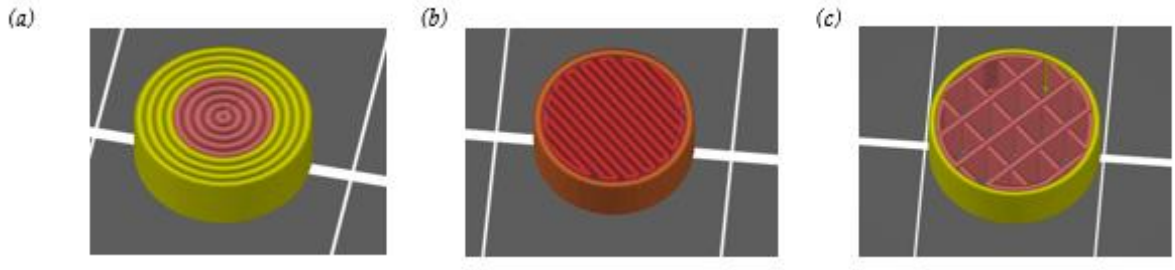

Figure 8. Design of different 3D printed tablets of the formulation containing bPMMA extruded at 70 °C with 100 % infill (**a**), and reduced infill of 25 % (**b**) and 20 % (**c**).

With another design (Figure 8b), the content of enalapril was 78.20 ± 0.42% (*n* = 3, mean ± SD) and the content of the diketopiperazine derivative 22.74 ± 0.54% (*n* = 3, mean ± SD) in the tablets. This did not show a higher content of enalapril despite reduced infill. The infill was further reduced to 20% and straight infill was chosen (Figure 8c). To achieve the same tablet weight of 100 mg, the tablet geometry had to be adjusted to a diameter of 9.6 mm and a height of 3.4 mm. The content of enalapril in these tablets was 81.93 ± 2.85% (*n* = 3, mean ± SD), whereas 19.27 ± 2.33% (*n* = 3, mean ± SD) diketopiperazine derivative was formed.

Compared to the 3D-printed tablets with 100% infill, no higher content has been found by printing more flexible structures with reduced infill or varying infill pattern.

3.5. Dissolution

In addition to the content, the release behavior of enalapril and DKP (Figure 9) from the bPMMA tablets extruded at 70 °C with 100% infill was also investigated compared to the extrudates which was already shown in [19]. As expected, fast drug release was observed. Due to the decrease of enalapril content in the tablets and the formation of the DKP, only 35.62 ± 5.52% enalapril and 14.78 ± 1.52% DKP were dissolved in the tablets after 30 min [27]. After 180 min, 68.85 ± 1.86% enalapril and 30.34 ± 0.72% DKP were released. However, despite the degradation of enalapril in the tablets, enalapril was almost completely released from the tablets which is shown by the formation of the calculated sum of ENP and DKP (Figure 9). The sum, which was formed from the mean values of the individual curves of both substances, amounts to 99.18% after 180 min.

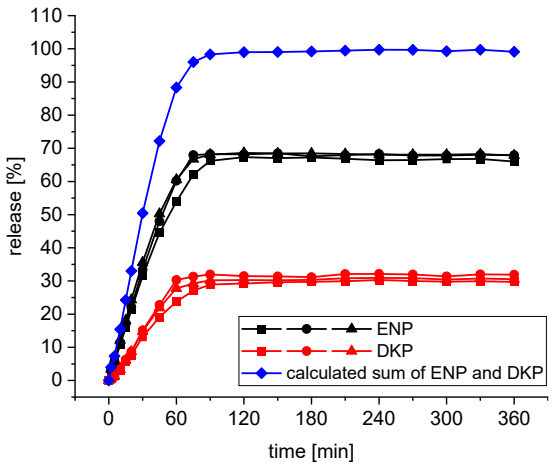

Figure 9. In vitro dissolution profiles of ENP and DKP from bPMMA tablets (*n* = 3) as well as the calculated sum of ENP and DKP, pH 1.2 buffer solution, USP Apparatus 1-basket, 37 °C, 50 rpm.

4. Conclusions

In this study, we investigated the thermal degradation of the peptidomimetic drug enalapril maleate in FDM 3D printing in two different formulations. Data showed that enalapril maleate was amorphous in extrudates and tablets of both formulations. Processed at 100 °C, a higher content of enalapril was observed in bPMMA-based extrudates compared to SOL-based extrudates. The same order was observed in tablets 3D printed at 180 °C, but the observed difference was larger. Enalapril maleate degraded more strongly during the 3D printing process in the formulation with SOL than in the formulation with bPMMA. The main thermal degradation product found in extrudates and 3D printed tablets was the diketopiperazine derivative (Imp-D). The lower degradation of enalapril maleate with bPMMA could be explained by a cation-anion interaction of enalapril with the basic bPMMA [19]. Degradation in extrudates could be avoided using bPMMA at an extrusion temperature of 70 °C. In FDM, a higher temperature gradient between nozzle and filament is necessary to plasticise the filament in the comparably short residence time and degradation was observed in all experiments. Selecting a larger nozzle diameter and higher printing speeds as well as varying the infill did not result in reduced degradation of the drug in the 3D printed tablets.

To our knowledge, this is the first study that not only investigates the extent of degradation of a thermo-sensitive drug during 3D printing but also quantifies both, the drug and also the resulting degradation product. This study revealed that despite selection of suitable polymers, FDM 3D printing with a commercial 3D printer is not feasible for the peptidomimetic enalapril maleate without degradation. Our study highlights one of the drawbacks of FDM 3D printing, as it excludes therapeutic important active ingredients such as enalapril maleate, which is especially important for pediatric care. It also demonstrates the need for the development and implementation of good manufacturing practice (GMP) compliant FDM 3D printers, designed to reduce the temperature stress during 3D printing. These could offer new opportunities for this important class of drugs. Enabling 3D printing with such drugs would be beneficial for personalized treatments.

Author Contributions: Conceptualization, L.H., J.Q and J.B.; methodology, L.H.; formal analysis, L.H.; investigation, L.H.; writing—original draft preparation, L.H.; writing—review and editing, L.H., J.Q.; visualization, L.H.; supervision, J.Q, J.B.; project administration, J.Q.; funding acquisition, J.Q., J.B. All authors have read and agreed to the published version of the manuscript.

Funding: This research was funded by German Federal Ministry of Education and Research—project 'ProMat Leben-Polymere-PolyPrint' (project no.: 13XP5064B).

Institutional Review Board Statement: Not applicable.

Informed Consent Statement: Not applicable.

Data Availability Statement: The data presented in this study are available upon request from the corresponding author.

Acknowledgments: The authors want to thank Tobias Auel for conducting the XRD measurements.

Conflicts of Interest: The authors 1,3 declare that they have no conflict of interest. Jörg Breitkreutz is a minority shareholder of Ethicare GmbH, a company developing a pediatric medicine with enalapril.

Abbreviations

ACEI	angiotensin-converting enzyme inhibitor
BJ	binder jetting
bPMMA	basic butylated methacrylate copolymer
CV	coefficient of variation
DKP	diketopiperazine derivative
DSC	Differential Scanning Calorimetry
EM	enalapril maleate
ENP	enalapril
EVA	ethylene-vinyl acetate
HME	hot melt extrusion
HPLC	High Performance Liquid Chromatography
FDM	fused deposition modeling
GMP	good manufacturing practice
Imp	impurity
LOD	limit of detection
LOQ	limit of quantification
PEG	polyethylene glycol
PEO	polyethylene oxide
PF	Pyrogen-free
PLA	polylactic acid
PVP	polyvinylpyrrolidone
SD	standard deviation
SEM	Scanning Electron Microscopy
SiO_2	fumed silica
SLA	stereolithography
SLS	selective laser sintering
SOL	Soluplus
SSE	semi-solid extrusion
TTSPP	time- and temperature-sensitive pharmaceutical product

USP	United States Pharmacopeia
UV	ultraviolet
VA	poly(vinylpyrrolidone-vinyl acetate)-copolymer
WHO	World Health Organization
XRD	X-ray diffractometer

References

1. Litman, T. Personalized medicine—concepts, technologies, and applications in inflammatory skin diseases. *Apmis*. **2019**, *127*, 386–424. [PubMed]
2. Beer, N.; Heggerm I.; Kaae, S.; De Bruin, M.L.; Genina, N.; Alves, T.L.; Hoebert, J.; Kälvemark Sporrong, S. Scenarios for 3D printing of personalized medicines - A case study. *Explor. Res. Clin. Soc. Pharm*. **2021**, *4*, 100073. [CrossRef] [PubMed]
3. Basit, A. Recent innovations in 3D-printed personalized medicines: An interview with Abdul Basit. *J. 3D Print. Med*. **2020**, *4*, 5–7. [CrossRef]
4. Vaz, V.M.; Kumar, L. 3D Printing as a Promising Tool in Personalized Medicine. *AAPS PharmSciTech*. **2021**, *22*, 49. [CrossRef]
5. El Aita, I.; Ponsar, H.; Quodbach, J. A critical review on 3D-printed dosage forms. *Curr. Pharm*. **2018**, *24*, 4957-4978. [CrossRef]
6. Manini, G.; Benali, S.; Mathew, A.; Napolitano; S.; Raquez; J.-M.; Goole, J. Paliperidone palmitate as model of heat-sensitive drug for long-acting 3D printing application. *Int. J. Pharm*. **2022**, *618*, 121662. [CrossRef]
7. Abdella, S.; Youssef, S.H.; Afinjuomo, F.; Song, Y.; Fouladian, P.; Upton, R.; Garg, S. 3D Printing of thermo-sensitive drugs. *Pharmaceutics*. **2021**, *13*, 1524. [CrossRef]
8. Azad, M.A.; Olawuni, D.; Kimbell, G.; Badruddoza, A.Z.M.; Hossain, M.S.; Sultana, T. Polymers for extrusion-based 3D printing of pharmaceuticals: A holistic materials–process perspective. *Pharmaceutics*. **2020**, *12*, 124. [CrossRef]
9. Alhnan, M.A.; Okwuosa, T.C.; Sadia, M.; Wan, K.-W.; Ahmed, W.; Arafat, B. Emergence of 3D printed dosage forms: Opportunities and challenges. *Pharm. Res*. **2016**, *33*, 1817-1832. [CrossRef]
10. Quodbach, J.; Bogdahn, M.; Breitkreutz, J.; Chamberlain, R.; Eggenreich, K.; Elia, A.G.; Gottschalk, N.; Gunkel-Grabole, G.; Hoffmann, L.; Kapote, D. Quality of FDM 3D printed medicines for pediatrics: Considerations for formulation development, filament extrusion, printing process and printer design. *Ther. Innov. Regul. Sci*. **2021**, *56*, 1-19. [CrossRef]
11. World Health Organization. WHO Technical Report Series, No. 961, 2011. Annex 9 Model guidance for the storage and transport of time- and temperature-sensitive pharmaceutical products (2011). Avaiable online: https://www.who.int/docs/default-source/medicines/norms-and-standards/guidelines/distribution/trs961-annex9-modelguidanceforstoragetransport.pdf?sfvrsn=b80e925f_2 (accessed on 27 July 2022).
12. do Pazo-Oubiña, F.; Alorda-Ladaria, B.; Gomez-Lobon, A.; Boyeras-Vallespir, B.; Santandreu-Estelrich, M.M.; Martorell-Puigserver, C.; Gomez-Zamora, M.; Ventayol-Bosch, P.; Delgado-Sanchez, O. Thermolabile drug storage in an ambulatory setting. *Sci Rep*. **2021**, *11*, 5959. [CrossRef] [PubMed]
13. Okwuosa, T.C.; Stefaniak, D.; Arafat, B.; Isreb, A.; Wan, K.-W.; Alhnan, M.A. A Lower temperature FDM 3D printing for the manufacture of patient-specific immediate release tablets. *Pharm. Res*. **2016**, *33*, 2704-2712. [CrossRef] [PubMed]
14. Kempin, W.; Domsta, V.; Grathoff, G.; Brecht, I.; Semmling, B.; Tillmann, S.; Weitschies, W.; Seidlitz, A. Immediate release 3D-printed tablets produced via fused deposition modeling of a thermo-sensitive drug. *Pharm. Res.* **2018**, *35*, 1-12. [CrossRef] [PubMed]

15. Kollamaram, G.; Croker, D.M.; Walker, G.M.; Goyanes, A.; Basit, A.W.; Gaisford, S. Low temperature fused deposition modeling (FDM) 3D printing of thermolabile drugs. *Int. J. Pharm*. **2018**, *545*, 144-152. [CrossRef]

16. Sadia, M.; Sośnicka, A.; Arafat, B.; Isreb, A.; Ahmed, W.; Kelarakis, A.; Alhnan, M.A. Adaptation of pharmaceutical excipients to FDM 3D printing for the fabrication of patient-tailored immediate release tablets. *Int. J. Pharm*. **2016**, *513*, 659-668. [CrossRef]

17. Neubeck, M. Commentary on Ph. Eur. 9.0, 2017. 57th Supply, enalapril maleate. *In Commentary on the European Pharmacopoeia*; Wissenschaftliche Verlagsgesellschaft mbH: Stuttgart, Germany; Govi-Verlag: Eschborn, Germany, 2017.

18. Brambilla, C.R.; Okafor-Muo, O.L.; Hassanin, H.; & ElShaer, A. 3DP printing of oral solid formulations: A systematic review. *Pharmaceutics*. **2021**, *13*, 358. [CrossRef]

19. Hoffmann, L.; Breitkreutz, J.; Quodbach, J. Hot-Melt Extrusion of the Thermo-Sensitive Peptidomimetic Drug Enalapril Maleate. *Pharmaceutics* **2022**, *14*, 2091. [CrossRef]

20. Tidau, M.; Kwade, A.; Finke, J.H. Influence of high, disperse API load on properties along the fused-layer modeling process chain of solid dosage forms. *Pharmaceutics*. **2019**, *11*, 194. [CrossRef]

21. Takahashi, Y.; Tadokoro, H. Structural studies of polyethers, (-(CH2)m-O-)n. X. Crystal structure of poly(ethylene oxide). *Macromolecules*. **1973**, *6*, 672–675. [CrossRef]

22. Lin, S.-Y.; Wang, S.-L.; Chen, T.-F.; Hu, T.-C. Intramolecular cyclization of diketopiperazine formation in solid-state enalapril maleate studied by thermal FT-IR microscopic system. *Eur. J. Pharm. Biopharm.* **2002**, *54*, 249-254. [CrossRef]

23. Gómez Pineda, E.A.; Martins Ferrarezi, A. D.; Ferrarezi, J.G.; Winkler Hechenleitner, A.A. Thermal decomposition of enalapril maleate studied by dynamic isoconversional method. J. *Therm. Anal. Calorim*. **2005**, *79*, 259-262. [CrossRef]

24. Ramírez-Rigo, M.V.; Olivera, M.E.; Rubio, M.; Manzo, R.H. Enhanced intestinal permeability and oral bioavailability of enalapril maleate upon complexation with the cationic polymethacrylate Eudragit E100. Eur. *J. Pharm. Sci.* **2014**, *55*, 1-11. [CrossRef] [PubMed]

25. Xu, X.; Jiang, L.; Zhou, Z.; Wu, X.-F.; Wang, Y. Preparation and properties of electrospun soy protein isolate/polyethylene oxide nanofiber membranes. *ACS Appl. Mater. Interfaces*. **2012**, *4*, 4331-7. 10.1021/am300991e. [CrossRef] [PubMed]

26. Ilyés, K.; Kovács, N.K.; Balogh, A.; Borbás, E.; Farkas, B.; Casian, T.; Marosi, G.; Tomuță, I.; Nagy, Z.K. The applicability of pharmaceutical polymeric blends for the fused deposition modelling (FDM) 3D technique: Material considerations–printability–process modulation, with consecutive effects on in vitro release, stability and degradation. *Eur. J. Pharm. Sci*. **2019**, *129*, 110-123. [CrossRef]

27. Lima, D.M.; dos Santos, L.D.; Lima, E.M. Stability and in vitro release profile of enalapril maleate from different commercially available tablets: possible therapeutic implications. *J. Pharm. Biomed. Anal*. **2008**, *47*, 934-937. [CrossRef]

5 Publication 4: FDM 3D Printing of Filaments with Escitalopram Oxalate

Pretext

In Chapter 5, the physical and chemical stability of the thermo-sensitive enantiomeric drug escitalopram oxalate (ESC-OX) during HME and FDM 3D printing was investigated. Three different formulations consisting of escitalopram with a drug load of 10 % and the polymers HPMC and bPMMA were processed into extrudates by HME and subsequently 3D printed tablets were produced by FDM 3D printing. Depending on the polymer matrix used, the aim was to investigate both the physical state of the active ingredient using DSC and XRD and the chemical stability using HPLC. Therefore, the content of ESC-OX and its degradation products was determined on the achiral column. In addition, due to the chiral structure of ESC-OX, a potential conversion to the R-enantiomer during these two processes was investigated. The stability in solution was also assessed. Comparative studies were conducted with the commercially available Cipralex® film-coated tablets.

Evaluation of authorship

The following research paper has been published in European Journal of Pharmaceuticals Sciences in 2023. Lena Hoffmann was responsible for conceptualisation, data curation, formal analysis, investigation, methodology, visualisation, writing – original draft, writing – review and editing. Jörg Breitkreutz was responsible for conceptualisation, funding acquisition, project administration, resources, supervision, writing – review and editing. Julian Quodbach was responsible for conceptualisation, funding acquisition, project administration, resources, supervision, writing – review and editing.

author/co-author	idea [%]	study design [%]	experimental [%]	evaluation [%]	manuscript [%]
Lena Hoffmann	85	80	100	100	85
Jörg Breitkreutz	10	10	0	0	5
Julian Quodbach	5	10	0	0	10

Investigation of the degradation and *in-situ* amorphization of the enantiomeric drug escitalopram oxalate during Fused Deposition Modeling (FDM) 3D printing

Lena Hoffmann[1], Jörg Breitkreutz[1] and Julian Quodbach[1,2]

[1]Institute of Pharmaceutics and Biopharmaceutics,

Heinrich Heine University, Düsseldorf, Germany

[2]Department of Pharmaceutics,

Utrecht University, Utrecht, The Netherlands

Eur. J. Pharm. Sci. 185 (2023) 106423

Abstract

Hot-melt extrusion (HME) and subsequent FDM 3D printing offer great potential opportunities in the formulation development and production of customized oral dosage forms with poorly soluble drugs. However, thermal stress within these processes can be challenging for thermo-sensitive drugs. In this work, three different formulations were prepared to investigate the degradation and the solid state of the thermo-sensitive and poorly soluble drug escitalopram oxalate (ESC-OX) during the two heat-intensive processes HME and FDM 3D printing. For this purpose, hydroxypropyl methyl cellulose (HPMC) and basic butylated methacrylate copolymer (bPMMA) were chosen as polymers. DSC and XRD measurements revealed that ESC-OX is amorphous in the HPMC based formulations in both, extrudates and 3D printed tablets. In contrast, *in-situ* amorphization of the drug from crystalline state in bPMMA filaments was observed during FDM 3D printing. With regard to the content, it was found that degradation of ESC-OX in extrudates with bPMMA could be avoided and in 3D printed tablets almost fully reduced. Furthermore, a possible conversion into the R-enantiomer in the formulation with bPMMA could be excluded using a chiral column. Compared to the commercial product Cipralex®, drug release from extrudates and tablets with bPMMA was slower but still qualified as immediate drug release.

Keywords: hot-melt extrusion; FDM 3D printing; thermal degradation; solid-state analysis; escitalopram oxalate; personalized medicine.

Article available online at:

https://doi.org/10.1016/j.ejps.2023.106423

1. Introduction

Fused deposition modeling (FDM) 3D printing is an additive manufacturing technique, which is widely explored in pharmaceutics for the production of personalized dosage forms (Khalid and Billa, 2022). It offers the opportunity to manufacture dosage forms with an individual dose and desired release profile on-demand in short time. Therefore, the dose can be adapted to the special needs of the patients (Awad et al., 2018; Konta et al., 2017; Fernandez-Garcia et al., 2020; Windolf, et al. 2022) as well as the needs of pediatric and geriatric patients (Scoutaris et al., 2018; Krause et al., 2021; Hoffmann et al., 2022a). This becomes increasingly important in personalized medicine (Goyanes et al., 2017; Varghese et al., 2022) and can also be beneficial in pandemic situations when shortages are present (Khalid and Billa, 2022).

To meet the growing interest in FDM 3D printed dosage forms, hot-melt extrusion can be applied for the production of filaments, the feed stock material for the subsequent 3D printing process (El Aita et al., 2018, Hoffmann et al., 2022b). HME, as an upstream process, can be considered as preferred method for the preparation of amorphous solid dispersions (ASDs) which can improve the solubility of poorly soluble drugs (Pawar et al., 2016; Tan et al., 2020). Besides the solubility enhancement of BCS class II and IV drugs, HME can improve bioavailability and dissolution rate (Douroumis, 2012; Kanaujia et al., 2015). This becomes a major concern in the pharmaceutical industry, because 40 % of approved medicines and up to 90 % of drugs in the discovery pipeline are poorly water soluble (Hiew et al., 2022; Kalepu and Nekkanti, 2015).

The production of amorphous solid dispersions should overcome this problem by converting the drug from the crystalline state to the amorphous state (Grohganz et al., 2013). However, the amorphous drug must be stabilized in a (polymer) matrix, prolonging the stability of the amorphous state and preventing recrystallization (Holm et al., 2022). Therefore, the combination of hot-melt extrusion followed by FDM 3D printing should enable the possibility to improve on the one hand, the solubility issues and, on the other hand, the production of customized 3D printed oral dosage forms with poorly soluble drugs. This is beneficial because oral dosage forms are still the preferred choice due to their ease of administration (Alhnan et al., 2016; Wang et al., 2022). Nevertheless, the combination of the two processes, hot-melt extrusion and FDM 3D printing, also have drawbacks. Thermo-sensitive drugs are subjected to high temperatures twice (Khalid and Billa, 2022).

Hence, the processing of thermo-sensitive drugs can be challenging (Abdella, et al. 2021; Kempin, et al. 2018). The first investigations were conducted by Goyanes et al. (2015), who explored the thermal degradation of 5-aminosalicylic acid (5-ASA) and 4-aminosalicylic acid (4-ASA) from previously made filaments during FDM 3D printing. It was shown that the degradation of the active ingredients during FDM 3D printing at a temperature of 210 °C was drug dependent. 4-aminosalicyclic acid, which initially melts and then decomposes at a temperature between 130 to 145 °C, degraded to 50 %, while the drug 5-aminosalicylic acid was stable with a melting temperature of 278 to 279 °C. Kollamaram et al. (2018) prepared filaments with the model drug ramipril, which has a low melting temperature of 109 °C, and the two immediate release polymers Kollidon VA 64 and Kollidon 12 PF via hot-melt extrusion at a temperature of 70 °C. They used them as feedstock material for the production of 3D printed tablets via FDM 3D printing at a temperature of 90 °C. Kempin et al. (2018) investigated the drug pantoprazole sodium, which is not only thermo-labile but also acid-labile during both heat-intensive processes HME and FDM. A thermal degradation of the active ingredient was observed during dual extrusion printing with a cellulose acetate phthalate coating and a tablet core of polyethylene glycol 6.000 at a printing temperature of 141 °C. After development of different tablets designs, the design of a tablet coating with a gastro-resistant cellulose acetate phthalate bottom part and an upper, nearly insoluble polycaprolactone part resulted in a printing temperature of 58 °C and no signs of degradation. Furthermore, Manini et al. (2022)

produced implants with the heat-sensitive active ingredient paliperidone palmitate below a temperature of 180 °C to avoid thermal degradation, due to the degradation temperature at approximately 180 °C and investigate the stability of the solid state and the release behavior of the implants over three months. Until now, the possibility of thermally induced racemization has not been investigated.

For the present study, we selected the chiral drug ESC-OX as model drug for the investigations of both the thermal instability and also the solid state during hot-melt extrusion and FDM 3D printing. ESC-OX is a selective serotonin (5-HT) reuptake inhibitor (SSRI) which is used for the treatment of major depressive disorder (MDD) and several anxiety disorders (Jagtap and Bhaskar, 2013). According to the WHO, mental disorders, with anxiety and depressive disorders as most common, affected approximately 970 million people in 2019 (Institute of Health Metrics and Evaluation. Global Health Data Exchange (GHDx), 2022). From these, 301 million people suffered from anxiety disorder and 280 million people suffered from depression (Institute of Health Metrics and Evaluation. Global Health Data Exchange (GHDx), 2022). Due to the COVID-19 pandemic, the Global Burden of Disease (GBD) 2020 estimated that the number of people suffering from these diseases increased significantly by 25.6 % and 27.6 % respectively within one year (Santomauro et al., 2021). SSRIs are considered as first-line treatment in antidepressant medication (Waugh and Goa, 2003) and are characterized by good tolerability due to the high selectivity and low interaction potential compared to other antidepressants (Kirino, 2012; O'Donnell and Shelton, 2015). Escitalopram (ESC) is the S-stereoisomer of racemic (R,S) citalopram (Fig. 1) (Pinto et al., 2018) and has been shown to have greater efficacy than the racemate citalopram while being equally well tolerated (Cipriani et al., 2009; Gartlehner et al., 2011; Cipriani et al., 2009).

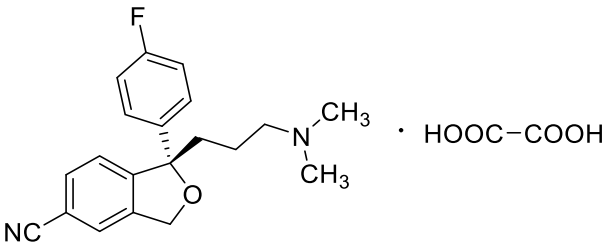

Fig. 1. Structural formula of ESC-OX.

ESC-OX is listed on the WHO Model List of Essential Medicines (WHO, 2021) and is marketed by Lundbeck GmbH under the trade names Cipralex® and Lexapro® (Akay et al., 2021). It is administered orally, with the dose equal to the free base (Akay et al., 2021). Although the oxalate salt is administered, the drug belongs to the BCS class II drugs with low solubility and high permeability (Akay et al., 2021). In addition to the poor solubility, ESC-OX also shows a pronounced pH instability in basic solution (Rao, et al., 2008; Dhaneshwar et al., 2008).

Thus, the main aim of this work was to investigate the thermal degradation of the thermo-sensitive and base-labile antidepressant ESC-OX and its degradation products during hot-melt extrusion and FDM 3D printing depending on a neutral and basic polymer matrix used. This also includes the investigations of a possible conversion of the enantiomer S-Citalopram into R-Citalopram during these two heat-intensive processes. Formulation development was carried out to prevent degradation of ESC-OX leading to the optimized formulation F3. Besides the chemical stability, the physical state of ESC-OX embedded in the different polymer matrices during HME and FDM 3D printing was examined. Lastly, the optimized formulation with the polymer bPMMA was compared with the commercially available Cipralex® 10 mg film-coated tablets regarding the physical state, the purity as well as dissolution.

2. Materials and methods

2.1 Materials

ESC-OX was purchased from F. & A. Pharma-Handels-GmbH (Marl, Germany) ex Micro Labs Limited (Bangalore, India). Hypromellose (HPMC, Affinisol™ HPMC HME 15 LV) and polyethylene oxid Mw 100.000 (PEO, Polyox™ WSR N10) were kindly provided by DuPont Nutrition & Biosciences (Neu-Isenburg, Germany). Basic butylated methacrylate copolymer (bPMMA, Eudragit® E PO) and fumed silica (Aerosil® 200 V/V Pharma) were kindly provided by Evonik (Essen, Germany). Polyethylene glycol (PEG) 6.000 (Polyglykol® 6000 P) was kindly provided by Clariant (Frankfurt, Germany). ESC-OX United States Pharmacopoeia (USP) reference standard, R-Citalopram oxalate USP reference standard, Citalopram Related Compound A USP reference standard (CIT-A), Citalopram Related Compound B USP reference standard (CIT-B) and Citalopram Related Compound C USP reference standard (CIT-C) were purchased by Eurofins PHAST GmbH (Homburg, Germany). Citalopram hydrobromide CRS was purchased at the European Directorate for the Quality of Medicine & Healthcare (Strasbourg, France).

2.2 Preparation of drug loaded extrudates

Hot-melt extrusion was carried out for the production of extrudates. Extrudates were prepared with three different formulations (Table 1).

Table 1. Formulation composition for the production of HME extrudates (*w/w*).

Formulation	API (%)	Matrix (%)				Plasticizer (%)		Glidant (%)	
F1	ESC-OX 12.78	HPMC	81.72	bPMMA	-	PEG 6.000	5	SiO_2	0.5
F2	ESC-OX 12.78	HPMC	71.72	bPMMA	10	PEG 6.000	5	SiO_2	0.5
F3	ESC-OX 12.78	-	-	bPMMA	42.61	PEO	42.61	SiO_2	2.0

To ensure a homogenous powder mixture of each formulation, ESC-OX and the polymers were separately sieved (355 µm) and mixed for 15 min in a turbula mixer (T2F, Willy A. Bachofen, Switzerland). The higher amount of SiO_2 in F3 compared to formulation F1 and F2 was used to improve the flowability of this powder mixture. The formulations were fed with a flat-bottom powder feeder (ZD 5 FB, Three-Tec, Seon, Switzerland) at a feed rate of 100 g/h into a co-rotating twin screw extruder (ZSE12 HP-PH, Leistritz, Nürnberg, Germany) with a screw diameter of 12 mm. Screws with two kneading zones and a die with a diameter of 2 mm were used. The extrusion temperature profiles are detailed in Table 2. The screw speed was set to 25 rpm in all cases.

Table 2. Temperature profiles across the different zones of the extruder barrel (°C).

Formulation	Zone 1	2	3	4	5	6	7	8	Die
F1 / F2	20	20	150	150	150	150	150	150	150
F3	20	20	80	80	80	80	80	80	80

Following the extrusion, the extruded strand was cooled and transported with a conveyor belt (model 846102.001, Brabender, Germany). The desired extrudate diameter of 1.75 mm was achieved using a belt hauled-off unit of a winder (Brabender, Duisburg, Germany).

2.3 3D printing of ESC-OX tablets

The extrudates were printed with a 0.4 mm nozzle into tablets using a FDM 3D printer (i3 Mk3, Prusa Research; Czech Republic). The tablet geometry was designed using Autodesk Fusion 360 (Mill Valley, USA) and then sliced using the PrusaSlicer (PRUSA Research; Hradec Králové, Czech Republic). For formulation F1 and F2, the extrudates were printed at 180 °C nozzle temperature and 65 °C print bed temperature with a printing speed of 30 mm/s. For formulation F3, the extrudates were printed at 180 °C nozzle temperature and 35 °C print bed temperature with a printing speed of 30 mm/s. A cylindrical tablet geometry (diameter: 6.8 mm and height: 2.4 mm) was selected to obtain a 100 mg tablet with a dose of 10 mg and a drug loading of 10 % ESC. All tablets were printed with a layer height of 0.2 mm and 100 % infill.

2.4 Microscopy

Images of the tablets were taken using a Keyence digital microscope VHX-6000 (Keyence, Essen, Germany) with a 20x magnification.

2.5 Thermal analysis

For thermogravimetric analysis (TGA) and derivative thermogravimetric analysis (DTG), ESC-OX was measured using a NETZSCH TG 209F1 Libra (NETSCH, Germany). The sample was placed in the form of powder in an 85 µL aluminium pan and was then heated from 35 °C to 600 °C with 10 °C / min heating rate. The thermal decomposition was analyzed using NETZSCH Proteus Software. The experiments were carried out under nitrogen gas flow of 20 mL / min. Thermal analysis of ESC-OX starting material, related substances, physical mixtures, extrudates and tablets were performed using differential scanning calorimetry (DSC, DSC 1, Mettler-Toledo, Giessen, Germany). ESC-OX and related substances were heated at 10 °C / min from 20 °C to 200 °C, whereas plasticizer, physical mixtures, extrudates, and tablets were heated over the temperature range of 20 °C to 160 °C.

2.6 X-ray diffractometer (XRD)

XRD analysis was carried out for starting materials, extrudates and tablets using a Rigaku Miniflex 300 diffractometer (Rigaku, Neu-Isenburg, Germany) in Θ/2Θ geometry at ambient temperature using Cu-Kα radiation (Θ = 1,54182 Å). The amperage was 15 mA and the voltage 40 kV. Scans were performed from 2θ = 2° to 50° with 0.01° step width. The scan resolution was 0.0025 and the scan speed 1.7°/min. The duration of each measurement was 30 min.

2.7 Polarized light microscopy

Microscopic images were taken using the light microscope DM LB (Leica Microsystems, Germany) with polarization filter with a 5x magnification. The raw materials ESC-OX and PEO were measured directly as powders, whereas for the extrudate and 3D printed tablet small pieces were examined.

2.8 FT-IR spectra measurements

FT-IR spectra measurements were performed to investigate possible interactions between the active ingredient ESC-OX and the polymers for all self-produced formulations. The raw materials were measured directly as powders, whereas for the extrudates and tablets, a small piece of each was cut using a scalpel. Infrared spectra were recorded with a Shimadzu IR Affinity-1 equipped with an ATR unit (Shimadzu, Germany).

2.9 Assay in extrudates, 3D printed tablets and in solution

A 3D printed tablet (n = 3, mean ± SD) or a section of a drug-loaded extrudate (approximately 0.1 g) (n = 10, mean ± SD) was placed in a 100 mL volumetric flask and dissolved in 100 mL of a mixture of methanol and 5 mM potassium dihydrogen phosphate buffer pH 3.8 (50/50, *V/V*). Samples of the solutions were then filtered through a 0.45 µm nylon filter. An Elite LaChrom system consisting of L-2200 automatic sampler, L-2130 high pressure pump, L-2300 column oven and L-2400 UV detector was used (all Hitachi-VWR, Darmstadt, Germany). Chromatographic separation of ESC-OX and related substances were carried out on an achiral XSelect CSH C18 column [3.0 x 150 mm, 3.5 µm (Waters, Germany)]. After injection of 20 µL sample solution the samples were separated with the aid of a gradient using a mobile phase of methanol and 5 mM potassium dihydrogen phosphate buffer pH 3.8 (Table 3). The flow rate was 0.7 mL/min and the column temperature was maintained at 45 °C. The eluent was screened due to the absorption maximum at a wavelength of 239 nm. The run time was 30 min. The identification and quantification of ESC-OX and related substances were done with solutions of the USP reference standards. The solutions were also used for the determination of the selectivity. The limit of detection (LOD) for ESC for the assay was determined to be 18.1 ng/mL and the limit of quantification (LOQ) to be 54.7 ng/mL. A LOD and LOQ for ESC of 19.4 ng/mL and 58.9 ng/mL were determined for the dissolution. Linearity was given for the assay of ESC in the concentration range of 60 to 140 µg/mL with an $R^2 > 0.999$, whereas for the dissolution linearity was given with an $R^2 > 0.999$ in the concentration range of 0.2-12 µg/mL. The accuracy of the content determination in the samples was verified by using USP reference standards. Precision, determined as repeatability, with a coefficient of variation of 0.78 % was determined for ESC.

To determine the stability of ESC-OX in solution, 100 mg ESC was dissolved in 100 mL 0.1 N hydrochloric acid, de-ionized water and 0.1 N sodium hydroxide and the content was also determined by HPLC at a wavelength of 240 nm.

Table 3. Gradient for the separation of ESC-OX and related substances.

Time (min)	Methanol (% *V/V*)	Buffer (% *V/V*)
0–3.0	30	70
3.0–5.0	30 → 35	70 → 65
5.0–24.0	35 → 40	65 → 60
24.0-25.5	40 → 95	60 → 5
25.5-27.5	95	5
27.5-27.6	95 → 30	5 → 70
27.6-30.0	30	70

2.10 Enantiomeric purity in extrudates, 3D printed tablets and in solution

A 3D printed tablet (*n* = 3, mean ± SD), a Cipralex® 10 mg film-coated tablet (*n* = 3, mean ± SD), or sections of a drug-loaded extrudate (*n* = 10, mean ± SD) (approximately 0.1 g) were placed in a 100 mL volumetric flask and were dissolved in 100 mL of a mixture of acetonitrile and potassium dihydrogen phosphate buffer pH 7.0 (15/85, *V/V*). In contrast, for the stability studies of ESC-OX in solution, such as on the achiral column, 100 mg ESC was dissolved in 100 mL 0.1 N hydrochloric acid, de-ionized water and 0.1 N sodium hydroxide. Samples of the solutions were then filtered through a 0.45 µm nylon filter. An Elite LaChrom system consisting of L-2200 automatic sampler, L-2130 high pressure pump, L-2300 column oven and L-2400 UV detector was used (all Hitachi-VWR, Darmstadt, Germany). Chromatographic separation was achieved according to the USP method of ESC-OX for “enantiomeric purity” on an Ultron ES-OVM column [4.6 x 150 mm, 5 µm (Shinwa Chemical Industries Ltd., Japan)]. The chiral column was additionally equipped with an Ultron ES-OVM holder, in which a guard cartridge with the dimensions 4.6 x 10 mm was integrated. The following chromatographic conditions as defined by the USP method were set: A mobile phase consisting of acetonitrile and potassium dihydrogen phosphate buffer pH 7.0 (15/85 *V/V*) was used. The flow rate was 0.6 mL/min and the column temperature was maintained at 25 °C. After injection of 15 µL, the eluent was screened due to the absorption maximum at a wavelength of 240 nm. The run time was set to 25 min. The samples were analyzed after establishment of the method according to the USP method.

2.11 Mass spectrometry

A UHR-QTOF maXis 4G mass spectrometer (Bruker Daltonics, MA, USA) equipped with an ESI source was used in positive ionization mode to detect ESC and degradation products in alkaline solution. For this purpose, 127.8 mg ESC-OX, equal to 100 mg ESC, was dissolved in 100 mL 0.1 N natrium hydroxide solution and heated for 1 h and 12 h at 70 °C respectively. The solutions were further diluted with methanol to achieve a target concentration of 100 µg/mL ESC. For the determination, the following mass spectrometric conditions were used: The capillary voltage was set to 4 kV and the temperature was adjusted to 180 °C. The gas flow was 4.0 L/min and the nebulizer pressure was 0.3 bar. The monitored mass-to-charge range (m/z) was 50 to 1500 m/z and mass spectra were presented in the range of interest from 320 to 350 m/z.

2.12 Dissolution

In vitro drug release studies from ESC-OX tablets with a target mass of 10 mg ESC were carried out using dissolution tester AT7 Smart (Sotax, Aesch, Switzerland) with USP type I apparatus (basket) and USP type II apparatus (paddle) at 37 °C ± 0.5°C with rotating speed of 75 rpm in 900 mL 0.1 N hydrochloric acid (n = 3, mean ± SD). Samples were withdrawn manually after 2 min, 5 min, 10 min, 15 min, 20 min, 30 min, 45 min, 60 min, 75 min, 90 min, 105 min and 120 min. The amount of ESC was quantified by HPLC. The eluent which was dissolved in the dissolution medium was analyzed with the above mentioned method for the content uniformity at the UV maximum of 238 nm.

3. Results

3.1 Hot-melt extrusion and 3D printing of tablets

Three formulations were selected with respect to temperature, physical properties of the polymers and printability for FDM 3D printing. For formulations F1 and F2, an extrusion temperature of 150 °C was chosen to study the degradation of ESC-OX near the melting temperature. In addition, the influence of the additional amount of basic bPMMA in formulation F2 compared to formulation F1 containing only HPMC on degradation of ESC-OX was investigated. Therefore, it was clarified in more detail whether the addition of the basic polymer bPMMA led to a greater degradation of the base-labile active substance. From these investigations and after formulation development, formulation F3, designated as optimized formulation, represented the most suitable formulation, which could be extruded at the lowest possible extrusion temperature of 80 °C and printed. Regarding the physical properties, changes in the solid-state of the crystalline ESC-OX starting material during both melting processes in extrudates and in 3D printed tablets were investigated. The degree to which ESC-OX existed in the crystalline state below the melting temperature and was amorphized by FDM 3D printing was examined. Furthermore, the printability was studied for the obtained extrudates of all three formulations from the extrusion process. All extrudates were sufficient flexible and could be successfully printed into 3D printed tablets with the help of the Prusa i3 Mk3 printer at a nozzle temperature of 180 °C, which could be seen in the microscopic images (Fig. 2). The images of the 3D printed tablets showed the different texture of the tablets depending on the polymer and temperature used. All tablets were printed with a concentric infill (Fig. 2a-c). The tablets of the originator product Cipralex® 10 mg film-coated tablets are shown in Fig. 2d for comparison.

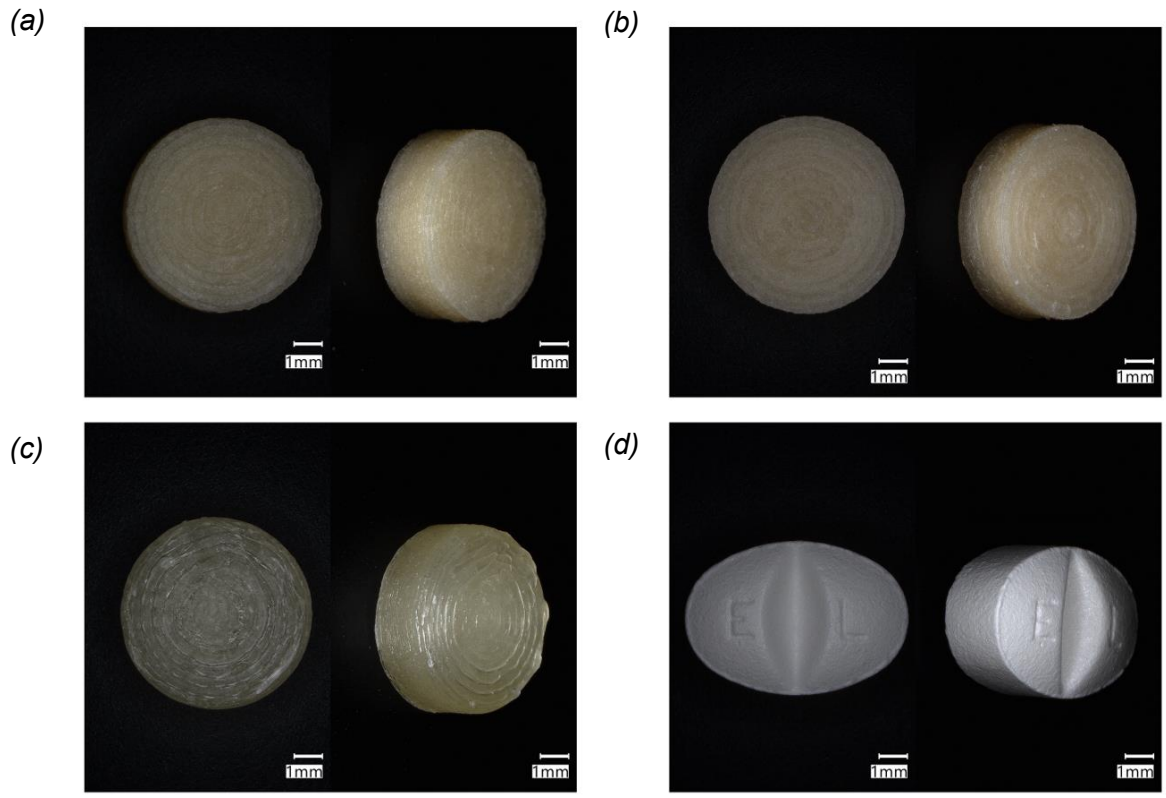

Fig. 2. Images of top and side view of the 3D printed tablets of formulation F1 (a), of formulation F2 (b), of formulation F3 (c) and Cipralex® 10 mg film-coated tablets (d) (scale bars: 1 mm).

For the tablets of formulations F1 and F2 based on HPMC, higher print bed temperatures of 65 °C were necessary to ensure sufficient adhesion of the layers to each other, but also to the print bed. As a result, the individual layers are more fused together and less recognizable (Fig. 2a and 2b). The tablets of formulation F3 based on bPMMA could be printed at a print bed temperature of 35 °C. Due to the lower glass transition temperature of bPMMA (57 °C vs. 115 ° for HPMC) (Parikh, et al. 2016; O'Donnell and Woodward 2015; Ilyés, et al. 2019), lower printing temperatures are sufficient to ensure complete solidification of the individual layers after the melting process. In addition, the concentric infill is clearly visible (Fig. 2c). The oval and white Cipralex® 10 mg film-coated tablet has a score, which allows the tablet to be divided into two equal halves. In addition, the tablets are marked on the front with "E" and "L" on each half of the score, which can be clearly seen in Fig. 2d.

3.2 Thermal analysis

3.2.1 Thermogravimetric analysis

TGA measurements confirmed that the degradation of ESC-OX took place in two consecutive events (Pinto et al., 2018; Akay et al., 2021). As already described by Pinto et al. (2018), the first major mass loss starting from the melt temperature of ESC-OX up to 237 °C is related to the decomposition of the oxalate, whereas the second major mass loss up to 300 °C is caused by the degradation of ESC (Pinto et al., 2018) (Fig. 3).

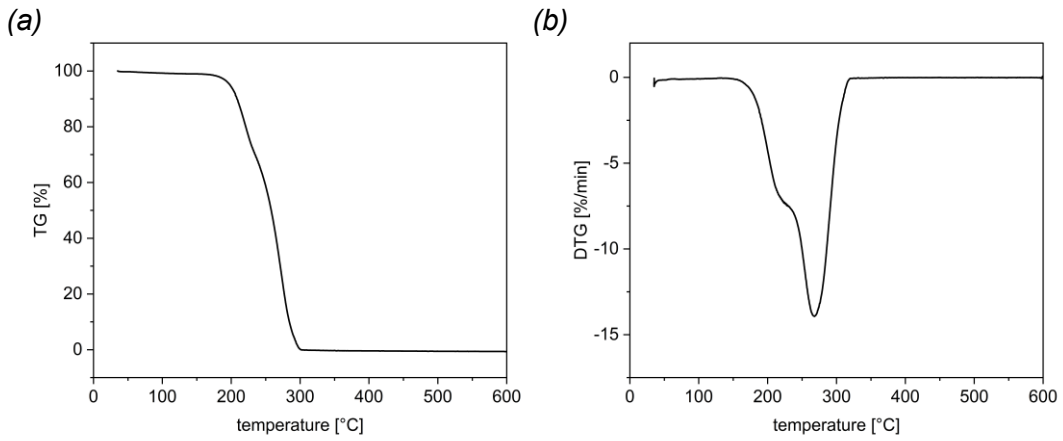

Fig. 3. TG (a) and DTG curves (b) of ESC-OX.

3.2.2 DSC analysis

DSC analysis of ESC-OX starting material showed an endothermic peak at approximately 153°C correlating to the melting temperature (Pinto, et al., 2018) (Fig. 4a). In addition to the DSC thermogram of ESC-OX, the thermograms of the degradation products are also depicted in Fig. 4b, c and d.

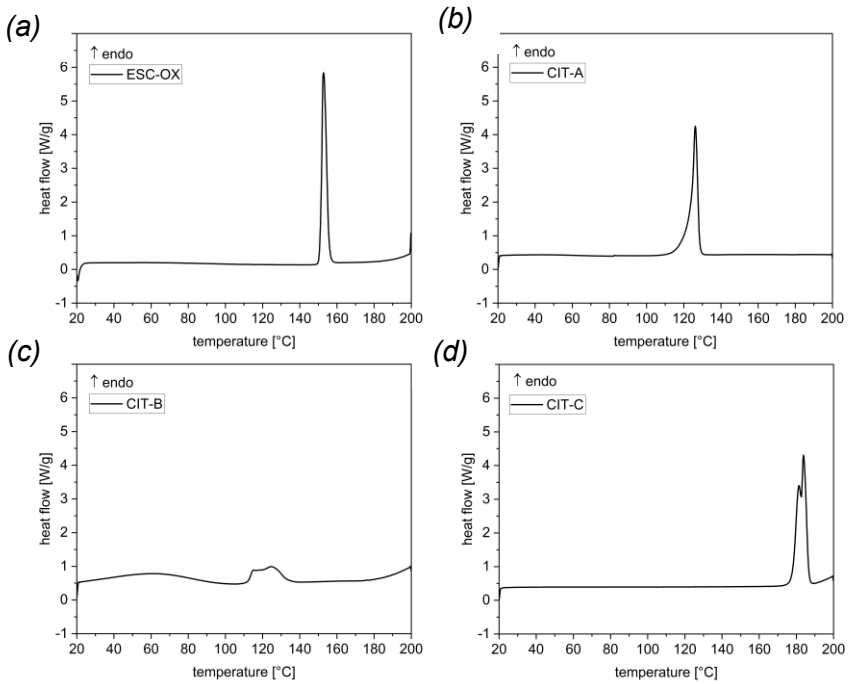

Fig. 4. DSC thermograms of ESC-OX (a), CIT-A (b), CIT-B (c) and CIT-C (d).

The DSC thermogram for the impurity CIT-A showed an endothermic event at 126 °C, whereas for the impurity CIT-B an onset could be observed at 107 °C with an endothermic peak at 125 °C. Finally, a higher melting point of 181 °C with subsequent decomposition could be observed for CIT-C.

Furthermore, the melting behavior of R-Citalopram oxalate and the racemate citalopram hydrobromide was investigated (Fig. 5). For R-Citalopram oxalate, an endothermic peak at

149 °C was observed (Fig. 5a). In contrast, a higher melting point of approximately 188 °C was determined for the racemate citalopram hydrobromide (Fig. 5b), which is consistent with the observations of Pinto et al. (2018). This shows the higher stability of the racemate compared to the enantiomers, which was also described by Diego et al. (2011) for the racemate present as an oxalate.

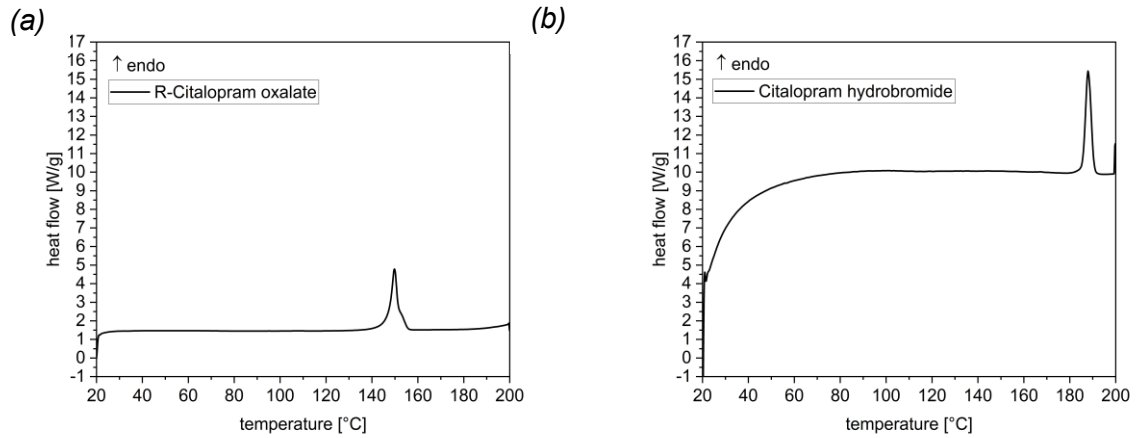

Fig. 5. DSC thermograms of R-Citalopram oxalate (a) and citalopram hydrobromide (b).

Additionally, the formulations with ESC-OX were examined. The physical mixtures of all formulations showed the endothermic event of ESC-OX at 153 °C (Fig. 6a-c). Furthermore, endothermic peaks could be observed for polyethylene glycole (PEG) 6.000 and polyethylene oxide (PEO) which diffractograms are shown in the Figure S1 of the Supplementary data. PEG 6.000 exhibited an endothermic event with an onset at 59.4 °C and a peak at 63.6 °C, whereas for the PEO an endothermic event with an onset at 62.4 °C and a peak at 67.9 °C could be observed. For formulation F1 and F2, which were extruded at a temperature of 150 °C and printed at 180 °C, the endothermic event of ESC-OX was not present in the extrudates and tablets. The absence of the endothermic event indicated that ESC-OX seems to be in amorphous form in the extrudates and 3D printed tablets of these formulations. For formulation F3, on the other hand, an endothermic event with an onset at 121.1 °C and a peak at 136.5 °C was observed in the extrudates from the extrusion process at 80 °C, which could not be detected in the 3D printed tablets printed at 180 °C (Fig. 6c). This indicated that ESC was crystalline in the extrudates in the formulation F3 and was amorphized during the 3D printing process. The crystalline parts of the PEO in F3 were still visible in both the extrudates and the 3D printed tablets. The thermogram of the Cipralex® 10 mg film-coated tablets clearly showed the endothermic peak of ESC-OX at 152.4 °C with an onset at 148.5 °C, indicating the crystalline state (Fig. 6d). To confirm these observations, XRD analysis were conducted.

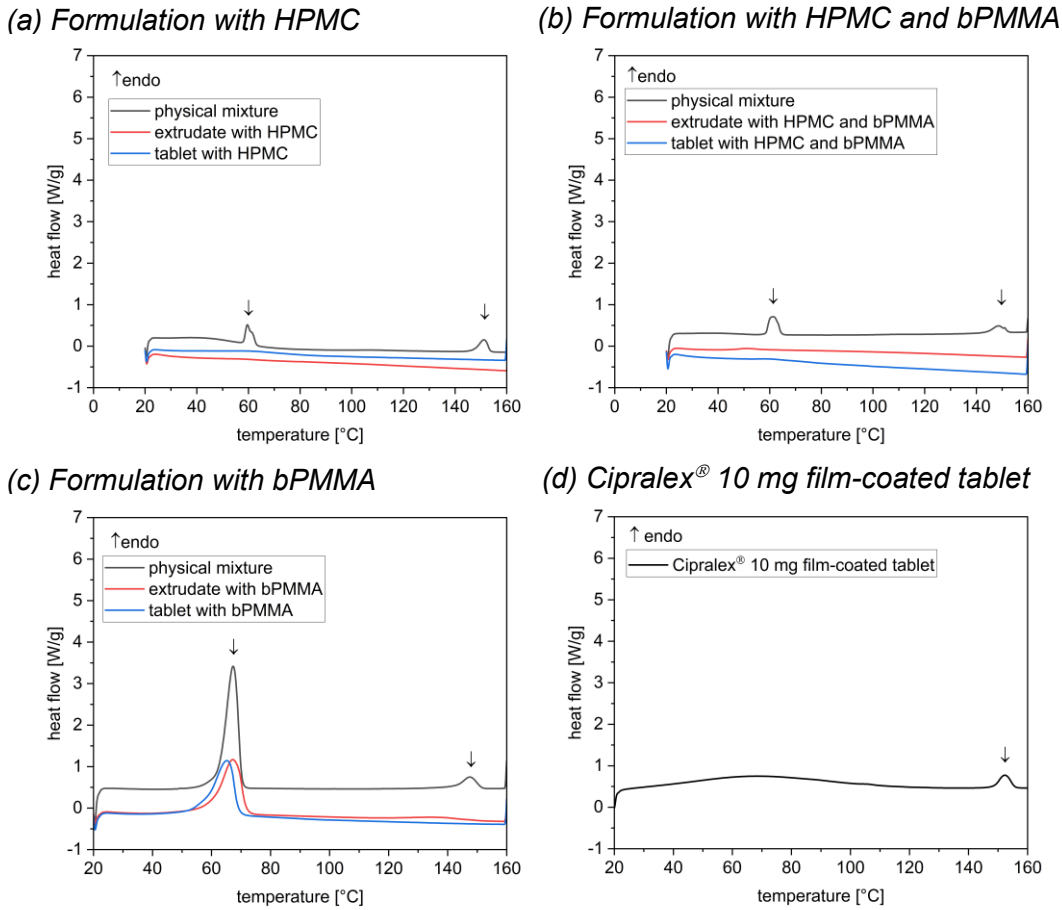

Fig. 6. DSC thermograms of formulation F1 (a), formulation F2 (b), formulation F3 (c) and Cipralex® 10 mg film-coated tablets (d), respectively.

3.3 X-ray diffraction (XRD)

XRD analysis were performed to investigate the physical form of ESC-OX in the physical mixtures, extrudates and 3D printed tablets (Fig. 7). The typical diffraction peaks in the starting material of ESC-OX agreed with those of Alkahtani et al. (2021) at 13.14°, 13.16°, 16.06°, 19.2°, 20.94°, and 27.12°. While the physical mixtures showed the crystalline peaks of ESC-OX, the absence of these peaks in extrudates and 3D printed tablets of formulations F1 and F2 indicated the amorphous state of the drug and the production of amorphous solid dispersions (Fig. 7a and b). For formulation F3, on the other hand, characteristic peaks of ESC can still be observed in the extrudates, which were absent in the 3D printed tablets (Fig. 7c). Only the crystalline parts of PEO with characteristic peaks at 19.0° and 23.2°, marked with an arrow in Fig.7c and depicted separately in Fig. S2 of the Supplementary Data, could still be seen in both, the extrudates and 3D printed tablets (Xu et al., 2012). This illustrates the possibility of *in-situ* amorphization of ESC-OX during FDM 3D printing and is shown in more detail in the diffractogram of Fig. 8. Furthermore, the results could be confirmed with polarization microscope images and were presented in Fig. S3 (Supplementary Data). Lastly, the Cipralex® 10 mg film-coated tablets were investigated and also showed crystalline peaks of ESC (Fig. 7d).

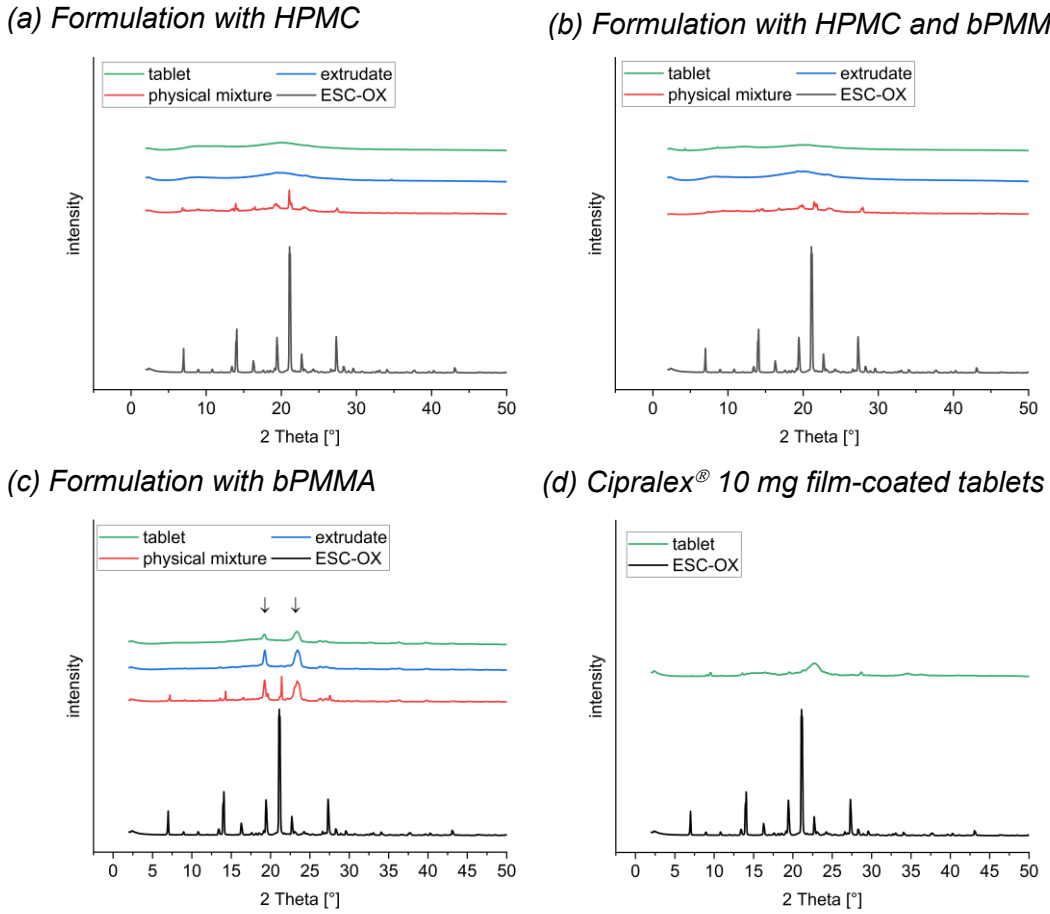

Fig. 7. X-ray diffractograms of formulation F1 (a), formulation F2 (b), formulation F3 (c) and Cipralex®10 mg film-coated tablets (d), respectively.

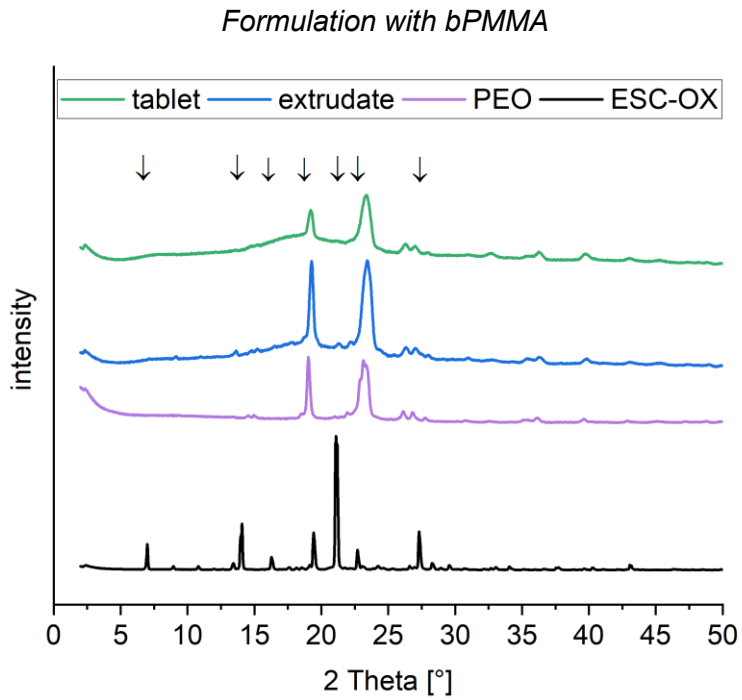

Fig. 8. X-ray diffractogram of ESC-OX, PEO, extrudate as well as 3D printed tablet of formulation F3.

3.4 FT-IR spectra measurements

FT-IR spectroscopy was used to investigate potential interactions between ESC-OX and the polymers (Fig. 9). The FT-IR spectrum of ESC-OX showed characteristic bands at 2953 cm^{-1} (C–H stretching), 2231 cm^{-1} (C≡N stretching vibration) and 1221 cm^{-1} (C–N stretching) (Alkahtani et al., 2021; Song, et al., 2016; Kumbhar, 2013). The polymer bPMMA showed characteristic bands for the dimethylamino groups at 2822 cm^{-1} and 2770 cm^{-1} (Evonik, Technical Information Eudragit® E 100, Eudragit® E PO and Eudragit® E 12,5., 2022). In addition, further characteristic peaks for the ester groups of bPMMA at 1267 cm^{-1}, 1238 cm^{-1} and 1144 cm^{-1} as well as the C=O ester vibration at 1724 cm^{-1} are also recognizable and in agreement with data from (Evonik, Technical Information Eudragit® E 100, Eudragit® E PO and Eudragit® E 12,5., 2022). FT-IR spectrum of HPMC showed characteristic bands for the O–H stretching vibration at 3458 cm^{-1}, for the C–H stretching vibration in the range from 2800 cm^{-1} to 3000 cm^{-1} as well as for the C–O stretching vibration at 1047 cm^{-1}. Deformation vibrations are visible for the C–H group at 1454 cm^{-1} and for the O-H group at 1373 cm^{-1} (Furqan et al., 2017). No specific interactions between the active ingredient ESC-OX and the polymers could be detected.

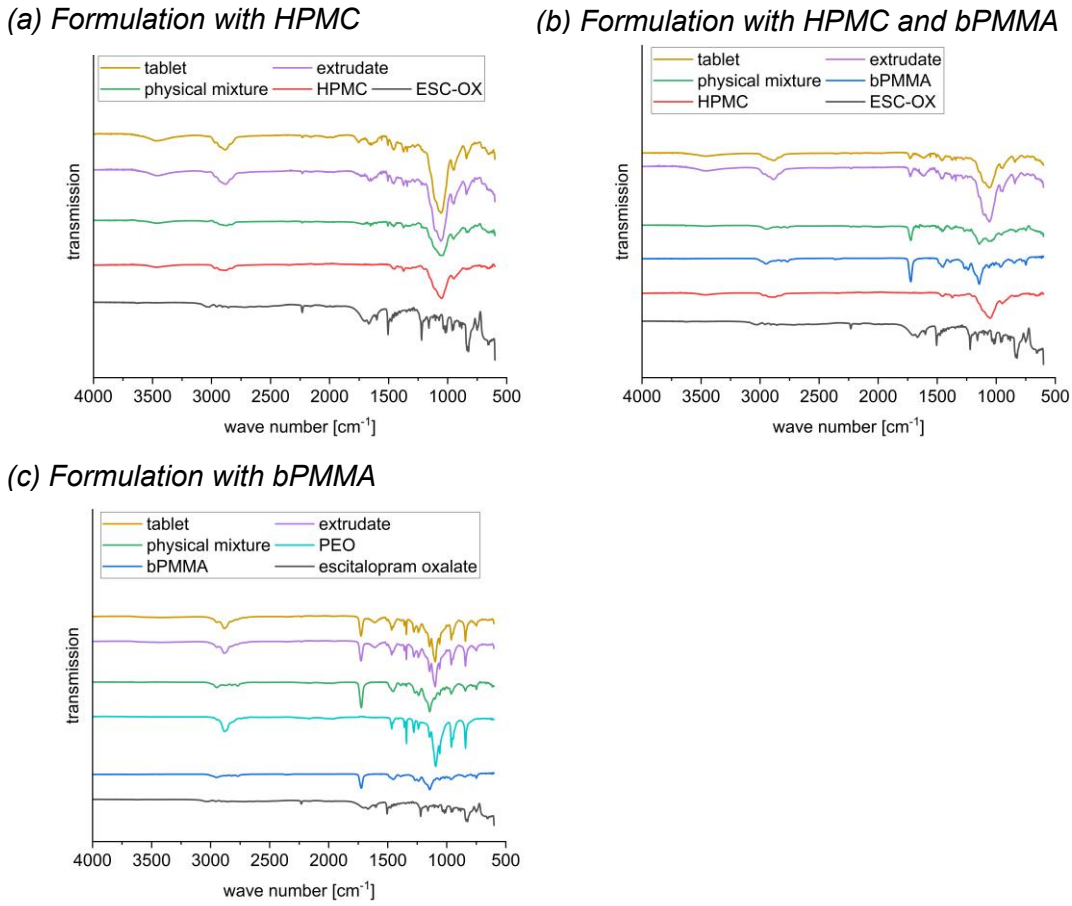

Fig. 9. FT-IR spectra of formulation F1 (a), formulation F2 (b) and formulation F3 (c), respectively.

3.5 Assay in solution

The content determination of ESC-OX on an achiral column in alkaline solution showed that ESC-OX is unstable at these conditions. After dissolving in 0.1 N NaOH and subsequent determination of the content of ESC, only 80.34 % ESC was present and impurity CIT-A was formed as the main degradation product. No instabilities were observed in acidic or neutral solution. The content in acidic solution was 103.63 %, while in neutral medium a content of 100.24 % was determined. These samples were also used to investigate the stability of ESC-OX in solution after 5 days on the chiral column. Furthermore, the stability of ESC-OX was also investigated when heating up the solution for 1 h at a temperature of 70 °C, in order to accelerate the degradation (Fig.10a).

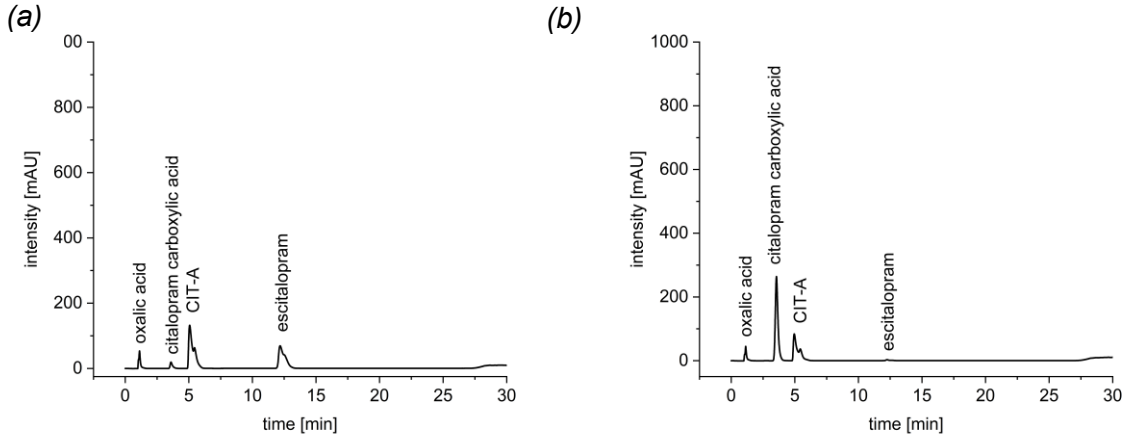

Fig. 10. HPLC chromatograms of ESC-OX in 0.1 N NaOH for 1 h at 70 °C (a) and for 12 h at 70 °C (b).

Additional degradation of ESC-OX was evident in basic solution. After 1h at 70 °C, only 29.78 % ESC was present. In addition to the degradation product CIT-A with a content of 64.44 %, another impurity with a content of 3.94 % was formed. The impurity was described in literature as citalopram carboxylic acid (Dhaneshwar, et al. 2008; Rao, et al., 2008) and could be confirmed on the basis of the mass-to-charge range (m/z) of 344.17 with mass spectrometric measurements. The content in acidic medium and also in water remained stable with 101.86 % and 101.06 %.

For further investigations, the samples were heated in 0.1 N NaOH for 12 h at a temperature of 70 °C (Fig. 10b). After 12 h, the content of ESC decreased further and only a small amount with 0.40 % ESC was present. CIT-A was formed with a content of 42.22 % and especially citalopram carboxylic acid originated to a higher content with 62.03 %, which was again conformed with mass spectrometric measurements. The obtained mass spectra and detailed explanations can be found in Fig. S4 of the Supplementary Data. Structural formulas of CIT-A and citalopram carboxylic acid are shown in Fig. 11a and b. Thus, the observations made on the instability of ESC in basic solution are consistent with the results of Dhaneshwar et al. (2008).

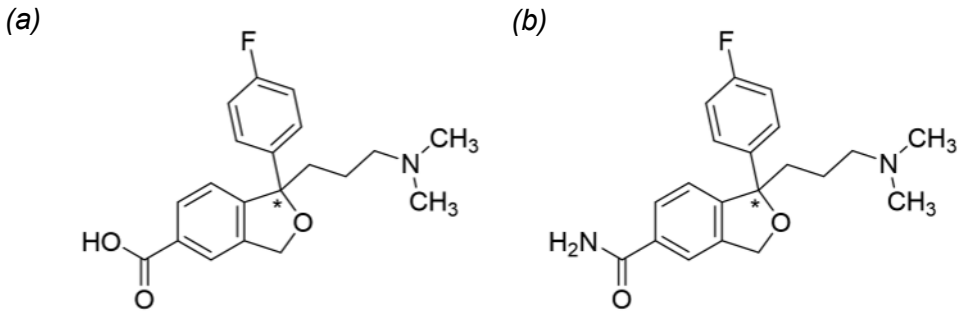

Fig. 11. Structural formulas of citalopram carboxylic acid (a) and CIT-A (b)

3.6 Assay in extrudates and 3D printed tablets

After the instability of ESC-OX in basic solution was confirmed, the thermal stress as well as the influence of different polymer matrices on the degradation of the active substance was investigated during hot-melt extrusion and FDM 3D printing on the achiral column. As a result, degradation of the active ingredient ESC-OX in the extrudates and 3D printed tablets could be observed and different degradation products were formed depending on the polymer matrix. For formulation F1 containing the polymer HPMC, the content in the extrudates after extrusion was 91.20 ± 0.71 %. After 3D printing, further minor degradation of the active ingredient was evident and a content of 89.65 ± 0.32 % ESC was found in the 3D printed tablets. Major degradation products in formulation F1 which could be identified were CIT-A, CIT-B and CIT-C which are shown in Fig. 11a as well as in Fig.12a and b.

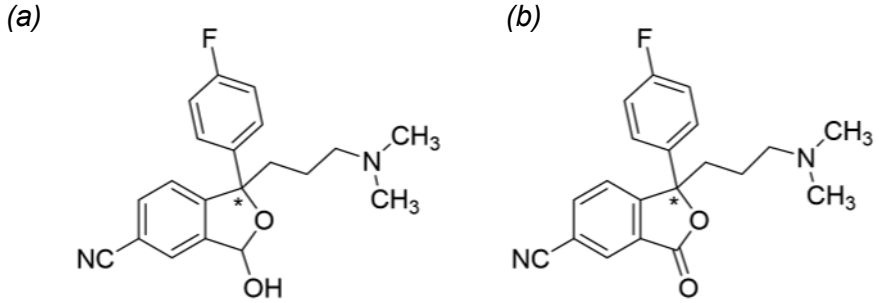

Fig. 12. Structural formulas of CIT-B (a) and CIT-C (b).

In the extrudates, the highest amount was found for CIT-C with 3.00 ± 0.18 % followed by CIT-A with a content of 1.41 ± 0.10 % and CIT-B with a content of 1.30 ± 0.19 %. In the 3D printed tablets, 2.73 ± 0.13 % CIT-C, 2.04 ± 0.03 % CIT-A and 1.84 % ± 0.12 % CIT-B were formed. For formulation F2, which contains the polymers HPMC and bPMMA, a higher content of ESC was achieved compared to the first formulation extruded at the same temperature. The content in the extrudates of formulation F2 was 98.29 ± 2.67 % ESC and 1.70 ± 0.09 % CIT-A as the major degradation product. After 3D printing, the content of ESC decreases to 98.16 ± 1.11 % and 2.48 ± 0.09 % CIT-A was recovered besides low amounts of CIT-B and CIT-C. The optimized formulation F3 containing only bPMMA could be extruded at a temperature of 80 °C. The content of ESC in the extrudates was 100.45 ± 1.21 % at 80 °C. After FDM 3D printing at a temperature of 180 °C, a content of 100.13 ± 0.52 % ESC and only 0.57 % ± 0.1 % CIT-A and 0.13 ± 0.001 % CIT-C could be found in the 3D printed tablets. The content of the Cipralex® 10 mg film-coated tablets on the market was also examined and a content of 104.09 ± 0.14 % was determined. No degradation products were detected in the tablets.

3.7 Enantiomeric purity in solution

The stability of ESC was also examined in different solvents on a chiral column. The investigations in different solvents and after several days, showed that no conversion to the R-enantiomer could be observed. As already on the achiral column, only the instability in basic medium could be identified (Fig. 13a). An increase in degradation could be seen over time, which could be established in the analyzed samples after 5 days (Fig.13b).

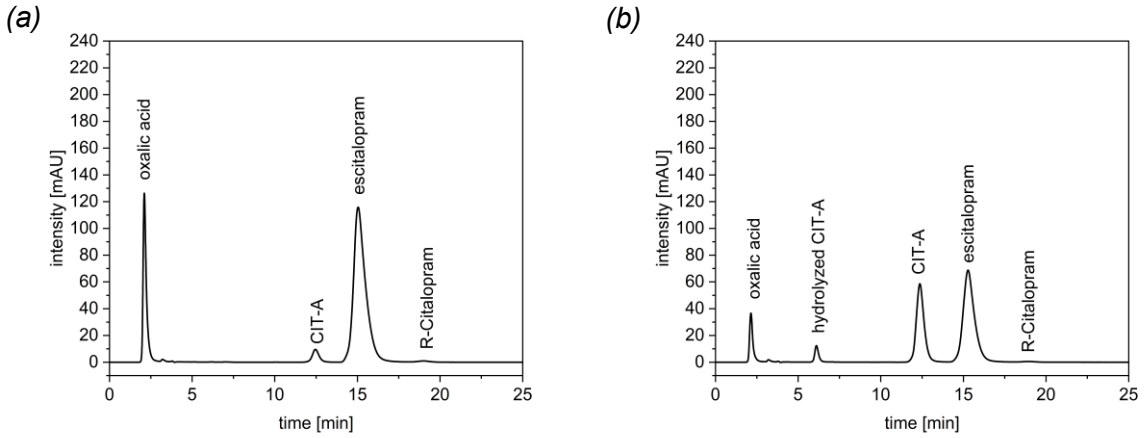

Fig. 13. HPLC chromatograms of ESC-OX in 0.1 N NaOH (a) and after 5 days (b).

Initially, a content of 85.43 % ESC in 0.1 N sodium hydroxide was found and 13.33 % CIT-A was formed. The content of R-citalopram in the basic solution was 0.62 %. As on the achiral column, no instability could be noted in acidic and neutral solution. The content was 103.62 % ESC in 0.1 N hydrochloric acid and 102.73 % in water. In contrast, a content of 0.57 % R-citalopram was determined in acidic solution and 0.63 % in neutral solution. After five days, a further reduction of the content of ESC was visible in 0.1 N sodium hydroxide. The content in 0.1 N sodium hydroxide was 48.99 % ESC and the impurities CIT-A with a content of 47.74 % and also the citalopram carboxylic acid with a content of 3.61 % were formed. The content of R-citalopram did not change and was 0.62 %.

3.8 Enantiomeric purity in extrudates and 3D printed tablets

In addition to the degradation of the drug, the potential conversion into the R-enantiomer was also investigated during the production of extrudates and 3D printed tablets on the chiral column. For this purpose, the extrudates of the optimized formulation F3 (extrusion temperature of 80 °C) as well as the corresponding 3D printed tablets were examined. In addition, the Cipralex® 10 mg film-coated tablets on the market were also analyzed (Fig. 14).

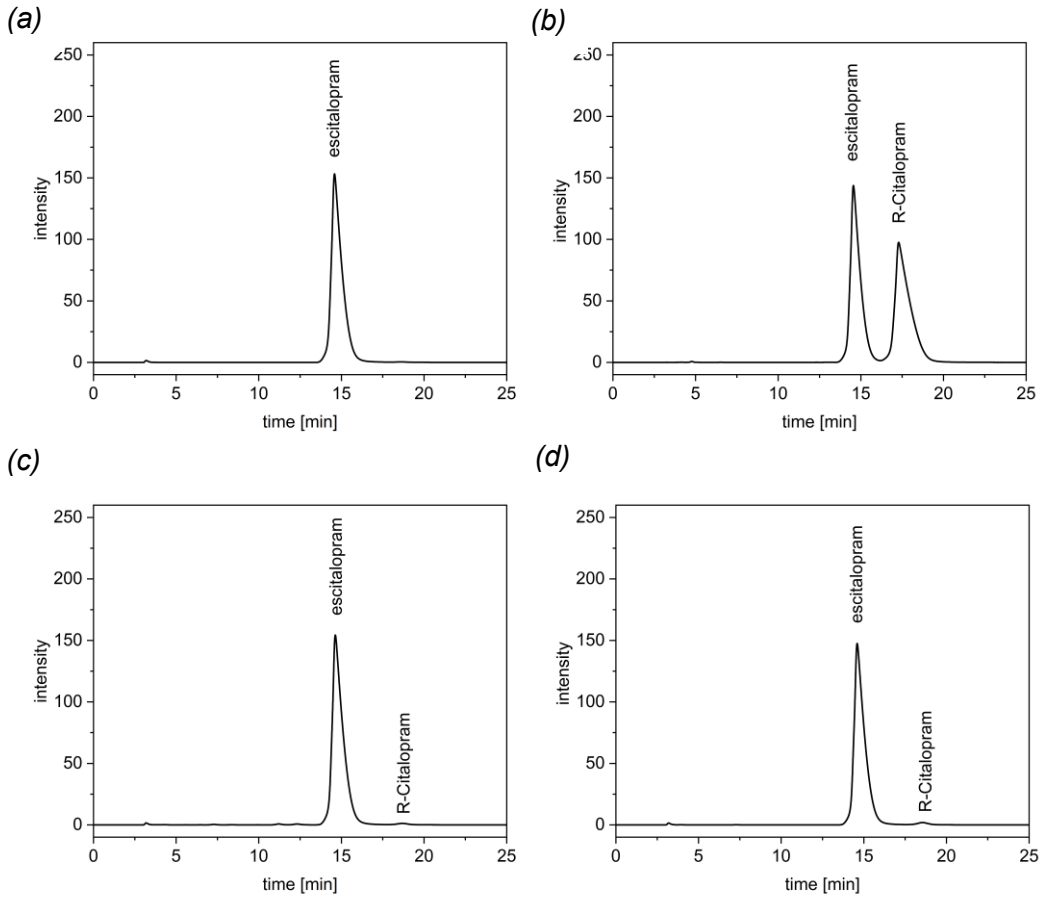

Fig. 14. HPLC chromatograms of ESC-OX (a), citalopram hydrobromide (b), the 3D printed tablet of F3 (c) and the Cipralex® 10 mg film-coated tablet (d).

The content of ESC in the extrudates was 98.74 ± 1.63 % after extrusion. After FDM 3D printing, the content amounts to 97.08 ± 0.58 %. For R-Citalopram, the content was 0.73 ± 0.01 % in the extrudates and 0.69 ± 0.04 % in the 3D printed tablets compared to 0.60 ± 0.03 % which was already contained in ESC starting material. Therefore, it can be concluded that also during heat intensive processes no racemization takes place. The limits of the USP are met with a maximum of 3 % R-Citalopram. In addition to the self-produced extrudates and tablets, the Cipralex® 10 mg film-coated tablets on the market were analyzed. A content of 104.76 ± 4.00 % ESC was detected in the tablets. In contrast, 1.24 ± 0.06 % R-Citalopram was present and the maximum permissible amount was not exceeded either.

3.9 Dissolution

In addition to the content, the release behavior of ESC from the bPMMA tablets extruded at 80 °C with 100 % infill was investigated and compared to the commercial product Cipralex® 10 mg film-coated tablets (Fig. 15). The USP monograph for ESC-OX tablets specified that at least 80 % ESC has to be released in 30 min in the paddle apparatus (USP II method) in 0.1 N hydrochloric acid at a rotational speed of 75 rpm. For the commercial product, it could be observed that after 30 min 95.11 ± 1.84 % ESC was released. Therefore, the requirements of the pharmacopoeia were met. Extrudates and 3D printed tablets floated on the surface of the dissolution medium and the basket apparatus was used for dissolution testing. The commercial product was also tested with the basket apparatus and it was observed that the complete active ingredient was released within two minutes (102.53 ± 6.43 %).

For extrudates and 3D printed tablets the release was slower. After 30 min, 97.84 ± 1.06 % ESC was released from the extrudates, whereas 80.66 ± 4.65 % ESC was released from the 3D printed tablets. The faster drug release from the extrudates in comparison to the 3D printed tablets can be explained by the larger surface area to volume ratio of the extrudates, which was already observed by Manini et al. (2022). But still, after 90 min, the active ingredient was completely released from both the extrudates and the 3D printed tablets (100.45 ± 5.15 % vs. 102.52 ± 2.59 %). Regarding the differences in physical state, no slower release from the crystalline extrudates could be observed compared to the amorphous 3D printed tablets.

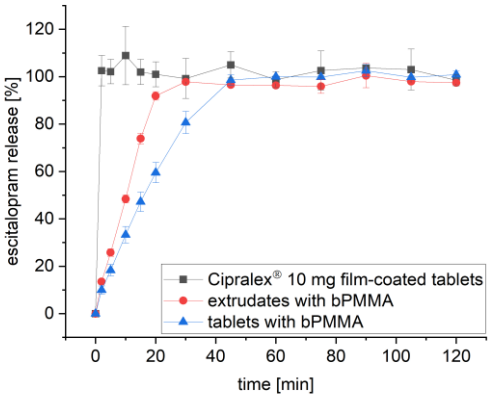

Fig. 15. In vitro dissolution profiles of ESC from bPMMA extrudates and tablets (n = 3) as well as from the commercial product Cipralex® 10 mg film-coated tablets, pH 1.2 buffer solution, USP Apparatus 1 (basket), 37 ± 0.2 °C, 75 rpm.

4. Discussion

Prepared extrudates and 3D printed tablets of three different formulations containing the active ingredient ESC-OX were investigated with regard to the physical state of ESC-OX. DSC and XRD results showed that amorphous solid dispersions could be prepared after hot-melt extrusion from formulations F1 and F2 with HPMC as main polymer. In these investigations it was found that amorphization of ESC-OX already took place below the melting temperature at 150 °C and thus sufficient energy was present to enable conversion of ESC-OX from the crystalline state to the amorphous state during hot-melt extrusion. Also after FDM 3D printing at 180 °C, the drug remained in amorphous form in both formulations F1 and F2. In contrast, for formulation F3 *in situ* amorphization of ESC-OX from crystalline extrudates with bPMMA was observed during FDM 3D printing. ESC-OX is still in its crystalline form in the extrudates of F3 due to hot-melt extrusion at only 80 °C, far below the melting temperature. 3D printing takes place at 180 °C, a temperature sufficient for the conversion from the crystalline state to the amorphous state of ESC-OX. *In-situ* amorphization is confirmed by DSC, XRD and polarized light microscopy. The crystalline parts of the semi-crystalline polymer PEO are still visible in extrudate and in small traces in the 3D printed tablet of F3. The phenomenon of *in-situ* amorphization can be of particular importance for production of customized dosage forms shortly before application, as stability of the amorphous form has only to be ensured until administration. The *in-situ* amorphization of drugs is not only relevant in FDM 3D printing. Also for the production of conventional dosage forms, e.g., tablets, *in situ* amorphization is researched. Approaches to achieve *in-situ* amorphization in conventionally produced tablets using microwave radiation have been investigated in detail. For example, tablets with indomethacin and polyvinylpyrrolidone K12 were prepared and the influence of moisture content and energy input on the degree of amorphization were investigated. It was found that up to 80 % indomethacin could be amorphized within the tablet (Doreth et al., 2017). *In situ* amorphization allows the preparation and administration even of unstable amorphous forms that were not accessible with traditional approaches.

Dissolution studies of ESC-OX from the crystalline bPMMA extrudates and the amorphous 3D printed bPMMA tablets revealed a faster drug release from the extrudates. This suggests that the larger surface area to volume ratio of the extrudates (S/V = 2.4) compared to the 3D printed tablets (S/V = 1.4) has a greater influence on the release of ESC than the solid state of the drug. In addition, a slower release of the 3D printed tablets was also observed compared to the commercial product Cipralex®. This can be explained by the higher density of the 3D printed tablet. FDM printed dosage forms are very compact and have either very low or no porosity, which reduces the surface area exposed to the dissolution medium drastically and further delays the drug release.

Due to the pronounced instability of ESC-OX in basic solution, the degradation of the active ingredient and the formation of degradation products in the extrudates and 3D printed tablets were studied using HPLC. Purity tests showed that the polymer matrix can have a decisive influence on the degradation products of ESC. In formulation F1 with the polymer HPMC, CIT-C was formed to the greatest extent, while in formulation F2 with the combination of HPMC and bPMMA, CIT-A was formed to the greatest extent. Formulation F3, which did not contain HPMC and consisted of the polymer bPMMA as matrix, CIT-A was also the main degradation product, but only in comparably small quantities. Regarding the amount of degradation, it could be depicted that a lower degradation of ESC-OX was seen in F2 compared to F1 despite the additional amount of the basic polymer bPMMA. F3 with bPMMA as the main polymer even represented the formulation with the highest content of ESC and lowest degradation. This illustrates that despite the use of a basic matrix polymer (bPMMA), processing in the melt and thus the absence of water could significantly reduce degradation of ESC. This is further supported by long term stability data after 6 months. Stored at atmospheric conditions for 6 months, 101.91 ± 0.77 % were recovered. With respect to enantiomeric purity, both temperature and pH of the solution do not appear to affect the conversion of the S-enantiomer to the R-enantiomer. No formation of the R-enantiomer could be observed, indicating sufficient stability of the S-enantiomer ESC-OX.

5. Conclusion

The obtained results showed that three formulations with the antidepressant ESC-OX could be hot-melt extruded and FDM 3D printed. The formulation F3 with bPMMA enabled *in-situ* amorphization from crystalline extrudates during FDM 3D printing which could be of decisive advantage, especially regarding their storage stability and clinical application. Thus, 3D printed tablets could be produced from stable extrudates according to the patient's needs just before application. Furthermore, formulation F3 with bPMMA showed no degradation of the active ingredient in the extrudates and only minor degradation in the 3D printed tablets. A possible racemization of the S-enantiomer into the R-enantiomer in formulation F3 could also be excluded. The dissolution of F3 extrudates and 3D printed tablets showed a fast drug release. Although ESC-OX was present in the extrudates in crystalline form, a rapid release of the active substance was achieved. The faster release compared to the tablets could be explained by the larger surface area to volume ratio. The slower release of the produced 3D printed tablets compared to the Cipralex® 10 mg film-coated tablets showed one of the hurdles of FDM 3D printing which can still be improved in the future.

Our study aimed to demonstrate the possibilities of formulation development, which on the one hand enabled *in-situ* amorphization of ESC-OX during FDM 3D printing, but also made it possible to avoid the degradation of the thermally unstable drug almost completely. Besides the content determination on an achiral column, to our knowledge, this was the first study that investigated the behavior of an enantiomer during hot-melt extrusion and FDM 3D printing compared to the stability in solution and analyzed the content of the active ingredient by using a chiral column.

CRediT authorship contribution statement

Lena Hoffmann: Conceptualization, Data curation, Formal analysis, Investigation, Methodology, Visualization, Writing – original draft, Writing – review & editing. **Jörg Breitkreutz:** Conceptualization, Funding acquisition, Project administration, Resources, Supervision, Writing – review & editing. **Julian Quodbach:** Conceptualization, Funding acquisition, Project administration, Resources, Supervision, Writing – review & editing.

Data availability

Data will be made available on request.

Acknowledgments:

The authors want to thank Dr. Tobias Auel for conducting the XRD measurements and Dr. Tom Kunde for conducting the FT-IR spectra measurements. Furthermore, the authors thank the CeMSA@HHU (Center for Molecular and Structural Analytics @ Heinrich Heine University) for recording the mass-spectrometric data.

Funding:

This work was supported by the German Federal Ministry of Education and Research - project 'ProMat Leben-Polymere-PolyPrint' [13XP5064B].

Supplementary materials

Supplementary material associated with this article can be found, in the online version, at doi:10.1016/j.ejps.2023.106423.

References

Abdella, S., Youssef, S.H., Afinjuomo, F., Song, Y., Fouladian, P., Upton, R., & Garg, S. 2021. 3D Printing of thermo-sensitive drugs. Pharmaceutics. 13(9), 1524.

Akay, S., Yang, Y., & Kayan, B. 2021. Investigation on the solubility of the antidepressant drug escitalopram in subcritical water. J. Chem. Eng. Data. 66(6), 2550-2560.

Alhnan, M.A., Okwuosa, T.C., Sadia, M., Wan, K.-W., Ahmed, W., & Arafat, B. 2016. Emergence of 3D printed dosage forms: opportunities and Challenges. Pharm. Res. 33(8), 1817-1832.

Alkahtani, M.E., Aodah, A.H., Abu Asab, O.A., Basit, A.W., Orlu, M., Tawfik, E.A. 2021. Fabrication and characterization of fast-dissolving films containing escitalopram/quetiapine for the treatment of major depressive disorder. Pharmaceutics. 13(6), 891.

Awad, A.; Trenfield, S.J., Goyanes, A.; Gaisford, S., Basit, A.W. 2018. Reshaping drug development using 3D printing. Drug Discov. Today. 23, 1547–1555.

Cipriani A, Furukawa T.A., Salanti G., et al. 2009. Comparative efficacy and acceptability of 12 new generation antidepressants: a multiple-treatments meta-analysis. Lancet. 373(9665),746-58.

Cipriani A., Santilli C., Furukawa T.A., et al. 2009. Escitalopram versus other antidepressive agents for depression. Cochrane Database Syst Rev; CD006532.

De Diego, H.L., Bond, A.D., & Dancer, R.J. .2011. Formation of solid solutions between racemic and enantiomeric citalopram oxalate. Chirality. 23(5), 408-416.

Dhaneshwar, S.R., Mahadik, M.V., Kulkarni, M.J. 2008. Column liquid chromatography-ultraviolet and column liquid chromatography/mass spectrometry evaluation of stress degradation behavior of escitalopram oxalate. J AOAC Int. 92, 138-47.

Doreth, M., Hussein, M.A., Priemel, P.A., Grohganz, H., Holm, R., de Diego, H.L., Rades, T., Löbmann, K. 2017. Amorphization within the tablet: Using microwave irradiation to form a glass solution in situ. Int. J. Pharm. 519(1-2), 343-351.

Douroumis, D. 2012. Hot-melt extrusion: Pharmaceutical Applications. Wiley Online Library.

El Aita, I., Ponsar, H., & Quodbach, J. 2018. A Critical Review on 3D-printed dosage forms. Curr. Pharm. Des. 24(42), 4957-4978.

Evonik, Technical Information Eudragit® E 100, EUDRAGIT® E PO and EUDRAGIT® E 12,5. www.pharmaexcipients.com/wp-content/uploads/attachments/TI-EUDRAGIT-E-100-E-PO-E-12-5-EN.pdf?t=1508413942 (Accessed 22 November 2022).

Fernandez-Garcia, R., Prada, M., Bolas-Fernandez, F., Ballesteros, M.P., Serrano, D. R. 2020. Oral fixed-dose combination pharmaceutical products: industrial manufacturing versus personalized 3D printing. Pharm. Res. 37, 132.

Furqan, M. & Iqbal, F. & Tulain, R. 2017. Microwave radiation induced synthesis of hydroxypropyl methylcellulose-graft-(polyvinylalcohal-co-acrylic acid) polymeric network and its in vitro evaluation. Acta Pol. Pharm. 74. 527-541.

Gartlehner G, Hansen R.A., Morgan L.C., Thaler, K., Lux, L., Van Noord, M., Mager, U., Thieda, P., Gaynes, B.N., Wilkins, T., Strobelberger, M., Lloyd, S., Reichenpfader, U., Lohr, K.N. 2011. Comparative benefits and harms of second-generation antidepressants for treating major depressive disorder: an updated meta-analysis. Ann. Intern. Med. 155(11), 772-85.

Goyanes, A., Buanz, A.B., Hatton, G.B., Gaisford, S., Basit, A.W. 2015. 3D printing of modified-release aminosalicylate (4-ASA and 5-ASA) tablets. Eur. J. Pharm. Biopharm. 89, 157–162.

Goyanes, A., Scarpa, M., Kamlow, M., Gaisford, S., Basit, A.W., & Orlu, M. 2017. Patient acceptability of 3D printed medicines. Int. J. Pharm. 530(1), 71-78.

Grohganz, H., Löbmann, K., Priemel, P., Jensen, K.T., Graeser K, Strachan, C, Rades, T. 2013. Amorphous drugs and dosage forms, J. Drug Deliv Sci. Technol. 23, 403–408.

Hiew, T.N., Zemlyanov, D.Y., Taylor, L.S., 2022. Balancing solid-state stability and dissolution performance of lumefantrine amorphous solid dispersions: the role of polymer choice and drug polymer interactions. Mol. Pharm. 19, 392–413.

Hoffmann L., Breitkreutz J., Quodbach J. 2022a. Fused deposition modeling (FDM) 3D printing of the Thermo-Sensitive Peptidomimetic Drug Enalapril Maleate. Pharmaceutics. 14(11), 2411.

Hoffmann, L., Breitkreutz, J., Quodbach, J. 2022b. Hot-Melt Extrusion of the thermo-sensitive peptidomimetic drug enalapril maleate. Pharmaceutics. 14(10), 2091.

Holm, T. P., Kokott, M., Knopp, M.M., Boyd, B.J., Berthelsen, R., Quodbach, J., Löbmann, K. 2022. Development of a multiparticulate drug delivery system for in situ amorphization. Eur. J. Pharm. Biopharm. 180, 170-180.

Ilyés, K.; Kovács, N.K.; Balogh, A.; Borbás, E.; Farkas, B.; Casian, T.; Marosi, G.; Tomut,ă, I.; Nagy, Z.K. 2019. The applicability of pharmaceutical polymeric blends for the fused deposition modelling (FDM) 3D technique: material considerations–printability– process modulation, with consecutive effects on in vitro release, stability and degradation. Eur. J. Pharm. Sci. 129, 110–123.

Institute of Health Metrics and Evaluation. Global Health Data Exchange (GHDx). https://vizhub.healthdata.org/gbd-results/ (Accessed 22 November 2022).

Jagtap A, Bhaskar M. 2013. Evaluation of antidepressant and antinociceptive activity of escitalopram. Ind. J. Pharm. Edu. Res. 47, 97–102.

Kalepu, S.; Nekkanti, V. 2015. Insoluble drug delivery strategies: Review of recent advances and business prospects. Acta Pharm. Sin. B. 5, 442–453.

Kanaujia, P., Poovizhi, P., Ng, W.K, Tan, R.B.H., 2015. Amorphous formulations for dissolution and bioavailability enhancement of poorly soluble APIs. Powder Technol. 285, 2-15.

Kempin, W., Domsta, V., Brecht, I., Semmling, B., Tillmann, S., Weitschies, W., Seidlitz, A. 2018.

Development of a dual extrusion printing technique for an acid- and thermo-labile drug. Eur. J. Pharm. Sci. 123, 191-198

Khalid, G. M., & Billa, N., 2022. Solid dispersion formulations by FDM 3D Printing - a review. Pharmaceutics. 14(4), 690.

Kirino, E. 2012. Escitalopram for the management of major depressive disorder: a review of its efficacy, safety, and patient acceptability. Patient Prefer. Adherence. 6. 853–861.

Konta, A.A.; Garcia-Pina, M.; Serrano, D.R. 2017. Personalised 3D Printed Medicines: which techniques and polymers are more successful? Bioengineering. 4, 79.

Krause, J., Müller, L., Sarwinska, D., Seidlitz, A., Sznitowska, M., Weitschies, W. 2021. 3D printing of mini tablets for pediatric use. Pharmaceuticals. 14, 143.

Kumbhar, M. S. 2013. Enhancement of solubility and dissolution rate of escitalopram oxalate by liquisolid compact technology. Int. J. Pharm. Chem. Sci. 2, 2277–5005.

Manini, G., Benali, S., Mathew, A., Napolitano, S., Raquez, J.-M., Goole, J. 2022. Paliperidone Palmitate as model of heat-sensitive drug for long-acting 3D printing application. Int. J. Pharm. 121662.

O'Donnell, J.M., & Shelton R. C. 2015. Drug therapy of depression and anxiety disorders. Brunton L. L., & Chabner B. A., & Knollmann B.C.(Eds.), Goodman & Gilman's: The Pharmacological Basis of Therapeutics, 12th ed. McGraw Hill. https://accesspharmacy.mhmedical.com/content.aspx?bookid=1613&sectionid=102158640 (Accessed 20 November 2022).

O'Donnell, K.P., & Woodward, W. H.H. 2015. Dielectric spectroscopy for the determination of the glass transition temperature of pharmaceutical solid dispersions. Drug Dev. Ind. Pharm. 41(6), 959-968.

Parikh, T.; Gupta, S.S.; Meena, A.; Serajuddin, A.T. 2016. Investigation of thermal and viscoelastic properties of polymers relevant to hot melt extrusion-III: Polymethacrylates and polymethacrylic acid based polymers. J. Excip. Food Chem. 5, 1003.

Pawar, J., Tayade, A, Gangurde, A., Moravkar, K., Amin. P. 2016. Solubility and dissolution enhancement of efavirenz hot melt extruded amorphous solid dispersions using combination of polymeric blends: a QbD approach. Eur. J. Pharm. Sci. 88, 37-49.

Pinto, B.V., Ferreira, A.P.G., & Cavalheiro, E.T.G. 2018. Thermal degradation mechanism for citalopram and escitalopram. J. Therm. Anal. Calorim. 133(3), 1509-1518.

Rao, R. N., Raju, A.N., Narsimha, R. 2008. Isolation and characterization of degradation products of citalopram and process-related impurities using RP-HPLC. J. Sep. Sci. 31(10), 1729-1738.

Santomauro D.F., Mantilla Herrera A.M., Shadid J., Zheng P., Ashbaugh C., Pigott D.M., et al. 2021. Global prevalence and burden of depressive and anxiety disorders in 204 countries and territories in 2020 due to the COVID-19 pandemic. Lancet, 398(10312),1700–1712.

Scoutaris, N., Ross, S.A. & Douroumis, D. 2018. 3D Printed "Starmix" drug loaded dosage forms for paediatric applications. Pharm. Res. 35, 34.

Song, T., Quan, P., Xiang, R., Fang, L. 2016. Regulating the skin permeation rate of escitalopram by ion-pair formation with organic acids. AAPS PharmSciTech. 17, 1267–1273.

Tan, D.K., Davis, D.A., Miller, D.A. et al. 2020. Innovations in thermal processing: hot-melt extrusion and KinetiSol® dispersing. AAPS PharmSciTech. 21, 312.

Varghese, R., Sood P., Salvi S., Karsiya, J., Kumar D. 2022. 3D printing in the pharmaceutical sector: advances and evidences. Sensors International. 3, 100177.

Wang, N., Shi, H., Yang. S. 2022. 3D printed oral solid dosage form: Modified release and improved solubility, J. Control. Release. 351, 407-431.

Waugh, J., and Goa, K.L. 2003. Escitalopram: a review of its use in the management of major depressive and anxiety disorders. CNS Drugs. 17, 343–362.

WHO Model List of Essential Medicines – 22nd list. 2021. https://www.who.int/publications/i/item/WHO-MHP-HPS-EML-2021.02 (Accessed 20 October 2022).

Windolf, H., Chamberlain, R., Breitkreutz, J., & Quodbach, J. 2022. 3D Printed mini-floating-polypill for Parkinson´s disease: combination of levodopa, benserazide, and pramipexole in various dosing for personalized therapy. Pharmaceutics. 14(5), 931.

Xu, X., Jiang, L., Zhou, Z., Wu, X.-F., Wang, Y. 2012. Preparation and properties of electrospun soy protein isolate/polyethylene oxide nanofiber membranes. ACS Appl. Mater. Interfaces. 4, 4331–4337.

Investigation of the degradation and *in-situ* amorphization of the enantiomeric drug escitalopram oxalate during Fused Deposition Modeling (FDM) 3D printing

Lena Hoffmann, Jörg Breitkreutz, Julian Quodbach

Supplemental Material

DSC analysis

DSC diffractograms of PEG 6.000 and PEO were presented in Figure S1.

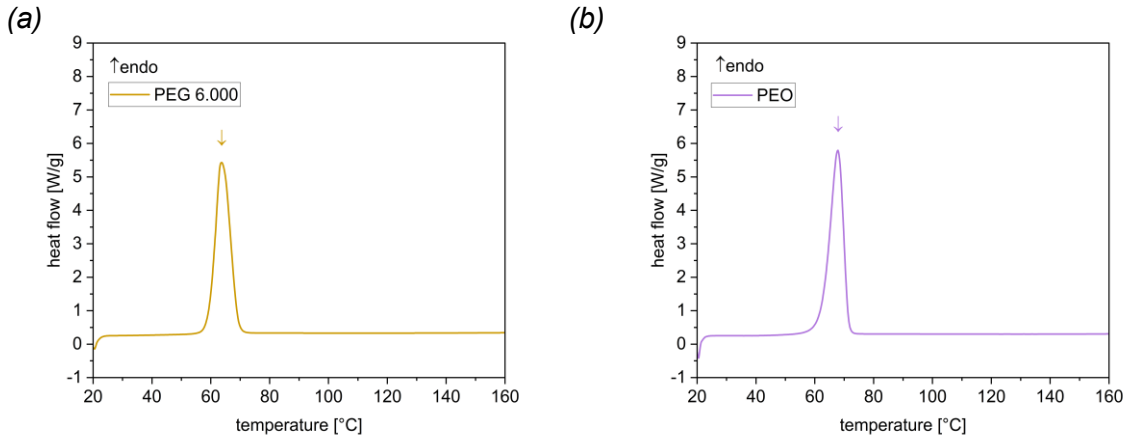

Figure S1. DSC diffractograms of PEG 6.000 (a) and PEO (b).

X-ray diffraction (XRD)

XRD diffractogram of the semi-crystalline PEO was shown in Figure S2.

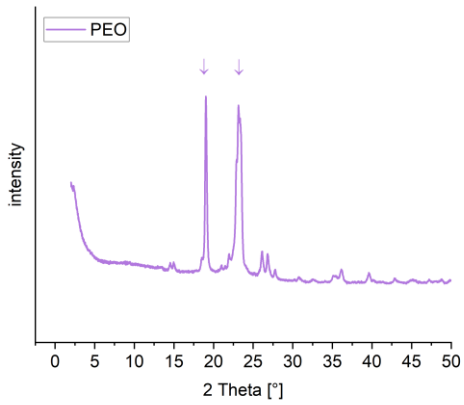

Figure S2. XRD diffractogram of PEO.

Polarized light microscopy

With the help of a polarized light microscope images were taken of ESC-OX, PEO, the extrudate of F3 with bPMMA as well as the 3D printed tablet of F3 with bPMMA (Figure S3). The image of the active ingredient ESC-OX clearly show its crystalline state in the form of individual crystals, whereas for the image of PEO some crystalline particles were visible. For the extrudate of F3 with bPMMA crystalline particles were also visible, which were absent in the 3D printed tablet of F3 with bPMMA. These results confirmed the DSC and XRD data regarding the previously made observations. ESC-OX is converted into an amorphous state during FDM 3D printing from crystalline extrudates with bPMMA.

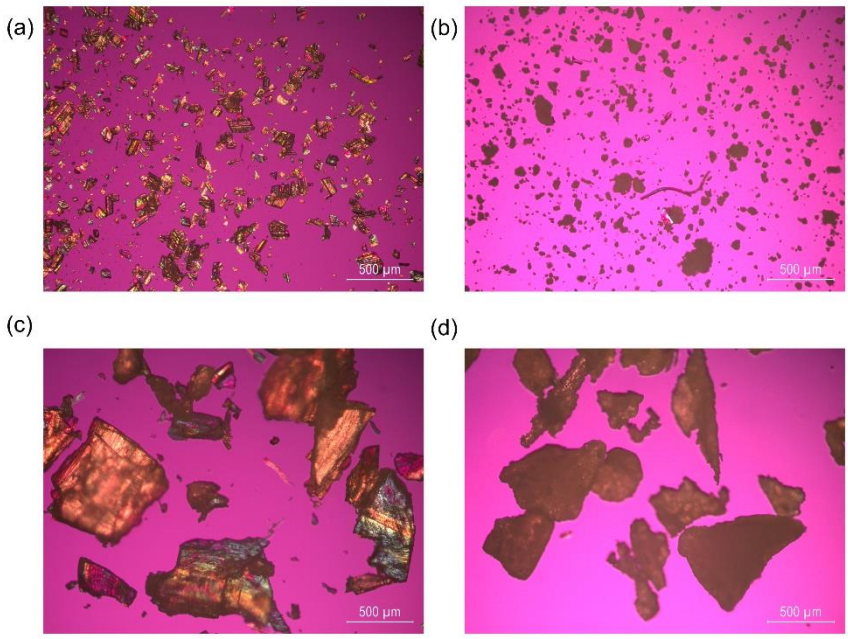

Figure S3. Polarization microscope images of ESC-OX (a), PEO (b), milled extrudate with bPMMA (c) and milled 3D printed tablet with bPMMA (d).

Mass spectrometry

Mass spectra were obtained for the stressed samples of escitalopram in 0.1 N NaOH at 70 °C for 1 h and 12 h (Figure S2). These should confirm the formation of the impurity citalopram carboxylic acid, which is not a pharmacopoeial impurity. However, this is formed from the known impurity CIT-A by hydrolysing the cyano group to the carboxyl group. The ESI spectrum for the alkali treated sample for 1 h showed the major peak of escitalopram at m/z 325.17 and also the two degradation products at m/z 343.18 and 344.17. These two impurities were confirmed as citalopram carboxylic acid and Citalopram Related Compound A (CIT-A) (Figure S4a). On the other hand, the ESI spectrum from the alkali treated sample for 12 h showed the major peak at m/z 344.17, which represented the citalopram carboxylic acid (Figure S4b). Furthermore, the Citalopram Related Compound A (CIT-A) could be seen at m/z 343.18. These results confirmed the observations from the HPLC analysis.

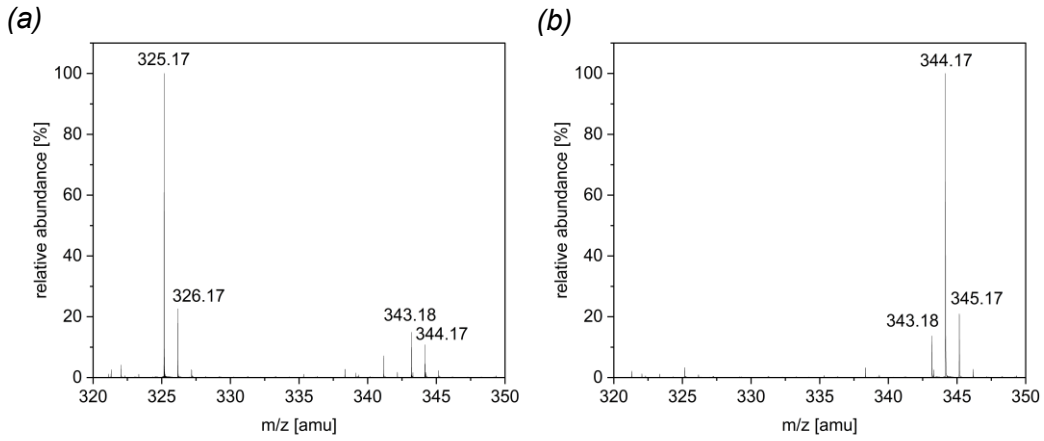

Figure S4. Mass spectra for the alkali treated samples of escitalopram at 70 °C for 1 h (a) and 12 h (b), respectively.

6 Discussion

The present work has shown that quality requirements must be set and matched for FDM 3D printed dosage forms, which are initially produced from extrudates by HME. As part of the work in the PolyPrint consortium, new polymers for FDM 3D printing (3DP), new formulations and a GMP-compliant FDM 3D printer were developed. Particularly for the production of FDM 3D printed dosage forms for paediatrics, special requirements may be necessary. Due to the lack of published literature on the quality of 3D printed dosage forms for paediatrics, considerations were compiled in a review article in the Therapeutic Innovation & Regulatory Science publication.

The focus of the research work was the processing of thermo-sensitive drug substances by HME and FDM 3DP, which poses a great challenge due to the double heat exposure. FDM 3DP in combination with HME was chosen as the printing method, because FDM 3DP is the most researched technology for the production of patient-specific dosage forms due to its simple, solvent-free process, its versatility and speed, and its low-cost equipment. An increasing number of thermo-sensitive drugs including biologically active molecules are becoming available, which are of great therapeutic relevance and require customisation that can be provided by FDM 3DP. To develop an understanding of the degradation of thermo-sensitive drug substances during the two processes of HME and FDM 3DP, the two thermo-sensitive drug substances enalapril maleate (EM) and escitalopram oxalate (ESC-OX) were selected.

EM was selected as a thermo-sensitive peptidomimetic drug substance, which was first processed into extrudates with various polymers by HME at temperatures of 100 °C to 150 °C. Within the scope of a polymer screening, extrudates from six different formulations with a drug load of 10 % EM were prepared at different temperatures and process conditions and the content in the extrudates was determined. In comparison to the DSC and TG measurements, it was found that the degradation of EM already occurred below the melting temperature of 153 °C. Following the development of a fast HPLC method to quantify EM and potential degradation products, the main degradation product in the extrudates was the cyclisation product enalapril diketopiperazine (DKP, Impurity D). DKP is also known as a thermal degradation product of proteins and peptides. It was found that not only the temperature, but also the shear forces had an influence on the degradation of the active ingredient. In addition, the selection of the polymer and thus the formulation is of crucial importance. Higher viscosity polymers such as HPMC led to greater degradation of enalapril (ENP) in the extrudates. On the contrary, it was found that low glass transition temperature polymers such as SOL can be extruded at a lower temperature of 100 °C. A higher feed rate of the feeder, which shortens the residence time, could also contribute to a lower degradation of the active ingredient. The polymer screening results indicated that two formulations of EM were suitable for extrusion at lower temperatures. These two formulations, which were referred to as "optimized formulations" in the publications, contained SOL and bPMMA as low glass transition temperature polymers. The process conditions for the extrusions were adjusted and a higher feed rate of 100 g/h was selected. The optimised formulations were fed at a feed rate of 100 g/h and extruded at a temperature of 100 °C, whereby the formulation with bPMMA allowed extrusion at 70 °C. The degradation of EM could be avoided in the extrudates with bPMMA extruded at 70 °C, confirming the advantageous use of low glass transition temperature polymers for the processing of thermo-sensitive drug substances. In addition, the interaction between EM and the basic bPMMA, which could be confirmed by FT-IR measurements, was found to have a stabilising effect on the EM content. The influence of a cation-anion interaction on the stability of an active substance during HME has already been described in the literature. It was also demonstrated that the polymer used had an influence on the dissolution of ENP from the extrudates.

Despite the amorphous form of ENP in the extrudates with SOL and bPMMA, which was determined with the help of DSC and XRD measurements, differences in the release behaviour of ENP could be observed. Dissolution tests in pH 1.2 and 6.8 showed a pH-independent release of ENP from the extrudates with SOL extruded at 100 °C and a pH-dependent release of ENP from the extrudates with bPMMA extruded at 70 °C. The polymer bPMMA dissolved at pH values below pH 5.5 and could thus lead to an immediate release of ENP from the extrudates.

The optimised formulations from HME at 100 °C were then processed into oral 3D printed tablets with a target dose of 10 mg EM and 100 % infill using a commercially available FDM 3D printer at a nozzle temperature of 180 °C and a print bed temperature of 35 °C and were evaluated for degradation. The amorphous state of ENP was also retained in the 3D printed tablets. After 3DP, the stabilising effect of bPMMA was again evident. As after extrusion, the content of enalapril was higher in the 3D printed tablets with bPMMA than in the tablets with SOL, although the differences in content were significantly greater. This corroborates the reduction in complex viscosity and increase in melt extrudability due to the cation-anion interaction during processing of the extrudates into 3D printed tablets. In addition, a printing study was conducted to investigate the thermal degradation of ENP during FDM 3DP. The extrudates with bPMMA from the extrusion of 70 °C without degradation were used and nozzle diameter (0.4 vs. 0.6 mm), nozzle temperature (180 and 190 °C) and printing speed (30, 60 and 90 mm/s) were selected as critical process parameters. The investigations showed that a higher nozzle temperature resulted in greater degradation of ENP at the same nozzle diameter and printing speed. Contrary to the expectations, a slight decrease in enalapril content was observed at a nozzle diameter of 0.4 mm and increasing printing speed at both nozzle temperatures. The decrease in content could be explained by the increased backpressure during 3DP at the same temperature due to the stronger backmixing. The use of a nozzle diameter of 0.6 mm resulted in a minor increase in the content of ENP at a printing temperature of 180 °C with increasing printing speed. This confirms the already known observations that the formation of degradation products is lower due to the shorter residence time and heat exposure during 3DP. However, this observation could not be confirmed for the higher temperature of 190 °C. Finally, the highest amount of ENP was found for the 0.4 mm nozzle at 180 °C and a printing speed of 30 mm/s. A non-significantly lower, but consistent active ingredient content was found when using a larger nozzle diameter of 0.6 mm and a printing speed of 90 mm/s. Further investigations, in which more flexible structures with reduced infill or different infill patterns were printed, also did not reveal a higher ENP content. Degradation of ENP could not be avoided during FDM 3DP due to the higher temperature gradient required between the nozzle and extrudate. The release of ENP from the bPMMA tablets confirms the degradation of the active ingredient and the presence of the degradation product DKP in the 3D printed tablets.

As a second thermo-sensitive drug, which is additionally unstable in 0.1 N sodium hydroxide solution, the enantiomeric drug ESC-OX and its degradation products were investigated during HME and FDM 3DP. The potential conversion of the S-citalopram to the R-enantiomer during both processes was also examined. The degradation avoidance strategies developed from HME and FDM 3DP of EM were applied and evaluated to the active ingredient ESC-OX with an approximate melting point of 153 °C. Three formulations based on the polymers HPMC and bPMMA with a drug load of 10 % ESC were used to manufacture extrudates and then printed into tablets with a target dose of 10 mg ESC. The two formulations based on HPMC or a combination of HPMC and bPMMA were extruded at a temperature of 150 °C and printed at a nozzle temperature of 180 °C and print bed temperature of 65 °C. In contrast, the formulation consisting of bPMMA could be extruded at 80 °C as the lowest possible temperature and printed at a nozzle temperature of 180 °C and a print bed temperature of 35 °C. Due to the known base lability of ESC-OX, the influence of a neutral and basic polymer on the content of

ESC and its degradation products as well as the physical state during the two processes was investigated. Quantification of ESC and degradation products was performed with HPLC measurements on both an achiral and a chiral column after prior method development and establishment. In 0.1 N sodium hydroxide solution, the impurity Citalopram related compound (CIT-A) was confirmed as the degradation product of ESC. If ESC was additionally exposed to temperature in basic solution at 70 °C for 1 h, an increase in the content of the impurity CIT-A and in small quantities, the impurity citalopram carboxylic acid was detected as a further degradation product. When ESC was stressed in basic solution at 70 °C for 12 h, almost complete degradation of ESC was observed. In contrast, CIT-A and in greatest quantities citalopram carboxylic acid were found. The formation of citalopram carboxylic acid was detected by mass spectrometry based on the mass-to-charge (m/z) ratio. The results on the instability of ESC in basic solution are in agreement with the observations described in literature. During the investigation in the melt, it was found that differences in the content of ESC and the presence of the degradation products were observed depending on the polymer matrix used, which also significantly influenced the process temperatures during HME and FDM 3DP. Similar to EM, the use of polymers with higher viscosity such as the HPMC resulted in faster degradation of ESC. The highest degradation was seen in the extrudates with the HPMC, followed by the extrudates with HPMC and bPMMA. The use of polymers with a low glass transition temperature also proved to be effective for processing the thermo-sensitive drug substance ESC-OX. Degradation of ESC could be avoided during extrusion with bPMMA at 80 °C. Thus, ESC-OX was stable in the extrudates with bPMMA. FDM 3DP at a nozzle temperature of 180 °C showed a reduction of the original content for all formulations. However, only slight degradation was observed in the 3D printed tablets of ESC-OX with bPMMA. Regarding the formation of the degradation products, the impurity Citalopram related compound C (CIT-C) could be detected as the main degradation product in the extrudates and 3D printed tablets with the neutral polymer HPMC. The extrudates and 3D printed tablets with the neutral HPMC and the basic bPMMA showed the impurity CIT-A as the main degradation product. In the 3D printed tablets with the basic bPMMA, CIT-A was observed as the main degradation product in small quantities. Melt processing was able to reduce the degradation of the active ingredient ESC-OX despite the basic matrix (bPMMA). In addition, comparative studies of the formulation of ESC with bPMMA to the commercially available product Cipralex® film-coated tablets were carried out and the content determined. The absence of degradation products in the Cipralex® film-coated tablets was demonstrated. So far, no studies have been reported on the transformation of an enantiomer during HME and FDM 3DP. The studies conducted on the chiral column showed no conversion of the S-citalopram to the R-enantiomer either in solution or in the extrudates, 3D printed tablets with bPMMA as well as the Cipralex® film-coated tablets. This confirms the sufficient stability of the S-enantiomer. DSC and XRD studies on the physical stability of ESC-OX in the extrudates and 3D printed tablets showed that amorphous solid dispersions (ASDs) could be produced with the polymer HPMC and the combination of HPMC and bPMMA. Due to the extrusion temperature of 150 °C and the printing temperature of 180 °C, sufficient energy was provided to convert ESC-OX into the amorphous state. In the extrudates with bPMMA from extrusion at 80 °C, ESC-OX was present in crystalline form. By extruding at a temperature below the melting point, crystals of ESC-OX could be detected. Only through FDM 3DP an *in-situ* amorphisation of ESC-OX took place. Thus, ESC-OX was in an amorphous form in the 3D printed tablets with bPMMA. Dissolution studies of ESC-OX with bPMMA showed a faster drug release from the extrudates compared to the 3D printed tablets which could be explained by the larger surface area to volume ratio and implicated the stronger influence on the release of ESC-OX than the physical state. The 3D printed tablets with bPMMA also showed a slower release than the commercially available Cipralex® film-coated tablets due to the greater density and lower porosity, confirming the previously described observations.

7 Summary and Outlook

The present work focused on the analytical characterisation of the two thermo-sensitive drug substances enalapril maleate and escitalopram oxalate, which are relevant for personalised therapy, in the manufactured extrudates and 3D printed tablets. The aim was to develop strategies to prevent degradation during the two heat-intensive processes. The quantification of both the thermo-sensitive drug substances and their degradation products was carried out by HPLC using in-house developed, sensitive and robust HPLC methods. In addition, the chiral drug S-citalopram and the R-enantiomer were quantified on a chiral column. The HPLC methods developed proved to be suitable for successfully determining the active ingredients and the degradation products, some of which are formed in small quantities, in the extrudates and 3D printed tablets. The control of impurities is of great relevance to ensure the quality of the dosage forms produced. Comprehensive formulation development confirmed that polymers with low glass transition temperature such as SOL and bPMMA are preferably used for processing thermo-sensitive drug substances. It was shown that by selecting suitable polymers and process conditions, degradation could be successfully avoided in the manufactured extrudates with EM and ESC-OX. By processing EM with the polymer bPMMA, a stabilising effect could be observed through the cation-anion interaction, which could be confirmed by FT-IR measurements. The release behaviour was also significantly influenced by the polymer used, which could be shown in the dissolution studies with SOL and bPMMA. Due to the known instabilities of the two active ingredients in solution, processing in the melt proved to be advantageous despite the thermolability to avoid degradation in the extrudates. This is highly relevant as the extrudates produced served as starting material for FDM 3DP for the production of patient-specific dosage forms. While degradation of EM and ESC-OX could be avoided during HME, degradation could not be completely avoided due to the higher printing temperature required during FDM 3DP. For both the formulations with EM and ESC-OX, printing temperatures with a nozzle temperature of at least 180 °C were required. For EM in particular, greater degradation was observed during FDM 3DP, despite the only short-term temperature exposure at 180 °C. In contrast, the degradation of ESC-OX could be almost completely avoided. Moreover, a possible conversion of the S-enantiomer into the R-enantiomer in the extrudates and 3D printed tablets on the chiral column could be excluded. It could be shown that S-citalopram was sufficiently stable and no conversion into the R-enantiomer occurred. With regard to the physical stability of the active ingredients, which was determined using DSC and XRD investigations, *in-situ* amorphisation from the crystalline extrudates with bPMMA was observed for ESC-OX during FDM 3DP. The *in-situ* amorphisation enables the production of unstable amorphous forms shortly before application and offers advantages especially with regard to storage stability and clinical applications. 3D printed tablets can be produced from physically stable extrudates shortly before use. From the insights gained, it became apparent that there is further potential for improvement in the development of FDM 3DP. Due to the current use of only commercially available FDM 3D printers, such as the Prusa 3D printer used in this work, the present work demonstrates the benefit for the development and implementation of a GMP-compliant printer, that could reduce the temperature load on the active ingredient and enable FDM 3DP at lower temperatures. This would open up new possibilities for thermo-sensitive drug substances and enable FDM 3DP of the two drug substances relevant to personalised medicine, EM and ESC-OX, for clinical applications. Further potential could lie in the coupling of the two processes of HME and FDM 3DP. Printing directly from the extruder nozzle could reduce the temperature load and enable printing at low temperatures due to better heat transfer.

8 Zusammenfassung und Ausblick

Im Rahmen der vorliegenden Arbeit wurde der Schwerpunkt auf die analytische Charakterisierung der beiden thermisch sensitiven, für die personalisierte Therapie relevanten Arzneistoffe Enalaprilmaleat und Escitalopramoxalat in den hergestellten Extrudaten und 3D-gedruckten Tabletten gelegt, mit dem Ziel der Erarbeitung von Strategien zur Vermeidung des Abbaus während der beiden wärmeintensiven Prozesse. Die Quantifizierung sowohl der thermisch-sensitiven Arzneistoffe als auch ihrer Zersetzungsprodukte erfolgte durch die Hochleistungsflüssigkeitschromatographie (HPLC) mithilfe eigens entwickelter, sensitiver und robuster Methoden. Zudem erfolgte die Quantifizierung des chiralen Arzneistoffes S-Citalopram und des R-Enantiomers zusätzlich auf einer chiralen Säule. Die entwickelten HPLC-Methoden erwiesen sich als geeignet, die Wirkstoffe sowie auch die in geringen Mengen entstehenden Abbauprodukte in den Extrudaten und 3D-gedruckten Tabletten erfolgreich zu bestimmen. Die Kontrolle von Verunreinigungen ist zur Sicherstellung der Qualität der hergestellten Darreichungsformen von großer Relevanz. Die umfangreiche Formulierungsentwicklung bestätigte, dass Polymere mit niedriger Glasübergangstemperatur, wie Soluplus® (SOL) und basische Polymethylmethacrylate (bPMMA, Eudragit® E), für die Verarbeitung von thermisch-sensitiven Arzneistoffen zu bevorzugen sind. Es konnte gezeigt werden, dass durch Auswahl geeigneter Polymere und Prozessbedingungen der Abbau in den hergestellten Extrudaten mit EM und ESC-OX erfolgreich vermieden werden konnte. Durch die Verarbeitung von EM mit dem Polymer bPMMA konnte eine stabilisierende Wirkung durch die Kationen-Anionen-Wechselwirkung beobachtet werden, welche durch FT-IR-Messungen bestätigt werden konnte. Des Weiteren wurde das Freisetzungsverhalten maßgeblich durch das verwendete Polymer beeinflusst, was in den Freisetzungsuntersuchungen mit Soluplus® und Eudragit® E gezeigt werden konnte. Aufgrund der bekannten Instabilitäten der beiden Wirkstoffe in Lösung erwies sich die Verarbeitung in der Schmelze trotz der Thermolabilität als vorteilhaft, um eine Degradation in den Extrudaten zu vermeiden. Dies ist von hoher Relevanz, da die hergestellten Extrudate als Ausgangsmaterial für den FDM-3D-Druck zur Herstellung von patientenspezifischen Darreichungsformen dienen. Während der Abbau von EM und ESC-OX während der Schmelzextrusion vermieden werden konnte, konnte der Abbau aufgrund der erforderlichen höheren Drucktemperatur während des FDM 3D-Drucks nicht vollständig vermieden werden. Sowohl für die Formulierungen mit EM als auch ESC-OX waren mindestens Drucktemperaturen mit einer Düsentemperatur von 180 °C erforderlich. Insbesondere für EM wurde trotz der nur kurzzeitigen Temperaturbelastung bei 180 °C ein größerer Abbau während des FDM 3D-Drucks festgestellt. Demgegenüber konnte der Abbau von ESC-OX fast vollständig vermieden werden. Zudem konnte eine mögliche Umwandlung des S-Enantiomers in das R-Enantiomer in den Extrudaten und 3D-gedruckten Tabletten auf der chiralen Säule ausgeschlossen werden. Es konnte gezeigt werden, dass S-Citalopram ausreichend stabil war und keine Umwandlung in das R-Enantiomer erfolgte. Bezüglich der physikalischen Stabilität der Wirkstoffe, welche mithilfe von DSC- und XRD-Untersuchungen bestimmt wurde, konnte für ESC-OX eine *in-situ* Amorphisierung aus den kristallinen Extrudaten mit bPMMA während des FDM 3D-Drucks beobachtet werden. Die *in-situ* Amorphisierung ermöglicht die Herstellung von instabilen amorphen Formen kurz vor der Anwendung und bietet vor allem Vorteile bezüglich der Lagerstabilität und der klinischen Anwendung. Es können 3D-gedruckte Tabletten kurz vor der Anwendung aus physikalisch stabilen Extrudaten hergestellt werden. Aus den gewonnenen Erkenntnissen wurde ersichtlich, dass weiteres Verbesserungspotenzial bei der Entwicklung der FDM 3D-Drucker liegt. Durch den bisherigen Einsatz von lediglich kommerziell erhältlichen FDM 3D-Druckern, wie z. B. den in dieser Arbeit verwendeten Prusa 3D-Drucker, zeigt die vorliegende Arbeit den Nutzen für die Entwicklung und Implementierung eines GMP-konformen Druckers auf, welcher die Temperaturbelastung des Wirkstoffes reduzieren und den FDM-Prozess bei niedrigeren Temperaturen ermöglichen könnte.

Dadurch würden neue Möglichkeiten für thermisch-sensitive Arzneistoffe eröffnet werden und den FDM 3D-Druck der beiden für die personalisierte Medizin relevanten Wirkstoffe EM und ESC-OX für klinische Anwendungen ermöglichen. Weiteres Potenzial könnte in der Kopplung der beiden Prozesse Schmelzextrusion und FDM 3D-Druck liegen. Das direkte Drucken aus der Düse des Extruders könnte die Temperaturbelastung reduzieren und das Drucken aufgrund des besseren Temperaturgradienten bei geringen Temperaturen ermöglichen.

9 List of original publications

1. Julian Quodbach, Malte Bogdahn, Jörg Breitkreutz, Rebecca Chamberlain, Karin Eggenreich, Alessandro Giuseppe Elia, Nadine Gottschalk, Gesine Gunkel-Grabole, Lena Hoffmann, Dnyaneshwar Kapote, Thomas Kipping, Stefan Klinken, Fabian Loose, Tristan Marquetant, Hellen Windolf, Simon Geißler, Tilmann Spitz

   Quality of FDM 3D printed medicines for pediatrics: Considerations for formulation development, filament extrusion, printing process and printer design

   Ther. Innov. Regul. Sci. 56 (2022) 910-928

   Own contribution: 5 %

   Lena Hoffmann was involved in planning the structure of the review and the study design. The chapter *3d Printed Dosage Forms for Pediatric Use* was co-written by Lena Hoffmann. Lena Hoffmann contributed to the revision and editing of the references.

2. Lena Hoffmann, Jörg Breitkreutz and Julian Quodbach

   Hot-melt extrusion of the thermo-sensitive peptidomimetic drug enalapril maleate

   Pharmaceutics 14(10) (2022) 2091

   Own contribution: 80 %

   Lena Hoffmann created the concept of the study and developed the study design, with the agreement of Jörg Breitkreutz and Julian Quodbach. Lena Hoffmann conducted the experimental work and evaluated the obtained data. Lena Hoffmann wrote the manuscript. Jörg Breitkreutz and Julian Quodbach reviewed the manuscript.

3. Lena Hoffmann, Jörg Breitkreutz and Julian Quodbach

   Fused deposition modeling (FDM) 3D printing of the thermo-sensitive peptidomimetic drug enalapril maleate

   Pharmaceutics 14(11) (2022) 2411

   Own contribution: 80 %

   Lena Hoffmann created the concept of the study and developed the study design, with the agreement of Jörg Breitkreutz and Julian Quodbach. Lena Hoffmann conducted the experimental work and evaluated the obtained data. Lena Hoffmann wrote the manuscript. Jörg Breitkreutz and Julian Quodbach reviewed the manuscript.

4. Lena Hoffmann, Jörg Breitkreutz and Julian Quodbach

   Investigation of the degradation and *in-situ* amorphization of escitalopram oxalate during FDM 3D printing

   Eur. J. Pharm. Sci. 185 (2023) 106423

   Own contribution: 80 %

   Lena Hoffmann created the concept of the study and developed the study design, with the agreement of Jörg Breitkreutz and Julian Quodbach. Lena Hoffmann conducted the experimental work and evaluated the obtained data. Lena Hoffmann wrote the manuscript. Jörg Breitkreutz and Julian Quodbach reviewed the manuscript.

10 Contributions to meetings

10.1 Oral presentations

1. Lena Hoffmann
   Hot-melt extrusion and 3D printing of a thermally unstable drug
   15th Annual PSSRC Symposium, online, 2021

10.2 Poster presentations

1. Lena Hoffmann, Jörg Breitkreutz, Julian Quodbach
   HPLC-Methodenentwicklung für die Untersuchung von thermolabilen Arzneistoffen während der Schmelzextrusion und des 3D-Druckes von Filamenten
   ProMatLeben-Polymere Doktorandenkonferenz, online, 2021

2. Lena Hoffmann, Jörg Breitkreutz, Julian Quodbach
   Analytische Entwicklung für die Untersuchung von thermolabilen Arzneistoffen während der Schmelzextrusion und des 3D-Druckes von Filamenten
   ProMatLeben-Polymere Midtermkonferenz, online, 2021

3. Lena Hoffmann, Jörg Breitkreutz, Julian Quodbach
   Hot melt extrusion and fused deposition modelling of a thermolabile drug
   13th World Meeting on Pharmaceutics, Biopharmaceutics and Pharmaceutical Technology (PBP), Rotterdam, 2022

11 Danksagung

Ich möchte mich ganz herzlich bei meinem Doktorvater, Prof. Dr. Jörg Breitkreutz, für die Aufnahme in seinen Arbeitskreis und die Betreuung während meiner Promotion am Institut für Pharmazeutische Technologie und Biopharmazie bedanken. Mein besonderer Dank gilt vor allem für seine Unterstützung und sein mir entgegengebrachtes Vertrauen bezüglich der Auswahl sowie freien Gestaltung meines Promotionsthemas. Dies ermöglichte mir die Aneignung eines fundierten Fachwissens. Weiterhin bedanke ich mich sowohl für die konstruktiven Gespräche als auch die Möglichkeit der Teilnahme an Fortbildungen und Konferenzen, welche Anregungen gaben und zum Gelingen der Arbeit beitrugen.

Bei meinem Mentor Prof. Dr. Dr. h.c. Peter Kleinebudde möchte ich mich für die freundliche Übernahme des Korreferats bedanken. Ich bedanke mich für die fachliche Betreuung im Rahmen der Fokusgruppen und Fortschrittsgespräche sowie der Möglichkeit der permanenten Ansprechbarkeit und Hilfsbereitschaft.

Bei Prof. Dr. Julian Quodbach möchte ich mich für die Betreuung im Rahmen des ´ProMatLeben-Polymere-PolyPrint´-Projektes und besonders für die Unterstützung durch kritisches Lesen von Abstracts, Postern, Publikationen und der Dissertation bedanken. Ebenfalls möchte ich mich bei Rebecca Chamberlain und Dr. Hellen Mazur für die freundliche Aufnahme in das Projekt sowie für unsere Zusammenarbeit seitens der Heinrich-Heine-Universität Düsseldorf bedanken. Zudem bedanke ich mich bei den Projektpartnern, der Technischen Hochschule Köln, Merck sowie Gen-Plus für den fachlichen Austausch in den gemeinsamen Gesprächen und Projektreffen, welche mir stets Freude bereitet haben.

Ein besonderer Dank gebühren Prof. Dr. Björn Burckhardt und Dipl. Chem. Simone Mönninghoff-Pützer für den fachlichen Austausch bei analytischen Fragestellungen, die Bereitstellung von Säulen sowie die tatkräftige Unterstützung bei HPLC-Reparaturen.

Andrea Michel danke ich für die Durchführung von DSC-Messungen sowie die freundlichen Gespräche während der Promotionszeit.

Stefan Klinken und Arne Schulzen danke ich für die Unterstützung bei der Durchführung von Extrusionsversuchen sowie beim Lösen von technischen Problemen.

Meinen Bürokolleginnen Annika Frings, Clara Grawe und Jennifer Kuck aus dem Büro 00.28 danke ich sehr für die angenehme Arbeitsatmosphäre, den Spaß und die schönen Erlebnisse während der gemeinsamen Zeit am Institut.

Zudem bedanke ich mich bei Claudia Köster für die gemeinsame Zeit und die netten Gespräche.

Zuletzt gilt mein größter Dank meinen Eltern Ellen und Heinrich Hoffmann, meinem Bruder Henry Hoffmann und ganz besonders meiner Schwester Laura Hoffmann für die grenzenlose Unterstützung und den Rückhalt.

12 Eidesstattliche Erklärung

Ich versichere an Eides Statt, dass die Dissertation von mir selbstständig und ohne unzulässige fremde Hilfe unter Beachtung der „Grundsätze zur Sicherung guter wissenschaftlicher Praxis an der Heinrich-Heine-Universität Düsseldorf“ erstellt worden ist. Die Dissertation wurde in der vorgelegten oder in ähnlicher Form noch bei keiner anderen Institution eingereicht. Ich habe bisher keinen erfolglosen Promotionsversuch unternommen.

Düsseldorf, den

Lena Hoffmann